



UNIVERSITÀ
DEGLI STUDI
FIRENZE

DOTTORATO DI RICERCA IN
SCIENZE DELLA TERRA

CICLO XXIX

COORDINATORE Prof. LORENZO ROOK

*Volatile Organic Compounds (VOCs) from Volcanic and Hydrothermal Systems:
Evidences from Field and Experimental Data*

Settore Scientifico Disciplinare GEO/08

Dottorando

Dott.ssa Venturi Stefania

Tutore

Prof. Tassi Franco

Co-Tutori

Prof. Shock Everett L.

Prof. Vaselli Orlando

Coordinatore

Prof. Lorenzo Rook

Anni 2013/2016

«*Considerate la vostra semenza:*

Consider well the seed that gave you birth:

fatti non foste a viver come bruti,

you were not made to live as brutes,

ma per seguir virtute e canoscenza»

but to follow virtue and knowledge

(Dante Alighieri, *Divina Commedia*,

Inferno, Canto XXVI)

Abstract

The PhD research project was aimed to improve the scientific knowledge about the composition and behaviour of volatile organic compounds (VOCs) in volcanic and hydrothermal systems, focusing on (*i*) primary processes occurring at high temperatures in deep fluid reservoirs and (*ii*) secondary processes occurring during the uprising of hydrothermal fluids toward the surface. The first goal was achieved following both experimental and empirical approaches. Laboratory experiments were performed in order to investigate the reaction pathways for benzene production under hydrothermal conditions, confirming that the aromatic compounds can be efficiently produced through dehydrocyclization and aromatization of normal-alkanes with cyclics as by-products. Moreover, the pivotal role of minerals in controlling organic reactivity and organic reaction pathways was demonstrated. The analysis of VOCs in fumarolic and venting gases from four volcanic-hydrothermal systems in the Mediterranean area characterized by different temperature and redox conditions at depth (Solfatara Crater, Nisyros Island, Poggio dell'Olivo and Cava dei Selci), supported by thermodynamic and experimental data, evidenced a strict control of physicochemical conditions of deep hydrothermal reservoirs on the composition of VOCs emitted at the surface. Alkanes were the most abundant VOCs, with decreasing abundances at increasing carbon chain length, in agreement with thermodynamic data. At relatively high temperatures, saturated hydrocarbons may undergo dehydrogenation to alkenes and/or dehydrocyclization and subsequent aromatization, as experimentally demonstrated. Accordingly, aromatics were enriched in fumarolic fluids from high temperature active volcanic systems, whilst cyclics were more abundant in hydrothermal systems characterized by lower temperatures, likely due

Abstract

to incomplete aromatization. The occurrence and abundances of S-bearing compounds were related to sulphur fugacity, whilst O-bearing compounds were mainly related to shallow processes. Interstitial soil gases were characterized by remarkably different compositions of VOCs when compared to those recorded in the fumarolic and venting gases, suggesting the relevant importance of secondary processes occurring at depth (dehydrocyclization of alkanes producing an enrichment in cyclics relative to fumarolic fluids) and at shallow depths (DMS oxidation, microbial production of O-bearing compounds). In particular, microbially-driven processes likely play a major role in modifying the composition of VOCs prior to their emission from soils in volcanic and hydrothermal systems.

Il progetto di ricerca sviluppato nei 3 anni di dottorato è stato finalizzato ad incrementare le conoscenze scientifiche circa la composizione e il comportamento dei composti organici volatili (COV) in sistemi vulcanici ed idrotermali, ponendo particolare attenzione allo studio di (i) processi primari in atto ad alte temperature nei serbatoi di fluidi idrotermali profondi, e (ii) processi secondari che avvengono durante la risalita dei fluidi idrotermali verso la superficie. I processi primari a carico dei COV sono stati indagati attraverso un approccio sia sperimentale che empirico. Esperimenti di laboratorio sono stati condotti per studiare i percorsi di reazione per la produzione di benzene a condizioni idrotermali, confermando che i composti aromatici possono essere efficientemente prodotti tramite deidro ciclizzazione e aromatizzazione di normal-alcani, con la produzione di ciclici come intermedi di reazione. Inoltre, gli esperimenti hanno dimostrato l'importante ruolo dei minerali nel controllare la reattività e i percorsi di reazione dei composti organici. L'analisi dei COV in gas fumarolici da quattro sistemi vulcanici-idrotermali nell'area mediterranea, caratterizzati da diverse condizioni di temperatura e redox in profondità (Cratere della Solfatara, Nisyros, Poggio dell'Olivo e Cava dei Selci), affiancata da dati termodinamici e sperimentali, ha evidenziato lo stretto controllo delle condizioni chimico-fisiche dei serbatoi idrotermali profondi sulla composizione dei COV emessi in superficie. Gli alcani sono risultati essere i COV più abbondanti, con concentrazioni decrescenti all'aumentare della lunghezza della catena carboniosa, in accordo con i dati termodinamici. A temperature relativamente alte, gli idrocarburi saturi possono andare incontro a deidrogenazione ad alcheni e/o deidro ciclizzazione e successiva aromatizzazione, come dimostrato sperimen-

talmente. Gli aromatici sono risultati essere più abbondanti nei fluidi fumarolici da sistemi vulcanici attivi ad alte temperature, mentre i ciclici risultano maggiormente presenti nei sistemi idrotermali caratterizzati da temperature minori, come probabile conseguenza di un'incompleta aromatizzazione. La presenza e l'abbondanza di composti S-sostituiti è risultata essere legata alla fugacità dello zolfo, mentre composti O-sostituiti sono principalmente legati a processi superficiali. Marcate differenze composizionali rispetto ai gas fumarolici sono state riscontrate nella frazione organica dei gas interstiziali del suolo, indicando il verificarsi di rilevanti processi secondari in atto in profondità (deidrociclizzazione degli alcani e conseguente arricchimento in ciclici rispetto ai fluidi fumarolici) e in livelli superficiali (ossidazione di DMS, produzione microbica di composti O-sostituiti). In particolare, i processi operati da microorganismi rivestono probabilmente un ruolo primario nella modificazione della composizione dei COV prima della loro emissione in aria dal suolo in sistemi vulcanici ed idrotermali.

Acknowledgments

I would like to express my special thanks to my supervisor Prof. Franco Tassi, for encouraging my research and for allowing me to grow as a research scientist, and to my co-supervisors, Prof. Orlando Vaselli and Prof. Everett L. Shock, for guiding and supporting me during my PhD study.

I also want to thank Prof. Jens Fiebig, Prof. Carlo Cardellini and Dr. Walter D'Alessandro for their valuable comments and suggestions on an earlier version of the manuscript.

I would like to convey my special and heartfelt gratitude to Dr. Jacopo Cabassi and Dr. Francesco Capecchiacci, two extraordinary colleagues and friends, for their priceless support and unvarying encouragement throughout these three years.

Gratitude is extended to Prof. Ian R. Gould, Prof. Edward D. Lorange, Prof. Hilairy E. Hartnett, Dr. Christiana Bockisch, Dr. Kristopher M. Fecteau, Dr. Kirtland Robinson, Dr. Kristin Johnson, Prof. Lynda Williams and all the GEOPIG and HOG members for their valuable advices and suggestions during my stay at ASU in Tempe (AZ, USA).

Many thanks go to all my colleagues at the DST-Unifi and to my friends, for their help and moral support.

Finally, special recognition goes to my family and Tommaso, for their limitless encouragement and support during my pursuit of the doctoral degree and for the draft-proofing services provided during the entire process. I thank all of you for your patience and enduring love and trust.

Contents

1	Introduction	1
2	Origin and fate of VOCs in volcanic and hydrothermal systems: from deep reservoirs to shallow environments	9
2.1	Introduction	9
2.2	Biotic vs. abiotic genesis	10
2.3	Abiotic synthesis	14
2.4	Thermogenic processes	16
2.4.1	Thermal cracking	16
2.4.2	Catalytic reforming	19
2.5	Organic functional group interconversions under hydrothermal conditions	23
2.6	Biogenic processes	29
2.6.1	Rudiments of biochemistry: metabolism and enzymes	31
2.6.2	Rudiments of biochemistry: microbial metabolic pathways	34
2.6.3	Biodegradation of VOCs	36
3	Experiments on organic reactions under hydrothermal conditions	41
3.1	Introduction	41
3.2	Preliminary considerations	42
3.3	Experimental methods	47
3.3.1	Reactants and minerals	47
3.3.2	Experimental procedure	47

CONTENTS

3.4	Results	51
3.4.1	Hexane and dodecane experiments	51
3.4.2	Cyclohexane experiments	52
3.4.3	Cyclohexene experiments	57
3.5	Discussion	62
3.5.1	Reactions in water with no minerals	62
3.5.2	Role of minerals	64
3.6	Concluding remarks	67
4	Study areas	69
4.1	Introduction	69
4.2	Active volcanoes-related hydrothermal systems	70
4.2.1	Solfatara Crater	70
4.2.2	Nisyros Island	76
4.3	Medium-low enthalpy hydrothermal systems	81
4.3.1	General settings	81
4.3.2	Poggio dell’Olivo	84
4.3.3	Cava dei Selci	88
5	Field sampling methods and analytical techniques	93
5.1	Sampling procedures for gases	93
5.1.1	Fumarolic gases	93
5.1.2	Gases from bubbling pool	96
5.1.3	Interstitial soil gases	97
5.2	Chemical and isotopic analysis of gases	98
5.3	Soil fluxes measurement	101
5.3.1	Soil CO ₂ flux measurement	101
5.3.2	Soil CH ₄ and C ₆ H ₆ flux measurement	102
6	Results	105
6.1	Introduction	105
6.2	Solfatara Crater	105
6.2.1	Fumarolic gases	105
6.2.2	Interstitial soil gases	115

CONTENTS

6.2.3	Soil flux measurements	147
6.2.4	Soil gases depth profiles	151
6.3	Nisyros Island	155
6.3.1	Fumarolic gases	155
6.3.2	Interstitial soil gases and soil flux measurements	161
6.4	Poggio dell'Olivo	163
6.4.1	Veza Creek bubbling gas	163
6.4.2	Interstitial soil gases	172
6.4.3	Soil gases depth profiles	174
6.5	Cava dei Selci	193
6.5.1	Gas vents	193
6.5.2	Interstitial soil gases and soil flux measurements	195
7	Distribution of VOCs from hydrothermal gas discharges: in- sights on primary processes	203
7.1	Introduction	203
7.2	General features of volcanic-hydrothermal systems	204
7.3	Thermal features	208
7.4	Inorganic constituents	209
7.5	Volatile organic compounds	213
8	Distribution of VOCs in interstitial soil gases: evidences of secondary processes	227
8.1	Introduction	227
8.2	Solfatara Crater	229
8.3	Nisyros Island	240
8.4	Poggio dell'Olivo	243
8.5	Cava dei Selci	255
9	Conclusions	259
	References	265

CONTENTS

Appendices	i
A Published Papers	i
B Conference Proceedings	v
C Research Projects	xi

Chapter 1

Introduction

Improvements in sampling techniques and analytical procedures, and the consequent lowering of the detection limit for gas trace constituents, have allowed the recognition of a number of different volatile organic compounds (VOCs) at low (generally $<1\%$), though detectable concentrations in natural fluid discharges from volcanic and hydrothermal systems (e.g. Capaccioni and Mangani, 2001; Capaccioni et al., 2001; Taran and Giggenbach, 2003; Schwandner et al., 2004; Tassi et al., 2005a, 2005b, 2010, 2012c; Schwandner et al., 2013; Tassi et al., 2013a). VOCs are defined as those organic species whose vapour pressure at $20\text{ }^{\circ}\text{C}$ is less than 760 torr (101.3 kPa) and greater than 1 torr (0.13 kPa), although the term VOC is generally related to any carbon-containing compound found in the atmosphere, excluding elemental carbon, carbon monoxide and carbon dioxide (Derwent, 1995).

The recognition of VOCs in volcanic and hydrothermal fluids is a relatively recent finding. The first studies revealing the presence of organic compounds in fumarolic gases date back to the 1960s-70s. White and Waring (1963) reported the presence of methane in fumarolic gases, whereas Findlayson et al. (1968) detected heavier hydrocarbons (not identified) in gases from Hawaiian lava lakes. Light $\text{C}_1\text{-C}_6$ hydrocarbons were then recognized in fumarolic gases from Vulcano (Aeolian Archipelago, Italy; Chaigneau and Conrad, 1970) and in magmatic and hydrothermal emissions from Kamchatka (Markhinin et al., 1975; Mukhin et al., 1978; Lebedev and Dekusar, 1980; Bondarev et al.,

1. Introduction

1982), whilst Stoiber et al. (1971), Isidorov et al. (1990) and Jordan et al. (2000) reported the presence of halocarbons in fumarolic gases from volcanic systems worldwide.

In the last decades, several studies (e.g. Capaccioni et al., 1993, 1995; Taran and Giggenbach, 2003; Tassi et al., 2012c; Schwandner et al., 2013) highlighted that the organic fraction of volcanic and hydrothermal gases is a complex mixture of a multitude of hydrocarbons (alkanes, alkenes, aromatics) and heteroatomic constituents (including O- and S-bearing compounds, and halocarbons). Most of these compounds have a strong impact on air quality and human health (HSDB: *Hazardous Substances Data Bank*). Once emitted in the atmosphere, they may undergo photochemical reactions with nitrogen oxides (NO_x) to form tropospheric ozone, or persist in the atmosphere (POPs, *Persistent Organic Pollutants*) acting as heat trapping gases (GHGs, *Greenhouse Gases*). For instance, methane (CH_4), the most abundant volatile organic compound emitted from volcanic and hydrothermal systems (e.g. Welhan, 1988; Fiebig et al., 2004; Tassi et al., 2012d), has an estimated Global Warming Potential 25 times higher than that of CO_2 (IPCC, 2007). The estimated methane emissions from European geothermal areas are in the order of 10^5 ton/yr; in Italy, the CH_4 contribution from volcanic and hydrothermal areas (up to 43,000 ton/yr) likely exceeds the emissions from vehicles and industrial activities (Etiope et al., 2007). Other VOCs recognized in volcanic and hydrothermal discharges are classified as Hazardous Air Pollutants (HAPs), i.e. substances that pose risk to human health even when they occur at low concentrations, due to their carcinogenic, mutagenic and teratogenic effects. They include halogenated organic compounds (e.g. vinyl chloride and chlorobenzenes), aldehydes, PAHs (Polycyclic Aromatic Hydrocarbons) and aromatics, among which benzene, particularly abundant in hydrothermal fluids, is commonly present at alarming levels in air in proximity of gas discharges (e.g. Tassi et al., 2013a,b). Notwithstanding the potentially severe impact of VOCs on air quality and human health, the composition of the organic fraction in gas emissions from volcanic and hydrothermal areas and their contributions to the global budgets of carbon are still poorly characterized, the available studies being limited to a relatively

small number of natural systems and the analysis of few organic species (e.g. Etiope et al., 2007; Etiope and Cicciole, 2009), whereas studies on diffused VOCs emissions from volcanic and hydrothermal systems are virtually lacking (Schwandner et al., 2004).

The comprehension of both (i) the primary processes on VOCs occurring at high temperatures in deep reservoirs and (ii) the secondary processes occurring during the uprising of hydrothermal fluids toward the surface, are crucial for a reliable estimation of VOCs emissions from volcanic and hydrothermal environments.

The origin of VOCs in volcanic and hydrothermal systems is mainly ascribed to the thermal decomposition of the organic material buried in sedimentary rocks and interacting with magma or hot fluids (thermogenic processes; e.g. Matsuo, 1961; Stoiber et al., 1971; Gunter, 1978; Des Marais et al., 1981; Giggenbach et al., 1986; Martini et al., 1986; Capaccioni et al., 1993, 1995; Darling, 1998; Mango et al., 2009), although abiotic synthesis was also hypothesized (e.g. Ingmanson and Dowler, 1977; Shock, 1990b, 1992; Shock and Schulte, 1998; Amend and Shock, 1998; McCollom and Seewald, 2007; McCollom, 2013). Whatever the starting material, clear analogies in relative abundances of the main classes of organic compounds have been recognized in gases collected from systems characterized by similar physicochemical conditions (i.e. temperature, pressure, redox; Capaccioni et al., 1993, 1995). Accordingly, the distribution of VOCs likely represents a useful parameter to evaluate the prevailing thermodynamic conditions at the fluid source(s) and their time-space variability, giving a promising contribution to the geochemical monitoring of active volcanic areas (Capaccioni et al., 1993; Capaccioni and Mangani, 2001; Taran and Giggenbach, 2003; Capaccioni et al., 2004; Tassi et al., 2005a,b; Agosto et al., 2013). The attainment of metastable equilibrium among organic compounds under hydrothermal conditions has been demonstrated both theoretically (Shock, 1990a,b) and experimentally (Seewald, 1994). Field studies on fumarolic gases (e.g. Taran and Giggenbach, 2004) have confirmed that alkane/alkene pairs approach equilibrium in natural environments and that their relative concentrations in volcanic gases are controlled by reversible and fast reactions. Hence, light alkane/alkene pairs

1. Introduction

(C₂ up to linear C₄) can successfully be used as organic geothermometers, as long as the appropriate mineral redox buffer is provided (e.g. Capaccioni and Mangani, 2001; Taran and Giggenbach, 2003; Capaccioni et al., 2004; Tassi et al., 2005a). Conversely, a detailed understanding of the influence of physicochemical conditions on the behaviour of VOCs could allow to predict the composition and fate of organics in natural environments.

Developing predictive models of organic reaction pathways at medium-to-high temperatures and pressures are particularly relevant as they are expected to better comprehend the behaviour of these substances in natural hydrothermal systems. Hypotheses on the reaction pathways for the production of VOCs in deep hydrothermal systems were carried out by comparing the composition of fumarolic gases with those recovered by (*i*) industrial refining processes (e.g. Capaccioni et al., 1993, 1995) and (*ii*) experimental studies (e.g. McCollom et al., 2001; Seewald, 2001, 2003; Yang et al., 2012; Shipp et al., 2013). Evidences from experimental studies suggest that reaction pathways among organic compounds consist of stepwise reversible and irreversible processes, including oxidation/reduction and hydration/dehydration reactions, which result in functional group interconversions (e.g. Seewald, 2001; Shipp et al., 2013). Water and minerals play a key role in chemical reactions involving VOCs since they act as both catalysts and reactants (e.g. Katritzky et al., 1996; Siskin and Katritzky, 2000; Seewald, 2001; Shipp et al., 2013, 2014). These findings are very promising not only for geochemical studies, but also in the framework of industrial applications and green chemistry (Shipp et al., 2014) and they open fascinating and appealing perspectives in studies on the origin of life on the Early Earth and astrobiology (e.g. Wächtershäuser, 1988; Russel and Martin, 2004; Sherwood Lollar, 2004; Williams et al., 2005). However, whilst laboratory experiments are invaluable tools to shed light on the *possible* organic reaction pathways occurring under specific physicochemical conditions and in the presence of different catalysts, it should be borne in mind that they represent simplified systems that cannot reflect the complexity of natural environments.

Hence, in order to (*i*) verify the representativeness of experimental results on natural settings and (*ii*) understand the *actual* processes governing the

organic composition of fluids in volcanic and hydrothermal systems, a comparison between experimental runs and natural samples, in particular fumarolic gases, is essential. Fumaroles are generally located along faults and fractures. These brittle structures, representing highly permeable zones, enhance a relatively fast uprising of hot fluids with respect to the time spent by fluids within the deep hydrothermal reservoir. Therefore, the chemical composition of fumarolic fluids is likely reflecting the (i) potential attainment of chemical equilibrium in the deep reservoirs (at least for saline geothermal fluids; Stefánsson and Arnórsson, 2002) and (ii) secondary processes occurring during the upflow of hydrothermal fluids towards the surface (e.g. Chiodini and Marini, 1998). The latter have a limited effect on the pristine fluid composition when the uprising of the deep-originated fluids is relatively fast. Hence, gases from high-flux fumarolic discharges may be considered the best proxy of the deep reservoirs. However, VOCs are released from volcanic and hydrothermal systems not only through punctual degassing vents (fumaroles), but also diffusively emitted through the Earth surface. Soil diffuse degassing significantly contributes to the atmospheric emissions of volatiles from volcanic and hydrothermal systems (e.g. Cardellini et al., 2001, 2003; Chiodini et al., 2004a; Granieri et al., 2010; Viveiros et al., 2010; Tassi et al., 2013b). Nevertheless, whilst the number of studies devoted to the characterization of the organic fraction of fumarolic gases and the comprehension of the organic reactions occurring under hydrothermal conditions have been increasing in the last twenty years, the composition of organic species in gases diffusively released from volcanic and hydrothermal areas is still almost unexplored. As already mentioned, the composition of the organic fraction in fumarolic fluids is expected to approach that of the deep hydrothermal fluids. On the contrary, the chemical features of VOCs in interstitial soil gases from diffuse degassing areas are likely controlled by secondary processes as fluids are uprising towards the surface. Gas fluxes from soil, depending on the pressure gradient (advective flux), and on the structure, porosity and permeability of the media encountered during the ascent towards the surface (e.g. Cardellini et al., 2003; Chiodini et al., 2010b), is orders of magnitude lower than those characterizing fumarolic discharges (e.g. Aiuppa et al., 2013).

1. Introduction

Thus, it is reasonable to suppose that the composition of the gases released as diffuse emissions significantly depends on chemical and physical processes (e.g. oxidation reactions, water vapour condensation, interactions with shallow aquifers), favoured by the strong changes in physicochemical conditions, which are particularly effective when fluids slowly approach the surface, i.e. within the soil (Tassi et al., 2013b). Similarly, secondary processes driven by microorganisms (Bacteria and Archaea), inhabiting hydrothermalized terrains at shallow depths, may affect the organic fraction of interstitial soil gases (e.g. Huber et al., 2000; Norris et al., 2002; Glamoclija et al., 2004; Henson et al., 2005; D’Alessandro et al., 2011; Gagliano et al., 2014). Actually, microbes reveal an incredible capability of adaptation to the harsh conditions characterizing hydrothermally altered soils (e.g. Stetter, 1999), where relatively high temperatures and concentrations of toxic gases (e.g. CO₂, H₂S, NH₃) and metals (e.g. Hg, As) and low pH prevail. Moreover, the abrupt lateral and vertical variations of the physicochemical conditions (occurring even in the order of few decimeters) that generally characterize the solfataric fields make hydrothermal systems (*i*) perfect natural laboratories to study the interplay between microbial communities and VOCs-bearing fluids uprising from deep reservoirs (e.g. Gagliano et al., 2015), and also (*ii*) suitable analogues for Early Earth or extraterrestrial environments to understand how life and phylogenetic diversity develop under extreme conditions (e.g. Glamoclija et al., 2004; Barbieri and Cavalazzi, 2014). Beyond the pure scientific interest, understanding how biochemical processes impact deep-sourced toxic or greenhouse organic gases can lead to relevant practical applications such as the development of bioremediation techniques (e.g. Wolicka et al., 2009; Gadd, 2010 and references therein; Chikere et al., 2011). The current PhD project was aimed to improve the scientific knowledge of the composition and behaviour of organic gas species released from volcanic and hydrothermal systems, covering most of the issues previously described. In the framework of the 3-year research project, several sampling campaigns were carried out from different sites in the Mediterranean area. The selection of the study areas was dictated by the need to compare the distribution of VOCs in different environments to understand how the speciation of or-

ganic compounds was affected by physicochemical conditions and geological settings. In particular, the selected areas included (*i*) hydrothermal systems associated with active volcanoes, i.e. Solfatara Crater (Campi Flegrei, Southern Italy) and Nisyros Island (Greece), and (*ii*) low-to-medium enthalpy hydrothermal systems feeding cold gas emissions (Poggio dell'Olivo and Cava dei Selci, Central Italy). Sampling strategies and analytical techniques were adopted in order to determine the composition of VOCs in both fumarolic discharges and interstitial soil gases at selected depths from each study area. The first goal was to investigate the primary processes controlling the distribution and behaviour of VOCs within hydrothermal reservoirs and their dependence on physicochemical conditions at depth. This objective was achieved (*i*) experimentally, by investigating specific organic reaction pathways, hypothesized on the basis of field data, through laboratory experiments carried out at conditions simulating those found in hydrothermal/volcanic systems (the experimental runs were performed in water and in the presence of different minerals to study their influence on organics reactivity), and (*ii*) empirically, by comparing the composition of organic fraction in fumarolic gases emitted from the different study areas.

The second goal was to study the secondary processes affecting the composition of VOCs in hydrothermal fluids during their uprising from the deep reservoirs to the surface. Consequently, the composition of fumarolic gases was compared with that of interstitial soil gases sampled within the same study area from sites affected by different deep fluids inputs. Soil gas samples were collected at regular interval depths along vertical profiles to provide further insights into the chemical modifications affecting VOCs at very shallow depths, where biochemical processes are expected to play a major role in controlling the fate of the deep-sourced organic compounds immediately prior to their release into the atmosphere.

This thesis includes data already presented at national and international scientific conferences (AGU 2014 and 2015 in USA), Congresso SIMP-SGI-So.Ge.I.-AIV 2015 in Italy, EGU 2016 in Austria; Appendix B) and published in (or submitted to) peer-reviewed international scientific journals (Applied Geochemistry, Organic Geochemistry, Journal of Volcanology and Geother-

1. Introduction

mal Research; Appendix A).

Chapter 2

Origin and fate of VOCs in volcanic and hydrothermal systems: from deep reservoirs to shallow environments

2.1 Introduction

In this chapter, a compendium of the current state of knowledge about (*i*) primary processes on VOCs under hydrothermal conditions and (*ii*) VOCs degradation processes in the soil is presented in order to provide a suitable background to the main topics of this PhD thesis.

First, an overview on the main hypotheses about the origin of organic compounds in volcanic and hydrothermal systems is described, with a special focus on thermogenic processes. Then, a summary of the possible organic functional group interconversions occurring under hydrothermal conditions is provided on the basis of experimental studies. These processes will be further investigated in Chapter 3 taking into account the experimental runs performed in this work.

These sections, shedding light on processes occurring at depth, are preparatory to the discussion on the composition of fumarolic gases sampled from

2. Origin and fate of VOCs in volcanic and hydrothermal systems

the selected study areas (Chapter 7).

Finally, the potential role played by biogenic processes at shallow depth on the fate of VOCs rising toward the surface is discussed through the description of the main microbial metabolic pathways involving organic compounds. The occurrence of biodegradation processes in hydrothermal systems affected by intense soil diffuse degassing is discussed in Chapter 8 by comparing the composition of interstitial soil gases with that of the fumarolic fluids for each study area.

2.2 Biotic vs. abiotic genesis

The controversy about the origin of organic compounds in volcanic and hydrothermal gases started immediately after they were detected in these environments, i.e. in the 1970s, arousing the interest of many researchers with the contraposition of two main different viewpoints.

The first one suggested that the organic compounds observed in volcanic and hydrothermal gases were deriving from the thermal decomposition of the organic material contained in sedimentary rocks and released upon heating by contact with magma or uprising hot gases (e.g. Matsuo, 1961; Stoiber et al., 1971; Giggenbach et al., 1986; Martini et al., 1986; Matsuo, 1988). It was estimated that more than 15,000,000 Gt of organic matter are sequestered beneath the Earth's surface (McSween et al., 2003 and references therein). When this organic matter is exposed to high temperatures and pressures, it undergoes physicochemical transformations that generally lead to the production of simpler organic compounds with respect to those characterizing the starting material. Detailed studies of these processes were developed in the framework of the petroleum geochemistry research (e.g. Girelli, 1969; Hunt, 1979; Pieri, 1988; North, 1995), which is beyond the aims of this work. Schematically, at increasing burial depth and temperature, the progressive evolution of the organic matter to petroleum hydrocarbons was distinguished into three steps, as follows: (i) diagenesis, occurring at temperatures < 50 °C, where microbial activity transforms previous biogenic biopolymers (e.g.

2.2 Biotic vs. abiotic genesis

proteins, carbohydrates) into kerogen and by-products, such as methane, (ii) catagenesis, occurring at temperatures ranging from 50 to 200 °C and consisting in the thermal degradation of kerogen to form liquid petroleum and then wet gas and condensate, where methane and hydrocarbons (oil and gas) are generated, and (iii) metagenesis, at temperatures >200 °C, producing methane and hydrocarbons (Hunt, 1984; Tissot and Welte, 1984). The transformations involved in these processes mainly consist of (i) degradation of complex organic molecules into simpler ones, and (ii) polymerization of organic molecules into heavier hydrocarbons. Polymerization occurs at high temperatures and in the presence of suitable catalytic agents, two requirements that are encountered in volcanic and hydrothermal systems.

According to the other viewpoint, volcanic and hydrothermal conditions are favourable environments to abiotic organic synthesis (e.g. Ingmanson and Dowler, 1977). The abiotic synthesis of organic compounds in hydrothermal systems is of particular relevance to the origin of life. Several current theories have proposed that the origin of life on Earth occurred in submarine hydrothermal systems, where abiotic synthesis would have supplied the prebiotic organic compounds from which life emerged (Sherwood Lollar, 2004; McCollom and Seewald, 2007 and references therein; Martin et al., 2008). The discovery of organic compounds in ultramafic-hosted hydrothermal fields along the Mid-Ocean Ridges (Konn et al., 2015 and references therein), meteorites (e.g. Botta and Bada, 2002; Pizzarello and Shock, 2010; Schmitt-Kopplin et al., 2010), comets (e.g. Goesmann et al., 2015; Wright et al., 2015) and Mars (e.g. Hand, 2015) demonstrated that abiotic synthesis is a possible pathway for the genesis of organic compounds. Hydrocarbons and organic compounds in natural environments can be produced abiotically through the reduction of inorganic carbon species (CO_2 , CO , HCO_3^-) by H_2 or other reducing reactants (e.g. H_2S , NH_3) (e.g. McCollom and Seewald, 2007). Thus, the abiotic synthesis of methane and other organic gas compounds in hydrothermal systems would be favoured by high CO_2 concentrations and reducing conditions (Shock, 1990b; McCollom and Seewald, 2007; McCollom, 2013). The production of hydrocarbons could be further increased as the H_2 - and CO_2 -rich hydrothermal fluids cool down during their ascent toward the

2. Origin and fate of VOCs in volcanic and hydrothermal systems

surface (Shock, 1990b; McCollom and Seewald, 2007; McCollom, 2013). Shock (1990b, 1992), Shock and Schulte (1998) and Amend and Shock (1998) clarified the thermodynamic basis for organic synthesis in hydrothermal systems. In the C-H-O chemical system, the stable equilibrium is dominated by CO_2 , CO, CH_4 , H_2O , H_2 , O_2 , graphite and/or diamond depending on temperature, pressure and bulk composition (Shock, 1990b and references therein). However, according to Shock (1990b), the achievement of stable thermodynamic equilibrium is prevented by kinetic constraints, and abiotic synthesis of organic compounds thus occurs in metastable states¹ (Figure 2.1). The

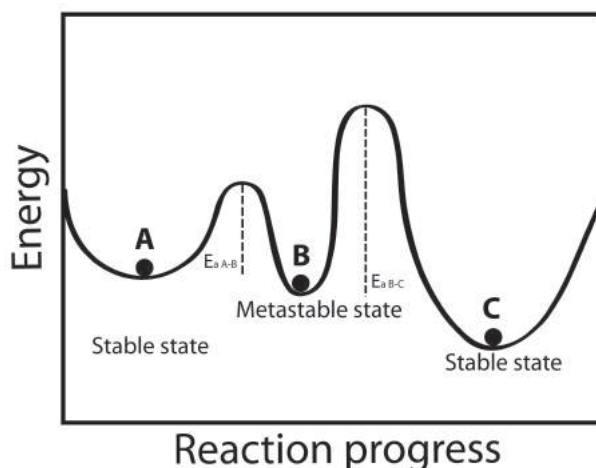


Figure 2.1: Plot of energy vs. reaction progress for a hypothetical system in which a metastable state (B) exists between two stable states (A and C). E_{aA-B} and E_{aB-C} indicate activation energies between states A and B and B and C, respectively.

presence of these barriers (i.e. the large temporal length involved in the conversion of organic compounds to the thermodynamically stable assemblages

¹Metastable thermodynamic equilibrium is a chemical state in which kinetic barriers prevent the system from attaining stable thermodynamic equilibrium (i.e. its lowest equilibrium energy state). At the same time, individual metastable species may reach a state of partial equilibrium in the presence of suitable reaction paths (Seewald, 1994, 2003; Anderson, 2005). Actually, the only thermodynamic difference between organic reactions (including those in living organisms) and inorganic reactions is that both reactants and products of organic reactions are invariably metastable compounds; metastable, that is, with respect to simple inorganic compounds and elements (Anderson, 2005).

2.2 Biotic vs. abiotic genesis

of compounds in the C-H-O system) allows the organic compounds to dominate the C-H-O systems in such states (Shock, 1990b).

Although reduction of inorganic carbon to methane and other hydrocarbons may be thermodynamically favoured at temperatures ≤ 350 °C (depending on redox conditions; McCollom and Seewald, 2007), kinetic inhibitions can still prevent the occurrence of spontaneous abiotic synthesis of organic compounds (McCollom and Seewald, 2007; McCollom, 2013). Hence, the reduction of CO₂ and CO to abiotic organic compounds requires the presence of suitable catalysts (McCollom and Seewald, 2007).

It is nowadays broadly accepted that organic compounds in geologic environments can be subdivided into three typologies, according to their source (e.g. McCollom and Seewald, 2007; Konn et al., 2011, 2015; Tassi et al., 2009):

- Abiotic compounds, formed from inorganic species through purely chemical reactions that have not been biologically catalyzed;
- Thermogenic compounds, derived from both thermal degradation of organic material buried in the soil, contained in sedimentary rocks or undergone diagenetic processes (e.g. kerogen or coal) and rearrangement of compounds under high temperature and pressure conditions;
- Biogenic compounds, formed by metabolic and biosynthetic activities of biological organisms.

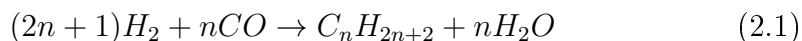
The attribution of organic compounds observed in natural systems to one of these classes rather than the others may be very challenging, as most of organic species can be originated by more than one process. For instance, methane and acetate can be formed as by-products of microbial metabolism, during thermal decomposition of organic matter, or by abiotic processes such as Fischer-Tropsch synthesis (McCollom and Seewald, 2007).

Organic compounds in volcanic and hydrothermal systems are likely the result of co-occurring abiotic, thermogenic and biogenic processes. Whilst biogenic processes may occur at shallow depths where temperatures decrease below 100-150 °C, both abiotic and thermogenic processes can develop in deep hydrothermal reservoirs.

2. Origin and fate of VOCs in volcanic and hydrothermal systems

2.3 Abiotic synthesis

The most widely invoked pathway for the abiotic synthesis of hydrocarbons in natural environments is the Fischer Tropsch-type (FTT) reaction (Fischer and Tropsch, 1923, 1926), an industrial process largely used during the World War II to generate fuels (McCollom and Seewald, 2007; Konn et al., 2015). As originally described, FTT reaction refers to the formation of organic compounds from a gaseous mixture of CO and H₂ in a high temperature and pressure surface-catalyzed process involving sequential reduction and polymerization of single-carbon units (McCollom and Seewald, 2007; McCollom, 2013; Konn et al., 2015), according to the following reaction (2.1):



However, the term is broadly used in the geological literature, being referred to the reduction of any inorganic carbon species to form organic compounds or just methane (the catalyzed reduction of CO₂ to methane is commonly related to the Sabatier process; McCollom and Seewald, 2007). In particular, for volcanic and hydrothermal gas environments, FTT reaction usually refers to the reduction of CO₂ and CO, the most abundant C-inorganic gas species, to organic compounds. FTT processes are considered likely candidates for the generation of abiogenic hydrocarbons in ultramafic-hosted hydrothermal systems (Shock and Schulte, 1998; Konn et al., 2009, 2015 and references therein).

During the FTT reaction (Figure 2.2), CO (or CO₂) is reduced to organic compounds through a series of steps occurring on the surface of a catalyst (McCollom and Seewald, 2007; McCollom, 2013). Typically, the primary products of the reaction are methane and normal-alkanes (with abundances that regularly decrease as the C-number increases; McCollom and Seewald, 2007). However, such a process also generates other compounds, though at a lower extent, including alkenes, branched hydrocarbons, and O-bearing species (McCollom and Seewald, 2007; McCollom, 2013). The relative abundance of normal-alkanes generated from FTT synthesis follows a log-linear

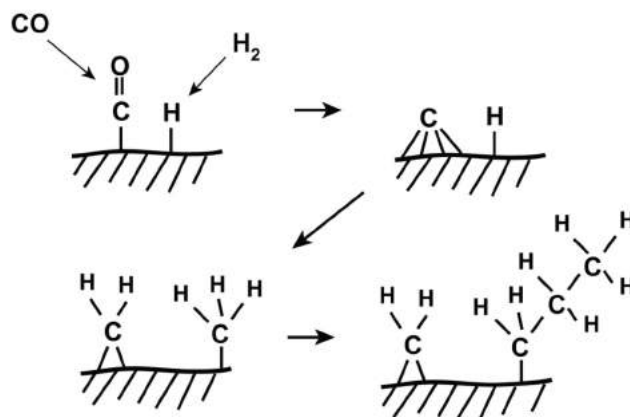


Figure 2.2: Reaction mechanism for Fischer-Tropsch synthesis of hydrocarbons (after McCollom, 2013). The CO molecule binds to the catalyst surface to form a carbonyl unit ($-\text{CO}$), which subsequently undergoes sequential reduction to surface-bound carbide ($-\text{C}$), methylene ($-\text{CH}_2$), and methyl ($-\text{CH}_3$) groups. Methylene groups can polymerize to one another resulting in the formation of C-C bonds and production of alkyl chains. Chain growth terminates when the alkyl chain combines with a methyl group or surface-bound H rather than an additional methylene, releasing the compound from the surface (McCollom and Seewald, 2007; McCollom, 2013).

decrease in abundance with increasing number of carbon atoms in the alkyl chain, which is commonly known as the Schulz-Flory or Anderson-Schulz-Flory (ASF) distribution. However, it is to mention that aliphatic hydrocarbons are also producing log-linear distributions during thermogenic processes. Therefore, this is not an unequivocal evidence for an abiotic origin of hydrocarbon gases (McCollom and Seewald, 2007).

Although abiotic synthesis of organic compounds in volcanic and hydrothermal systems is thermodynamically possible, it is generally considered negligible with respect to thermogenic processes under volcanic-hydrothermal conditions (Des Marais et al., 1981; Darling, 1998; Mango et al., 2009).

2. Origin and fate of VOCs in volcanic and hydrothermal systems

2.4 Thermogenic processes

Thermogenic processes are a series of reactions involving pre-existing organic compounds and occurring at temperatures $>120-150$ °C. In particular, they refer to both (*i*) thermal degradation of large organic molecules (e.g. proteins, lipids, DNA) to smaller and simpler ones and (*ii*) rearrangement of compounds under high temperature and pressure conditions (Konn et al., 2015). In analogy with processes used in petroleum refining industry, Capaccioni et al. (1993, 1995) referred to these processes as (*i*) thermal cracking and (*ii*) catalytic reforming (including polymerization processes).

2.4.1 Thermal cracking

Thermal decomposition of organic matter (or thermal cracking, also referred to as pyrolysis) is considered the most important source of hydrocarbons in volcanic and hydrothermal systems (Taran and Giggenbach, 2003 and references therein), where the presence of VOCs in gas discharges is likely the result of interactions between uprising hot magmatic gases and hydrothermal fluids circulating within organic-rich sedimentary rocks (Tassi et al., 2013a and references therein). The analysis of twenty-two samples from Yellowstone National Park by Gunter (1978) evidenced that the distribution of C_1-C_4 hydrocarbons in hydrothermal gases was more consistent with an organic origin (e.g. thermal degradation of kerogen) than that related to an abiotic production of methane ($CO_2 + 4H_2 \rightarrow CH_4 + 2H_2O$) followed by pyrolysis. Des Marais et al. (1981) confirmed the thermal decomposition of organic matter as the most important source of organic compounds in geothermal gases on the basis of isotopic measurements carried out on individual hydrocarbons. Thermal cracking defines a series of reactions involving the breaking of bonds in organic molecules, i.e. C-C, C-H or C-R bonds (where R refers to any heteroatom, such as O, S, N or halogens, or group of atoms), resulting in the fragmentation of molecules into smaller structures (Capaccioni et al., 1993, 1995; Guéret et al., 1997). The molecule fractionation preferentially occurs by breaking of C-C bonds as the result of the larger dissociation energy of the C-H bonds (Guéret et al., 1997). For instance, the cracking of

2.4 Thermogenic processes

normal-alkanes, during which the C-C or C-H bonds are broken, leads to the formation of an alkane and/or an alkene (Guéret et al., 1997). Consequently, ethane may decompose to ethene, propane to propene or ethene, butanes to methane, ethane, ethene, propene and 1-butene (Gunter, 1978). Methane, which cannot be fractionated into lighter hydrocarbons, undergoes thermal coupling to form heavier molecules (Holmen et al., 1995). Accordingly, the thermal decomposition of methane at high temperature may produce ethene, ethyne, benzene and H₂, the yields of these products depending on the temperature (Figure 2.3; Holmen et al., 1995).

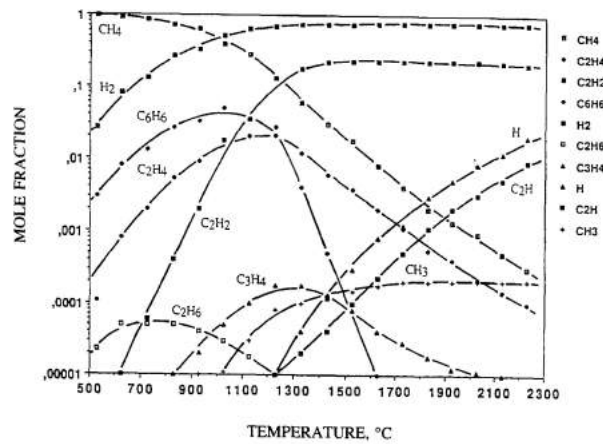


Figure 2.3: Mole fractions of 10 species in gas-phase equilibrium calculated from the thermodynamic data for the thermal decomposition of methane (after Holmen et al., 1995).

The dissociation reaction is highly endothermic and hence, it requires high temperatures. The standard free energy of formation (Figure 2.4) provides an indication of the stability of each hydrocarbon molecule. At a given temperature, the most stable compound has the lowest ΔG_f^0 . The stability of hydrocarbons generally decreases with increasing temperatures, with the exception of ethyne (Figure 2.4). Methane is the most stable hydrocarbon up to 1,300 K (1,027 °C), where benzene becomes more stable than methane (Guéret et al., 1997). In fact, the stability of aromatics increases faster as a function of temperature (the slopes of lines $\Delta G_f^0=f(T)$ are lower than those for alkanes and cycloalkanes; Figure 2.4). However, hydrocarbons in Fig-

2. Origin and fate of VOCs in volcanic and hydrothermal systems

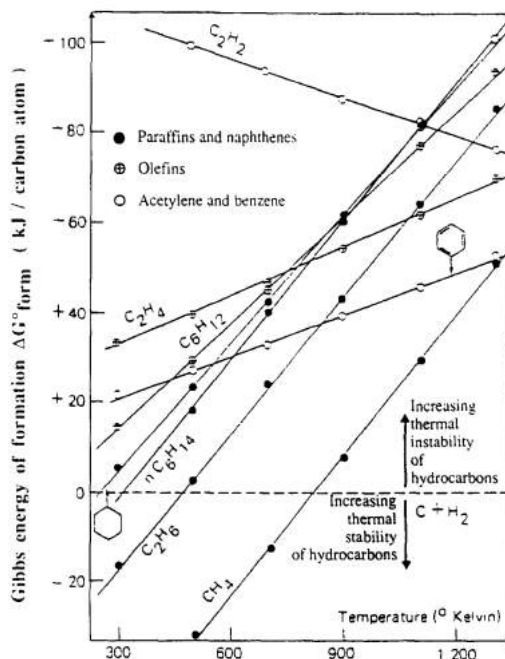


Figure 2.4: Thermodynamic stability of hydrocarbons (after Guéret et al., 1997). The standard Gibbs energy of formation is related to a carbon atom to facilitate comparison.

Figure 2.4 are unstable for all T relative to C and H_2 , except for methane and ethane at T lower than 800 K (527 °C) and 400 K (127 °C), respectively (Guéret et al., 1997). To prevent the decomposition of hydrocarbons into C and H the reaction has to be stopped (quenched) at a certain time (or reaction progress), i.e. before C is formed (Holmen et al., 1995; Guéret et al., 1997). The rates of cracking reactions are considered negligible at temperatures below 350 °C (Capaccioni et al., 1995). At temperatures from 150 to 350 °C, catalytic reforming processes prevail (Capaccioni et al., 1995).

2.4.2 Catalytic reforming

In reforming processes, catalytic agents, rather than temperature and pressure, play the most important role (Capaccioni et al., 1993).

A catalyst is a substance that increases the rate of a chemical reaction by providing an alternative pathway for breaking and making of bonds without undergoing a permanent chemical change itself in the process (Killops and Killops, 2005; Brown et al., 2012). The catalyst partially bonds to the reactants, weakening one or more of the bonds that are to be broken (Killops and Killops, 2005). In other words, a catalyst lowers the overall activation energy for a specific chemical reaction (Figure 2.5), without being involved as a reactant, and allows the reaction to proceed faster. The

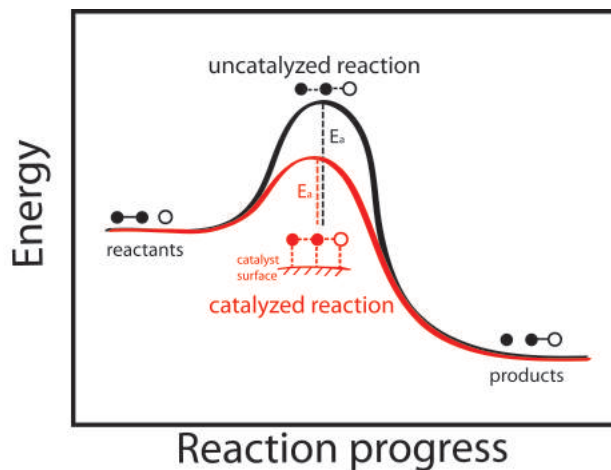


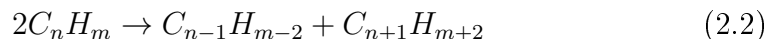
Figure 2.5: Effect of a catalyst on the activation energy of a reaction.

catalyst may be present in the same phase of the reacting molecules (homogeneous catalyst) or in a different phase (heterogeneous catalyst), usually as a solid in contact with either gaseous or liquid reactants. The distinction between hetero- and homo-catalytic processes is important. While homogeneous catalyzed reactions are subject to the probability (clearly small under dilute conditions) of favourable reactant collision in solution, heterogeneous catalysts scavenge dilute solutions for reactants through surface adsorption, significantly enhancing the reaction rate (Cody et al., 2004). Heterogeneous catalysis usually starts with adsorption of reactants, i.e. reactant molecules

2. Origin and fate of VOCs in volcanic and hydrothermal systems

bind to the catalyst surface. Adsorption occurs because atoms and ions at the surface of a solid are extremely reactive as they have unused bonding capability that can be used to bond molecules from the gas or liquid phase to the surface of the solid (Brown et al., 2012).

Catalytic agents may enhance a series of structural transformations of organic molecules, including e.g. polymerization (addition to make larger molecules) and many organic functional interconversions (e.g. by condensation, cleavage, cyclization, hydrolysis, oxidation and hydrogenation reactions; Shock et al., 2013 and references therein). An example of catalytic reforming reaction is metathesis, consisting in interconversions among homologues (2.2), as follows:



For instance, propene may undergo metathesis reaction to form ethene and butene (2.3), by breaking and making C=C double bonds and redistributing carbons to new compounds, as follows:



Other examples include (i) the metathesis of methane, ethane and propane (Mango et al., 2009), as follows (2.4):



, or (ii) the dehydrogenation of alkanes to the corresponding alkenes (Capaccioni et al., 1995), as follows (2.5):



The prevailing of catalytic processes as source of organic compounds in gases originated at temperature lower than 350 °C is confirmed by the achievement of thermodynamic equilibrium among light hydrocarbons in natural gases, as argued by Mango et al. (2009). Equilibrium requires the easy exchange of carbon atoms between organic compounds, i.e. C-C and C-H σ bonds are

2.4 Thermogenic processes

broken and reformed with overall bond conservation. This is unlikely in thermal reactions, which are generally under kinetic control and whose products are then far from thermodynamic equilibrium; contrarily, catalytic reactions are often under thermodynamic control and the products may approach a complete equilibrium (i.e. metastable equilibrium; Mango et al., 2009 and references therein).

The possibility for organic compounds to approach equilibrium under hydrothermal conditions is a crucial point. If the relative abundances of some compounds were controlled by thermodynamic equilibria (and hence by physical and chemical variables such as temperature, redox, pressure), measurements of the concentrations of these compounds would be potentially powerful tools for evaluating chemical conditions in subsurface environments (McCollom et al., 2001).

The attainment of metastable equilibrium among organic compounds under hydrothermal conditions was demonstrated both theoretically (Shock, 1990b) and experimentally (Seewald, 1994). The patterns in the relative abundances of organic compounds in volcanic and hydrothermal gases originated at similar temperature and redox conditions (e.g. Capaccioni et al., 1993, 1995) support these findings, enhancing the possibilities for studying the distribution of organic compounds in hydrothermal fluids as functions of T, P and redox conditions, using a thermodynamic approach (e.g. Plyasunov and Shock, 2000). For instance, studies on fumarolic gases (Taran and Giggenbach, 2004) have shown that alkane/alkene pairs can approach equilibrium in natural environments and that their relative concentrations in volcanic gases are controlled by reversible reactions, enhancing the use of ethane/ethene and propane/propene pairs as geothermometers (e.g. Capaccioni and Mangani, 2001; Taran and Giggenbach, 2003; Capaccioni et al., 2004; Tassi et al., 2005a,b; Agosto et al., 2013). Hence, the achievement of metastable equilibrium among organic compounds is possible because of the presence of specific catalysts.

Organic reactions are known to be catalyzed by a variety of transition metals. Nickel, palladium, copper, rhodium, etc. are commonly used for organic synthesis in technological applications in chemical and refining industry. How-

2. Origin and fate of VOCs in volcanic and hydrothermal systems

ever, these catalysts are rarely observed in natural environments. Instead, catalytic activity on organic reactions is known to be exerted by both hot water and minerals in hydrothermal systems.

Organic hydrocarbons in waters are expected to be rather unreactive. However, the physicochemical properties of water change as temperature increases. In particular, the solvent properties of liquid water (density, dielectric constant) at high temperature become similar to those of polar organic solvents at room temperature, thus enhancing (more than expected for the effect of temperature) the solubility of organic compounds and their reactions in an environmentally friendly medium (Katritzky et al., 1996; Siskin and Katritzky, 2000). Laboratory experiments have demonstrated that water participates to organic reactions not only as a solvent, but also as reactant and catalyst (Katritzky et al., 1996; Siskin and Katritzky, 2000; Seewald, 2001; Shipp et al., 2013). In fact, the increase in the dissociation constant allows water at high temperature to act as an acid, base or acid-base bi-catalyst (Katritzky et al., 1996; Siskin and Katritzky, 2000).

Minerals were demonstrated to catalyze organic reactions as well (e.g. Soma and Soma, 1989; Dale Ortego et al., 1991; Seewald, 2001, 2003; Ferris, 2005; Fu et al., 2008; Kaur and Kishore, 2012; Shipp et al., 2014; He et al., 2015). Al-silicates, such as zeolites and clays (in particular smectites), which are generally present in hydrothermally altered volcanic terrains, are known to act as catalysts for organic reactions (Soma and Soma, 1989; Capaccioni et al., 1995; Ferris, 2005; Williams et al., 2005; Kaur and Kishore, 2012). Owing to its sorbent and catalytic properties, montmorillonite has extensively been used in organic chemical applications for technological and environmental purposes (e.g. selective removal of organic pollutants; Dale Ortego et al., 1991 and references therein). Moreover, transition metal sulphides (e.g. pyrite, pyrrhotite) were proposed as possible catalysts for prebiotic organic synthesis in the Early Earth² (Wächtershäuser, 1988). The reducing capability of the FeS/FeS₂-system was experimentally demonstrated by Kaschke

²According to Wächtershäuser's surface metabolism theory, the formation of organic molecules on the primitive Earth occurred from the reaction of iron sulphide (FeS) with hydrogen sulphide and CO₂ to form pyrite (FeS₂). The energy released by this redox reaction could have been utilized for an autotrophic origin of life.

2.5 Organic functional group interconversions under hydrothermal conditions

et al. (1994). Recent experiments by Shipp et al. (2014) demonstrated that sphalerite significantly favours the breaking and making of C-H bonds. Similarly, magnetite was found to catalyze oxidation/reduction reactions (He et al., 2015). Moreover, since many organic reactions involve changes in the oxidation state of carbon, the relative stability of organic compounds may be strongly dependent on the redox state of the system which in turn is buffered by mineral assemblages (e.g. Seewald, 2001).

2.5 Organic functional group interconversions under hydrothermal conditions

An increasing interest in geochemistry is devoted to the study of reaction pathways of organic compounds under hydrothermal conditions. The development of predictive models for thermodynamic properties of organic compounds (e.g. Shock and Helgeson, 1990; Helgeson et al., 1998; Plyasunov and Shock, 2000, 2003) and organic reaction pathways at elevated temperatures and pressures in aqueous solutions is particularly relevant for the improvement of knowledge around the organic chemistry in natural hydrothermal systems. Several authors performed experimental studies under hydrothermal conditions in order to understand the chemical transformations of organic compounds in fluids at high temperatures and pressures (e.g. Seewald, 1994; McCollom et al., 2001; Seewald, 2001; McCollom and Seewald, 2003; Seewald, 2003; Watanabe et al., 2004; Yang et al., 2012; McCollom, 2013; Shipp et al., 2013). Evidences from these studies suggest that the reaction pathways among organic compounds consist of stepwise reversible and irreversible processes (e.g. oxidation/reduction, hydration/dehydration, carboxylation/decarboxylation) resulting in functional group interconversions (e.g. Seewald, 2001; Shipp et al., 2013).

Seewald (2001, 2003) proposed a general reaction scheme (Figure 2.6) connecting alkane to carboxylic acids through a series of reversible and irreversible functional group interconversions: alkanes interconvert with alkenes, followed by hydration of alkenes to alcohols, dehydrogenation to ketones, and

2. Origin and fate of VOCs in volcanic and hydrothermal systems

conversion to carboxylic acids, which can undergo decarboxylation and/or oxidation reactions to produce CO_2 and shorter-chain saturated hydrocarbons.

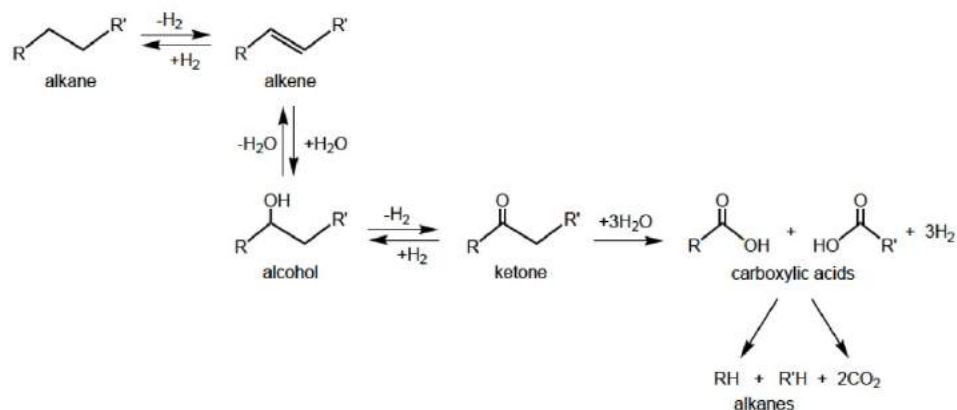


Figure 2.6: Reaction scheme of functional group interconversions, as proposed by Seewald (2001, 2003), involving reversible hydration/dehydration, hydrogenation/dehydrogenation and C-C bond cleavage reactions (after Shock et al., 2013).

This model was based on hydrothermal experiments focusing on specific functional group reactions. The stepwise reactions in Figure 2.6 mainly consist of hydrogenation/dehydrogenation and hydration/dehydration reactions, in which the reactants and products were experimentally shown to approach metastable equilibrium states (Seewald, 1994, 2001; McCollom and Seewald, 2003). Shipp et al. (2013) found that the reaction path connecting alkanes to ketones is completely reversible under hydrothermal conditions (300 °C, 100 MPa) and that the various functional group interconversions exhibit quite different rates. In particular, the reactivity was found to decrease in the following order: diene > alcohol > alkene > ketone > alkane.

Hydrogenation/dehydrogenation reactions are common among organic compounds during geochemical processes (Shock et al., 2013 and references therein). In hydrogenation reactions, a carbon atom in an organic compound gains a bond to hydrogen and loses a bond to a heteroatom (or to another carbon atom), resulting in higher electron density on the carbon atom (hydrogen is the least electronegative element). Thus, hydrogenation consists of a reduc-

2.5 Organic functional group interconversions

tion of the organic molecule. Conversely, during dehydrogenation reactions, a carbon atom loses a bond to hydrogen and gains a bond to a heteroatom (or to another carbon atom), resulting in an overall loss of electron density, i.e. oxidation.

Common hydrogenation/dehydrogenation reactions include the alkane-alkene (e.g. Seewald, 1994; Shipp et al., 2013) and the alcohol-ketone (e.g. Leif and Simoneit, 1995; Seewald, 2001) interconversions. The reversibility of these redox reactions was observed in hydrothermal experiments, demonstrating that reactants and products can approach metastable equilibrium states (Shock et al., 2013 and references therein). For instance, Seewald (1994) experimentally proved the reversibility of the reaction between ethane and ethene (2.6), i.e.:



, in water at 325 °C and 350 bar.

Considering the equilibrium constant K for this reaction, it can be derived that (2.7):

$$\log aH_2 = \log K - \log \frac{aC_2H_4}{aC_2H_6} \quad (2.7)$$

Setting the activities of the hydrocarbons equal to each other, the corresponding equilibrium activity of hydrogen can be computed from $\log K$ (Shock et al., 2013) (Figure 2.7). Alkanes show relatively high stabilities at redox conditions common to many mineral assemblages, being consistent with the higher abundance of saturated hydrocarbons relative to alkenes in natural systems (Shock et al., 2013). Moreover, dehydrogenation (i.e. oxidation) of alkanes to alkenes is thermodynamically enhanced at increasing temperatures (Shock et al., 2013) (Figure 2.7). Based on hydrothermal experiments, Seewald (2001) found that the rate of hydrocarbon dehydrogenation (i.e. oxidation) decreases substantially under reducing conditions and in the absence of catalytically active aqueous sulphur species.

Hydration/dehydration reactions consist of the addition/removal of H_2O in the organic molecule. The reversible hydrothermal hydration reaction of alkenes to form alcohols is well known (e.g. Leif and Simoneit, 1995; Seewald, 2001; Akiya and Savage, 2001). The overall reaction (2.8) can be

2. Origin and fate of VOCs in volcanic and hydrothermal systems

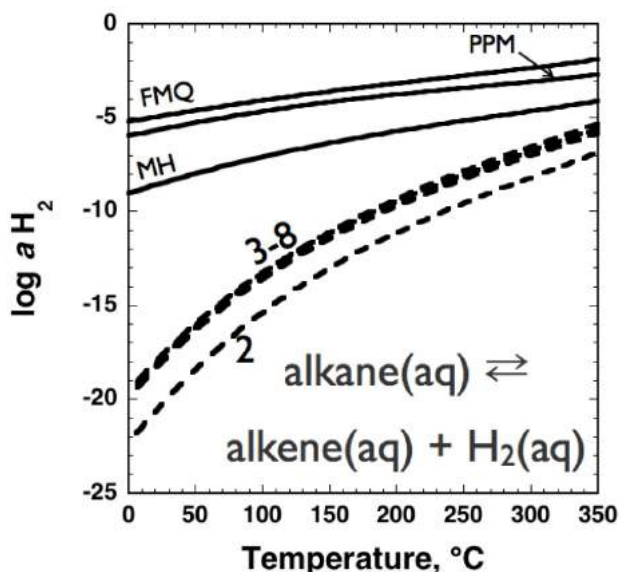


Figure 2.7: Equilibrium values of a_{H_2} corresponding to (i) equal activities of alkanes and alkenes (dashed curves; numbers refer to number of carbon atoms in the alkane and alkene), or (ii) mineral assemblages (solid curves; MH = magnetite-hematite; PPM = pyrrhotite-pyrite-magnetite; FMQ = fayalite-magnetite-quartz) as a function of temperature at P_{SAT} (after Shock et al., 2013).

written as follows:



, or, in terms of the equilibrium constant K (2.9):

$$\log \frac{a_{C_nH_{2n}}}{a_{C_nH_{2n+1}}} = \log K - \log a_{H_2O} \quad (2.9)$$

Assuming $a_{H_2O} \approx 1$ (that is true unless the ionic strength of the solution is significantly higher than that of seawater), the alkene to alcohol activity ratio is equivalent to the equilibrium constant, which is dependent on the temperature (Figure 2.8). The alkene/alcohol ratios increase at increasing temperatures (up to 5 orders of magnitude from 0 to 350 °C), highlighting the existence of a thermodynamic drive towards dehydration at high T,

2.5 Organic functional group interconversions

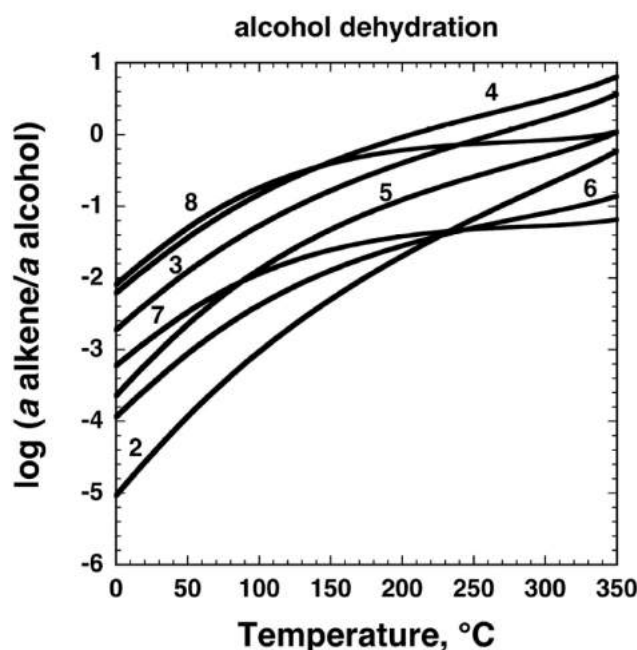


Figure 2.8: Metastable equilibrium ratios of alkenes to alcohols as a function of temperature at P_{SAT} . Numbers refer to the number of carbon atoms in the alkene and alcohol (after Shock et al., 2013).

whereas hydration is thermodynamically favoured as temperature decreases. Hence, as fluids cool, hydration of alkenes to alcohols may compete with hydrogenation of alkenes to alkanes (Shock et al., 2013). Dehydration reactions may also lead to the production of larger molecules through condensation of smaller organic compounds (Shock et al., 2013 and references therein).

Some of the transformations described above involve parallel processes. For instance, for the cyclic structures, aromatization processes may compete with the other functional group interconversions. Shipp et al. (2013) found that the formation of aromatic structures may dominate the product distribution for alkylated cyclohexanes at hydrothermal conditions (300 °C and 100 MPa), eventually prevailing over the reaction path connecting alkanes to ketones. Aromatization of alkanes consists of a dehydrogenation reaction, highly endothermic and favoured at high temperatures, likely proceeding through the formation of alkenes and dienes as by-products (Crittendon and Parsons, 1994; Shipp et al., 2013). Transition metals are known to be heterogeneous

2. Origin and fate of VOCs in volcanic and hydrothermal systems

catalysts for aromatization at high temperature conditions (Crittendon and Parsons, 1994 and references therein). The reaction pathways leading to the production of aromatics under hydrothermal conditions were investigated in the framework of this PhD thesis through a series of experiments, carried out in water and in the presence of various minerals, which are presented in Chapter 3.

2.6 Biogenic processes

As hydrothermal fluids approach the surface and encounter decreasing temperatures, thermogenic processes are expected to be progressively replaced by biogenic processes, i.e. metabolism-driven reaction pathways regulated by microbial communities. Owing to the presence of liquid water and energy sources, hydrothermal systems provide suitable habitats for numerous chemosynthetic (hyper-)thermophilic³ microorganisms, both in deep-ocean and sub-aerial settings. In continental settings, chemosynthetic microbes compete with photosynthetic organisms (Barbieri and Cavalazzi, 2014). Brock (1967) first recognized the existence of bacteria able to live and grow at temperatures up to the boiling point of water in hot springs from the Yellowstone National Park. More recently, Takai et al. (2008) found hyperthermophiles able to grow at 122 °C, that is the current highest growth temperature for microbes on Earth. More than 90 species of hyperthermophilic organisms, represented by bacterial and archaeal species, have been isolated from hot terrestrial and marine environments (Vieille and Zeikus, 2001; Meyer-Dombard et al., 2005; Stetter, 2006). These chemosynthetic organisms gain energy by catalyzing oxidation/reduction reactions. These reactions have to be thermodynamically favoured but kinetically inhibited in order to serve as energy sources: at elevated temperatures, unassisted reaction rates are too fast to allow organisms to take advantage of catalyzing the reaction (Amend and Shock, 2001). In other words, *things that burst into flame are not good to eat* (Shock and Boyd, 2015). This explains why temperature is one of the limiting factors for the biosphere.

Volcanic and hydrothermal areas represent extreme environments, affected by high temperatures, low pH, significant diffuse gas emissions and high interstitial soil gas and metal contents. Hence, they offer ideal biotopes to extremophilic microbes. In such areas, microbial populations grow in a harsh

³Thermophiles and hyperthermophiles are defined as extremophilic microbes, i.e. organisms (mainly microorganisms, i.e. Archaea and Bacteria) that thrive at extreme conditions. Thermophiles grow readily at temperatures above 45 °C, whereas hyperthermophiles live at temperatures >80 °C (Madigan and Mairs, 1997). Other extremophiles include psychrophiles, acidophiles, alkaliphiles, barophiles and halophiles (Rampelotto, 2013).

2. Origin and fate of VOCs in volcanic and hydrothermal systems

and spatially rapidly changing environment, affecting and being affected by the local geochemical conditions (Gagliano et al., 2015). The variety of habitats offered in volcanic-hydrothermal areas may even increase the number of individuals and the richness of metabolically diverse species (Amend et al., 2003). Thus, biochemical processes (biogenic processes) may play a critical role in controlling the composition of the uprising volcanic and hydrothermal fluids prior to their release in the atmosphere.

Biochemical processes are expected to be particularly relevant when volatile organic compounds are investigated in interstitial soil gases. Organics are strictly related to microbial activity, being consumed and/or produced by the metabolism of archaea and bacteria. On the one hand, VOCs are used as carbon and energy sources by chemoorganotrophs (biodegradation). Soil may act as a sink of VOCs due to microbe capability of degrading organic compounds under both aerobic and anaerobic conditions (Insam and Seewald, 2010; Peñuelas et al., 2014; Gennadiev et al., 2015). On the other hand, soil may be a source of VOCs (Leff and Fierer, 2008; Peñuelas et al., 2014 and references therein), as these compounds may be produced by primary metabolism, as cell growth-associated by-products, and secondary metabolism, as (i) products not required for the survival of the organisms but that may serve for specific functions, (ii) competitive weapons used against other microbes, (iii) agents of symbiosis between organisms, (iv) sexual hormones, and so on. For instance, VOCs are known to be used for communication (infochemicals) between plants and rhizobacteria (e.g. Wheatley, 2002; Mendes et al., 2013 and references therein; Peñuelas et al., 2014), or in microbes-microbes interactions (Schmidt et al., 2015; Schulz-Bohm et al., 2015; Schmidt et al., 2016). Based on the mVOC database (<http://bioinformatics.charite.de/mvoc/>), which includes approximately 1,000 VOCs released from about 350 bacterial and 80 fungal species, bacteria mainly emit alkenes, alcohols, ketones and terpenes, whereas fungal VOCs are largely represented by alcohols, benzenoids, aldehydes and ketones (Figure 2.9).

In the following sections, the basic principles of biochemistry and microbial metabolism are summarized in order to provide a necessary knowledge

2.6 Biogenic processes

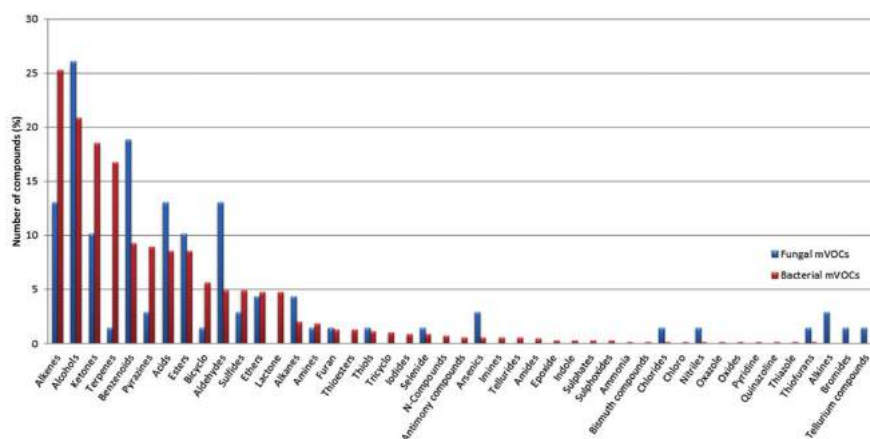


Figure 2.9: Distribution of microbial VOCs emitted by bacteria (red columns) and fungi (blue columns) (after Peñuelas et al., 2014).

background to understand how VOCs can be involved in and affected by microbial activity. The last sections will then be devoted to the biodegradation pathways of VOCs under aerobic and anaerobic conditions.

2.6.1 Rudiments of biochemistry: metabolism and enzymes

Biochemistry is “the chemistry of life”, i.e. the study of chemical compounds and processes related to living organisms. Living organisms are classified into three kingdoms (or domains) that define three phylogenetic branches of evolution from a Last Universal Common Ancestor (LUCA), i.e. Archeobacteria, Eubacteria and Eukaryotes (Figure 2.10). The domains of Archeobacteria and Eubacteria (also named Archaea and Bacteria) include prokaryotes that can be distinguished into aerobic and anaerobic (and obligate anaerobic) according to their tolerance to oxygen.

Since all living organisms must perform work to stay alive, to grow and to reproduce, they must obtain energy and materials necessary for cellular processes via food (nutrients). Microbes may either (*i*) make their own food, fixing CO₂ into organic compounds (autotrophs) or (*ii*) require a source of nutrients (heterotrophs). Organisms can further be classified on the basis

2. Origin and fate of VOCs in volcanic and hydrothermal systems

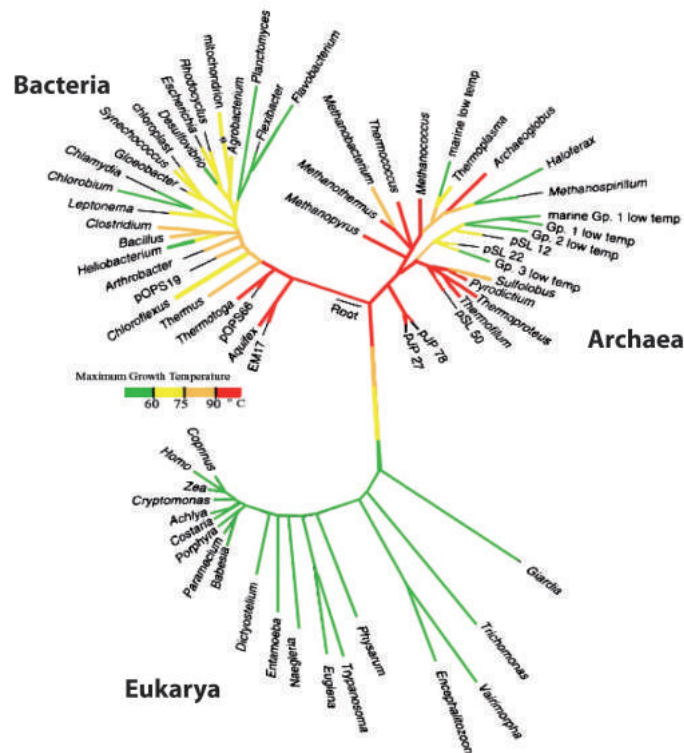


Figure 2.10: Phylogenetic tree of life. The colours of the branches correspond to the maximal growth temperatures: (i) green: $< 60\text{ }^\circ\text{C}$, (ii) yellow: from 60 to $75\text{ }^\circ\text{C}$, (iii) orange: from 75 to $90\text{ }^\circ\text{C}$, and (iv) red: $>90\text{ }^\circ\text{C}$ (after Lineweaver and Schwartzman, 2003).

of how they obtain energy. Organisms may gain energy from the sunlight (phototrophs) or by the oxidation of electron donors within their habitats (chemotrophs). Chemotrophs may use either inorganic (lithotrophs) or organic compounds (organotrophs) as electron donors (Nelson and Cox, 2005). The sum of chemical transformations taking place in a living organism that, starting from nutrients, leads to the synthesis of new proteins, nucleic acids (DNA, RNA) etc., and makes energy available for cellular processes, is called metabolism. Metabolic reactions are divided into two categories: (i) catabolism, in which nutrients are converted into simpler products with energy release, and (ii) anabolism (or biosynthesis), requiring input of energy to convert simpler substances into larger and more complex molecules. The overall

2.6 Biogenic processes

transformation of nutrients occurs through a series of enzyme-catalyzed reactions, i.e. metabolic pathways, whose intermediate products are called metabolites. They include e.g. oxidation-reduction reactions, making or breaking of C-C bonds, isomerizations, eliminations, free radical reactions and group transfers (Nelson and Cox, 2005). Enzymes are biocatalysts, mainly proteins that greatly enhance the rate of specific chemical reactions without being consumed in the process (Nelson and Cox, 2005). The chemical reaction is catalyzed at a specific location in the enzyme, called the active site, whereas the molecule, bound in the active site, and whose chemical transformation is catalyzed by the enzyme, is called the substrate (Nelson and Cox, 2005; Brown et al., 2012). Enzymes are very efficient, catalyzing 10^3 to 10^7 reactions per second at a particular active site (Brown et al., 2012). Some of them require no chemical groups for activity while others need an additional chemical component (cofactor), i.e. either one or more inorganic ions or a complex organic or metallo-organic molecule called coenzyme (Nelson and Cox, 2005). Enzymes are divided into 6 classes based on the type of reaction catalyzed (Nelson and Cox, 2005): (*i*) oxidoreductases for transfer of electrons (hydride ions or H atoms), (*ii*) transferases for group transfer reactions, (*iii*) hydrolases for hydrolysis reactions (transfer of functional groups to water), (*iv*) lyases for addition of groups to double bonds or formation of double bonds by removal of groups, (*v*) isomerases for transfer of groups within molecules to yield isomeric forms, (*vi*) ligases for formation of C-C, C-S, C-O, and C-N bonds by condensation reactions coupled to ATP cleavage.

Interestingly, it is an increasingly convincing hypothesis that metabolic pathways arose from the evolution of inorganic processes. Starting from the Oparin-Haldane theory of the origin of life and the Miller-Urey prebiotic soup experiment (Miller and Urey, 1959 and references therein), the strict connection between inorganic and organic spheres has become increasingly evident. Enzymes show clear similarities with inorganic catalysts and it has been hypothesized that metal centres in many enzyme cofactors are vestiges of mineral catalysis (Russel and Martin, 2004). In this perspective, biochemical processes would have a geochemical origin. In particular, Rus-

2. Origin and fate of VOCs in volcanic and hydrothermal systems

sel and Martin (2004) proposed that biochemistry arose on Early Earth at submarine hydrothermal vents, where an inorganically-catalyzed analogue of present metabolic pathways, involving metal sulphides as catalysts, hydrothermal H₂ as the initial electron donor and volcanogenic CO₂ as the initial acceptor, may have occurred leading to the synthesis of organic precursors to fuel primordial biochemical reactions. Accordingly, thermophiles from hot springs and hydrothermal vents are found near the root of the phylogenetic tree (Figure 2.10), suggesting that (i) the last common ancestor likely lived in similar hot environments (Lineweaver and Schwartzman, 2003 and references therein), and (ii) the origin and evolution of many metabolic reactions and pathways may be rooted in thermophiles (Amend and Shock, 2001).

2.6.2 Rudiments of biochemistry: microbial metabolic pathways

Through metabolic pathways, living organisms convert a carbon source into the building blocks needed for the synthesis of new cellular materials. As stated above, heterotrophs are capable to break down complex organic compounds, such as carbohydrates, proteins, lipids, into simpler end-products through catabolism, i.e. the degradative phase of metabolism. The catabolic pathways consist of oxidative stepwise reactions that result in the transfer of electrons from electron donors to an electron acceptor. Energy may be obtained by (i) respiration, involving transfer of electrons to inorganic acceptors, i.e. either molecular oxygen (aerobic respiration) or other species such as SO₄, NO₃, NO₂, CO₃, CO₂ (anaerobic respiration), or (ii) fermentation, involving transfer of electrons to an organic substrate. Whilst part of the energy released during these electron transfers is lost as heat, the rest is used to form electron carriers or high-energy compounds (such as ATP, NADH, NADPH and FADH₂), which are the central goal of catabolism. These compounds, in particular ATP, provide energy for anabolic pathways and cell growth.

Both cellular respiration and fermentation may start with glycolysis, i.e.

2.6 Biogenic processes

the breaking down of glucose (derived from carbohydrates breakdown) to pyruvate (Figure 2.11). Pyruvate may either (*i*) convert, depending on the

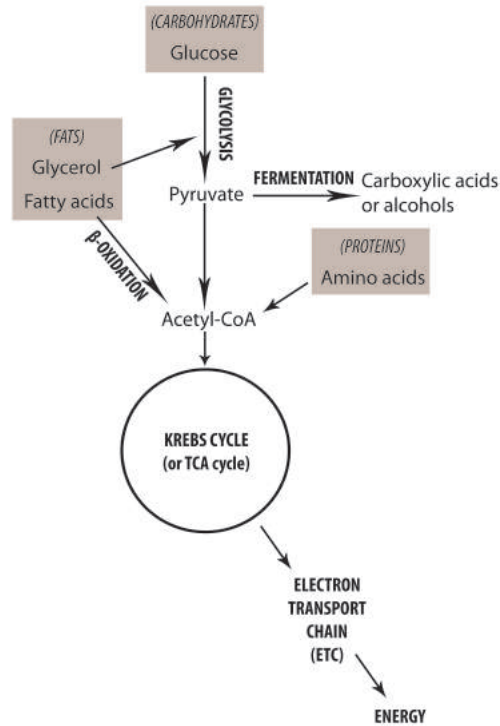


Figure 2.11: Simplified scheme of the metabolic pathways related to cellular respiration and fermentation. See text for details.

enzymes involved, into acids or alcohols producing energy in anaerobic conditions (fermentation), or (*ii*) be oxidized and converted, together with coenzyme A (CoA), into acetyl-CoA (cellular respiration). In cellular respiration, acetyl-CoA enters the so-called Krebs cycle, or TCA (tricarboxylic acid) cycle (Figure 2.11), that leads to the production of many more reduced electron carriers (e.g. NADH) than glycolysis. Also amino acids from proteins breakdown can enter the TCA cycle after deamination (removal of an amino group). Glycerol and fatty acids from fats breakdown are changed into, respectively, (*i*) one of the intermediate products of glycolysis entering the cell respiration pathway, and (*ii*) acetyl-CoA molecules through a series of reactions called β -oxidation, hence entering cell metabolism at the Krebs cycle (Figure 2.11).

2. Origin and fate of VOCs in volcanic and hydrothermal systems

In the final stage of cellular respiration, the reduced electron carriers pass through the electron transport chain (ETC), which consists of a series of compounds at increasing electronegativity that transfer electrons to the final electron acceptor (oxygen in aerobic respiration, other acceptors in anaerobic respiration) via oxidation/reduction reactions. The resulting electrochemical gradient drives the synthesis of ATP (i.e. energy) through the ATP synthase enzyme (Figure 2.11).

Differently from heterotrophs, autotrophic organisms are capable to fix carbon atoms from inorganic species (CO_2) into organic compounds. They may obtain energy, in the form of ATP and NADPH, from sunlight or oxidation of chemicals. Six autotrophic carbon fixation pathways are known (reviewed by Berg, 2011), including the Calvin cycle (a cyclic pathway through which carbon atoms from CO_2 are fixed into sugars, e.g. glucose), the reductive TCA (rTCA) cycle (widespread in anaerobic or microaerobic bacteria, it reverses the reactions of the oxidative TCA cycle forming acetyl-CoA from CO_2 ; acetyl-CoA is assimilated to pyruvate by the pyruvate synthase), and the reductive acetyl-CoA pathway (a non-cyclic pathway that results in the fixation of CO_2 into acetyl-CoA and proceeds via pyruvate synthase). The latter, also known as Wood-Ljungdahl pathway, is preferred by, for instance, methanogens, acetogens and sulphur-reducing bacteria (Berg, 2011). According to a recent study (Weiss et al., 2016), the Wood-Ljungdahl pathway was also used by the last universal common ancestor, which would have been an autotrophic thermophilic microbe living in hydrothermal settings.

2.6.3 Biodegradation of VOCs

As stated above, VOCs participate to microbial metabolism as energy and carbon sources, or products of primary or secondary metabolism. Accordingly, microbes are used, for instance, for the production of biofuels and chemicals (e.g. Mukhopadhyay, 2015), and in bioremediation techniques to biodegrade VOCs in contaminated soils and waters (e.g. Megharaj et al., 2011; Lien et al., 2016). Biodegradation is defined as the biologically catalyzed reduction in molecular complexity of chemical compounds (Alexander,

1994). It may occur in the presence of oxygen (aerobic conditions) or without oxygen (anaerobic conditions) through the metabolic activity of microorganisms. Chemoorganotrophic species are able to use a huge number of organic compounds as carbon and energy sources, some microbial species utilizing more than 100 different organic compounds (Fritsche and Hofrichter, 2008). In general, an organic compound may be (i) used by microbes as the primary carbon and energy source for cell growth and ATP production, (ii) used as an electron acceptor to aid cellular respiration (anaerobic respiration), or (iii) transformed by a microbe without nutritional benefit in the presence of a growth substrate that is used as the primary carbon and energy source (cometabolism). For example, methanotrophs are capable to cometabolize a variety of aromatic, aliphatic and halogenated compounds (e.g. oxidizing alkanes to organic acids, or trichloroethylene to TCE epoxide; Little et al., 1988; Fritsche and Hofrichter, 2008 and references therein) and have been applied for bioremediation of chlorinated solvents in polluted sites (Semrau, 2011 and references therein).

The cell growth-associated degradation of VOCs may occur through cellular respiration (aerobic or anaerobic) and/or fermentative processes. In the following sections, the aerobic and anaerobic metabolic pathways for alkanes and aromatics, i.e. the most abundant VOCs found in hydrothermal gases, are schematically described.

Aerobic biodegradation

Aerobic degradation of organic compounds is initiated by oxygenases, i.e. oxydoreductase enzymes that oxidize the organic substrate by transferring oxygen from molecular oxygen (O_2 , the initial electron donor) to it (Fritsche and Hofrichter, 2008). Oxygenases may be either monooxygenases (incorporating one atom of oxygen into the substrate and reducing the other oxygen of O_2 to H_2O) or dioxygenases (incorporating both oxygen atoms of O_2 into the substrate). These enzymes allow to overcome the low chemical reactivity of saturated hydrocarbons and lead to the generation of reactive oxygen species.

2. Origin and fate of VOCs in volcanic and hydrothermal systems

Under aerobic conditions, alkanes are degraded by terminal or sub-terminal oxidation (Figure 2.12), with the formation of a primary or secondary alcohol that is subsequently converted to aldehyde or ketone, respectively (e.g. Fritsche and Hofrichter, 2008; Rojo, 2009). The aldehyde is finally oxidized

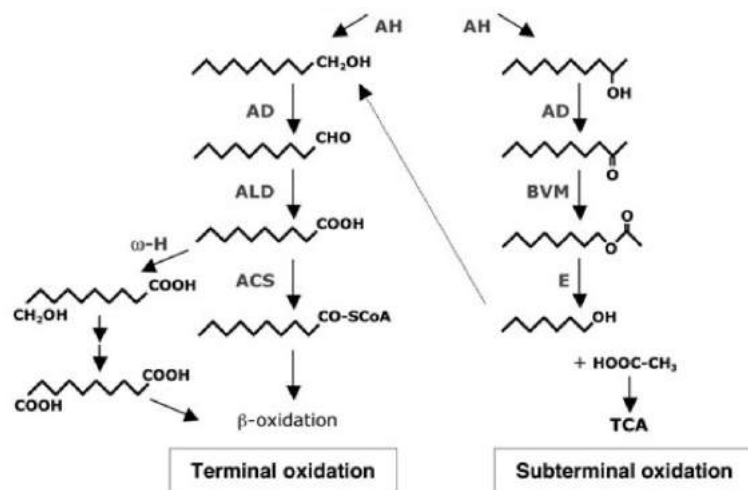


Figure 2.12: Aerobic pathways for the degradation of n-alkanes by terminal and sub-terminal oxidation. The initial attack needs O₂ as reactant. AH: alkane hydroxylase; AD: alcohol dehydrogenase; ALD: aldehyde dehydrogenase; ACS: acyl-CoA synthetase; ω-H: ω-hydroxylase; BVM: Baeyer-Villiger monooxygenase; E: esterase; TCA: tricarboxylic acids cycle (after Rojo, 2009).

to a fatty acid, whereas the ketone is converted into an ester that is then hydroxylated generating an alcohol and a fatty acid (Figure 2.12). β-oxidation of the fatty acids leads to the formation of acetyl-CoA that is incorporated into the intermediary metabolism (Figure 2.11).

Branched alkanes are generally more difficult to degrade than the corresponding linear homologues (Rojo, 2009), although simple methyl side groups do not drastically decrease the biodegradability (Fritsche and Hofrichter, 2008). In cyclic alkanes, the absence of an exposed terminal methyl group complicates the initial attack of the molecule (Fritsche and Hofrichter, 2008).

Aromatic compounds are characterized by a higher thermodynamic stability than aliphatic hydrocarbons. However, some bacteria are able to attack benzene

exist (Fritsche and Hofrichter, 2008 and references therein). The classical strategy for degrading the ring structure under aerobic conditions consists in an attack by oxygenases, forming compounds such as catechol or protocatechuate as central intermediates. The attack of these compounds by specific dioxygenases cleaves the aromatic ring and, after further reaction steps, acetyl-CoA is produced (Fritsche and Hofrichter, 2008; Fuchs, 2011). In general, the introduction of a substituent group on the aromatic ring makes the molecule initial attack easier. For instance, toluene degradation may occur via hydroxylation of the methyl group with its overall oxidation to the corresponding alcohol, aldehyde and carboxylic acid, before being converted to catechol (Fritsche and Hofrichter, 2008).

Anaerobic biodegradation

While microorganisms able to utilize hydrocarbons under aerobic conditions have been known since the beginning of the 20th century, it was only in the 1980s that bacteria capable of degrading organic compounds in the absence of oxygen were recognized (Widdel and Rabus, 2001).

Under anaerobic conditions, electron acceptors other than free O₂ have to be used for the initial attack of the organic molecule. Anaerobic microorganisms use nitrate, ferric iron, sulphate or organic species (e.g. chlorinated compounds; Holliger et al., 1999) as electron acceptors for anaerobic respiration, and may grow in syntrophic cocultures with other anaerobes (e.g. methane is oxidized by archaea in a syntrophic association with sulphate-reducing bacteria; Widdel and Rabus, 2001).

Two general metabolic strategies for degrading alkanes under anaerobic conditions were recognized (Rojo, 2009 and references therein). The first one involves the activation of the alkanes by the addition of a fumarate molecule to a sub-terminal position, yielding an alkyl succinate derivative. The latter is then linked to CoA and converted into an acyl-CoA that can further be metabolized by β -oxidation, which results in the production of acetyl-CoA (Figure 2.13). The second strategy consists in the addition of the fumarate molecule to one of the terminal carbon atom of the alkane (Figure 2.13).

2. Origin and fate of VOCs in volcanic and hydrothermal systems

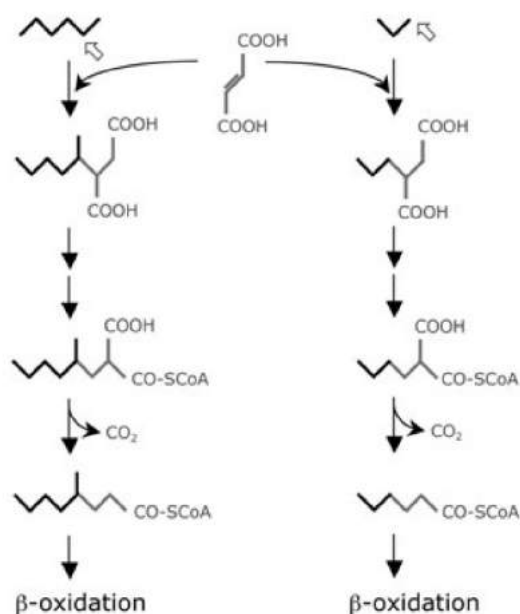


Figure 2.13: Anaerobic pathways for the degradation of n-alkanes. The initial activation of the alkane (in black) occurs by addition of a fumarate molecule (in grey) either at a sub-terminal position (on the left) or at a terminal position (on the right). The products are likely processed by β -oxidation (after Rojo, 2009).

Initial activation of aromatic hydrocarbons in the absence of free O₂ may occur through different enzymatic reactions, including (i) addition of fumarate, (ii) methylation of unsubstituted aromatics, (iii) hydroxylation of an alkyl substituent via a dehydrogenase, and (iv) direct carboxylation (Foght, 2008 and references therein; Fuchs et al., 2011). These activation reactions lead to a central intermediate (benzoyl-CoA) that is dearomatized and processed by ring-cleaving yielding acetyl-CoA, which is eventually completely oxidized to CO₂ via the TCA cycle.

Although benzene can be degraded aerobically, its thermodynamic stability results in its high persistence under anaerobic conditions. Contrarily, toluene is the most readily degraded among the BTEX compounds (Foght, 2008 and references therein).

Chapter 3

Experiments on organic reactions under hydrothermal conditions

3.1 Introduction

Laboratory experiments designed to simulate hydrothermal conditions are useful tools to investigate the behaviour of VOCs at high temperatures. When compared with empirical data from fumarolic gases, experimental results can be invaluablely informative on the processes that possibly control the distribution of VOCs within natural deep hydrothermal reservoirs. Accordingly, specific experiments can be devised to corroborate hypotheses, based on the composition of natural gas discharges, on primary processes occurring at depth. In this chapter, laboratory experiments carried out at high temperatures in order to investigate the mechanisms of benzene production under hydrothermal conditions are presented.

The experiments were performed at the laboratories of the School of Molecular Sciences and the School of Earth and Space Exploration (SESE) at Arizona State University (ASU) in Tempe (Arizona, USA) in collaboration with the GEOPIG (Group Exploring Organic Processes in Geochemistry) and HOG (Hydrothermal Organic Geochemistry) research groups coordinated by Prof. Everett L. Shock (<http://geopig.asu.edu/>). The experimental work was carried out in the framework of the 4-months research stay abroad (February

3. Experiments on organic reactions

to June 2015) required by the “Pegaso” PhD regulations.

Most of the data here discussed were presented (*i*) at the Italian national conference Il Pianeta Dinamico (Congresso SIMP-SGI-SoGeI-AIV) 2015 in Florence (Italy) and (*ii*) at the 2015 AGU Fall Meeting in San Francisco (California, USA; see Appendix B). Moreover, they were included in a research paper titled “*Mineral-assisted production of benzene under hydrothermal conditions: insights from experimental studies on C₆ cyclic hydrocarbons*”, (see Appendix A) presently under review for publication on the JVGR (Journal of Volcanology and Geothermal Research) special issue “*Volcano-Hydrothermal Systems*”, edited by Prof. Yuri Taran.

3.2 Preliminary considerations

Benzene (C₆H₆) is one of the most abundant non-methane VOCs in volcanic/hydrothermal fluid discharges (e.g. Capaccioni et al., 2001; Taran and Giggenbach, 2003; Tassi et al., 2012c, 2013b), and is of particular interest for its impact on (*i*) human health, being associated with acute and long-term diseases including cancer and aplastic anaemia, and (*ii*) the environment, contributing to smog, and contaminating waters and soils (WHO, 2000; Huff, 2007; Galbraith et al., 2010). Benzene levels up to 40 $\mu\text{g}/\text{m}^3$ (i.e. significantly higher than the Italian national law threshold for benzene in ambient air, 5 $\mu\text{g}/\text{m}^3$) were recorded at Solfatara Crater (Campi Flegrei, Italy), where a total output of benzene from diffuse degassing of 0.10 kg/d was estimated (Tassi et al., 2013b). Nevertheless, the conditions and the processes that favour the production and release of benzene from volcanic and hydrothermal environments are still poorly understood. Whilst the relatively high concentrations of benzene found in natural hydrothermal fluids have univocally been interpreted to be a consequence of the stability of the aromatic ring over a wide range of temperature conditions (e.g. Darling, 1998; Katritzky et al., 1990; Tassi et al., 2012c), different hypotheses have been proposed to explain its origin. Taran and Giggenbach (2003) suggested that benzene is likely produced via oxidative aromatization of methane at high temperatures. Accordingly, as described in Chapter 2 (Section 2.4.1), thermal decomposi-

3.2 Preliminary considerations

tion of methane may yield small amounts of benzene (Guéret et al., 1997; Holmen et al., 1995). Differently, Capaccioni et al. (1993) proposed that the production of benzene in volcanic and hydrothermal environments is occurring through mechanisms that resemble the catalytic reforming processes used in the refining industry. These processes take place at high temperatures (700-800 K) in the presence of solid catalysts (e.g. alumina supported Pt, Pt-Re, and Pt-Ir catalysts and zeolites; Turata and Ramanathan, 2003; Rahimpour et al., 2013) and the reaction pathways include dehydrogenation, isomerization, cyclization and fragmentation, which lead to the overall conversion of alkanes and cycloalkanes to aromatic hydrocarbons. Similarly, benzene in natural volcanic and hydrothermal systems may be originated from saturated hydrocarbons through multi-step dehydrogenation reactions (e.g. Capaccioni et al., 1993, 1995, Tassi et al., 2010).

The conversion of normal alkanes to aromatics consists of (*i*) cyclization of normal alkanes (which in the laboratory usually requires metal catalysts), and (*ii*) dehydrogenation of cycloalkanes to aromatics (which in the laboratory is usually acid catalyzed), as follows:



The equilibrium constants for reactions (3.1) and (3.2) can be expressed, as follows:

$$K_1 = \frac{a_{C_6H_{12}} f_{H_2}}{a_{C_6H_{14}}} \quad (3.3)$$

and

$$K_2 = \frac{a_{C_6H_6} (f_{H_2})^3}{a_{C_6H_{12}}} \quad (3.4)$$

The K_1 and K_2 values at the saturated vapour pressure (P_{SAT}), calculated using the SUPCRT database (Johnson et al., 1992), increase from 3 to 15 orders of magnitude from 0 to 350 °C, respectively (Figure 3.1). Both the cyclization and the dehydrogenation reactions are endothermic, and thus, the stability of benzene is favoured by increasing temperatures. Moreover, as these reactions consist of the loss of bonds to hydrogen (oxidation), they

3. Experiments on organic reactions

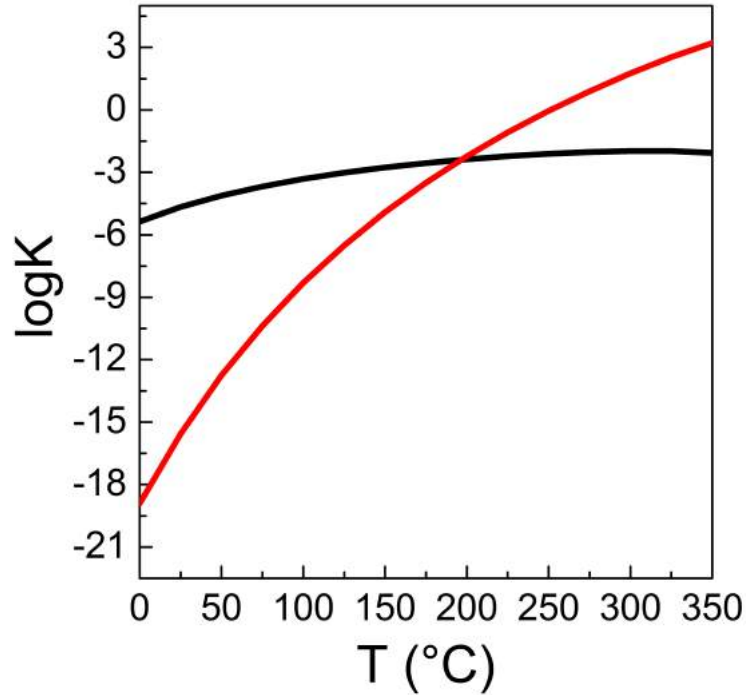


Figure 3.1: The temperature dependence of equilibrium constants K_1 (black line) and K_2 (red line), referred to reactions (3.1) and (3.2), is shown (see text for further details).

are sensitive to redox conditions.

The dependence of K_1 and K_2 on hydrogen fugacity can be conveniently expressed on a log-basis, as follows:

$$\log K_1 = \log \frac{(a_{C_6H_{12}})}{(a_{C_6H_{14}})} + \log fH_2 \quad (3.5)$$

$$\log K_2 = \log \frac{(a_{C_6H_6})}{(a_{C_6H_{12}})} + 3 \log fH_2 \quad (3.6)$$

At equilibrium conditions, the products of both reactions (3.1) and (3.2) are thermodynamically favoured by decreasing fH_2 values (Figure 3.2). Accordingly, field data on volcanic and hydrothermal fluids showed a positive

3.2 Preliminary considerations

correlation between cyclohexane/benzene ratios and H_2 contents in fumarolic discharges (Capaccioni et al., 2004).

In a hydrothermal reservoir, where redox conditions are generally controlled by the fayalite-hematite-quartz ($FeO-FeO_{1.5}$) mineral buffer (Giggenbach, 1987), hexane and benzene production from cyclohexane, as described by reactions (3.1) and (3.2), are favoured at temperatures higher than 150 °C (field D; Figure 3.2). Accordingly, linear alkanes and aromatics were found to dominate the composition of the organic gas fraction in fumarolic fluids emitted from volcanic/hydrothermal systems, whereas cyclics were rarely detected (e.g. Schwandner et al., 2013). On the other hand, benzene hydrogenation to produce cyclohexane is favoured at relatively low temperatures (field C; Figure 3.2), as confirmed by the relatively high concentrations of cyclics compared to those of aromatics found in hydrothermal discharges fed by reservoirs having temperatures <150 °C (Tassi et al., 2012a).

Hence, both thermodynamic calculations and empirical data support the hypothesis that the production of benzene from cyclohexane through dehydrogenation is energetically favoured at high temperatures, and can, and likely does, occur in natural volcanic and hydrothermal environments.

All this considered, a series of experiments were performed at 300 °C and 85 bar on both normal- and cyclic-alkanes, in order to confirm the hypothesized dehydrogenation reaction pathway as the mechanism responsible for benzene production under hydrothermal systems. The experimental runs were performed in the presence of water and different minerals (sphalerite, quartz, hematite, magnetite and pyrite) commonly found in a hydrothermal environment, in order to investigate the role that minerals may have in enhancing reactivity, catalyzing or participating in organic reactions.

3. Experiments on organic reactions

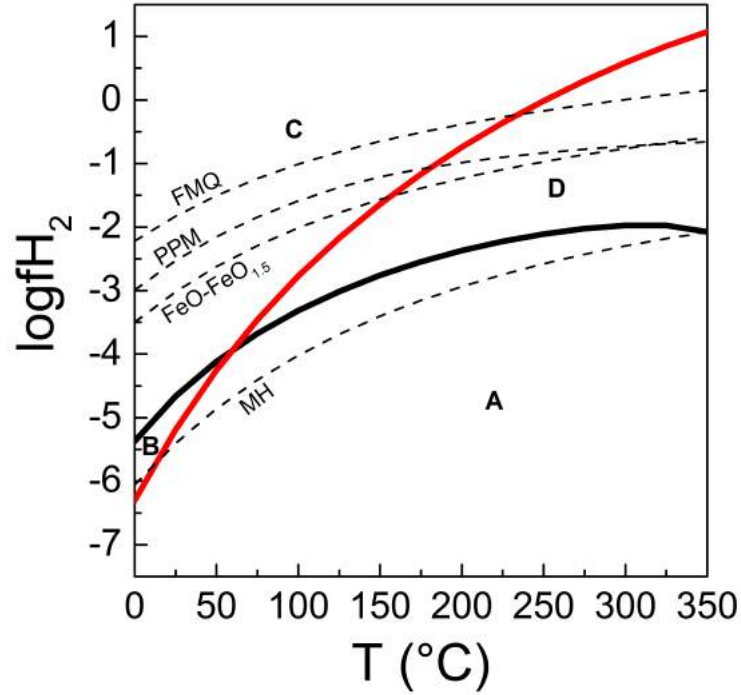


Figure 3.2: The equilibrium values of hydrogen fugacity corresponding to equal activities of cyclohexane to hexane (i.e. $\log fH_2 = \log K_1$, referred to reaction (3.1); black line) and benzene to cyclohexane (i.e. $3 \log fH_2 = \log K_2$, referred to reaction (3.2); red line) are plotted as a function of temperature at P_{SAT} . Four fields are depicted in the diagram, corresponding to T and fH_2 at which the following products are favoured: (i) cyclohexane from reaction (3.1) and benzene from reaction (3.2) (field A), (ii) cyclohexane from both reaction (3.1) and (3.2) (field B), (iii) hexane from reaction (3.1) and cyclohexane from reaction (3.2) (field C), and (iv) hexane from reaction (3.1) and benzene from reaction (3.2) (field D). Dashed curves represent hydrogen fugacity values buffered by specific mineral assemblages: magnetite-hematite (HM), fayalite-hematite-quartz (FeO-FeO_{1.5}), pyrrhotite-pyrite-magnetite (PPM) and fayalite-magnetite-quartz (FMQ).

3.3 Experimental methods

3.3.1 Reactants and minerals

Organic reactants, i.e. cyclohexane ($\geq 99.0\%$), cyclohexene ($\geq 99.9\%$), 1,4-cyclohexadiene (97%), hexane ($\geq 99.7\%$), and dodecane ($\geq 99.0\%$), were purchased from Sigma-Aldrich. Powdered minerals (Figure 3.3), i.e. sphalerite (99.99% ZnS), quartz (99.5% Silicon(IV) oxide), hematite (99.5% Iron(III) oxide), magnetite (97% Iron(II, III) oxide), pyrite (99.9% Iron(II) sulphide), were purchased from Alfa Aesar. The crystal structures of the powdered minerals were confirmed by X-ray diffraction. The BET surface areas (Table 3.1) were measured as described by Shipp et al. (2014).

Powdered Mineral	Surface area (m^2/g)
Sphalerite	12.7
Quartz	5.32
Hematite	12.9
Magnetite	7.82
Pyrite	2.34

Table 3.1: Surface areas (expressed in m^2/g) for each powdered mineral used in the experimental runs.



Figure 3.3: Powdered minerals used in the experimental runs.

3.3.2 Experimental procedure

Experiments were performed using 0.1 or 0.2 M organic reactants added to water and sealed in silica glass tubes (Figure 3.4). Under the conditions of the

3. Experiments on organic reactions

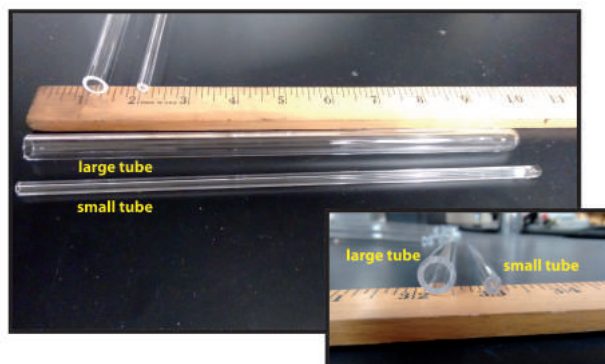


Figure 3.4: Silica glass tubes employed for the experiments (small tubes with 6 mm outer diameter and 2 mm inner diameter; large tubes, with 10 mm outer diameter and 8 mm inner diameter).

experiment, the organic reactants are soluble in aqueous media. The solvent was either (i) Ar-purged 18.2 M Ω -cm water (NANOpure[®] DIamondTM UV, Barnstead International; Figure 3.5) or (ii) deuterium oxide (99.9 % D₂O, Sigma-Aldrich), both added up to a fixed volume in the silica tubes (200 μ L in small tubes and 4 mL in large ones). Powdered minerals were added



Figure 3.5: Ar was purged in MilliQ water for 20 minutes in order to remove air.

to the samples so that the total mineral surface areas were 0.1 or 0.6 m², depending upon the experimental run. Hence, the headspace of the tubes was purged with ultra-high purity Ar to remove air (step 1; Figure 3.6).

3.3 Experimental methods

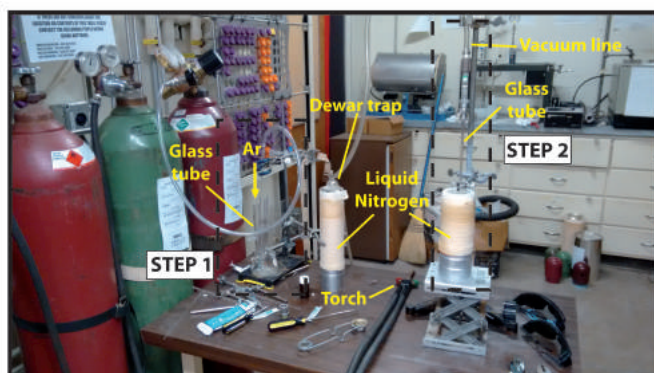


Figure 3.6: Glass tube sealing apparatus. See text for further details.

The tubes were then cooled using liquid nitrogen to solidify the contents and minimize the reactant loss due to volatilization, and connected to a vacuum pump to evacuate the headspace (pressure < 60 mtorr). The open ends of the tubes were then sealed using a hydrogen-oxygen flame while the bottom of the tubes containing the reactants were submerged in the liquid nitrogen (step 2; Figure 3.6). The sealed tubes were placed in a pre-heated oven at $300\text{ }^{\circ}\text{C}$ for 10, 14 or 30 days.

After each experimental run, the glass tubes were quickly cooled down by submerging them in water at ambient temperature and the organic products were extracted using dichloromethane (DCM, 99.9 %, Fisher Scientific) in silanized glass vials (Supelco, Inc.). The samples (organic products in DCM) were then removed from the aqueous layer and transferred to glass vials equipped with a PTFE-lined septum using a disposable glass pipette (Figure 3.7).

The analysis of organic products was carried out by gas chromatography (GC; Thermo Trace GC Ultra) coupled with Quadrupole Mass Spectrometry (MS; Thermo DSQ) at the Department of Earth Sciences of the University of Florence. An aliquot ($20\text{ }\mu\text{L}$) of samples was transferred to the GC through an injection port operating at $230\text{ }^{\circ}\text{C}$ in splitless mode. Peak separation was carried out using a TR-V1 fused silica capillary column (Thermo) and He as carrier gas at a flow rate of 1.3 mL/min in constant pressure mode. The column oven temperature was set, as follows: $35\text{ }^{\circ}\text{C}$ (hold 10 min), ramp at

3. Experiments on organic reactions

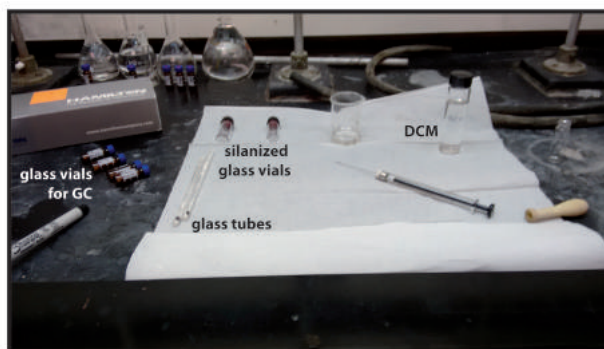


Figure 3.7: Equipment for the extraction of samples after experimental runs (see text).

5.5 °C/min to 180 °C (hold 3 min), ramp at 20 °C/min up to 230 °C (hold 6 min). The GC-MS transfer-line was set at 230 °C, the MS was operated in positive electron impact mode (EI) with an ionization energy of 70 eV, and the source was maintained at 250 °C. A mass-to-charge range from 35 to 400 m/z in full scan mode was analyzed. Retention time of the chromatographic peaks and the mass spectra were both used to identify organic compounds detected by the quadrupole detector, using the mass spectra database of the NIST05 database (NIST, 2005) for comparison. Quantitative analyses were carried out by external standard calibration procedure using Accustandard® mixtures in methanol or, alternatively, hexane solvent. Relative Standard Deviation (RSD), calculated from five replicate analyses of the standard mixtures, was <5%. The amounts of products yielded from each experiment were calculated by dividing each quantifiable product by the sum of products plus the unreacted starting material and expressed as percent abundances.

The product analysis for experiments in D₂O (carried out at the Department of Chemistry at Vanguard University in Costa Mesa, California, USA) was performed using GC-MS (Thermo Electron Trace 1300-ISQ with a TG-SQC column) with the following parameters: 1 μ L split (30:1) injection, 225 °C injection port, 30 °C oven (5 minute hold) with at 15 °C/min ramp to 105 °C, constant flow mode (1 mL/min with vacuum compensation), 250 °C transfer line and ion source, electron-impact ionization (70 eV) scanning 29-400 m/z 5 times per minute.

3.4 Results

3.4.1 Hexane and dodecane experiments

The results of the experiments carried out using normal-alkanes (hexane and dodecane) as reactants are reported in Table 3.2. The yield of the quantified products (cyclohexane and benzene) are expressed as percent abundance relative to the unreacted starting material.

Starting reactant	organic species	hexane		dodecane	
	molality (m)	0.1	0.1	0.1	0.1
Mineral	name	-	sphalerite	-	sphalerite
	formula	-	ZnS	-	ZnS
	surface area (m ²)	-	0.6	-	0.6
Reaction time	days	14	14	14	14
Products	cyclohexane	0.33	0.17	0.21	0.37
	benzene	0.11	0.24		
	hexanol			x	x
	thiophene		x		x
	methylthiophene		x		x
	other S-bearing species				x

Table 3.2: The details and results of experiments performed starting from hexane and dodecane at 300 °C and 85 bar are reported. In this case, the yield of each product is expressed as percent abundance with respect to the amount of unreacted starting material (x = present but not quantified).

Reaction of hexane in water for 14 days at 300 °C produced cyclohexane as main product (0.33 %), followed by benzene (0.11 %). In the presence of sphalerite, the yield of benzene (0.24 %) increased relative to cyclohexane (0.17 %). S-bearing compounds (thiophene and methylthiophene) were also recognized Table 3.2.

Reaction of dodecane in water at 300 °C produced cyclohexane after 14 days both in the absence of minerals (0.21 %) and in the presence of sphalerite (0.37 %). Hexanol was similarly detected in both the experiments, whereas S-bearing compounds (thiophene, methylthiophene and others) were found after the reaction of dodecane in the presence of sphalerite (Table 3.2).

3. Experiments on organic reactions

3.4.2 Cyclohexane experiments

The results of the experiments carried out using cyclohexane as reactant are reported in Table 3.3. Reaction of cyclohexane (0.2 m) in water at 300 °C after 10 days generated only trace amounts of benzene, cyclohexadiene and cyclohexene (0.36, 0.34 and 0.27 %, respectively; Figure 3.8). No ap-

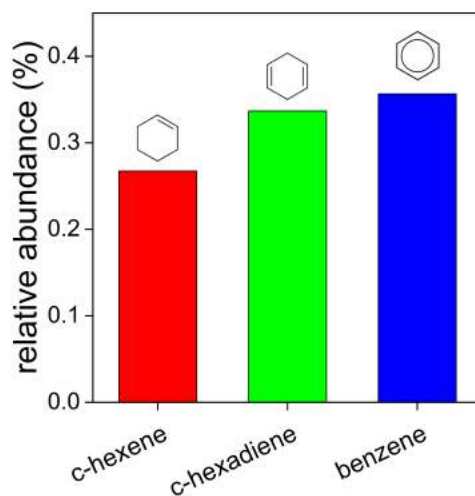


Figure 3.8: Relative abundances (% of total products plus unreacted starting material) of products yielded after 10 days from reaction of cyclohexane in water at 300 °C and 85 bar.

preciable amount of deuterated cyclohexane was observed in the experiment performed at the same conditions in heavy water (Figure 3.9; Table 3.4).

Under the same experimental conditions but in the presence of 0.1 m² sphalerite, benzene was produced as the major product (Figure 3.10a), followed by cyclohexene and phenol (0.23, 0.13 and 0.07 %, respectively; Table 3.3). In this sample, no cyclohexadiene was detected. Increasing the sphalerite/cyclohexane ratios (i.e. increasing ZnS surface area from 0.1 to 0.6 m² and/or decreasing cyclohexane initial concentration from 0.2 to 0.1 m) caused the ratio of products to remaining starting structure to increase (Table 3.3; Figure 3.10b,c). Most (69 %) cyclohexane remaining at the end of the experiment in heavy water (D₂O) with 0.1 m² sphalerite incorporated deuterium atoms, 41 % of which contained a single deuterium atom (Ta-

Starting reactant	molality (m)		0.2		0.2		0.1		0.2		0.2		0.2	
Mineral	name	formula	surface area (m ²)	days	sphalerite ZnS	sphalerite ZnS	sphalerite ZnS	sphalerite ZnS	hematite Fe ^{III} O ₃	magnetite Fe ^{II,III} O ₄	quartz SiO ₂			
Reaction time				10	0.1	0.6	10	0.6	0.1	0.1	10	0.1	10	10
Products	cyclohexane			99.0	99.6	95.1	90.4	98.0	97.4	98.4				
	cyclohexene			0.27	0.13	0.85	1.30	0.18	0.19	1.16				
	benzene			0.36	0.23	2.69	5.91	1.81	2.35	0.25				
	cyclohexadiene			0.34	-	-	-	-	0.05	0.08				
	phenol			-	0.07	1.39	2.36	-	-	0.07				

Table 3.3: The details and results of experiments performed starting from cyclohexane at 300 °C and 85 bar are reported. The yield of each product is expressed as percent abundance with respect to the sum of quantifiable products plus unreacted starting material.

3. Experiments on organic reactions

Starting reactant	molality (m)	0.2	0.2
Mineral	name	-	sphalerite
	formula	-	ZnS
	surface area (m ²)	-	0.1
Reaction time	days	10	10
Deuterated cyclohexane	D0	100	31.0
	D1	-	40.9
	D2	-	18.3
	D3	-	8.43
	D4	-	1.39

Table 3.4: The details and results of experiments performed starting from cyclohexane in heavy water (D₂O) at 300 °C and 85 bar are shown. The relative amounts (%) of cyclohexane containing from 0 (D0) up to 4 (D4) deuterium atoms obtained at the end of experimental runs in heavy water are reported.

ble 3.4; Figure 3.9).

Reaction of cyclohexane in water with hematite (0.1 m²) produced benzene and cyclohexene, the former being 10 times more abundant than the latter (Figure 3.11). No cyclohexadiene and phenol were detected. A similar benzene/cyclohexene ratio (12:1) was also measured in the presence of magnetite (Figure 3.11), where cyclohexadiene was detected at very low relative amount (0.05 %; Table 3.3). In the presence of quartz, cyclohexene was the main product (Figure 3.11), whereas cyclohexadiene and phenol were measured at very low amounts (Table 3.3). The benzene/cyclohexene ratio (~ 0.2) was markedly lower than that measured in the water alone experiment (~ 1.3).

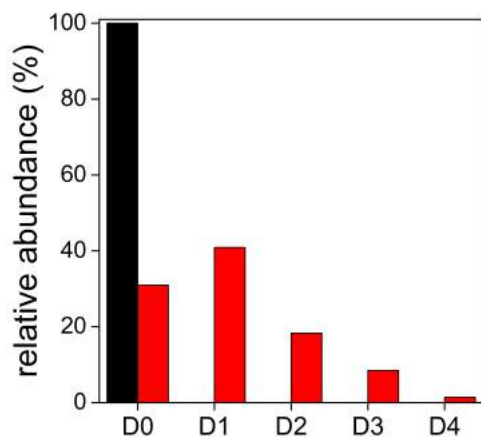


Figure 3.9: Relative abundances (% of cyclohexane) of undeuterated (D0) and deuterated (D1 to D4) cyclohexane yielded after 10 days from reaction of cyclohexane (i) in heavy water (black bars) and (ii) in D_2O and in the presence of sphalerite (red bars) at 300 °C and 85 bar.

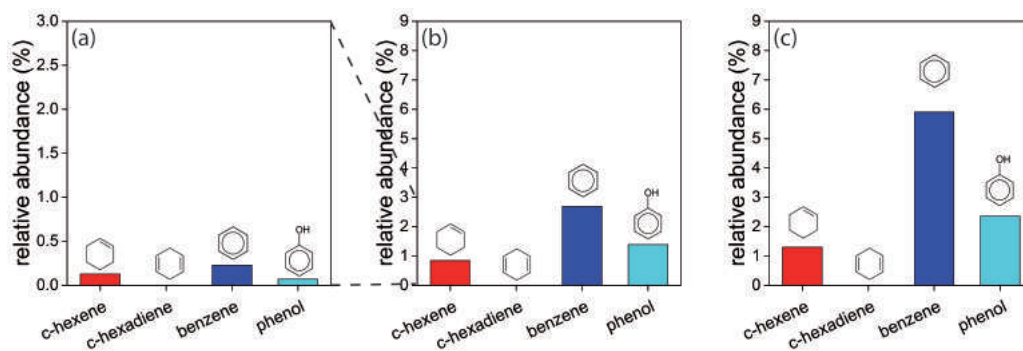


Figure 3.10: Relative abundances (% of total products plus unreacted starting material) of products yielded after 10 days from reaction in water at 300 °C and 85 bar of (a) 0.2 m cyclohexane in the presence of 0.1 m² sphalerite, (b) 0.2 m cyclohexane in the presence of 0.6 m² sphalerite, and (c) 0.1 m cyclohexane in the presence of 0.6 m² sphalerite.

3. Experiments on organic reactions

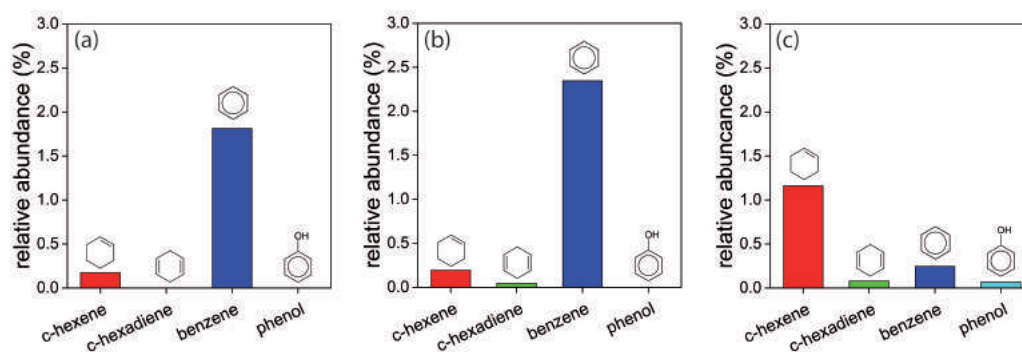


Figure 3.11: Relative abundances (% of total products plus unreacted starting material) of products yielded after 10 days from reaction in water at 300 °C and 85 bar of 0.2 m cyclohexane in the presence of (a) 0.1 m² hematite, (b) 0.1 m² magnetite, and (c) 0.1 m² quartz.

3.4.3 Cyclohexene experiments

Further experiments were carried out using cyclohexene as reactant, which is expected to be an intermediate in the aromatization reaction pathway from cyclohexane to benzene. The results are reported in Table 3.5.

Reaction of cyclohexene in water for 10 days at 300 °C produced mainly cyclohexanol and methylcyclopentenes (0.23 and 0.20 %, respectively), with minor amounts of benzene (0.05 %), cyclohexanone (0.01 %) and methylcyclopentanol (0.01 %; Figure 3.12). After 30 days, the products were domi-

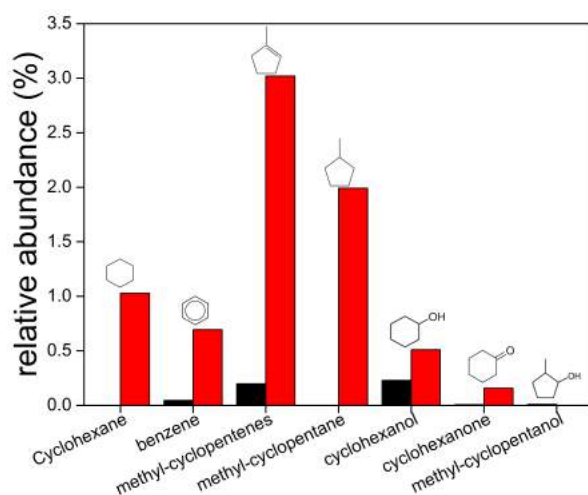


Figure 3.12: Relative abundances (% of total products plus unreacted starting material) of products yielded from reaction of cyclohexene in water at 300 °C and 85 bar (i) after 10 days (black bars) and (ii) after 30 days (red bars).

nated by methylcyclopentenes, methylcyclopentanes and cyclohexane (3.02, 1.99 and 1.03 %, respectively), whereas benzene, cyclohexanol and cyclohexanone were present at lower abundances (0.69, 0.51 and 0.16 %, respectively; Figure 3.12). Reaction of cyclohexene 0.2 m with 0.1 m² sphalerite mainly produced methylcyclopentenes (0.58 %), followed by cyclohexanol (Figure 3.13a). Benzene, cyclohexane, methylcyclopentanol and cyclohexanone were only present at very low relative amounts (≤ 0.05 %). A S-containing product (cyclohexanethiol) was also detected for reaction of cyclohexene 0.2 m with 0.6 m² sphalerite. The major products of this reaction

3. Experiments on organic reactions

Starting reactant	molality (m)	0.2	0.2	0.2	0.2	0.1	0.2	0.2
Mineral	name formula surface area (m ²)	-	-	sphalerite ZnS 0.1	sphalerite ZnS 0.6	sphalerite ZnS 0.6	pyrite Fe ¹¹ /S ₂ 0.1	quartz SiO ₂ 0.1
		-	-	-	-	-	-	-
Reaction time	days	10	30	10	10	10	10	10
Products	cyclohexene	99.5	92.6	99.1	99.7	94.4	86.4	99.8
	cyclohexane	-	1.03	0.02	0.02	0.08	1.07	-
	benzene	0.05	0.69	0.05	0.09	3.88	1.11	0.004
	methylcyclopentenes	0.20	3.02	0.58	0.02	0.32	5.84	0.02
	methylcyclopentanes	-	1.99	-	-	0.02	3.95	-
	cyclohexanol	0.23	0.51	0.19	0.09	0.56	0.08	0.15
	cyclohexanone	0.01	0.16	0.004	0.04	0.20	1.22	-
	methylcyclopentanol	0.01	-	0.01	0.003	-	0.18	-
	methylcyclopentanone	-	-	-	0.01	0.27	-	-
	cyclohexanethiol	-	-	0.01	0.03	0.17	0.19	-
phenol	-	-	-	-	0.10	-	-	

Table 3.5: The details and results of experiments performed starting from cyclohexene at 300 °C and 85 bar are reported. The yield of each product is expressed as percent abundance with respect to the sum of quantifiable products plus unreacted starting material.

were benzene and cyclohexanol (0.09 %), followed by cyclohexanone and cyclohexanethiol (0.04 and 0.03 %, respectively). Methylcyclopentanone was also detected, whereas the relative abundance of methylcyclopentenes was lower with respect to that measured using the lower quantity of sphalerite (Figure 3.13b). Reaction of 0.1 m cyclohexene in the presence of 0.6 m² sphalerite significantly increased the relative yield of products compared to consumed reactant. Benzene was by far the most abundant product under these conditions (3.88 %) and a small yield of phenol (0.10 %) was also observed (Figure 3.13c).

Reaction of cyclohexene 0.2 m in water with pyrite (0.1 m²) mainly produced methylcyclopentenes and methylcyclopentanes (Figure 3.14a), followed by cyclohexanone (5.84, 3.95, 1.22 %, respectively). Benzene and cyclohexane were produced in quite similar amounts (1.11 and 1.07 %, respectively). Methylcyclopentanol, cyclohexanethiol and cyclohexanol were also detected. Reaction of cyclohexene 0.2 m in water with quartz (0.1 m²) yielded low amounts of cyclohexanol, methylcyclopentenes and benzene (Figure 3.14b).

3. Experiments on organic reactions

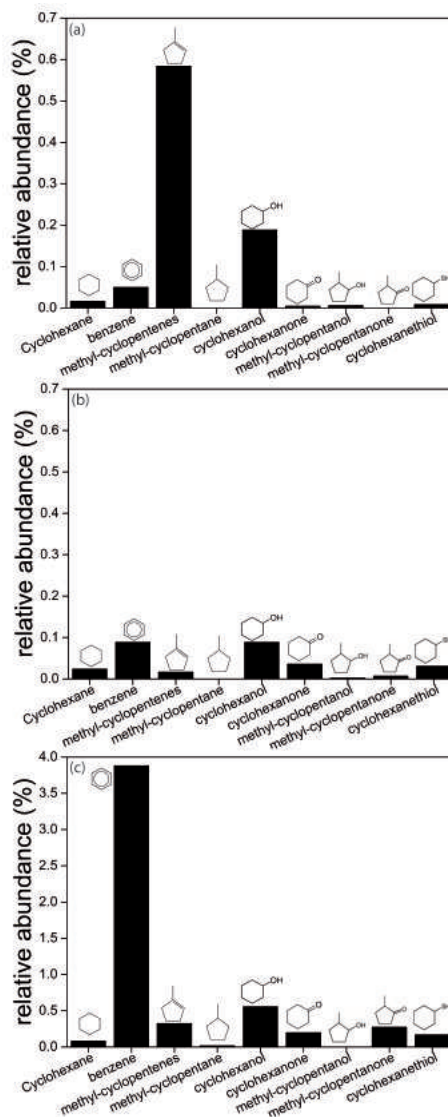


Figure 3.13: Relative abundances (% of total products plus unreacted starting material) of products yielded after 10 days from reaction in water at 300 °C and 85 bar of (a) 0.2 m cyclohexene in the presence of 0.1 m² sphalerite, (b) 0.2 m cyclohexene in the presence of 0.6 m² sphalerite, and (c) 0.1 m cyclohexene in the presence of 0.6 m² sphalerite.

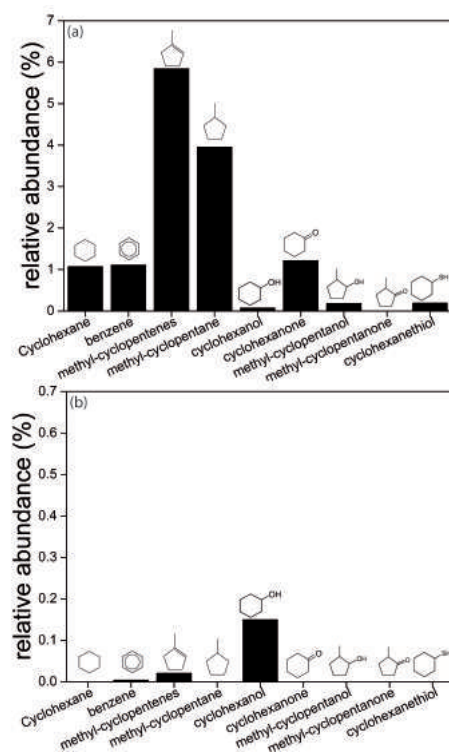


Figure 3.14: Relative abundances (% of total products plus unreacted starting material) of products yielded after 10 days from reaction in water at 300 °C and 85 bar of 0.2 m cyclohexane in the presence of (a) 0.1 m² pyrite, and (b) 0.1 m² quartz.

3. Experiments on organic reactions

3.5 Discussion

The results of the experiments performed at 300 °C in water on normal alkanes yielded cyclohexane after 14 days. Benzene was produced after only 10 days in all the experiments involving cyclic C₆ hydrocarbons, suggesting that (i) the cyclization of normal alkanes and (ii) the aromatization of cycloalkanes and cycloalkenes readily occur under hydrothermal conditions in natural systems, where the reactions of organic materials can occur at even higher temperatures and over longer time periods than those of the current experiments. Experiments carried out with varying reaction times, with added minerals and using different initial compounds (hexane, dodecane, cyclohexane or cyclohexene) gave different product distributions. In particular, the experiment data showed that minerals are likely to play a major role in controlling the aromatization reaction of cyclic C₆ compounds under the experimental hydrothermal conditions.

3.5.1 Reactions in water with no minerals

The main product yielded from the reaction of C₆ and C₁₂ normal-alkanes in water with no mineral catalysts at 300 °C after 14 days was cyclohexane, suggesting that the production of C₆ cyclics from saturated hydrocarbons takes place under hydrothermal conditions. Accordingly, cyclohexane is, as well as cyclic C₅ species, the most commonly cyclic organic compound found in natural fumarolic gases (Tassi, 2004; Tassi et al., 2009; Capecciacci, 2012; Schwandner et al., 2013). Benzene was detected among the products formed from hexane, indicating that the dehydrogenation pathway may further proceed forming aromatic compounds and supporting the hypothesis put forward by Capaccioni et al. (1993). However, the recognition of hexanol among the products formed from dodecane suggests that hydration may compete with the aromatization process, as expected according to the general reaction scheme for organics interconversions (Figure 2.6) proposed by Seewald (2001, 2003).

The production of small amounts of cyclohexene and cyclohexadiene from cyclohexane after 10 days suggests that aromatization to form benzene as

a final product proceeds through a multi-step dehydrogenation mechanism, with cyclohexene and the cyclohexadiene as intermediates (Figure 3.15). The

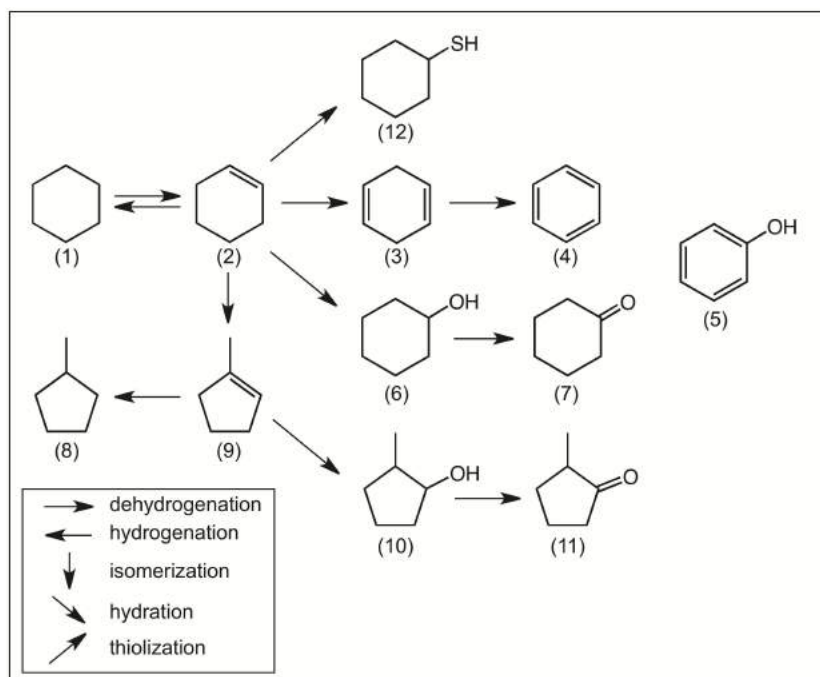


Figure 3.15: A general reaction scheme for the organic transformations consistent with the observed product distributions, involving hydrogenation, dehydrogenation, isomerization, hydration and thiolization reactions. (1) cyclohexane, (2) cyclohexene, (3) cyclohexadiene, (4) benzene, (5) phenol, (6) cyclohexanol, (7) cyclohexanone, (8) methylcyclopentane, (9) methylcyclopentene, (10) methylcyclopentanol, (11) methylcyclopentanone, (12) cyclohexanethiol. Diene (3), alkene (9) and alcohol (10) may be present as more than one structural isomer. Phenol (5) may be formed via more than one pathway, specifically from benzene (4) or cyclohexanol (6), the current data do not allow these pathways to be distinguished.

production of methylcyclohexene and toluene from methylcyclohexane in water at 300 °C after 24 hours (Shipp et al., 2013), may have the same origin, although in that case no diene could be detected.

Experiments carried out with cyclohexene at 300 °C did produce benzene in 10 days. However, the main products under these conditions were cyclohexanol and methylcyclopentenes, suggesting that hydration and isomerization reactions dominate over dehydrogenation (Figure 3.15). This hypothesis was

3. Experiments on organic reactions

confirmed by longer timescale experiments (30 days).

The number of products formed from cyclohexane at 300 °C after 10 days was smaller than that observed with cyclohexene as reactant, pointing to a lower reactivity of cyclohexane under the experimental conditions. This hypothesis is supported by the absence of deuteration of cyclohexane in the experiment performed in heavy water (Table 3.4). The results are consistent with those reported by Crittendon and Parsons (1994), who observed no reaction of cyclohexane in supercritical water (375 °C) after 20 min.

3.5.2 Role of minerals

Experiments on normal-alkanes were replicated at 300 °C and 85 bar in the presence of sphalerite. Differently from what observed in the absence of minerals, benzene was produced from hexane in concentration higher than cyclohexane, suggesting that the presence of sphalerite favoured the dehydrogenation reaction. Contrarily, benzene was not detected among the products resulting from the experiment on dodecane, where hexanol was instead found. Both hexane and dodecane in the presence of sphalerite yielded S-bearing compounds, in particular thiophene and methylthiophene, pointing to the involvement of the mineral (directly or indirectly) to organic reactions. Further information was derived from the experiments on cyclic compounds. The products obtained from the reaction of cyclohexane at 300 °C in the presence of small quantities of sphalerite were slightly different with respect to those obtained from the same reactant in water with no minerals. In particular, in the presence of sphalerite, cyclohexadiene was not detected, presumably because of its high reactivity (e.g. Shipp et al., 2013). The presence of phenol on the other hand, suggested that some oxidation still occurs (Figure 3.15), although detailed reaction pathways cannot be determined from the present data. In contrast to the experiments in heavy water in the absence of minerals, the extensive deuteration of cyclohexane observed in the presence of sphalerite suggests a dramatic enhancement in the reactivity of C-H bonds. Under these conditions, most recovered cyclohexane contained a single deuterium atom. This is consistent with deuteration of

3.5 Discussion

cyclohexane proceeding by cleavage of single C-H bonds rather than via addition of two deuterium atoms to cyclohexene, which would result in the incorporation of pairs of deuterium atoms from the solvent. In laboratory experiments performed at 300 °C and 100 MPa, Shipp et al. (2014) demonstrated that the addition of sphalerite dramatically increased the kinetics of the stereoisomerization reaction of cis- and trans-1,2-dimethylcyclohexane, suggesting that the mineral efficiently acted as a catalyst through a surface-catalyzed mechanism. These observations are consistent with our results. In analogy with the previous suggestion (Shipp et al., 2014), the active sites on the sphalerite surface presumably interact with the cyclohexane to weaken or break the C-H bonds via formation of a surface-bound intermediate that is able to bond to a deuterium atom derived from the solvent (Figure 3.16). Repetition of this process would be expected to result in the incorpora-

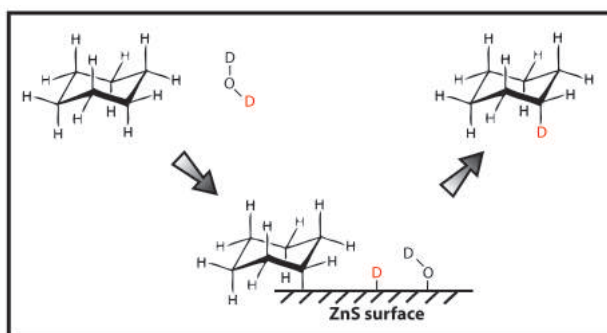


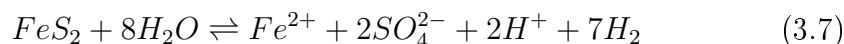
Figure 3.16: Surface-catalyzed mechanism operated by sphalerite and leading to the incorporation of a single deuterium atom in the cyclohexane structure, as described in the text (figure modified from Shipp et al., 2014).

tion of a progressively increasing number of deuterium atoms (Shipp et al., 2014). Accordingly, cyclohexane incorporating up to four deuterium atoms was found in reactions in heavy water with sphalerite. A surface-catalyzed reaction mechanism was suggested by the enhanced conversion of both the cyclohexane and cyclohexene experiments with sphalerite, presumably via C-H bond cleavage, with increasing the sphalerite surface area. More isomerization and hydration of cyclohexene to form methylcyclopentenes and cyclohexanol (Figure 3.15) was observed at the lower sphalerite/cyclohexene

3. Experiments on organic reactions

ratios, since these reactions proceed even in the absence of minerals. On the other hand, aromatization of cyclohexene to benzene was observed to be the dominant reaction pathway at higher sphalerite/cyclohexene ratios, consistent with a catalytic role for sphalerite in the aromatization reaction. However, the observation of cyclohexanethiol as a product of reaction of cyclohexene in the presence of sphalerite also suggests that the mineral can act as a reagent under experimental conditions. Therefore, sphalerite not only can enhance the reactivity of organic compounds, but it can apparently participate to reactions of organic compounds, as previously suggested on the basis of the production of S-bearing compounds from normal alkanes. In fact, the presence of sulphur-containing organic products implies the involvement of mineral-derived dissolved sulphur in solution that can act as a reactant, perhaps in the form of H_2S (Figure 3.15). The increasing production of the sulphur-bearing compounds at increasing sphalerite/cyclohexene ratios for the 0.2 m cyclohexene experiments may be the result of increasing fH_2S (or increasing concentration of other soluble sulphur species) and/or the increasing number of available active sites on the sphalerite surface if the reaction is surface catalyzed.

Cyclohexanethiol production from cyclohexene was also observed in the presence of pyrite. In this case, isomerization of cyclohexene to methylcyclopentenes and subsequent hydrogenation to form methylcyclopentanes was likely the main reaction pathway under experimental conditions (Figure 3.15). Hydration products including methylcyclopentanol and cyclohexanol were observed, but this was not a major pathway in the presence of pyrite. Benzene and cyclohexane were produced in similar amounts, consistent with enhanced C-H bond activation similar to sphalerite. The observed hydrogenation may be related to the oxidation of pyrite, i.e. by the oxidation of sulphur to sulphate (3.7) and/or by the successive oxidation of ferrous iron to ferric iron (3.8), as follows:



3.6 Concluding remarks

Experiments carried out in the presence of iron oxide minerals (hematite and magnetite) demonstrated the formation of benzene from cyclohexane. Interestingly, the benzene/cyclohexene ratios in the presence of these oxide hematite and magnetite were significantly higher with respect to those where sphalerite was added, suggesting that iron oxides may be quite efficient in enhancing reactivity and that further work with these minerals is to be taken into account. In contrast, experiments in the presence of quartz showed no evidence of enhanced reactivity compared to those carried out in the absence of mineral catalysts. In fact, quartz may have reduced the reactivity of cyclohexene, as suggested by the somewhat lower benzene/cyclohexene ratio for reaction starting with cyclohexane and the slightly lower yields of products observed starting cyclohexene.

3.6 Concluding remarks

The capability of dehydrocyclization processes to occur under hydrothermal conditions, as expected on the basis of thermodynamic calculations and empirical observations, was proven by the results of the specifically designed experiments here presented, confirming the hypothesis proposed by Capaccioni et al. (1993) who suggested the occurrence of benzene production from normal- and cyclic-alkanes in natural hydrothermal environments. Cyclohexane was obtained from both C₆ and C₁₂ normal-alkanes, while benzene production starting with cycloalkanes was found at 300 °C. The observed product distributions were consistent with a reaction pathway characterized by multi-step dehydrogenations, with cycloalkenes and cyclic dienes as intermediate products. Although further experiment work is necessary to determine the detailed reaction kinetics and to more definitely define the reaction pathways, the data of the present study demonstrated that starting with cyclic hydrocarbons, aromatization prevails over other reaction pathways that yield alcohols and ketones proposed by Seewald (2001). Benzene production was observed even in the absence of catalyzing minerals, as expected on thermodynamic grounds. However, minerals, in particular sulphides (sphalerite and pyrite) and iron oxides (magnetite and hematite), gave significantly higher

3. Experiments on organic reactions

yields of benzene and clearly enhanced the reactivity of alkanes and cycloalkanes. In particular, sphalerite efficiently increased the reactivity of C-H bonds, presumably via a surface-catalyzed mechanism, and also participated in organic reactions as an indirect reactant in the production of cyclohexanethiol. The latter was also produced from cyclohexene in the presence of pyrite. Similarly, thiophene and methylthiophene were obtained from hexane and dodecane in the presence of sphalerite. The absence of thiophenes in experiments involving cyclic compounds suggests that the formation of these species likely occurs through the incorporation of sulphur prior to cyclization of the organic molecule. Eventually, although quartz exhibited virtually no catalytic effect on organic reactivity, hematite and magnetite significantly enhanced the conversion of cyclohexane to benzene, even more efficiently than sphalerite.

These experiments demonstrated that benzene is effectively and efficiently produced at hydrothermal conditions through cyclization of normal alkanes and subsequent dehydrogenation of cyclic organic structures. Moreover, they highlighted the crucial role played by minerals in this process, suggesting that iron oxides and sulphides may act as suitable catalysts and participate as reactants in organic reactions under hydrothermal conditions.

The experiments here presented produced useful insights into the reactivity of VOCs. Although they represent simplified systems, experimental results provided valuable clues for understanding the primary processes governing the distribution of VOCs in hydrothermal fluids from natural systems and the response of organics to variable physicochemical conditions.

Chapter 4

Study areas

4.1 Introduction

In order to investigate VOCs variability over a wide range of environmental conditions, four study areas displaying different physical and chemical conditions, were selected among the Mediterranean hydrothermal systems, including (*i*) hydrothermal systems associated with active volcanoes, i.e. Solfatara Crater (Campi Flegrei, Southern Italy) and Nisyros Island (Greece), and (*ii*) low-to-medium enthalpy hydrothermal systems, associated with quiescent volcanism, feeding cold gas emissions in Central Italy, i.e. Poggio dell'Olivo (Viterbo) and Cava dei Selci (Alban Hills, Rome). Gases were sampled from hydrothermal degassing vents, i.e. fumarolic discharges and bubbling pools, and soils at sites characterized by variable soil diffuse degassing.

In the following sections, the geological setting and geochemical features for each study area and the sampling strategy adopted during the campaigns are described in detail.

4. Study areas

4.2 Active volcanoes-related hydrothermal systems

4.2.1 Solfatara Crater

The Solfatara Crater is a 0.6 km wide tuff cone located NE of the town of Pozzuoli at 180 m a.s.l. (Bruno et al., 2007). The crater formed about 3.9 ka BP within the Campi Flegrei caldera (Figure 4.1a), an active volcanic field of about 100 km² NW of Naples (Southern Italy).

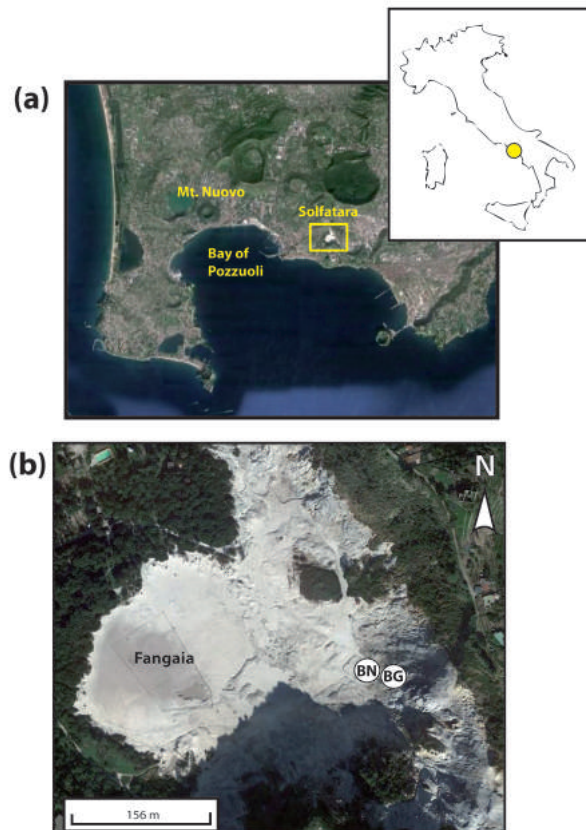


Figure 4.1: **(a)** Location of the Solfatara Crater (yellow rectangle) within the Campi Flegrei caldera (Italy); **(b)** satellite photo of the Solfatara Crater: the location of *(i)* main fumarolic discharges, i.e. Bocca Grande (BG) and Bocca Nuova (BN) and *(ii)* Fangaia mud pool are reported.

4.2 Active volcanoes-related hydrothermal systems

The Campi Flegrei caldera is one of the most dangerous volcanic areas in the world, as it hosts Pozzuoli and numerous densely populated villages and moreover, it is just a few kms west of Naples (Chiodini et al., 2010a). The caldera structure formed during two large eruptions: the Campanian Ignimbrite (39 ka; De Vivo et al., 2001) and the Neapolitan Yellow Tuff (14.9 ka; Deino et al., 2004). The last eruptive event occurred in 1538 AD (Di Vito et al., 1987), after about 3,000 years of quiescence, producing the monogenic tuff cone of Monte Nuovo (Figure 4.1a). The Campi Flegrei caldera is known for frequent episodes of ground uplift and subsidence, accompanied by seismic activity. These *bradyseismic events* (from the ancient Greek words “bradus” and “seism”, meaning “slow movement”) have repeatedly occurred during the past century, with two main uplift phases in 1968-1972 and in 1982-1984 (Caliro et al., 2007; Todesco et al., 2003), the latter episode causing the partial evacuation of Pozzuoli. According to some authors (e.g. Corrado et al., 1977; Berrino et al., 1984; Dvorak and Berrino, 1991; Berrino, 1994), these episodes were related to mass/density/pressure changes within the magmatic reservoir, whereas other authors (e.g. Bonafede and Mazzanti, 1998; Chiodini et al., 2003; Battaglia et al., 2006; Gottsmann et al., 2006) concluded that the bradyseismic episodes were caused by fluid pressure variations within the subsurface hydrothermal system. The Campi Flegrei caldera has recently given signs of potential reawakening, i.e. increased magmatic component in the fumaroles, more frequent seismic swarms and an accelerating ground uplift trend (Chiodini et al., 2012). These events, suggesting a possible resuming of the volcanic activity, have been supposedly ascribed to two overlapping processes: (i) short-time episodes of gas pressurization caused by injection of magmatic fluids into the hydrothermal system, and (ii) a long-period progressive heating of the system (Chiodini et al., 2015).

The Solfatara Crater (Figure 4.1b) is the most prominent surface hydrothermal evidence of the Campi Flegrei volcanic area. It was known to the Romans as the *Forum Vulcani* (or in Greek *Agora of Hephaistos*, home of the god of fire), as it was named by Strabone in its “*Strabonis geographica*”. This crater hosts one of the largest fumarolic fields in the world and a significantly large soil degassing area. The main fumarolic discharges from the Solfatara Crater

4. Study areas

are Bocca Grande and Bocca Nuova (Figure 4.1b), with temperatures of ~ 165 and ~ 155 °C, respectively (Vaselli et al., 2011), although several fumarolic vents are present in the crater, especially in its NE and SE sectors. A bubbling mud pool, named Fangaia, with a temperature < 50 °C and a pH < 2 , is hosted at the centre of the crater (Figure 4.1b).

About 460 ± 160 tons of CO_2 are emitted daily by the fumarolic emissions (Aiuppa et al., 2013), whilst 113 t d^{-1} of hydrothermal CO_2 are released through diffuse soil degassing (Cardellini et al., 2003). Chiodini et al. (2001) calculated a value of $1.19 \times 10^{13} \text{ J d}^{-1}$ for the thermal energy related to the diffuse soil degassing at the Solfatara Crater, i.e. one order of magnitude higher than the conductive heat flux released through the whole Campi Flegrei caldera ($1 \times 10^{12} - 1.5 \times 10^{12} \text{ J d}^{-1}$; Corrado et al., 1998). The anomalously high diffuse CO_2 degassing from the soil (e.g. Tedesco and Scarsi, 1999; Chiodini et al., 2001, 2005; Caliro et al., 2007; Granieri et al., 2003, 2010; Tassi et al., 2013b), evidenced by the lack of vegetation in most of the crater area, occurs together with a significant emission of CH_4 and C_6H_6 (Cardellini et al., 2003; Castaldi and Tedesco, 2005; Tassi et al., 2013b).

The physicochemical features of the hydrothermal-magmatic system feeding the fluid emissions at the Solfatara Crater were investigated since the 1980s (e.g. Cioni et al., 1984, 1989). According to Caliro et al. (2007), the Solfatara fumaroles discharge a mixture of magmatic gases (about 26 %) and hydrothermal fluids (about 74 %), as the results of the degassing from a magma body (at about 5 km depth; Gottsmann et al., 2006) and the boiling of the overlying aquifer(s). The magmatic fluids, rich in CO_2 ($X_{\text{CO}_2} \sim 0.4$) and a steam characterized by an isotopic composition similar to ‘andesitic’ water type ($\delta\text{D} \sim -20$ ‰, $\delta^{18}\text{O} \sim 10$ ‰; Taran et al., 1989), mix with meteoric-originated hydrothermal liquids at the bottom of the hydrothermal system (2,000-2,500 m depths), generating vapours at temperature and pressure of ≥ 360 °C and 200-250 bar, respectively (Caliro et al., 2007). Below this mixing zone, magmatic conditions, i.e. high temperatures and presence of oxidized acid species (SO_2 , HCl , HF), prevail, whereas hydrothermal conditions dominate the upper zone favouring the formation of reduced gas species (e.g. CH_4 and H_2S) and the disappearance of the acidic oxidant magmatic

4.2 Active volcanoes-related hydrothermal systems

species (Caliro et al., 2007). According to the model proposed by Caliro et al. (2007), the central column of ascending fluids is characterized by the presence of a separated vapour phase that moves from the high temperature injection zone to a shallow single phase gas zone (spgz) at temperatures ranging from 190 to 230 °C and 100-300 m depths (Figure 4.2). These physic-

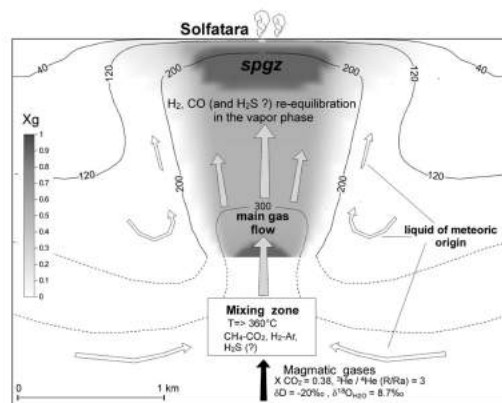


Figure 4.2: Geochemical conceptual model of the Solfatara volcanic-hydrothermal system according to Caliro et al. (2007).

ochemical conditions were also indicated by the chemical composition of light alkanes and alkenes in the Solfatara fumaroles, although the origin of most VOCs recognized in these fluids (e.g. Capaccioni and Mangani, 2001; Vaselli et al., 2011) is basically considered as related to organic matter buried in the sedimentary formations embedding the magmatic-hydrothermal system (Capaccioni and Mangani, 2001; Tassi et al., 2010; Fiebig et al., 2013).

Sampling strategy

Two sampling campaigns were conducted in the Solfatara Crater. The first sampling campaign was performed in September 2013 and it was mainly devoted to (i) the study of the spatial variability of the composition of interstitial soil gases within the crater and (ii) the comparison between the chemical features of soil gases and fumarolic discharges. In particular, fumarolic gas samples were collected from the two main vents, i.e. Bocca Grande and Bocca Nuova, while 52 sites were selected within the crater floor in order to perform

4. Study areas

(i) measurements of the soil CO₂ and CH₄ gas fluxes, and (ii) sampling of interstitial soil gases at 30 cm depth (Figure 4.3). The sampling sites were chosen in the field after a preliminary evaluation of the soil CO₂ gas flux in order to cover a wide range of physical and chemical conditions.

The second sampling campaign, carried out in January 2016, was aimed at investigating the VOCs degradation processes occurring at very shallow depths and likely related to the interplay between soil gases and microbiological communities. Five sampling sites affected by different soil degassing of hydrothermal fluids were selected (Figure 4.4) for the collection of interstitial soil gases at 10 and 30 cm depth along vertical profiles. The campaign was developed in the framework of a project entitled “*A geomicrobiological study on soils and sediments affected by hydrothermal fluids from Solfatara Crater (Campi Flegrei, Italy): life adaptation in extreme environments*” (in progress; see Appendix C), which was one of the selected proposals for the Census of Deep Life (CoDL) Sequencing Opportunities 2016 Phase 8 (<https://deepcarbon.net/content/deep-life>).

4.2 Active volcanoes-related hydrothermal systems

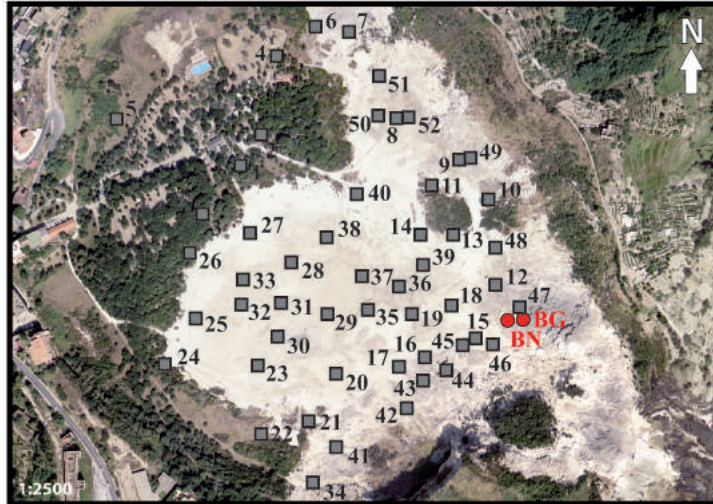


Figure 4.3: Location of the sampling sites for (i) fumarolic gases (red circles; BG= Bocca Grande, BN = Bocca Nuova) and (ii) 52 interstitial soil gases at 30 cm depth (grey squares) referred to the sampling campaign carried out in September 2013.

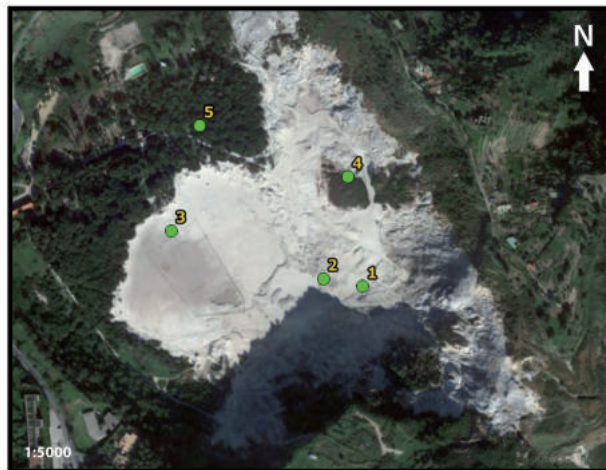


Figure 4.4: Location of the five sampling sites where interstitial soil gases at 10 and 30 cm depths (green circles) were collected in the sampling campaign carried out in January 2016.

4. Study areas

4.2.2 Nisyros Island

Nisyros Island is a Quaternary stratovolcano located in the Aegean Sea (Greece), at the easternmost edge of the South Aegean active volcanic arc (SAAVA; Figure 4.5a). The SAAVA, formed by the subduction of the conti-

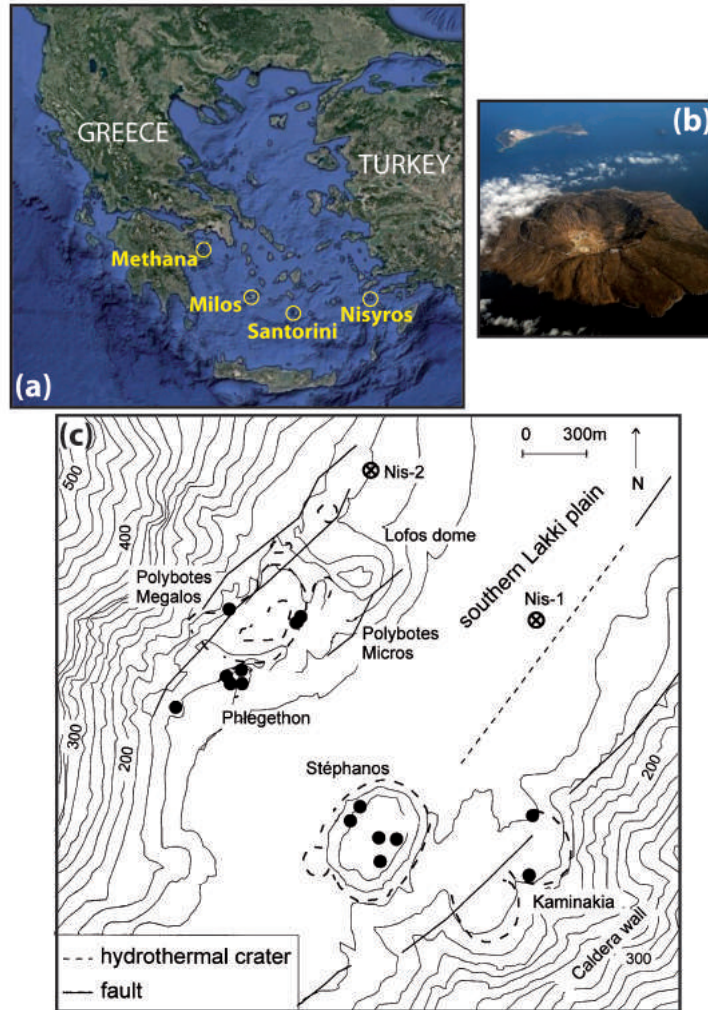


Figure 4.5: (a) Location map and (b) aerial photograph of Nisyros Island. The location of main hydrothermal craters is shown (c) together with the location of fumaroles (filled circles) and geothermal wells Nis-1 and Nis-2 (circles with a cross; from Brombach et al., 2003).

mental African crust beneath the Aegean-Anatolian plate, extends from the Gulf of Saronikos (Susaki, Aegina, Methana, Poros) to the West to Nisy-

4.2 Active volcanoes-related hydrothermal systems

ros, Yali and Kos close to the Anatolian coast to the East, through Milos, Santorini, Christiana and Kolumbo in the central part (Figure 4.5a; Francalanci et al., 2005). The volcanic activity of the SAAVA started in the Lower Pliocene at Aegina (4.7 Ma) in the northwest and lasted until historic times at Methana, Milos, Santorini, Kolumbo and Nisyros (Pe-Piper and Piper, 2005).

Nisyros Island has a truncated cone shape, with a base diameter of 8 km and a surface area of about 42 km² (Figure 4.5b). The island built up on a basement of Mesozoic limestones and Neogene sediments during the last 100 ka (Brombach et al., 2003 and references therein). Five major phases were distinguished in the evolution of Nisyros Island: (1) a submarine volcano erupting basaltic and andesitic pillow-lavas, (2) a 500-700 m high subaerial stratovolcano grown up in more than 100 ka, (3) several eruptive phases with gas and steam explosions followed by two major rhyodacitic plinian eruptions with the emplacement of pumice fall and pyroclastic flow deposits (<30 ka), (4) a major collapse of the volcano forming a large (4 km in diameter) summit caldera, namely Lakki Plain, at <20 ka, and (5) a post-caldera stage characterized by the extrusion of a series of rhyodacitic domes in the western part of the caldera (Tibaldi et al., 2008 and references therein).

No magmatic activity is known to have occurred in the last 25 Ka (Hurni et al., 2005). However, an active high-temperature hydrothermal system is present underneath the Lakki Plain. Several phreatic explosions formed a series of hydrothermal craters in the southern part of the Lakki Plain, such as Kaminakia, Polybotes, Stephanos and Phlegethon (Figure 4.5c), which presently host a widespread fumarolic activity and extended zones characterized by anomalously high diffuse degassing (e.g. Chiodini et al., 2002; Cardellini et al., 2003; Caliro et al., 2005). The most recent hydrothermal eruptions occurred in the 19th century (1871-1873 and 1888), forming the craters of Polybotes and Phlegethon, and Polybotes Micros, respectively, partly destroying the Lofos dome (Marini et al., 1993 and references therein). More recently, during 1996-1998, Nisyros experienced an intense seismic crisis (Papadopoulos et al., 1998), accompanied by ground deformation (Lagios et al., 2005) and changes in the chemistry of fumarolic gases (Chiodini et al.,

4. Study areas

2002), pointing to a renewed unrest, so that Nisyros volcano has been ranked in the “Very High Treat (VHT)” category (Kinvig et al., 2010).

Direct information on the hydrothermal system was retrieved from two deep geothermal wells (Nis-1 and Nis-2; Figure 4.5c) drilled in the southern part of the Lakki Plain (Geotermica Italiana, 1983, 1984). Differences in the stratigraphic logs of the two boreholes suggested a deepening of the caldera depression towards its centre (Brombach et al., 2003). The terrains encountered by the two wells consisted of (i) alluvial, lacustrine and tephra deposits up to 600 and 1,000 m thick in Nis-1 and Nis-2, respectively, (ii) carbonate rocks, found at >1,000 m depth in Nis-1 and not present in Nis-2, and (iii) diorites with associated thermometamorphic rocks at 1,816 m in Nis-1 and underneath the sedimentary-volcanic series in Nis-2. The geological cross-section through the two geothermal wells is shown in Figure 4.6.

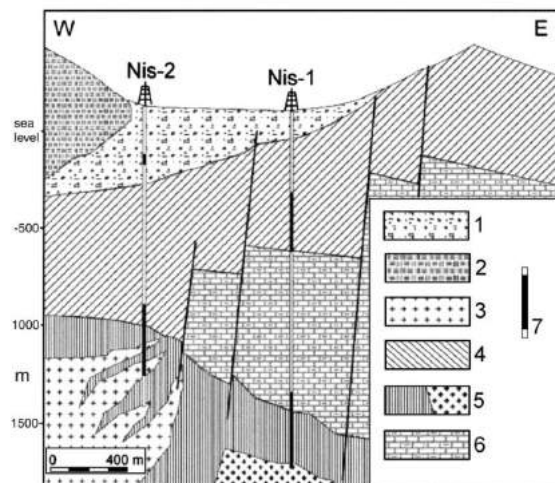


Figure 4.6: Geological section through the two deep geothermal wells Nisyros 1 and Nisyros 2 (from Geotermica Italiana, 1984). Symbols as follows: 1= Talus and alluvial debris filling the caldera depression; 2= Post-caldera dacitic-rhyodacitic domes; 3 = Subintrusive quartz-dioritic rocks, probably related to post-caldera activity; 4 = Andesitic to dacitic tephra and lavas; 5 = Diorites and thermometamorphic rocks related to the composite volcano magma chamber; 6 = Carbonate rocks and thermometamorphic marbles; 7 = Permeable intervals in geothermal wells.

Two distinct hydrothermal aquifers were recognized, consisting of (i) a shal-

4.2 Active volcanoes-related hydrothermal systems

low permeable zone (from 431 to 695 m depth in Nis-1 and from 30 to 365 m depth in Nis-2), characterized by a phyllitic-zeolitic hydrothermal mineral paragenesis likely produced at 120-180 °C, and (ii) a deep aquifer (found at 1,421 - 1,816 m depth in Nis-1 and at 1,070 - 1,360 m depth in Nis-2), characterized by a high temperature propylitic hydrothermal mineral assemblage (Geotermica Italiana, 1983, 1984; Brombach et al., 2003; Caliro et al., 2005; Ambrosio et al., 2010). Maximum temperatures of 340 and 320 °C were measured at the bottom of Nis-1 (1,816 m depth) and Nis-2 (1,547 m depth) wells, respectively. The deep hydrothermal reservoir has 81.5 g/L of Cl, whereas the shallow aquifer has a chloride content close to that of seawater (Chiodini et al., 1993). Although the hydrothermal system of Nisyros is mainly fed by seawater, partial contribution from arc-type magmatic water was also suggested on the basis of δD and $\delta^{18}O$ values of fumarolic condensates (Brombach et al., 2003). Vapours from the shallow aquifer feed the fumarolic vents in the southern portions of the Lakki Plain (Chiodini et al., 1993; Ambrosio et al., 2010). Accordingly, the fumaroles have outlet temperatures close to the boiling point of water and compositions dominated by H₂O, CO₂, H₂S with minor amounts of N₂, H₂, CH₄, CO, Ar, and He, whereas strongly acidic gases (i.e. SO₂, HCl, HF) are absent (Chiodini et al., 1993). The organic fraction of hydrothermal gases discharged from the fumarolic vents, dominated by aromatics and alkanes, was interpreted as mainly related to thermogenic degradation of organic matter (Tassi et al., 2013a), although abiotic processes were also invoked (e.g. Fiebig et al., 2007; 2009).

As hydrothermal fluids approach the surface, vapour condensates partly flow from the hydrothermal craters area towards the northern and southern coasts of the island, contributing to feed the thermal springs (Chiodini et al., 1993; Brombach et al., 2003; Ambrosio et al., 2010). Steam condensation also produces altered terrains and thermal anomalies in the craters area. The same zones are characterized by a significant CO₂ soil degassing, quantified in 67.9 t d⁻¹ and corresponding to a total thermal energy flux in the order of 43 MW (Caliro et al., 2005). Tectonic structures play a major role in controlling the hydrothermal fluids uprising. NE-SW elongated CO₂ anomalies were

4. Study areas

recognized on the basis of soil flux measurements, corresponding to brittle structures (Caliro et al., 2005). Similarly, hydrothermal craters are aligned along two narrow NE-SW directed zones, corresponding to a main active fault system in Nisyros, associated with a main E-W extension (Caliro et al., 2005; Tibaldi et al., 2008). Deep-reaching faults and fractures likely act as uprising channels for the deep fluids. The main upflowing zones were recognized in the hydrothermal craters of Stephanos, Kaminakia and Phlegethon and at the southeastern base of the Lofos dome (Brombach et al., 2001; Caliro et al., 2005).

Sampling strategy

The sampling campaign at Nisyros Island was conducted in June 2015. Fumarolic gases were sampled from 5 discharges located within Phlegethon, Kaminakia, Stephanos and Micros Polybotes craters and Lofos dome (Figure 4.7). Five soil gas samples were collected in selected sites from the same areas (Figure 4.7) at 20 or 40 cm depth. CO₂ soil flux measurements were also carried out.

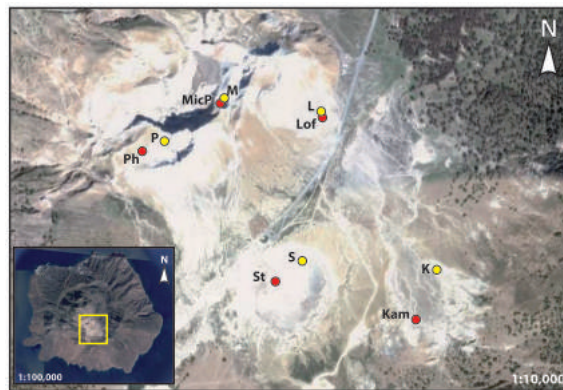


Figure 4.7: Location of sampling sites for (i) fumarolic gases (red circles), and (ii) interstitial soil gases (yellow circles) referred to the sampling campaign carried out in June 2015.

4.3 Medium-low enthalpy hydrothermal systems

4.3.1 General settings

Areas of quiescent volcanism and seismically active zones are often characterized by cold CO₂-rich gas manifestations (e.g. Kerrick et al., 1995; Evans et al., 2002; Lewicki et al., 2003; Bergfeld et al., 2006; Doğan et al., 2009; Gal and Gadalia, 2011; Kämpf et al., 2013). These emissions differ from both volcanic and geothermal discharges since CO₂ is the main constituent of the gas phase, rather than H₂O. Such manifestations characterize the western sector of Central Italy, in particular Southern Tuscany, Northern Latium and Campania. This area, extending from the Apennine chain to the Tyrrhenian Sea and from the Larderello geothermal field in Tuscany to the Alban Hills volcanic complex in Latium (the Tuscan Roman Degassing Structure: TRDS) and from Southern Latium to Southern Campania (the Campanian Degassing Structure: CDS; Figure 4.8; Chiodini et al., 2004b), is affected by extensive CO₂ degassing, resulting in (*i*) high pCO₂ in groundwater and soda springs (Chiodini et al., 1995, 1999, 2000; Minissale, 2000; Gambardella et al., 2004; Frondini et al., 2008), (*ii*) CO₂-rich gas manifestations (Chiodini, 1994; Minissale, 2000; Rogie et al., 2000; Chiodini, 2008) and high diffuse CO₂ soil degassing (Chiodini et al., 1995, 1999; Chiodini and Frondini, 2001; Chiodini et al., 2004b; Frondini et al., 2008; Carapezza et al., 2012).

According to Chiodini et al. (2004b), in the TRDS a large portion of the CO₂ degassed at the surface or dissolved in ground waters is derived from a deep mantle-related source, which would account for a total CO₂ release of 1.4×10^{11} mol/y. The recycling of sedimentary limestone deposits via subduction of Adriatic Plate and the subsequent thermal decomposition of carbonates into the mantle would be the main responsible process for the regional CO₂ degassing in Central-Southern Italy affecting non-volcanic areas (Chiodini et al., 2000, 2004b, 2013), although carbonate assimilation in the upper crust might represent an important supplementary mechanism of CO₂ production in active volcanic zones (Iacono Marziano et al., 2007).

The huge degassing is favoured by the geological features of the Tyrrhe-

4. Study areas

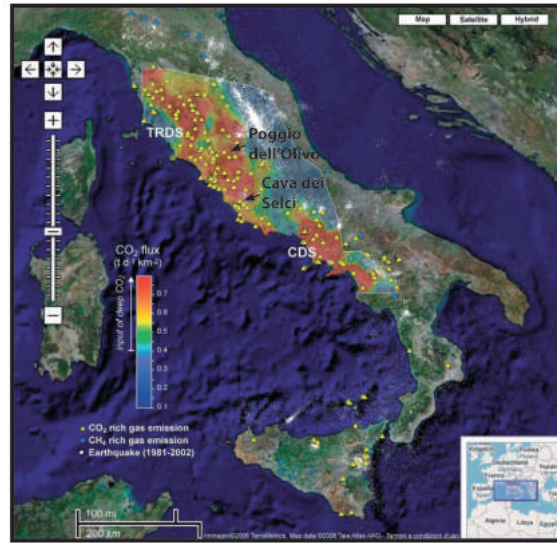


Figure 4.8: Location of the CO₂- and CH₄-rich gas emissions archived in GOOGAS (yellow and blue triangles) and CO₂ degassing map (color scale; after Chiodini, 2008). The location of Poggio dell'Olivo and Cava dei Selci is shown.

nian margin of the Italian peninsula, including (*i*) crustal thinning (<25 km; Scrocca et al., 2003), (*ii*) seismic activity (Frepoli and Amato, 1997; Mariucci et al., 1999; Chiodini et al., 2004b and references therein), (*iii*) Quaternary volcanism (i.e. a sequence of NW-SE aligned volcanic complexes, including Mt. Amiata, Latera, Vulsini, Cimino, Vico, Sabatini, Alban Hills; Mattei et al., 2010) and (*iv*) high heat flow (>80 mW/m², and locally higher than 200 mW/m²; Cinti et al., 2014 and references therein).

The post-orogenic extensional tectonic regime, related to the opening of the Tyrrhenian basin, was responsible for both intense magmatic activity (Barberi et al., 1971; Marinelli, 1975; Civetta et al., 1978; Mattei et al., 2010) and NW-SE trending fault systems (Acocella and Funicello, 2006 and references therein), which spatially control the distribution of soil-gas anomalies (e.g. Chiodini et al., 1995; Beaubien et al., 2003). Chiodini et al. (1995) evidenced a clear correspondence between high pCO₂ in ground waters and Bouguer positive gravity anomalies, which were interpreted as related to buried structural highs of the carbonate basement. Apenninic (NW-SE) and

4.3 Medium-low enthalpy hydrothermal systems

anti-Appenninic (NE-SW) trending horsts and grabens characterize the Mesozoic carbonate-evaporite formations of the Tuscan series, which are overlaid by clays, shales and marls of the Ligurian units and Neoautochthon complex and volcanic deposits (Fron dini et al., 2008). The low-permeability cover favours the accumulation of CO₂, mainly as dissolved phases, in the aquifer hosted in the Mesozoic limestone formations, producing pressurized reservoirs (Figure 4.9). When pCO₂ of the deep fluid exceeds the hydrostatic

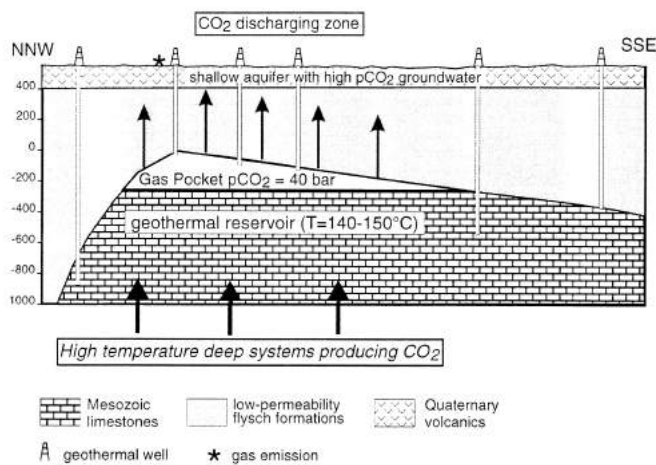


Figure 4.9: Degassing model of one of the geothermal fields from Central Italy (Torre Alfina; from Chiodini et al., 1999).

pressure, gas-liquid separation occurs and the gas phase may escape toward the surface through the permeable pathways offered by extensional faults and fractures (Chiodini et al., 1995), as confirmed by sudden increases of the gas emissions associated with seismic activity (e.g. Chiodini et al., 2004b; Heinicke et al., 2012). In the correspondence of these permeable structures, the main emission sites of TRDS are found (e.g. Chiodini, 2008), including Poggio dell’Olivo and Cava dei Selci (Figure 4.8).

4. Study areas

4.3.2 Poggio dell'Olivo

Poggio dell'Olivo is an area of about 1.5 km² located at about 3 km W-SW of the Grotte Santo Stefano village and few tens of km NE of Viterbo (Latium, Central Italy; Figure 4.10), on the eastern side of Vezza Creek.

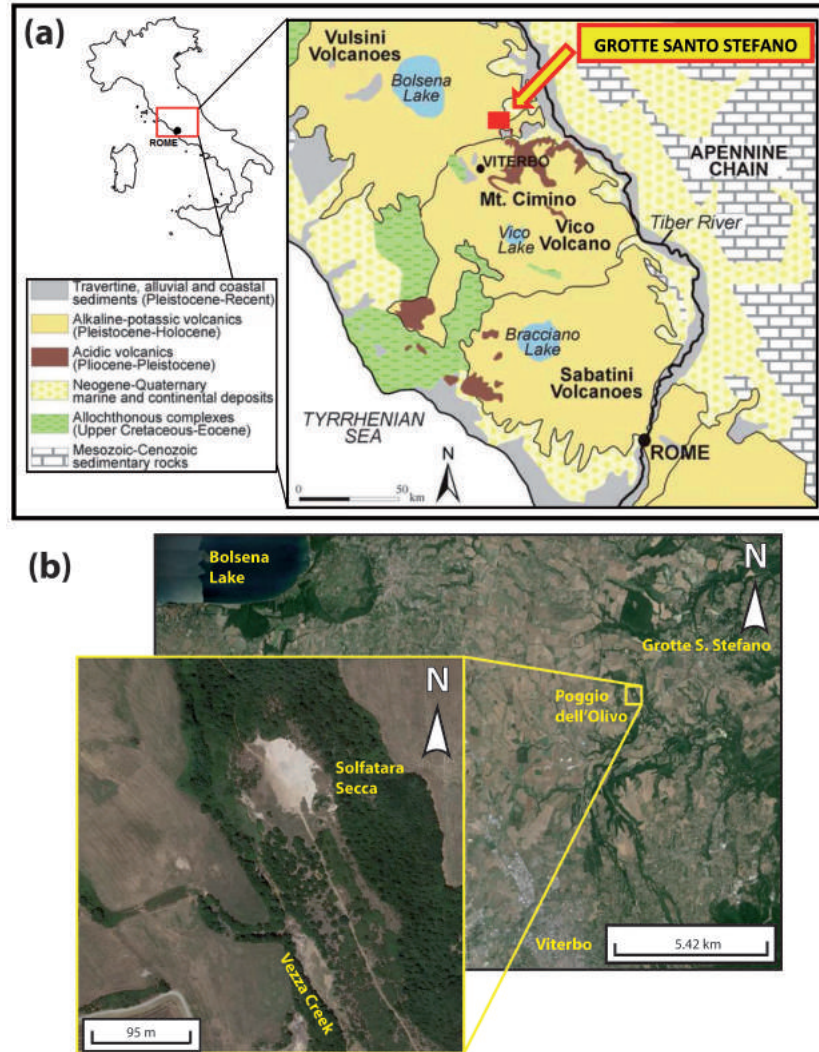


Figure 4.10: (a) Schematic map of Central Italy (modified from Baiocchi et al., 2012) with the location of the study area (red square); (b) satellite image of the Poggio dell'Olivo site, showing in the inset the Vezza creek and the main degassing area of Solfatara Secca.

This area, characterized by intense diffuse cold degassing and cold bubbling

4.3 Medium-low enthalpy hydrothermal systems

gas manifestations along the stream (Chiodini, 1994), is situated within the Vicano-Cimino Volcanic District (VCVD).

The VCVD is a hydrothermally active area of approximately 1,400 km² extending from the Apennine chain to the Tyrrhenian Sea (Figure 4.10a) in Central Italy, where cold gas discharges and thermal springs, related to the Quaternary magmatic activity of the Vicano and the Cimino volcanoes, occur.

The Cimino and Vicano volcanic complexes were active from 1.35 to 0.94 Ma (Nicoletti, 1969) and from 0.42 to 0.09 Ma (Laurenzi and Villa, 1987), respectively. The former consists of rhyodacite domes, ignimbrites, latitic and olivine-latitic lavas (Lardini and Nappi, 1987; Cimarelli and De Rita, 2006). The latter, a stratovolcano developed on a NW-SE elongated graben with a central depression caldera presently hosting Lake Vico, consists of fall deposits, lava and pyroclastic flows with leucitites, phono-tephrites and leucite-phonolites (Perini et al., 2000). The volcanic products lie on a sedimentary sequence consisting of, from the top to the bottom, (i) Plio-Pleistocene conglomerates, sandstones and mudstones, (ii) Cretaceous-Oligocene Ligurian and Sub-Ligurian units and (iii) Mesozoic carbonates overlying the Triassic evaporitic Burano Fm. (Cinti et al., 2014). The Mesozoic unit hosts a regional hydrothermal reservoir, which is responsible for the presence of widespread thermal emissions, mineral springs and diffuse soil degassing areas in the VCVD. The water-dominated reservoir has a SO₄-HCO₃ composition at about 220 °C (Cinti et al., 2014). NW-SE-trending extensional faults, and NE-SW-trending transtensive/transfer structures, developed during post-collisional extension in Plio-Quaternary (Barberi et al., 1994; Cinti et al., 2014 and references therein), provide the permeable pathways for the uprising of the deep-seated fluids towards the surface (Minissale, 2004, and references therein). During their ascent, hydrothermal fluids eventually mix with a cold, shallow and mainly unconfined regional aquifer hosted in the volcanic deposits and separated from the deep reservoir by the low-permeable Plio-Pleistocene deposits and/or the Ligurian and Sub-Ligurian units (Baiocchi et al., 2006; Cinti et al., 2014).

In the study area, vigorous and structurally controlled CO₂-rich gas bub-

4. Study areas

bling sites occur in the Vezza Creek, the stream being imposed along a NW-striking, SW-dipping high-angle normal fault (Cinti et al., 2014). Strong CO₂ diffuse degassing (estimated to be 200×10^3 kg d⁻¹; Chiodini et al., 1999) characterizes the Poggio dell'Olivo area, inhibiting the growth of a vegetative cover in several zones (Figure 4.10b). Relatively high CO₂ fluxes (30×10^3 kg d⁻¹) were measured in a relatively small area (19,600 m²) called Solfatara secca (Figure 4.10b; Chiodini et al., 1999). The NW-SE orientation of the highest fluxes confirms the fault control on the gas emissions (Chiodini et al., 1995, 1999).

The CO₂-dominated hydrothermal fluids discharged from the VCVD are mainly produced by thermometamorphic reactions (e.g. decarbonation and sulfate reduction) occurring within the Mesozoic carbonates in the underlying Triassic anhydrites and/or in the metamorphic basement of the Tuscan series, with a minor contribution from a deeper seated source (mantle degassing) (Chiodini et al., 1995, 2000; Minissale et al., 2000; Cinti et al., 2014 and references therein). Significant concentrations of CH₄, mainly produced by CO₂ reduction (Tassi et al., 2012d), and light hydrocarbons originating from thermogenic processes (Cinti et al., 2014) were also recognized.

Sampling strategy

The sampling campaign at Poggio dell'Olivo was carried out in May 2014. Up to 25 sampling sites were selected within the Solfatara secca (Figure 4.11) in order to collect (*i*) interstitial soil gases from regular depth intervals (5 cm) from 10 to 50 cm depth along 5 vertical profiles, and (*ii*) interstitial soil gases at 40 cm depth from 20 sites. The sampling sites were selected on the basis of (*i*) a preliminary evaluation of the CO₂, CH₄ and O₂ concentrations in the interstitial soil gases and (*ii*) the presence or absence of vegetation cover. Moreover, one gas sample was collected from a bubbling pool located close to the Vezza Creek (Figure 4.11).

4.3 Medium-low enthalpy hydrothermal systems

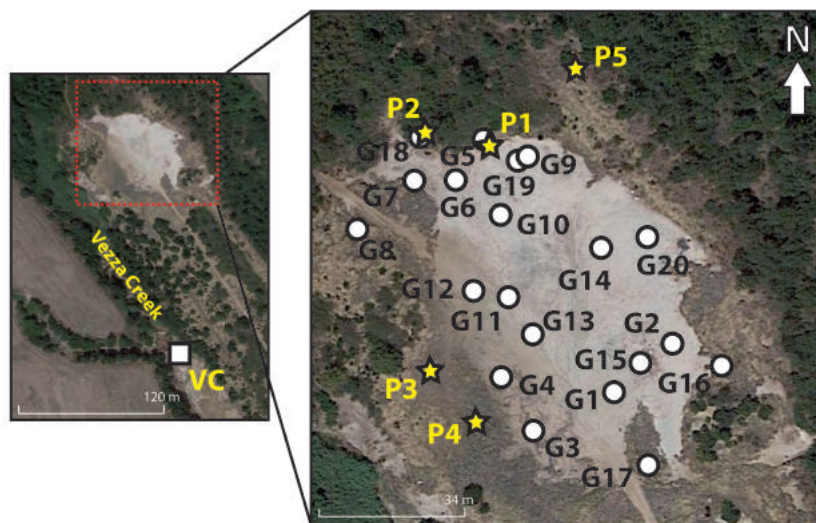


Figure 4.11: Location of the sampling sites for (i) interstitial soil gases at 40 cm depth (white circles), and (ii) interstitial soil gases along vertical profiles from 10 to 50 cm depth (yellow stars) from the Solfatara Secca area, and (iii) the position of the bubbling gas pool close to the Vezza Creek (white square in the inset) referred to the sampling campaign carried out in May 2014.

4. Study areas

4.3.3 Cava dei Selci

Cava dei Selci is an area of high CO₂ gas emission of about 10,000 m² located ca. 20 km SE of Rome (Latium, Central Italy; Figure 4.12a), in an intensely urbanized zone close to the Ciampino International Airport. It is located on

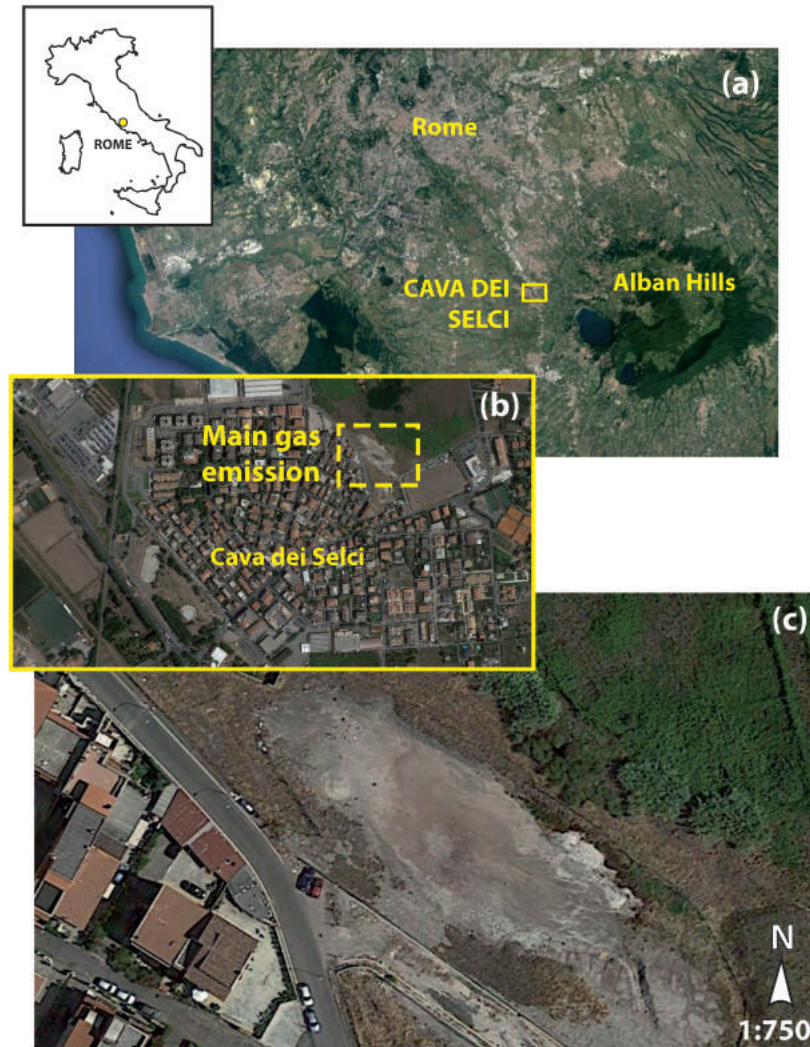


Figure 4.12: (a) Location map and aerial photographs of (b) Cava dei Selci and (c) the main gas emission area.

the NW side of the Quaternary Alban Hills volcanic complex (Figure 4.12b), on the western border of a NW-SE oriented structural high of the Meso-

4.3 Medium-low enthalpy hydrothermal systems

zoic carbonate basement (the Ciampino horst), situated at 700 m depth (Di Filippo and Toro, 1995). Its volcanic activity, emitting SiO₂-poor, strongly alkaline potassic products (Trigila et al., 1995; Peccerillo, 1999, 2005; Giordano et al., 2006), lasted from about 0.7 to ca. 0.01 Ma (Voltaggio and Barbieri, 1995). The magmatic reservoir that fed the past large eruptive events is believed to be located at the base of, or within, the Mesozoic-Cenozoic carbonatic succession (Giordano et al., 2006 and references therein). The Alban Hills volcano is considered to be quiescent, as suggested by (i) the recognition of a low-velocity region at >5 km depth beneath the youngest eruptive center (Chiarabba et al., 1997), (ii) shallow and frequent seismic activity (Amato and Chiarabba, 1995), and (iii) significant volcano uplift (Riguzzi et al., 2009). Moreover, the area is characterized by intense CO₂ emissions, both as (i) surface cold gas discharges (gas vents and diffuse degassing; Hooker et al., 1985; Minissale, 2004; Carapezza et al., 2012) and (ii) dissolved CO₂ in shallow ground waters, sometimes reaching oversaturation and producing sudden and hazard gas leaks at the surface (Chiodini and Frondini, 2001; Annunziatellis et al., 2003). The total CO₂ discharged from the Alban Hills volcanic district was estimated to be higher than 4.2×10^9 mol/y over an area of about 1,500 km² (Chiodini and Frondini, 2001). One of the main degassing sites of the area, namely Cava dei Selci, is located very close to the densely inhabited town of Cava dei Selci (Figure 4.12c), at the north-western margin of the NE volcanotectonic active structure bordering the Ciampino high (Amato and Chiarabba, 1995; Carapezza et al., 2003). Buildings and houses are at ca. 20 m from the degassing site, posing serious gas hazard problems (Annunziatellis et al., 2003; Beaubien et al., 2003; Carapezza et al., 2003, 2012). Several lethal accidents, caused by gas inhalation, occurred in the area, involving both humans (a man in December 2000) and animals (29 cows in 1999, a sheep in March 2000 and 3 sheep in 2001; Annunziatellis et al., 2003; Carapezza et al., 2003). Until the 1970s, the site was a stone quarry. The excavation removed the superficial low permeability volcano-sedimentary cover and formed a depression, which was filled with loose material after the closure of the quarry. The highly permeable filling deposits, which favoured the gas to escape towards the surface, were progres-

4. Study areas

sively altered by the acidic fluids, and turned to be clay-rich (Carapezza et al., 2003; Carapezza and Tarchini, 2007; Carapezza et al., 2012). The shallow aquifer emerges at the bottom of the depression during the rainy season, producing a stagnant water pool that disappears in the summer months. The gas is released either diffusively from the soil or advectively from vents, as evidenced by gas bubbles rising from the water pool (Carapezza et al., 2003). The origin of CO₂ emitted from Cava dei Selci has been ascribed to (i) metamorphic reactions involving carbonate formations, (ii) magmatic source, possibly affected by carbonate assimilation, or (iii) mantle degassing, likely affected by crustal contamination (Giggenbach et al., 1988; Rogie et al., 2000; Chiodini and Frondini, 2001; Minissale, 2004; Carapezza and Tarchini, 2007; Iacono Marziano et al., 2007). N₂, H₂S and CH₄ are minor constituents of the emitted gases (Annunziatellis et al., 2003; Chiodini and Frondini, 2001; Carapezza et al., 2003) together with the short-lived Rn, whose presence suggests that fluids rise quite rapidly through high permeable pathways, i.e. faults and fractures (Beaubien et al., 2003), from the low-to-medium-enthalpy geothermal reservoir (Giggenbach et al., 1988) hosted in the structural highs of the Mesozoic carbonate basement and trapped by the low-permeability volcanic products. This is supported by the low concentrations of CH₄, H₂, unsaturated hydrocarbons and benzene, which suggest prolonged residence of the rising gases at shallow, low temperature (<150 °C) and possibly oxidizing conditions (Giggenbach et al., 1988; Carapezza et al., 2003).

Sampling strategy

The sampling campaign at Cava dei Selci was performed in April 2016 in the framework of a field trip project (“*Studio multiparametrico sulle emissioni gassose naturali presso Cava dei Selci e Solfatarà di Pomezia (Colli Albani, Roma): sviluppo di un protocollo di misura per la definizione di traccianti geochimici atti alla valutazione dell’impatto ambientale di aree affette da degassamento diffuso dal suolo*”; Appendix C) patronized by So.Ge.I. (Società Geochimica Italiana) and involving two departments of Earth Sciences (Florence and Bologna), two research centres (INGV-Palermo and CNR-IGG

4.3 Medium-low enthalpy hydrothermal systems

Pisa) and a private company (WEST Systems Ltd.).

Two main gas vents (CS1 and CS2) were sampled from the main emission area (Figure 4.13), together with interstitial soil gases at 20 cm depth from 30 sites (Figure 4.12). The sites from where the soil gases were collected were selected after measuring the CO₂ soil fluxes with the accumulation chamber method.



Figure 4.13: Location of the sampling sites for (i) interstitial soil gases at 20 cm depth (yellow circles), and (ii) gas vents (red squares) referred to the sampling campaign carried out in April 2016.

Chapter 5

Field sampling methods and analytical techniques

5.1 Sampling procedures for gases

5.1.1 Fumarolic gases

Fumarolic gases were sampled by inserting a 70 cm long Titanium tube into the fumarolic conduit in order to convey the gas into a sampling flask for laboratory investigations. The fumarolic outlet temperatures, measured by a thermocouple, were lower than 650 °C. At these conditions, Titanium tubes are inert, i.e. they do not undergo oxidation reactions (i.e. $\text{Ti}_{(g)} + 2\text{H}_2\text{O} \rightarrow \text{TiO}_{2(s)} + 2\text{H}_{2(g)}$) that may introduce secondary H_2 to the original composition of the gas discharge (Vaselli et al., 2006). A sampling line was connected to the Titanium tube, consisting of dewared glass tubes directly linked and sealed by ball-and-socket joints assembled with steel pincers (Figure 5.1; Vaselli et al., 2006). Dewared tubes consist of two coaxial cylindrical tubes with an evacuated space between them that avoids temperature drop and condensation processes while the gas flows through the sampling apparatus (Vaselli et al., 2006). Moreover, the dewared connections ensure safer operating conditions allowing to operate slightly away from the fumarolic vents. The final part of the sampling line was made of a two-ways dewar (Figure 5.1). A pre-weighted and pre-evacuated 60 mL glass flask was connected

5. Field sampling methods and analytical techniques

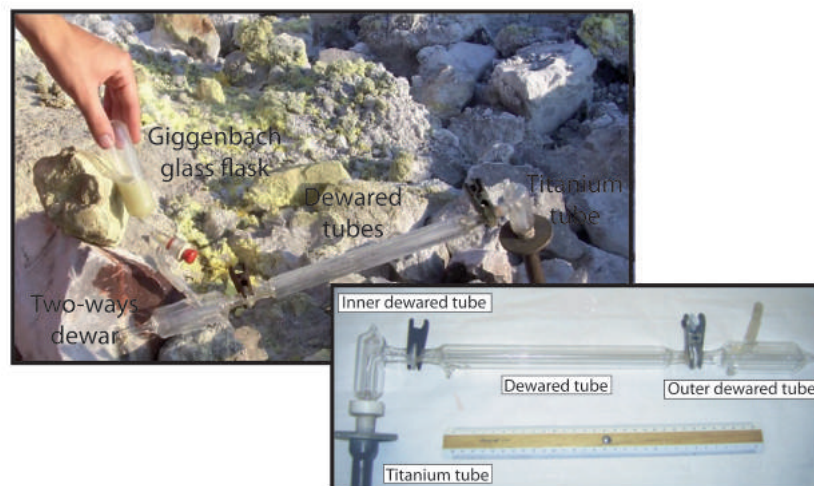


Figure 5.1: Sampling line from the Titanium tube to the two-ways dewars connected to the Giggenbach glass flask.

at one of its ends, sampling only a part of the fumarolic gas, whereas the remaining part of the gas was free to flow out through the other end. This allowed to keep the flux of fumarolic discharge unmodified during sampling, hence preventing condensation effects (Vaselli et al., 2006). The glass flask was equipped with a Thorion[®] valve and partially filled with 20 mL of a 4 M NaOH solution (Giggenbach, 1975; Montegrossi et al., 2001). The alkaline solution allowed to separate the condensable and reactive gas species (H_2O , CO_2 , H_2S) from the inert and incondensable gases (H_2 , CO , O_2 , N_2 , noble gases, C_1 - C_3 hydrocarbons), which accumulate in the headspace of the flask (Montegrossi et al., 2001; Vaselli et al., 2006).

Since VOCs are expected to interact with the highly alkaline solution (Vaselli et al., 2006), their analysis (with the exception of the C_1 - C_3 hydrocarbons) cannot be performed on the gas phase enriched by the soda solution of the Giggenbach flask. The collection of fumarolic gas samples for the analysis of VOCs was then performed through a different sampling apparatus, which included a Graham condenser after the dewared glass tubes, connected by ball-and-socket joints assembled with steel pincers (Figure 5.2; Tassi et al., 2012b). The dry gas fraction was pumped with a 100 mL plastic syringe connected to the sampling line through a PTFE three-way valve. The gas

5.1 Sampling procedures for gases

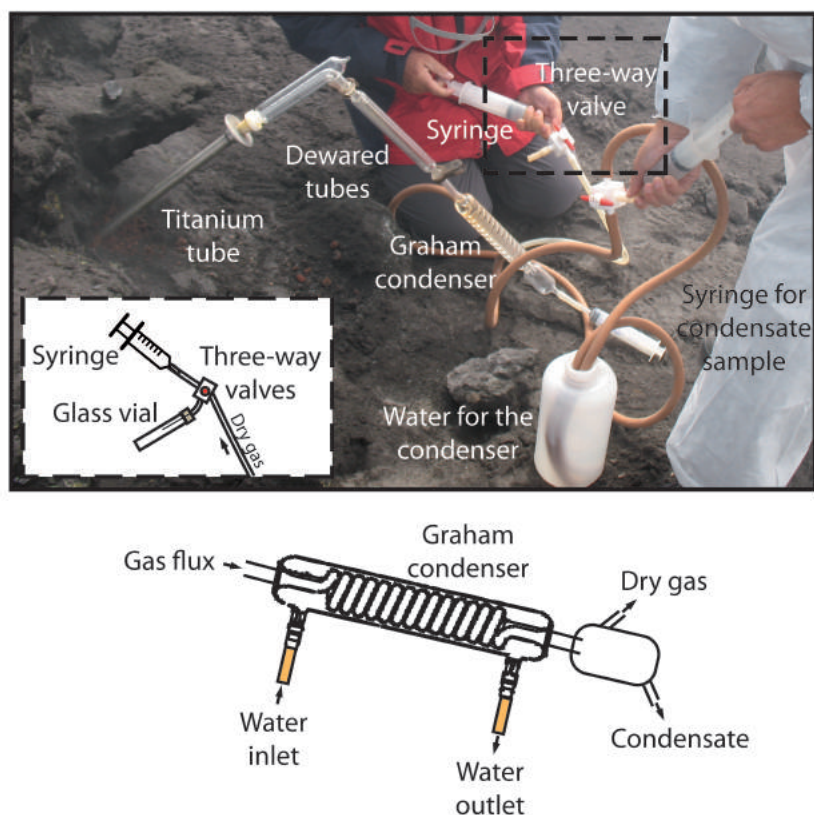


Figure 5.2: Sampling apparatus including dewared tubes and a Graham condenser. The sample for the analysis of VOCs is conveyed into a glass vial by pumping the gas with a syringe (see text for further details). The apparatus allows the simultaneous collection of steam condensate samples.

sample was transferred into a 12 mL Labco Exetainer[®] glass vial tapped with a porous membrane through a second PTFE three-way valve and silicon connections ending with a needle. A second needle, inserted into the glass vial before sampling, allowed to rinse repeatedly (at least 3 times) the vial with the fumarolic gas by flushing the entire gas content of the syringe (Figure 5.2). The collection of gas samples for the analysis of VOCs after water vapour condensation prevents the presence of condensable H_2S , which may corrupt the Solid Phase Micro Extraction (SPME) fibre (see Section 5.2), and allows to enrich VOCs and increase the sensitivity of the analytical method by up to one order of magnitude (Tassi et al., 2012b). Moreover, the dry gas

5. Field sampling methods and analytical techniques

fraction composition is not dependent on water vapour condensations that are strongly affected by both outlet temperatures and the presence of liquid water at shallow depth. Therefore, the analysis of different fluid discharges, i.e. low-to-high temperature fumaroles, bubbling pools and interstitial soil gases, is directly comparable (Tassi et al., 2012b).

A second dry gas fraction aliquot collected in another 12 mL Labco Exetainer[®] glass vial was destined to the analysis of $\delta^{13}\text{C-CO}_2$, whereas $\delta^{13}\text{C-CH}_4$ was determined on the gas enriched in the headspace of the glass flask.

5.1.2 Gases from bubbling pool

Gas from bubbling pools was conveyed to a pre-evacuated 60 mL glass flask, equipped with a Thorion[®] valve and containing 20 mL of 4 M NaOH (Giggenbach, 1975), using a funnel positioned upside down above the emission (Figure 5.3). During sampling, acidic gas species (CO_2 and H_2S) entering the



Figure 5.3: Sampling system for the collection of gas samples from bubbling pools.

flask were dissolved in the alkaline solution, whereas gas compounds with low solubility were stored in the flask headspace. The sampling lasted until the

5.1 Sampling procedures for gases

pressure in the flask headspace reached the inlet pressure. Two glass vials for the analysis of (i) VOCs and (ii) $\delta^{13}\text{C}\text{-CO}_2$ and $\delta^{13}\text{C}\text{-CH}_4$ were also collected through the two-needle system (see Section 5.1.1).

5.1.3 Interstitial soil gases

Interstitial soil gases were collected inserting a 1 m long stainless steel tube, having an inner diameter of 4 mm, down to the sampling depth. Once inserted in the soil, the tube was first connected to a GA2000 gas analyzer (Geotechnical Instruments, UK), equipped with an infrared (IR) detector and a low flux ($100\text{ cm}^3/\text{min}$) pump, for a preliminary semi-quantitative in situ measurement of CO_2 , CH_4 and O_2 concentrations. After pumping for 2 min in order to remove the air filling the sampling line, soil gases were collected using a 60 cm^3 syringe connected to the tube through a PTFE three-way valve placed between the tube and the analyzer. The gas sample was then transferred into a 12 cm^3 glass vial (Labco Exetainer[®]) equipped with a porous membrane using a second PTFE three-way valve and silicon connections ending with a needle. A second needle was inserted, prior to sampling, into the glass vial to rinse repeatedly (at least 3 times) the vial with the soil gas by flushing the entire gas content of the syringe (Figure 5.4).

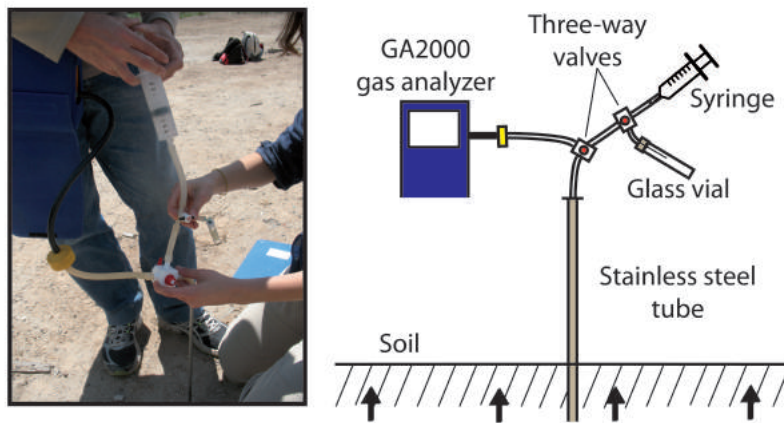


Figure 5.4: Apparatus for (i) soil CO_2 , CH_4 and O_2 preliminary determination in situ, and (ii) interstitial soil gas sampling, as detailed in the text.

5. Field sampling methods and analytical techniques

A second glass vial for isotopic analysis ($\delta^{13}\text{C-CO}_2$ and $\delta^{13}\text{C-CH}_4$) was also collected. Soil temperature was measured using a thermocouple.

5.2 Chemical and isotopic analysis of gases

Inorganic gases both in the headspace of fumarolic and bubbling pool sampling flasks (N_2 , O_2 , H_2 , Ar , CO) and in the glass vials (CO_2 , H_2S , N_2 , O_2 , H_2 , Ar , CO) were analyzed using a Shimadzu 15A gas chromatograph (GC; Figure 5.5) equipped with a thermal conductivity detector (TCD) and a 10 m long 5A Molecular Sieve column or, for CO_2 and H_2S analysis in the glass vials, a 3 m long column packed with Porapak Q 80/100 mesh.



Figure 5.5: Shimadzu 15A gas chromatograph for the analysis of inorganic gases.

Light hydrocarbons ($\text{C}_1\text{-C}_3$) in the headspace of the flasks and in the glass vials were analyzed using a Shimadzu 14A gas chromatograph (Figure 5.6) equipped with a Flame Ionization Detector (FID) and a 10 m long stainless steel column packed with Chromosorb PAW 80/100 mesh coated with 23% SP 1700. CO_2 and H_2S dissolved in the alkaline solution of the flasks were analyzed as CO_3^{2-} by automatic titration (AT) with 0.5 M HCl solution (Metrohm 794 Basic Titrino; Figure 5.7a) and SO_4^{2-} by ion-chromatography (IC; Metrohm 761 Compact IC; Figure 5.7b) after oxidation with H_2O_2 (Montegrossi et al., 2001; Vaselli et al., 2006).

The analysis of VOCs in the fumarole, bubbling pool and soil gas samples was carried out by Solid Phase Micro Extraction (SPME; Arthur and Pawliszin, 1990), using a 2 cm long three-phase fibre made of DiVinylBenzene (DVB) -

5.2 Chemical and isotopic analysis of gases



Figure 5.6: Shimadzu 14A gas chromatograph for the analysis of light hydrocarbons.

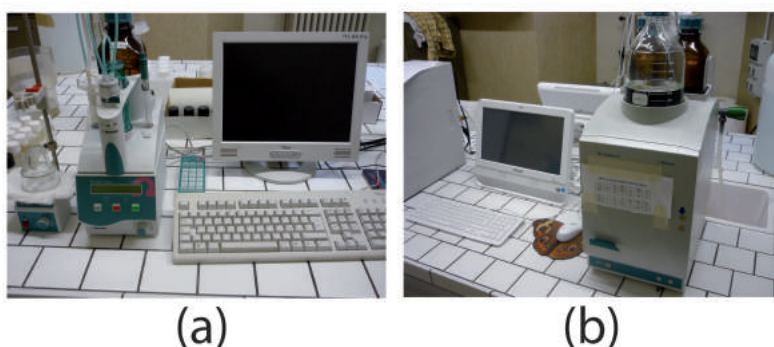


Figure 5.7: (a) Metrohm 794 Basic Titrino and (b) Metrohm 761 Compact IC for the determination, respectively, of CO_2 and H_2S dissolved in the alkaline solution in the Giggenbach flasks.

Carboxen (Car) - PolyDiMethylSiloxane (PDMS) (Supelco; Bellefonte, PA, USA). The fibre was introduced into the glass vials through their porous membrane using a manual SPME device and exposed to the sampled gases for 30 min at 20 °C (Figure 5.8). VOCs absorbed by the SPME fibre were then desorbed for 2 min at 230 °C in the column headspace of a Thermo Trace GC Ultra gas chromatograph coupled to a Thermo DSQ Quadrupole Mass Spectrometer (Figure 5.9). Desorbed gases were injected through a port operating in splitless mode and equipped with a SPME liner (0.75 mm inner diameter) into a 30 m \times 0.25 mm (1.4 μm inner diameter) film thickness TR-V1 fused silica capillary column (Thermo), using He as carrier gas at a flow rate of 1.3 mL/min in constant pressure mode. The column oven

5. Field sampling methods and analytical techniques



Figure 5.8: Solid Phase Micro Extraction (SPME) device.



Figure 5.9: Thermo Trace GC Ultra gas chromatograph and Thermo DSQ Quadrupole Mass Spectrometer (GC-MS) for the analysis of VOCs.

temperature was set, as follows: 35 °C (hold 10 min), ramp at 5.5 °C/min to 180 °C (hold 3 min), ramp at 20 °C/min up to 230 °C (hold 6 min) (Tassi et al., 2012c). After chromatographic separation, gases passed, through a transfer-line set at 230 °C, to the mass spectrometer operating in positive electron impact mode (EI), with an ionization energy of 70 eV and a source temperature of 250 °C. A mass range from 35 to 400 m/z in full scan mode was analyzed. Retention times of the chromatographic peaks and the mass spectra were both used to identify VOCs detected by the quadrupole detector, using the mass spectra database of the NIST05 library (NIST, 2005) for comparison. Quantitative analyses were carried out by external standard calibration procedure using Accustandard[®] mixtures in methanol or, alternatively, hexane solvent (Tassi et al., 2012c). Relative Standard Deviation (RSD), calculated from five replicate analyses of the standard mixtures, was

5.3 Soil fluxes measurement

<5%. The limit of quantification (LOQ) was determined by linear extrapolation from the lowest standard in the calibration curve using the area of a peak having a signal/noise ratio of 5 (Tassi et al., 2012b).

Analytical errors for AT, GC and IC were <5%.

The $^{13}\text{C}/^{12}\text{C}$ ratios in CO_2 (expressed as $\delta^{13}\text{C}\text{-CO}_2$ ‰ vs. V-PDB) were determined by using a Finningan Delta S mass spectrometer after a two-step extraction and purification procedures of the gas mixtures by using liquid N_2 and a solid-liquid mixture of liquid N_2 and trichloroethylene (Evans et al., 1998; Vaselli et al., 2006). Internal (Carrara and San Vincenzo marbles) and international (NBS18 and NBS19) standards were used for estimation of external precision. The analytical uncertainty and the reproducibility were ± 0.05 ‰ and ± 0.1 ‰, respectively. The $\delta^{13}\text{C}\text{-CH}_4$ values were determined by mass spectrometry (Varian MAT 250) according to the procedure reported by Schoell (1980). The analytical uncertainty was ± 0.15 ‰.

5.3 Soil fluxes measurement

5.3.1 Soil CO_2 flux measurement

Carbon dioxide soil fluxes (ΦCO_2) were measured according to the “accumulation chamber (AC) method” (e.g. Chiodini et al., 1998; Tassi et al., 2013b). The instrument consists of (i) an inverted chamber (a cylindrical metal vase with a basal area of 200 cm^2 and an inner volume of $3,060\text{ cm}^3$), (ii) an Infra-Red (IR) spectrophotometer (Licor[®] Li-820, measuring range of 0-20,000 ppm, accuracy of 4% of reading), (iii) an analog-to-digital (AD) converter, and (iv) a palmtop computer (Figure 5.10). Once the chamber is placed firmly on the ground, the soil gas is continuously extracted from the chamber through a low-flux pump (20 mL/s), conveyed to the IR spectrophotometer, and then injected back into the chamber to minimize the disturbance effects due to changes of barometric conditions. The values of CO_2 concentration inside the chamber, measured over time by the IR spectrophotometer, are acquired by the AD converter and sent to the palmtop PC, which displays a CO_2 concentration vs. time plot by a specifically de-

5. Field sampling methods and analytical techniques

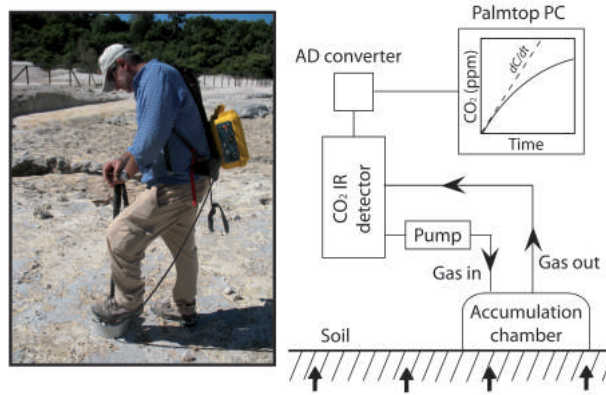


Figure 5.10: System device for the measurement of ΦCO_2 (accumulation chamber method).

veloped software (Palm Flux 5.36 software). From the plot, the initial slope dC_{CO_2}/dt of the concentration-time curve is calculated, which is directly proportional to the CO_2 flux from the soil (ΦCO_2), according to the following equation (Chiodini et al., 1998):

$$\Phi\text{CO}_2 = cf \times dC_{\text{CO}_2}/dt \quad (5.1)$$

, where the proportionality factor (cf) between dC_{CO_2}/dt and the ΦCO_2 , depending on the geometry of the measuring equipment, was determined by laboratory tests (Chiodini et al., 1998).

5.3.2 Soil CH_4 and C_6H_6 flux measurement

Soil methane (CH_4) and benzene (C_6H_6) fluxes were measured using the “static closed-chamber (SCC) method” (Tassi et al., 2013b, and references therein). The equipment consisted of a plastic cylindrical chamber (basal area of 177 cm^2 and inner volume of $4,415 \text{ cm}^3$) equipped on its top with a rubber septum connected to a PTFE three-way valve (Figure 5.11). Once the chamber was positioned on the ground, gas samples (5–10 cc) were taken from the chamber at fixed time intervals (i.e. after 16, 32 and 48 min) using a syringe, and transferred into 12 mL pre-evacuated Labco Exetainer[®] glass

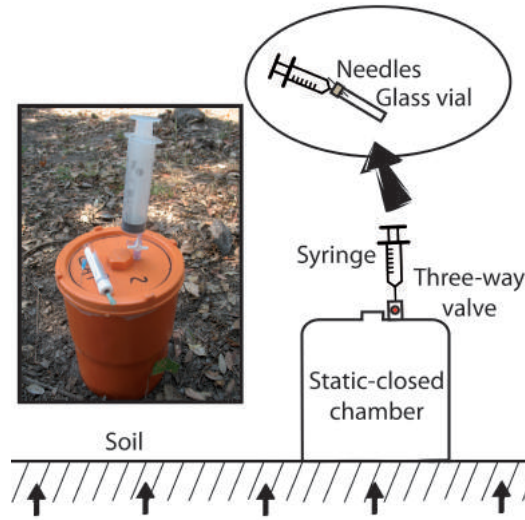


Figure 5.11: System apparatus for the measurement of ΦCH_4 and $\Phi\text{C}_6\text{H}_6$ (static closed-chamber method).

vials tapped with a porous membrane through the three-way valve and a silicon connections ending with a needle. A second needle inserted into the glass vial allowed to rinse repeatedly (3 times) the vial with the chamber gas before sampling.

CH_4 and C_6H_6 concentrations in the vials were determined by using a Shimadzu 14A gas chromatograph (GC) equipped with a Flame Ionization Detector (FID) and a 3 m long stainless steel column packed with Chromosorb PAW 100/120 mesh coated with 10% TCEP. The values of the CH_4 (ΦCH_4) and C_6H_6 ($\Phi\text{C}_6\text{H}_6$) fluxes from the soil were then computed according to the following equation:

$$\Phi X = dC_X/dt \times V/A \quad (5.2)$$

, where dC_X/dt is the rate of concentration change of the X gas compound (CH_4 or C_6H_6) within the chamber (calculated from the linear regression of the concentrations of the X compound in samples collected from the chamber starting from zero time), whereas V and A are the volume and the basal area of the chamber, respectively.

Chapter 6

Results

6.1 Introduction

In this chapter, the results of field measurements and laboratory analyses of gas samples from the studied natural systems are presented. The chemical and isotopic features of (i) hydrothermal fluids discharged from high-flux punctual vents, and (ii) soil gases are described separately for each selected area.

6.2 Solfatara Crater

6.2.1 Fumarolic gases

The chemical composition (in mmol/mol) of the main gas compounds (CO_2 , H_2S , CH_4 , N_2 , O_2 , Ar, H_2 , CO) of the dry fraction of the Bocca Grande and Bocca Nuova fumaroles (BG and BN, respectively, collected in January, February, May and September 2013) is reported in Table 6.1.

The outlet temperatures were ranging from 161 to 164 °C in BG and from 150 to 153 °C in BN (Table 6.1). CO_2 was the most abundant compound (up to 991 mmol/mol), followed by H_2S (up to 15 mmol/mol), N_2 (from 2.3 to 3.1 mmol/mol), and H_2 (from 0.48 to 0.85 mmol/mol). Minor concentrations of CH_4 , O_2 , Ar and CO (up to 0.098, 0.026, 0.020 and 0.010

6. Results

	Date	East	North	T	CO ₂	H ₂ S	CH ₄	N ₂	O ₂	Ar	H ₂	CO	$\delta^{13}\text{C-CO}_2$
BG	Jan13	427648	4519919	163	983	14	0.069	2.6	0.018	0.010	0.85	0.0090	
	Feb13	427648	4519919	164	984	13	0.067	2.5	0.017	0.0077	0.77	0.0083	
	May13	427648	4519919	161	983	14	0.070	2.3	0.017	0.0074	0.55	0.0088	-1.82
	Sep13	427648	4519919	163	981	15	0.098	3.0	0.018	0.013	0.76	0.0086	
BN	Jan13	427632	4519918	151	991	5.3	0.077	2.9	0.024	0.016	0.53	0.0086	
	Feb13	427632	4519918	153	985	11	0.091	3.4	0.022	0.020	0.61	0.0098	
	May13	427632	4519918	150	984	12	0.097	3.0	0.026	0.017	0.48	0.010	
	Sep13	427632	4519918	152	985	11	0.096	3.1	0.022	0.015	0.49	0.0090	

Table 6.1: Location (in UTM), outlet temperature ($^{\circ}\text{C}$) and chemical composition (in mmol/mol) of the main gas species (CO₂, H₂S, CH₄, N₂, O₂, Ar, H₂, CO) of the BG and BN fumaroles from the Solfatara Crater. The isotopic composition of CO₂ is also reported ($\delta^{13}\text{C-CO}_2$, in ‰ vs. V-PDB).

mmol/mol, respectively) were measured. Such concentrations were consistent with those reported in literature for the Solfatara fumaroles (Caliro et al., 2007, and references therein). Strong acidic gases (SO_2 , HCl, HF) released from the magmatic source were not detected since they were scrubbed by the hydrothermal aquifer (Cioni et al., 1984; Chiodini et al., 2001).

The isotopic composition of CO_2 ($\delta^{13}\text{C}\text{-CO}_2$; Table 6.1) analyzed in two gas samples (BG collected in May and September 2013) was -1.82 and -1.90 ‰, respectively. These values were within the range of $\delta^{13}\text{C}\text{-CO}_2$ values (from -2.2 to -0.41 ‰) reported by Vaselli et al. (2011) for the inland and submarine fumarolic gases discharged from the Campi Flegrei caldera.

The organic fraction of BG and BN samples (in nmol/mol; Table 6.2) was dominated by alkanes and aromatics (Figure 6.1), whose sum was ranging from 91 to 94 % of total VOCs (ΣVOCs).

Table 6.2: Chemical composition (in nmol/mol) of VOCs of the BG and BN fumaroles from the Solfatara Crater.

			BG				BN			
			Jan13	Feb13	May13	Sep13	Jan13	Feb13	May13	Sep13
Alkanes	C ₂ H ₆	ethane	1740	1709	1624	2154	3658	3723	3658	3073
	C ₃ H ₈	propane	235	213	174	240	354	372	407	308
	C ₄ H ₁₀	methylpropane	241	222	185	236	321	395	410	311
	n-C ₄ H ₁₀	normalbutane	257	261	198	256	355	387	433	354
	i-C ₅ H ₁₂	(2)methylbutane	231	215	196	241	336	416	418	351
	n-C ₅ H ₁₂	normalpentane	264	233	241	255	315	428	436	368
	i-C ₆ H ₁₄	(3)methylpentane	216	194	155	219	287	351	354	318
	n-C ₆ H ₁₄	normalhexane	478	341	318	487	511	589	597	555
	i-C ₇ H ₁₆	(3)methylhexane	167	111	158	161	157	221	236	217
	n-C ₇ H ₁₆	normalheptane	186	123	169	156	168	234	261	227
	i-C ₈ H ₁₈	(3)methylheptane	85	89	95	91	96	108	121	114
	i-C ₈ H ₁₈ *	(2,5)dimethylhexane	85	97	81	76	88	95	94	86
	n-C ₈ H ₁₈	normaloctane	158	133	156	165	161	238	218	236
Aromatics	C ₆ H ₆	benzene	1651	1755	1618	2085	3547	3669	3687	3128
	C ₇ H ₈	toluene	21	23	21	19	25	24	29	27
	C ₈ H ₈	styrene	1.5	1.6	1.7	1.9	1.7	1.6	1.8	1.4
	C ₈ H ₁₀	ethylbenzene	2.6	2.5	2.4	2.1	2.6	2.7	2.8	2.9
	m,p-C ₈ H ₁₀	m,p xylene	16	18	14	19	20	21	26	23
	o-C ₈ H ₁₀	o xylene	2.3	2.5	2.7	2.4	2.1	1.8	2.3	2.2
	C ₉ H ₁₂	(1)methyl(4)ethylbenzene	0.89	0.87	0.71	1.1	1.2	1.4	1.3	1.2

(To be continued)

			BG				BN			
	C ₉ H ₁₂ *	(1,2,3)trimethylbenzene	1.3	1.2	1.1	1.5	1.4	1.6	1.5	1.5
	C ₉ H ₁₂ **	(1,3,5)trimethylbenzene	1.1	0.89	1.2	1.4	1.3	1.4	1.3	1.1
	C ₉ H ₁₂ ***	(1)methyl(4)methylethylbenzene	0.31	0.36	0.38	0.34	0.39	0.41	0.39	0.44
	C ₁₀ H ₈	naphthalene	4.1	3.5	2.9	3.2	3.8	4.4	4.2	4.1
	C ₁₀ H ₁₄	(1,2,3,4)tetramethylbenzene	0.54	0.61	0.38	0.66	0.68	0.81	0.86	0.69
	C ₁₀ H ₁₄ *	(1,2,3,5)tetramethylbenzene	0.33	0.55	0.21	0.36	0.51	0.68	0.64	0.77
Cyclics	C ₅ H ₁₀	cyclopentane	0.21	0.19	0.16	0.21	0.17	0.16	0.13	0.24
	C ₆ H ₁₀	(1)methylcyclopentane	0.08	0.06	0.1	0.12	0.08	0.13	0.14	0.09
	C ₆ H ₁₂	(1)methylcyclopentane	0.11	0.06	0.05	0.08	0.08	0.09	0.11	0.07
	C ₆ H ₁₂ *	cyclohexane	0.06	0.14	0.09	0.16	0.08	0.16	0.14	0.18
	C ₇ H ₁₄	(1)methylcyclohexane	0.26	0.31	0.28	0.15	0.19	0.24	0.26	0.17
	C ₇ H ₁₄ *	(1,3)dimethylcyclopentane						0.06		0.05
	C ₈ H ₁₆	(1,3)dimethylcyclohexane				0.08	0.06		0.06	
	C ₈ H ₁₆ *	(1,5)dimethylcyclohexane								
	C ₈ H ₁₆ **	cyclooctane				0.05			0.06	0.05
	C ₉ H ₁₈	(1)ethyl(3)methylcyclohexane								
	C ₉ H ₁₈ *	(1,3,5)trimethylcyclohexane								
	C ₉ H ₁₈ **	(1,3,4)trimethylcyclohexane								
Alkenes	C ₃ H ₆	propene	16	14	13	16	19	22	23	21
	C ₄ H ₈	(1)butene	87	91	88	76	75	156	161	174
	C ₅ H ₁₀	(2)pentene	0.51	0.44	0.38	0.26	0.27	0.29	0.51	0.26
	C ₆ H ₁₂	(3)methyl(2)pentene	0.21	0.15	0.16	0.08	0.11	0.08	0.13	0.12
	C ₆ H ₁₂ *	(2)hexene	1.2	0.89	1.5	1.1	1.6	0.88	0.96	1.2
	C ₇ H ₁₄	(3)heptene	0.06			0.07	0.05	0.06		0.08

(To be continued)

			BG				BN			
	C ₇ H ₁₄ *	(4,5)dimethyl(2)hexene	0.07				0.06	0.05	0.05	
	C ₈ H ₁₈	(2,3,4)trimethyl(2)pentene	0.06				0.08	0.06	0.08	
S-bearing	CS ₂	carbon disulphide	169	171	156	219	368	351	333	306
	C ₄ H ₄ S	thiophene	51	66	80	56	69	57	46	72
	C ₂ H ₆ S	dimethylsulphide	37	41	78	41	53	44	41	60
	C ₅ H ₆ S	(3)methylthiophene	25	39	45	26	31	27	21	29
	C ₆ H ₈ S	(2,5)dimethylthiophene	26	41	39	24	39	24	26	31
	C ₂ H ₆ OS	dimethylsulphoxide	1.3	0.85	0.66	1.1	0.94	1.3	0.74	0.66
	C ₂ H ₆ O ₂ S	dimethylsulphone	0.32	0.29	0.21	0.29	0.24	0.18	0.36	0.51
	C ₇ H ₅ NS	benzothiazole	0.13	0.15	0.19	0.21	0.11	0.13	0.14	0.12
O-bearing	C ₄ H ₄ O	furan	0.91	1.1	1.5	1.3	1.2	1.4	1.9	1.4
	C ₄ H ₈ O	tetrahydrofuran	1.3	1.9	2.1	1.9	1.6	1.8	2.5	1.7
	C ₅ H ₆ O	(2)methylfuran	0.87	0.89	1.6	1.1	1.4	1.1	1.5	1.2
	C ₄ H ₈ O ₂	ethyl acetate	1.1	0.85	1.3	0.56	0.66	0.71	0.56	0.51
	C ₅ H ₁₂ O	(2,2)dimethyl(1)propanol	0.11	0.21	0.23	0.15	0.17	0.08	0.09	0.12
	C ₅ H ₁₂ O*	(2)methyl(1)butanol	0.06	0.15	0.16	0.08	0.19	0.06	0.08	0.07
	C ₆ H ₁₄ O	hexanol	0.08	0.07			0.11			
	C ₆ H ₆ O	phenol	3.8	2.8	4.1	2.6	3.4	3.2	2.8	2.7
	C ₆ H ₁₄ O*	(2)methoxy(2)methylbutane	0.52	0.69	1.1	0.23	0.51	0.77	0.21	0.15
	C ₃ H ₆ O ₂	methyl acetate	0.78	1.1	0.61	0.38	0.44	0.51	0.71	0.16
	C ₆ H ₁₂ O ₂	butyl acetate	0.13	0.27	0.15	0.21	0.07	0.06	0.11	0.13
	C ₆ H ₁₂ O ₂ *	ethyl butanoate	0.11	0.07	0.16	0.15	0.09	0.11	0.06	0.11
	C ₆ H ₁₆ O ₂	acid (2)ethylhexanoic								
	C ₄ H ₁₀ O ₂	(2)ethoxyethanol								

(To be continued)

			BG				BN				
	C ₅ H ₁₂ O ₂	(1)methoxy(2)methyl(2)propanol	0.09								
	C ₆ H ₁₄ O ₂	(2)butoxyethanol	0.06			0.11	0.08		0.06		
	C ₇ H ₁₆ O	(1)methoxyhexane	0.11	0.09	0.13	0.07	0.06	0.09	0.11	0.12	
	C ₄ H ₈ O*	butanone	0.84	0.76	0.72	0.55	0.61	0.54	0.59	0.44	
	C ₆ H ₁₂ O	hexanone	0.31	0.22	0.19	0.21	0.18	0.31	0.26	0.17	
	C ₈ H ₈ O	acetophenone	0.06					0.09	0.08		
	C ₄ H ₈ O**	butanal	0.71	0.66	0.65	0.51	0.48	0.44	0.45	0.37	
	C ₅ H ₁₀ O	pentanal	0.54	0.41	0.26	0.27	0.21	0.16	0.22	0.21	
	C ₆ H ₁₂ O*	hexanal	0.18	0.16	0.13	0.12	0.11	0.05	0.08	0.15	
	C ₇ H ₁₄ O	heptanal	0.11	0.07	0.08	0.05					
	C ₈ H ₁₆ O	octanal	0.06	0.05	0.07						
	C ₇ H ₆ O	benzaldehyde	0.77	0.61	0.46	0.45	0.39	0.49	0.51	0.45	
Halocarbons	CCl ₃ F	CFC11									
	CCl ₂ F ₂	CFC12									
	CClF ₃	CFC13									
	CH ₃ Cl	chloromethane									
	CCl ₄	carbon tetrachloride	0.09	0.11	0.07	0.06	0.05		0.09	0.07	
	C ₂ H ₂ Cl ₂	(1,2)dichloroethene	0.06	0.09	0.05	0.07	0.05		0.11	0.09	
	C ₂ HCl ₃	trichloroethene					0.06	0.06	0.08	0.08	
	C ₂ H ₃ Cl	vinylchloride	0.05					0.06	0.07	0.07	
	C ₆ H ₅ Cl	chlorobenzene	0.07	0.09	0.06	0.05	0.07		0.13	0.08	

Table 6.2: Chemical composition (in nmol/mol) of VOCs of the BG and BN fumaroles from the Solfatara Crater.

6. Results

S-bearing compounds and alkenes were present at significant concentrations (ca. 5 and 1.5 % Σ VOCs, respectively), whilst cyclics, halocarbons and O-bearing compounds were <0.3 % Σ VOCs (Figure 6.1). The Σ VOCs values were ranging from 5,935 to 12,070 nmol/mol, corresponding to <15 % of the CH_4 concentrations.

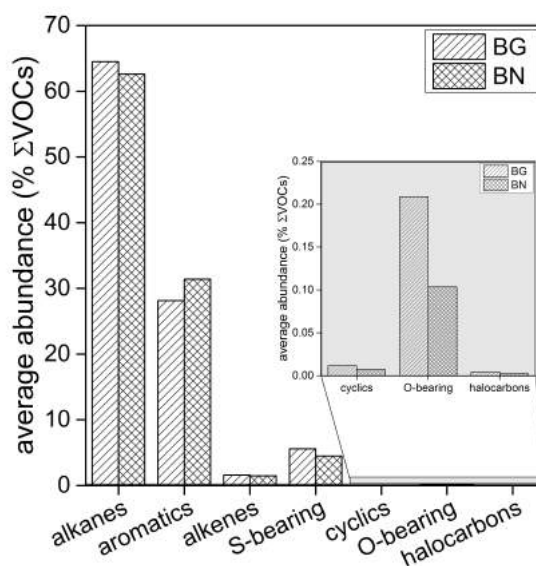


Figure 6.1: Average relative abundances (in % Σ VOCs) of the different families of VOCs (alkanes, aromatics, alkenes, S-bearing compounds, cyclics, O-bearing compounds and halocarbons) from the BG and BN fumaroles.

In the following paragraphs, the results for the main homologous series of VOCs are presented in detail.

Alkanes

Alkanes (CH_4 excluded) represented 61-67 % of the Σ VOCs. Ethane (C_2H_6) was the most abundant species, with concentrations ranging from 1,624 to 3,723 nmol/mol (up to 57 % Σ VOCs), i.e. one order of magnitude higher than the other alkanes (Table 6.2). The concentrations of alkanes generally decreased with increasing molecular weight (or increasing number of carbon atoms), with the exception of normal-hexane (C_6H_{14}). The latter was the

second most abundant alkane, whose concentration was varying between 318 and 597 nmol/mol (i.e. up to 9 % Σ VOCs; Table 6.2).

Iso-alkanes showed abundances lower than the corresponding normal-alkanes (Table 6.2), the normal- to iso- ratios ranging from 0.72 to 2.22.

Aromatics

Aromatics constituted from 26 to 33 % of Σ VOCs and were largely dominated by benzene (ca. 98 % Σ aromatics), followed by toluene (≤ 1.3 % Σ aromatics) and m,p-xylene (≤ 1.0 % Σ aromatics). The concentrations of benzene, ranging from 1,618 to 3,687 nmol/mol (Table 6.2), were comparable to those of ethane. Toluene and m,p-xylene were up to 29 and 26 nmol/mol, respectively. Other aromatic compounds exhibited maximum concentrations, varying from 1.4 to 4.4 nmol/mol (styrene, ethylbenzene, o-xylene, methylethylbenzene, trimethylbenzenes and naphthalene) or ≤ 0.86 nmol/mol (methylmethylethylbenzene and tetramethylbenzenes; Table 6.2).

Alkenes

Alkenes (from 0.86 to 1.88 % Σ VOCs) were mostly represented by butene (78-89 % Σ alkenes, up to 174 nmol/mol), followed by propene (10-19 % Σ alkenes, up to 23 nmol/mol) and hexene (≤ 1.67 % Σ alkenes, up to 1.6 nmol/mol; Table 6.2). Methylpentene was present at concentrations ranging from 0.08 to 0.21 nmol/mol, whilst heavier alkenes (C_{7-8}) displayed contents ≤ 0.08 nmol/mol and below detection limit (Table 6.2).

S-bearing compounds

S-bearing species (from 3.88 to 6.72 % Σ VOCs) were dominated by carbon disulphide (39-71 % Σ S-bearing, up to 368 nmol/mol), thiophene (10-20 % Σ S-bearing, up to 80 nmol/mol), and dimethylsulphide (3-20 % Σ S-bearing, up to 78 nmol/mol), with minor amounts of methylated thiophenes (up to 11 % Σ S-bearing; Table 6.2). Other S-bearing compounds, consisting of O- and N-substituted species, were present at concentrations ≤ 0.51 nmol/mol (≤ 0.42 % Σ S-bearing; Table 6.2).

6. Results

O-bearing compounds

O-bearing species accounted for ≤ 0.27 % of Σ VOCs. Furans (furan, tetrahydrofuran and methylfuran) and alcohols (dimethylpropanol, methylbutanol, hexanol and phenol) were the most abundant compounds, with relative abundances ranging from 22.8 to 45.6 and from 23.0 to 32.2 % Σ O-bearing species, respectively. Among alcohols, phenol was by far the most abundant compound, showing the highest concentrations among the O-bearing species (up to 4.1 nmol/mol; Table 6.2). Esters (ethyl acetate, methyl acetate, butyl acetate and ethyl butanoate) and aldehydes (butanal, pentanal, hexanal, heptanal, octanal and benzaldehyde) ranged from 8.9 to 17 and from 10 to 18 % Σ O-bearing species, respectively. Ketones (butanone, hexanone and acetophenone), ethers (methoxymethylbutane and methoxihexane) and glycol ethers (ethoxyethanol, methoxymethylpropanol and butoxyethanol) were detected at concentrations ≤ 8.95 , 7.79 and 1.00 % Σ O-bearing species, respectively.

Cyclics

Cyclic compounds represented a very small fraction of the VOCs in the fumarolic discharges (from 0.006 to 0.012 % Σ VOCs), mainly represented by methylcyclohexane, cyclopentane, methylcyclopentene, methylcyclopentane, and cyclohexane (up to 0.31 nmol/mol; Table 6.2). Dimethylated cyclopentanes and cyclohexanes, and cyclooctane were only occasionally detected (Table 6.2).

Halocarbons

Halocarbons were ≤ 0.006 % Σ VOCs, consisting of carbon tetrachloride, dichloroethene, trichloroethene, vinylchloride and chlorobenzene. These compounds were only sporadically recognized and their concentrations were ≤ 0.11 nmol/mol (Table 6.2).

6.2.2 Interstitial soil gases

The concentrations (in mmol/mol) of the main inorganic gas constituents (CO_2 , H_2S , CH_4 , N_2 , O_2 , Ar and H_2) in the interstitial soil gas samples collected in September 2013 are reported in Table 6.3. CO_2 (from 106 to 964 mmol/mol) and N_2 (from 20.2 to 811 mmol/mol) were the dominant species, followed by O_2 , Ar and H_2S (up to 78, 13 and 20 mmol/mol, respectively; Table 6.3). Minor contents of H_2 and CH_4 (up to 1.70 and 0.18 mmol/mol) were also measured (Table 6.3). The $\delta^{13}\text{C}\text{-CO}_2$ values (Table 6.3) were measured in 22 samples and were included in a relatively narrow interval: from -2.33 to -1.26 ‰, i.e. consistent with the isotopic signature of CO_2 in the fumaroles (Table 6.1) and pointing to a dominant hydrothermal fluid contribution.

Although CO_2 and N_2 largely dominated the composition of all the collected interstitial soil gases, the CO_2/N_2 ratio values were highly variable, ranging from 0.13 to 47.8. These values were significantly lower than those measured in the fumarolic gases (CO_2/N_2 ratios from 293 to 430; Table 6.1), suggesting that the composition of soil gases was affected by air contribution, at variable degree, diluting the CO_2 -rich fluids fed by the deep hydrothermal system. Accordingly, at decreasing CO_2/N_2 ratios, i.e. increasing air fraction, the concentrations of the reduced gas species (H_2S , H_2 and CH_4) also decreased (Figure 6.2). The N_2/Ar ratios ranged from 41 and 95, i.e. between air and air saturated water (ASW) values (Figure 6.3), confirming the involvement of air in the collected soil gases. Hence, soil gases were conveniently subdivided into three groups: (*i*) group A, characterized by CO_2/N_2 ratios >10 , includes those samples with a chemical composition approaching that of the fumaroles, (*ii*) group C, with CO_2/N_2 ratios <1 , consists of those samples strongly affected by air dilution, and (*iii*) group B, with CO_2/N_2 ratios ranging from 1 to 10, related to soil gas samples with intermediate composition between group A and group C (Figure 6.4).

6. Results

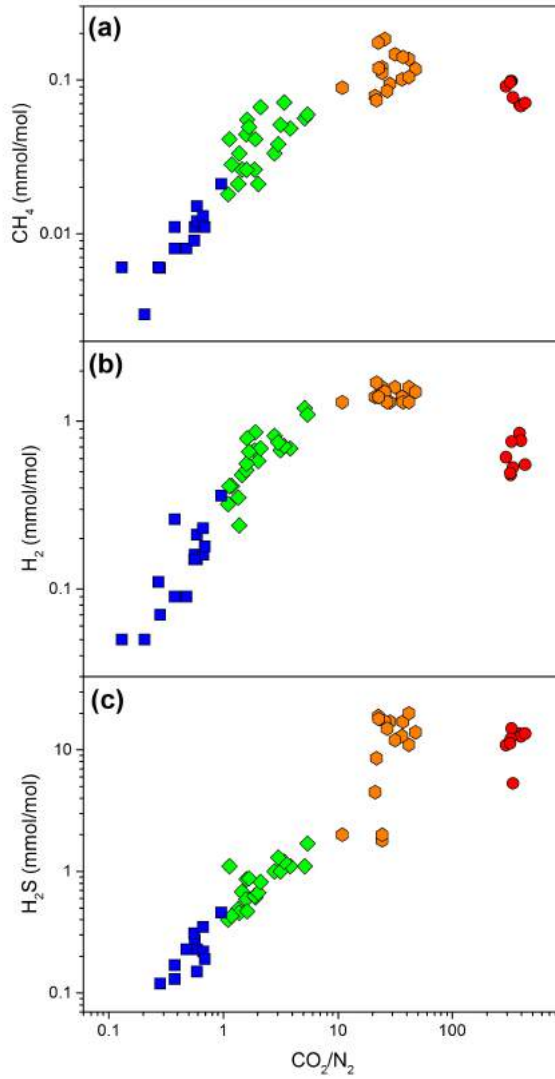


Figure 6.2: **(a)** CH_4 , **(b)** H_2 , and **(c)** H_2S (in mmol/mol) vs. CO_2/N_2 ratio binary diagram for fumarolic gases (red circles) and A (orange hexagons), B (green diamonds) and C (blue squares) soil gas types.

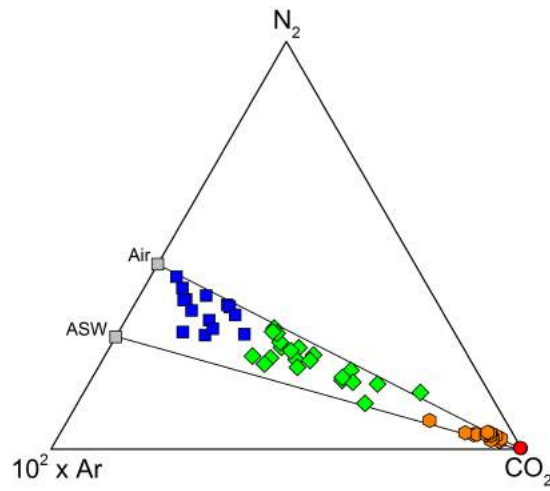


Figure 6.3: CO_2 - N_2 -Ar ternary diagram. Symbols and colours as in Figure 6.2.

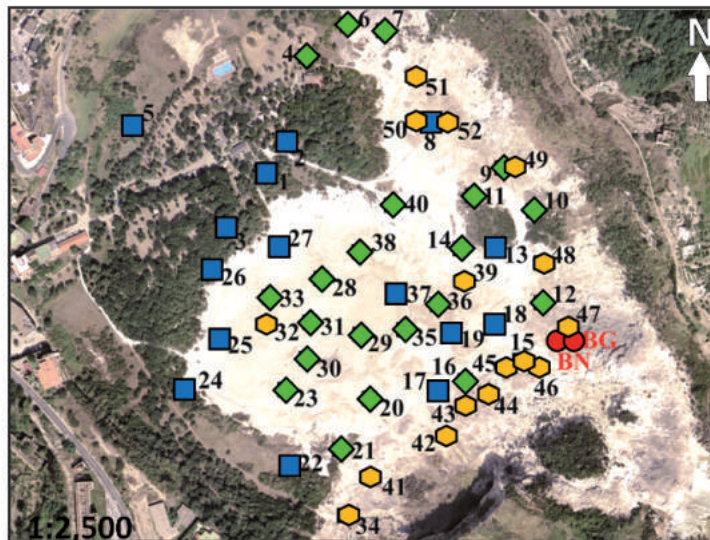


Figure 6.4: Location of the sampling sites for the fumaroles and A, B and C soil gas types (see text for details). Symbols and colours as in Figure 6.2.

Table 6.3: Location (in UTM), chemical composition (in mmol/mol) of the main gas species (CO_2 , H_2S , CH_4 , N_2 , O_2 , Ar , H_2), and isotopic composition of CO_2 ($\delta^{13}\text{C}\text{-CO}_2$, in ‰ vs. V-PDB) in soil gas samples from the Solfatara Crater. The soil gas type (A, B, or C) is also indicated, as described in the text.

ID	Date	East	North	CO_2	H_2S	CH_4	N_2	O_2	Ar	H_2	$\delta^{13}\text{C}\text{-CO}_2$	Type
1	Sep13	427353	4520079	352	0.3	0.011	625	13	10.00	0.16		C
2	Sep13	427374	4520111	268	0.2	0.008	711	12	9.10	0.09	-1.39	C
3	Sep13	427313	4520029	215	0.1	0.006	763	11	11.00	0.07		C
4	Sep13	427391	4520193	587	0.7	0.026	402	3.9	6.20	0.48		B
5	Sep13	427223	4520128	364	0.2	0.015	617	11	7.90	0.15		C
6	Sep13	427431	4520224	568	0.5	0.021	419	6	6.10	0.35		B
7	Sep13	427466	4520218	606	0.6	0.044	382	4	7.20	0.51	-1.91	B
8	Sep13	427516	4520128	308	0.2	0.008	648	31	13.00	0.09		C
9	Sep13	427581	4520085	650	0.6	0.041	339	5	4.80	0.86	-1.78	B
10	Sep13	427611	4520044	563	0.5	0.033	409	19	8.20	0.24		B
11	Sep13	427552	4520058	611	0.5	0.055	378	4.9	5.30	0.79		B
12	Sep13	427619	4519955	834	1.1	0.056	162		1.70	1.20		B
13	Sep13	427574	4520007	156	0.0	0.003	756	78	10.00	0.05		C
14	Sep13	427540	4520007	644	0.6	0.026	345	4	5.80	0.67	-1.64	B
15	Sep13	427598	4519900	956	1.8	0.121	39		0.92	1.60		A
16	Sep13	427545	4519880	660	0.7	0.021	325	8.8	5.10	0.58		B
17	Sep13	427518	4519870	204	0.0	0.006	751	34	11.00	0.11		C
18	Sep13	427573	4519934	387	0.2	0.011	578	24	11.00	0.16		C
19	Sep13	427531	4519925	344	0.3	0.009	615	33	7.80	0.15	-2.12	C

(To be continued)

ID	Date	East	North	CO ₂	H ₂ S	CH ₄	N ₂	O ₂	Ar	H ₂	$\delta^{13}\text{C-CO}_2$	Type
20	Sep13	427452	4519863	510	0.4	0.018	465	18	5.90	0.32		B
21	Sep13	427424	4519813	537	0.4	0.028	451	5	6.00	0.41	-1.38	B
22	Sep13	427374	4519800	476	0.5	0.021	496	19	7.90	0.36	-2.33	C
23	Sep13	427371	4519872	731	1.0	0.033	261	2	3.60	0.82		B
24	Sep13	427274	4519873	355	0.2	0.012	604	33	7.70	0.21		C
25	Sep13	427306	4519920	387	0.4	0.013	581	21	10.00	0.23	-1.38	C
26	Sep13	427300	4519988	106	0.0	0.006	811	73	10.00	0.05	-1.74	C
27	Sep13	427363	4520009	399	0.2	0.011	578	15	7.80	0.18		C
28	Sep13	427406	4519978	786	1.1	0.048	204	5	2.90	0.69	-1.56	B
29	Sep13	427443	4519925	839	1.7	0.059	155		3.80	1.10		B
30	Sep13	427391	4519901	754	1.0	0.051	238	2	4.20	0.67	-1.87	B
31	Sep13	427395	4519936	609	0.9	0.026	379	4	5.80	0.56	-1.33	B
32	Sep13	427354	4519935	911	2.0	0.089	83		1.90	1.30		A
33	Sep13	427356	4519961	767	1.2	0.071	226	1.9	3.80	0.71	-2.11	B
34	Sep13	427428	4519750	956	2.0	0.111	39		0.83	1.50		A
35	Sep13	427486	4519929	664	0.8	0.066	315	13	5.90	0.69	-1.34	B
36	Sep13	427518	4519953	616	0.9	0.049	369	5	7.80	0.66		B
37	Sep13	427479	4519964	266	0.1	0.011	704	19	11.00	0.26		C
38	Sep13	427443	4520005	742	1.3	0.038	247	4.9	4.10	0.75		B
39	Sep13	427543	4519976	948	4.5	0.078	45		1.10	1.40		A
40	Sep13	427474	4520049	518	1.1	0.041	457	17	6.10	0.41	-1.26	B
41	Sep13	427452	4519786	963	11.0	0.136	23		0.41	1.60	-1.94	A
42	Sep13	427526	4519827	964	14.0	0.117	20	0.22	0.38	1.50	-1.62	A
43	Sep13	427543	4519856	959	13.0	0.100	26	0.12	0.31	1.40	-1.86	A

(To be continued)

ID	Date	East	North	CO ₂	H ₂ S	CH ₄	N ₂	O ₂	Ar	H ₂	$\delta^{13}\text{C-CO}_2$	Type
44	Sep13	427567	4519866	948	17.0	0.094	33	0.26	0.39	1.30	-1.74	A
45	Sep13	427584	4519892	955	12.0	0.146	30	0.32	0.50	1.60		A
46	Sep13	427616	4519893	955	17.0	0.140	26		0.50	1.30		A
47	Sep13	427644	4519932	955	20.0	0.104	23		0.56	1.30		A
48	Sep13	427618	4519994	944	17.0	0.183	37		0.60	1.50		A
49	Sep13	427592	4520088	937	19.0	0.174	41	0.39	0.52	1.40	-1.78	A
50	Sep13	427496	4520132	948	15.0	0.084	35	0.12	0.50	1.30		A
51	Sep13	427497	4520172	939	18.0	0.119	41		0.49	1.40	-1.95	A
52	Sep13	427527	4520129	946	8.5	0.073	43		0.54	1.70	-1.78	A

Table 6.3: Location (in UTM), chemical composition (in mmol/mol) of the main gas species (CO₂, H₂S, CH₄, N₂, O₂, Ar, H₂), and isotopic composition of CO₂ ($\delta^{13}\text{C-CO}_2$, in ‰ vs. V-PDB) in soil gas samples from the Solfatara Crater. The soil gas type (A, B, or C) is also indicated, as described in the text.

The Σ VOCs contents (Table 6.4), ranging from 273 to 17,066 nmol/mol (corresponding to ≤ 3.33 % of the CH_4 concentration), showed significant differences among groups A ($\geq 3,136$ nmol/mol), B (from 789 to 3,789 nmol/mol) and C (≤ 977 nmol/mol), similarly to what evidenced by the composition of the organic fraction (Figure 6.5). The composition of VOCs in soil gases was

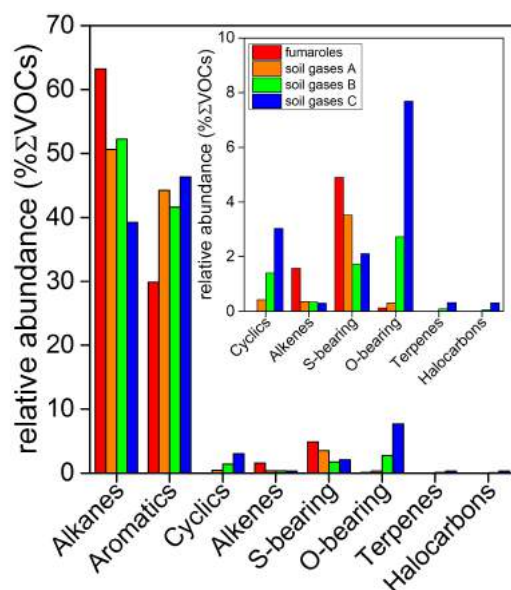


Figure 6.5: Average relative abundances (in % Σ VOCs) of the different families of VOCs (alkanes, aromatics, alkenes, S-bearing compounds, cyclics, O-bearing compounds and halocarbons) in soil gases of type A (orange), B (green) and C (blue). The average composition of VOCs in fumarolic gases (red) is also reported for comparison.

largely dominated by alkanes and aromatics, whose sum ranged from 73 to 98 % Σ VOCs, whereas alkenes were present at low concentrations (from 0.10 to 0.73 % Σ VOCs).

In the soil gas samples pertaining to group A, S-bearing compounds (from 0.94 to 12 % Σ VOCs), cyclics (from 0.23 to 1.29 % Σ VOCs), O-bearing species (from 0.14 to 1.29 % Σ VOCs) and alkenes (from 0.16 to 0.48 % Σ VOCs) showed subordinate concentrations with respect to those of alkanes and aromatics. Halocarbons were present at concentrations ≤ 0.013 % Σ VOCs.

6. Results

The soil gases of group B were characterized by relatively high percentages of cyclics (from 0.91 to 2.22 % Σ VOCs), O-bearing compounds (from 1.04 to 5.35 % Σ VOCs) and halocarbons (from 0.02 to 0.19 % Σ VOCs), and lower amounts of S-bearing species (from 0.77 to 2.75 % Σ VOCs), whereas alkenes displayed concentrations (from 0.21 to 0.67 % Σ VOCs) similar to those measured in the soil gases of group A. Relatively high contents of cyclics (1.53 to 4.93 % Σ VOCs), O-bearing species (4.79 to 19 % Σ VOCs) and halocarbons (0.14 to 0.76 % Σ VOCs) were also recorded in the soil gases of group C, whereas S-bearing compounds (from 1.08 to 2.90 % Σ VOCs) and alkenes (from 0.10 to 0.73 % Σ VOCs) were detected at concentrations comparable to those measured in the soil gases belonging to group B.

The principal features of the main homologous series of VOCs in interstitial soil gases are presented in detail below.

Table 6.4: Chemical composition (in nmol/mol) of VOCs in soil gases from the Solfatara Crater.

		1	2	3	4	5	6	7	8	9	10	11	12	13	14
Alkanes	C ₂ H ₆	230	170	80	510	290	330	790	150	750	620	960	910	60	510
	C ₃ H ₈	36	33	14	56	33	34	110	37	100	60	130	120	10	40
	C ₄ H ₁₀	7.8	7.1	4.4	7.7	6.1	5.6	11	4.7	12	9.7	7.2	7.8	1.5	6.6
	n-C ₄ H ₁₀	9.1	8.5	5.1	9.8	7.8	7.5	17	6.4	16	12	18	19	3.5	8.3
	i-C ₅ H ₁₂	3.1	2.6	2.3	3.6	3.2	3.4	5.6	2.4	5.1	3.8	3.2	3.3	0.6	2.1
	n-C ₅ H ₁₂	3.9	2.8	3.1	4.4	4.5	4.7	6.9	3	6.7	4.4	3.6	4.1	0.92	2.5
	i-C ₆ H ₁₄	2.5	2.5	1.9	2.4	2.3	2.8	3.1	1.8	3.3	3.2	2.4	2.6	0.62	1.1
	n-C ₆ H ₁₄	5.5	4.6	3.9	5.1	5.5	5.7	7.7	4.4	7.7	6.4	5.6	5.5	1.5	2.7
	i-C ₇ H ₁₆	0.66			0.71	0.82	0.52	0.93			1.1	0.54	0.73	0.55	
	n-C ₇ H ₁₆	1.1	0.74	0.54	1.3	1.4	1.1	1.9	0.72	2.1	1.5	1.8	1.4		0.56
	i-C ₈ H ₁₈								0.84		1.2		0.57		
	i-C ₈ H ₁₈ *								0.63		1.1		0.68		
	n-C ₈ H ₁₈	1.2	0.95	0.53	1.5	1.1	1.2	1.5	0.92	2.5	1.7	1.7	1.3		
Aromatics	C ₆ H ₆	310	270	120	470	340	410	750	260	710	560	880	850	120	450
	C ₇ H ₈	3.5	2.1	1.5	2.6	2.6	3.3	6.5	2.1	6.7	4.4	7.8	7.1	0.97	3.2
	C ₈ H ₈	1.7	0.92		0.61	0.73	1.2	2.1	0.94	2.6	2.1	3	3.1		1.3
	C ₈ H ₁₀	1.5	1.3		1.1	0.92	1.1	2.3	0.85	2.3	2.9	3.4	3.5		1.5
	m,p-C ₈ H ₁₀	2.1	1.5		1.8	1.1	1.3	2.9	2.1	3.4	4.4	3.2	3.9		1.9
	o-C ₈ H ₁₀	0.8	0.72		1.1	0.54	0.55	1.1	1.2	1.6	2.4	1.5	1.3		0.7
	C ₉ H ₁₂				0.53						0.75	0.65	0.57		
	C ₉ H ₁₂ *										0.95	0.86			

(To be continued)

		1	2	3	4	5	6	7	8	9	10	11	12	13	14
	C ₉ H ₁₂ ** C ₉ H ₁₂ *** C ₁₀ H ₈ C ₁₀ H ₁₄ C ₁₀ H ₁₄ *				0.55					1.1	0.64				
Cyclics	C ₅ H ₁₀ C ₆ H ₁₀ C ₆ H ₁₂ C ₆ H ₁₂ * C ₇ H ₁₄ C ₇ H ₁₄ * C ₈ H ₁₆ C ₈ H ₁₆ * C ₈ H ₁₆ ** C ₉ H ₁₈ C ₉ H ₁₈ * C ₉ H ₁₈ **	1.6 1.9 2.9 2.6 0.57 1.5 1.1 1.3 0.57	2.1 0.54 1.8 2.1 0.85 1.1 0.82 0.52 0.68	1.5 1.2 1.7 2.6 1.1 1.9 1.5 1.3 1.1	2.9 3.8 1.9 2.8 1.3 1.5 0.81 0.57	1.4 0.75 2.6 2.1 1.7 0.87 1.2 0.52 0.85	1.9 0.63 3.2 2.9 1.4 1.5 1.3 1.7	3.8 1.9 2.8 4.7 1.2 1.1 0.53 0.64	2.2 2.5 2.6 2.1 1.1 0.84 1.2 1.1	2.7 0.77 3.9 3.4 1.6 0.63 1.3 0.64	2.9 3.6 3.5 4.1 1.2 0.76 0.63 0.75	2.7 3.1 3.9 3.1 0.53 0.68 1.1 1.1	2.6 2.8 2.7 3.7 0.74 0.86 1.6 1.9	0.74 0.54 1.6 1.4 0.74 0.86 1.5 1.3	1.6 1.6 2.5 3.6 1.5 1.1 1.4 1.6
Alkenes	C ₃ H ₆ C ₄ H ₈ C ₅ H ₁₀ C ₆ H ₁₂ C ₆ H ₁₂ * C ₇ H ₁₄ C ₇ H ₁₄ *	1.2 1.3	1.1 0.71	0.53 0.15	2.1 1.2	1.3 1.1	1.1 0.75	3.4 3.1	0.93 1.5	3.1 3.5	2.1 1.7	3.6 2.1	3.8 2.7	0.56 0.21	1.4 0.94
								1.7 1.3		0.94 1.1		0.57 0.74			

(To be continued)

		1	2	3	4	5	6	7	8	9	10	11	12	13	14
	C ₈ H ₁₈														
S-bearing	CS ₂	4.1	1.5	1.1	3.2	4.5	6.7	16	4.1	13	6.7	5.1	11	1.1	11
	C ₄ H ₄ S	1.5			1.1	3.1	2.1	11	2.7	6.7	4.5	2.3	4.1		5.3
	C ₂ H ₆ S	3.7	0.7	0.9	0.8	4.5	2.7	3.1	1.5	7.8	5.3	3.4	3.3		3.9
	C ₅ H ₆ S					1.1	0.6	3.4	0.8	2.4	1.9	0.6	1.2		1.9
	C ₆ H ₈ S							1.7		0.6	0.8		0.8		0.9
	C ₂ H ₆ OS	2.1	2.9	3.4	1.8	5.4	3.7	2.8	1.7	2.7	2.9	2.4	1.5	3.8	3.3
	C ₂ H ₆ O ₂ S	1.8	1.1	2.9	1.6	4.1	2.6	2.1	2.3	2.5	1.9	2.1	2.9	1.7	1.9
	C ₇ H ₅ NS				1.1					0.52			0.54	0.51	
O-bearing	C ₄ H ₄ O												1.1		
	C ₄ H ₈ O				0.74					0.63			1.3		0.72
	C ₅ H ₆ O				0.65								1.5		1.1
	C ₄ H ₈ O ₂	2.1	1.5	1.9	1.9	1.7	1.6	2.6	2.1	2.4	2.8	1.7	1.5	1.3	1.9
	C ₅ H ₁₂ O	0.54		0.22	0.52	0.63	0.55	0.44	0.41	0.23	0.31	0.56		0.45	0.67
	C ₅ H ₁₂ O*		0.53	0.63	0.85	1.1	0.96	0.64	0.55		0.73	0.97		0.76	1.1
	C ₆ H ₁₄ O	0.66	0.74	0.98	1.4	1.3	0.8	0.66	0.73	0.56	0.85	0.63	0.52	0.73	0.87
	C ₆ H ₆ O	2.6	2.8	2.7	3.6	3.5	3.1	2.7	2.5	2.4	2.7	2.1	1.6	1.9	3.9
	C ₆ H ₁₄ O*	2.1	3.4	2.2	2.2	1.8	1.6	1.5	1.8	2.1	2.5	2.3	1.5	2.6	2.1
	C ₃ H ₆ O ₂	1.6	2.7	1.6	3.8	4.6	1.9	2.1	3.1	3.5	3.3	3.3	2.6	2.4	1.5
	C ₆ H ₁₂ O ₂	1.5	3.9	2.5	2.4	1.6	1.5	1.9	1.6	2.8	3.1	3.6	1.5	2.1	1.5
	C ₆ H ₁₂ O ₂ *	1.4	1.6	2.7	2.1	2.5	2.3	2.3	2.8	2.5	2.1	1.3	1.6	1.9	1.7
	C ₆ H ₁₆ O ₂		0.62			0.74	0.94			0.65			1.8		0.76
	C ₄ H ₁₀ O ₂		0.83	0.21	0.15	0.54		0.56	0.19	0.24		0.78	1.3	1.1	1.7
	C ₅ H ₁₂ O ₂		0.66			0.86		1.6		0.32			0.98	1.7	0.88

(To be continued)

		1	2	3	4	5	6	7	8	9	10	11	12	13	14
	C ₆ H ₁₄ O ₂	2.2	2.3	2.7	2.4	2.6	2.1	2.9	1.5	1.9	1.6	1.7	1.8	2.2	2.5
	C ₇ H ₁₆ O	1.6	2.8	2.6	2.4	1.5	1.6	2.1	2.7	2.5	2.6	2.3	2.8	2.1	2.4
	C ₄ H ₈ O*	4.1	3.6	3.1	2.7	1.6	1.7	4.1	4.6	3.5	3.3	2.9	2.5	4.1	2.6
	C ₆ H ₁₂ O	3.5	2.7	2.6	2.5	1.7	1.6	5.3	3.3	2.9	3.1	3.7	3.3	3.8	2.2
	C ₈ H ₈ O	0.74	0.56		0.75	1.5	1.6	1.9	0.54		1	1.3	1.7	1.6	
	C ₄ H ₈ O**	2.7	2.8	3.4	3.6	3.1	2.5	2.9	2.7	2.4	3.4	3.6	3.8	5.4	2.6
	C ₅ H ₁₀ O	2.6	2.1	3.3	3.8	2.5	2.7	2.5	2.1	1.5	2.6	3.3	4.1	4.7	2.1
	C ₆ H ₁₂ O*	2.9	3.6	3.4	2.7	2.9	3.6	4.1	3.3	3.1	3.4	3.6	4.4	4.6	1.8
	C ₇ H ₁₄ O	1.1	1.5	1.6	1	1.6	1.6	1.1	1.9	0.7	0.9	2.1	1.9	3.4	2.6
	C ₈ H ₁₆ O	0.63	0.75	0.55		1.1	0.65		0.84			0.85	0.66	1.6	1.7
	C ₇ H ₆ O	1.6	1.7	2.4	1.5	1.9	0.75		1.5			1.5	1.6	1.3	2.1
Halocarbons	CCl ₃ F	0.17	0.17	0.19	0.11	0.15	0.11	0.09	0.16	0.08	0.11	0.08		0.22	0.08
	CCl ₂ F ₂	0.36	0.4	0.42	0.21	0.35	0.22	0.21	0.38	0.2	0.24	0.22	0.09	0.47	0.18
	CClF ₃	0.08	0.09	0.11	0.05	0.08	0.05	0.05	0.09		0.06	0.05		0.11	
	CH ₃ Cl	0.36	0.4	0.43	0.23	0.35	0.24	0.22	0.38	0.21	0.22	0.22	0.09	0.46	0.21
	CCl ₄	0.15	0.16	0.09	0.08	0.13	0.21	0.09	0.17		0.09	0.16	0.21	0.27	0.22
	C ₂ H ₂ Cl ₂	0.06	0.07	0.08	0.05	0.07			0.06		0.08	0.15		0.09	
	C ₂ HCl ₃	0.08	0.09	0.11	0.06	0.07	0.06	0.05	0.09	0.05		0.06		0.05	0.06
	C ₂ H ₃ Cl	0.17	0.15	0.12	0.16	0.21	0.13	0.06	0.11	0.06	0.09	0.08	0.07	0.06	0.05
	C ₆ H ₅ Cl	0.51	0.56	0.66	0.28	0.38	0.34	0.34	0.47	0.26	0.24	0.18	0.08	0.35	0.19

(To be continued)

		15	16	17	18	19	20	21	22	23	24	25	26	27	28	
Alkanes	C ₂ H ₆	3600	370	120	220	180	290	450	390	610	180	190	110	180	770	
	C ₃ H ₈	510	51	14	15	13	33	57	65	72	20	34	15	31	110	
	C ₄ H ₁₀	9.8	2.3	2.3	2.9	1.5	2.3	6.8	7.9	8.3	3.1	5.4	1.5	3.4	7.7	
	n-C ₄ H ₁₀	25	2.6	4.4	4.7	3.8	5.9	9.1	11	13	5.6	7.1	3.2	5.8	15	
	i-C ₅ H ₁₂	4.4	1.1	0.85	1.1	0.5	1.2	3.1	3.3	3.8	1.3	2.3	0.7	1.4	3.5	
	n-C ₅ H ₁₂	4.9	1.2	1.3	1.5	0.83	1.7	4.3	3.9	4.6	1.8	3.5	1.5	1.9	4.5	
	i-C ₆ H ₁₄	2.9	1.3	1.7	1.3	0.8	1.6	2.5	3.4	2.1	2	2.3	0.96	2.2	2.5	
	n-C ₆ H ₁₄	6.7	1.7	3.1	2.5	1.8	3.3	5.9	6.2	5.5	3.3	4.9	2.4	6.7	6.4	
	i-C ₇ H ₁₆	0.66							0.57	0.88	0.66				0.77	1.3
	n-C ₇ H ₁₆	1.4		0.61	0.51		0.73	1.5	1.7	1.3	0.83	1.1		1.4	2.1	
	i-C ₈ H ₁₈								1.2	0.72						0.83
	i-C ₈ H ₁₈ *								0.73	0.54						0.64
	n-C ₈ H ₁₈	1.1						0.54	1.8	1.5	1.1	0.97	1.4		1.1	2.2
Aromatics	C ₆ H ₆	3200	470	160	310	260	360	530	380	530	280	350	190	260	710	
	C ₇ H ₈	62	11	1.1	2.1	1.5	2.4	3.9	2.1	3.3	1.9	2.6	1.3	1.9	6.6	
	C ₈ H ₈	43	5.1		0.55		0.8	1.4	0.74	0.95		1.2			2.6	
	C ₈ H ₁₀	51	6.2		0.87		1.1	1.5	0.61	0.72		1.3		0.67	1.3	
	m,p-C ₈ H ₁₀	66	7.1		1.1		1.5	2.5	2.1	1.5		2.7		0.86	1.1	
	o-C ₈ H ₁₀	41	4.2				0.76	1.2	1.1	0.65		1.1			0.55	
	C ₉ H ₁₂	7.6	0.77													
	C ₉ H ₁₂ *	6.1	0.61													
	C ₉ H ₁₂ **	4.4	0.58													
	C ₉ H ₁₂ ***	1.5														

(To be continued)

		15	16	17	18	19	20	21	22	23	24	25	26	27	28
	C ₁₀ H ₈ C ₁₀ H ₁₄ C ₁₀ H ₁₄ *	1.1													
Cyclics	C ₅ H ₁₀	3.7	2.2	3.3	2.9	2.6	4.1	7.8	8.5	8.6	4.6	5.7	2.6	4.4	11
	C ₆ H ₁₀	0.65	1.3	1.7		0.92	2.7	2.6	0.81		0.68	2.2	2.1	0.77	0.96
	C ₆ H ₁₂	5.7	2.5	2.1	2.6	2.5	2.9	5.8	5.1	4.5	3.3	2.7	3.3	3.9	3.5
	C ₆ H ₁₂ *	5.5	1.2	1.6	1.8	1.5	2.5	5.5	4.6	4.2	2.6	4.1	2.6	2.4	3.1
	C ₇ H ₁₄	2.8	1.1				1.3	1.6	2.4	2.1	1.2	1.8	1.6	0.94	0.73
	C ₇ H ₁₄ *	1.5	0.55	0.52	0.51		0.95	1.7	1.5	1.6	0.86	2.1	0.74	0.53	1.1
	C ₈ H ₁₆	0.83	0.61	1.1	1.3	1.1	0.85	0.76		1.5	1.8	0.63	0.87	1.5	0.74
	C ₈ H ₁₆ *	1.1	1.2	1.6	1.5	0.75	0.63			1.6	1.4	1.1	1.7	1.6	0.94
	C ₈ H ₁₆ **	0.75	1.1	1.3	1.4	0.91	0.84	0.62	0.61	1.1	1.6	1.5	1.7	1.3	1.1
	C ₉ H ₁₈		0.55	0.63									0.77		
	C ₉ H ₁₈ *		0.87		0.73						0.85		1.1	0.51	0.62
	C ₉ H ₁₈ **		1.1		0.94							0.53	1.3		0.7
Alkenes	C ₃ H ₆	7.8	1.5	0.57	0.64	0.51	1.5	2.3	3.1	3.5	0.73	1.2	3	1.5	3.9
	C ₄ H ₈	6.7	1.6	0.16		0.15	0.95	2.5	2.1	2.9	0.52	0.93		1.1	3.3
	C ₅ H ₁₀	1.4						1.1	0.72	0.64					1.1
	C ₆ H ₁₂														
	C ₆ H ₁₂ *	1.1					0.53	0.65		0.56					1.1
	C ₇ H ₁₄														
	C ₇ H ₁₄ *														
	C ₈ H ₁₈														
S-bearing	CS ₂	66	5.6	1.3	2.1	3.7	4.7	6.1	5.6	10	2.4	4.4	1.5	3.2	11

(To be continued)

		15	16	17	18	19	20	21	22	23	24	25	26	27	28
	C ₄ H ₄ S	34	2.9		1.6	1.9	4.1	5.5	3.4	3.9		1.7		1.1	5.3
	C ₄ H ₆ S	45	2.8		2.1	2.3	5.5	6.1	3.5	3.7		2.3		1.5	2.3
	C ₅ H ₆ S	8.7	3.4				1.4	1.5	0.8	2.1					1.5
	C ₆ H ₈ S	3.4	1.5							0.87					1.3
	C ₂ H ₆ OS	4.1	2.8	2.8	2.7	1.9	1.1	0.93	1.6	1.2	3.1	3.9	2.8	5.7	2.7
	C ₂ H ₆ O ₂ S	3.9	2.1	3.5	2.1	1.6	0.85	1.1	1.6	1.2	3.3	2.8	2.5	2.7	1.9
	C ₇ H ₅ NS	1.1	0.62				0.74				1.9		1.1		
O-bearing	C ₄ H ₄ O	1.3								0.76					
	C ₄ H ₈ O	2.1	0.54							0.55					1.1
	C ₅ H ₆ O	1.9	0.66							1.3					
	C ₄ H ₈ O ₂	2.2	2.5	2.6	2.2	2.9	3.1	4.6	2.1	2.8	4.1	4.4	3.1	2.6	2.1
	C ₅ H ₁₂ O	0.55	0.66	0.71	0.66	0.73	0.62	0.54	0.21		0.89	0.72	0.46	0.21	
	C ₅ H ₁₂ O*	0.65	0.82	0.53	0.95	1.3	1.1	0.86	0.54		1.1	1.4	1.1	0.86	
	C ₆ H ₁₄ O	1.1	1.4	1.1	1.5	1.6	1.3	0.75	0.87	0.57	1.4	1.7	1.3	1.2	0.86
	C ₆ H ₆ O	4.1	2.1	4.6	2.7	4.1	4.6	2.7	1.7	1.6	2.8	2.7	5.1	5.6	2.8
	C ₆ H ₁₄ O*	1.6	1.7	1.9	0.86		0.58	1.6	1.4	0.85	1.5	1.6	1.8	1.6	1.3
	C ₃ H ₆ O ₂	1.9	1.8	1.6	1.3	1.8	1.9	2.1	2.6	2.7	3.4	3.5	3.7	3.4	2.4
	C ₆ H ₁₂ O ₂	1.9	2.7	2.4	2.5	2.6	1.1	1.6	1.6	1.5	1.3	1.7	1.9	2.6	1.7
	C ₆ H ₁₂ O ₂ *	1.8	2.1	2.6	2.7	2.2	1.6	1.9	1.4	1.5	2.1	2.8	2.2	2.6	2.1
	C ₆ H ₁₆ O ₂			0.67		1.9			1.3	0.75		0.75	0.86		
	C ₄ H ₁₀ O ₂			0.79		2.1			1.9		0.86	0.87	1.2	0.74	
	C ₅ H ₁₂ O ₂			1.3		1.1			1.1		0.86	1.5	0.88	0.23	0.51
	C ₆ H ₁₄ O ₂	2.6	2.4	2.6	2.8	2.4	1.9	1.6	1.6	1.6	1.7	1.5	1.8	1.3	1.6
	C ₇ H ₁₆ O	2.6	2.2	2	4.2	5.1	3.3	3.1	2.6	2.4	2.8	2.9	1.9	0.6	2.9

(To be continued)

		15	16	17	18	19	20	21	22	23	24	25	26	27	28
	C ₄ H ₈ O*	2.3	1.6	2.4	2.7	1.6	5.5	4.6	4.1	3.1	2.7	1.6	2.8	3.9	3.2
	C ₆ H ₁₂ O	2.4	1.9	2.7	1.6	1.5	2.8	2.2	2.7	2.6	2.7	1.7	2.6	2.6	2.4
	C ₈ H ₈ O	0.53	0.65	0.82		0.65	1.6	1.4	1.7	0.65		0.83		0.93	0.54
	C ₄ H ₈ O**	2.5	2.9	3.4	3.5	3.8	3.3	4.3	4.6	4.4	5.2	5.9	5.4	6.1	6.8
	C ₅ H ₁₀ O	1.8	1.6	1.5	2.7	2.9	2.5	3.8	3.4	3.3	3.7	5.4	4.1	5.6	5.9
	C ₆ H ₁₂ O*	2.4	2.6	2.7	3.1	3.3	3.7	4.5	4.1	3.6	4.1	3.3	5.1	3.4	3.4
	C ₇ H ₁₄ O	1.4	0.65	0.73	2.1	2.6	1.7	2.2	2.6	2.4	2.1	3.4	3.6	2.9	2.7
	C ₈ H ₁₆ O	0.67			1.1	0.96		0.82	0.82	0.75	0.64	1.9	1	1.3	1.7
	C ₇ H ₆ O				1.5	1.9		1.7	1.8	1.3	1.9	2.4	1.5	2.7	2.1
Halocarbons	CCl ₃ F		0.08	0.2	0.15	0.17	0.12	0.1	0.13	0.07	0.16	0.15	0.2	0.15	
	CCl ₂ F ₂		0.18	0.42	0.34	0.36	0.27	0.24	0.25	0.15	0.38	0.31	0.45	0.33	0.12
	CClF ₃			0.1	0.06	0.08	0.06	0.06	0.07		0.09	0.08	0.12	0.08	
	CH ₃ Cl		0.19	0.44	0.35	0.38	0.27	0.26	0.31	0.15	0.36	0.35	0.5	0.35	0.13
	CCl ₄		0.15	0.19	0.21	0.17	0.13	0.08	0.09	0.11	0.16	0.15	0.17	0.23	
	C ₂ H ₂ Cl ₂			0.07	0.09	0.08	0.06	0.11	0.09		0.06		0.08	0.09	
	C ₂ HCl ₃			0.07	0.07	0.06	0.08	0.05	0.06		0.09	0.06	0.08	0.05	
	C ₂ H ₃ Cl		0.08	0.16	0.15	0.13	0.18	0.08	0.13	0.06	0.14	0.13	0.21	0.09	0.05
	C ₆ H ₅ Cl		0.21	0.26	0.26	0.34	0.31	0.27	0.26	0.15	0.27	0.34	0.46	0.41	0.09

(To be continued)

		29	30	31	32	33	34	35	36	37	38	39	40	41	42
Alkanes	C ₂ H ₆	950	910	440	1800	1700	3600	1700	870	160	580	1700	760	6800	7300
	C ₃ H ₈	130	130	56	250	190	340	250	120	35	66	240	110	550	840
	C ₄ H ₁₀	11	9.5	5.4	12	11	13	15	7.7	4.5	7.8	14	8.8	14	17
	n-C ₄ H ₁₀	17	15	9.5	23	21	27	31	16	7.7	9.8	25	13	35	42
	i-C ₅ H ₁₂	5.5	4.1	2.7	6.8	5.4	5.7	5.5	3.1	2.2	2.9	6.6	4.1	7.9	8.1
	n-C ₅ H ₁₂	5.9	4.5	3.3	7.7	6.6	6.3	6.9	4.4	3.6	3.9	7.9	6.2	9.9	11
	i-C ₆ H ₁₄	3.4	3.1	2.3	6.2	3.8	4.4	4.8	3.1	2.3	3.4	4.1	4.4	7.6	8.3
	n-C ₆ H ₁₄	7.7	7.1	5.4	12	9.8	8.9	8.8	6.6	5.1	7.2	9.8	8.8	14	19
	i-C ₇ H ₁₆	1.1	1.4	0.91	1.7	1.6	1.6	1.1	0.72	0.53	0.54	2.1	1.9	1.1	
	n-C ₇ H ₁₆	2.4	2.5	1.7	3.3	2.5	2.3	2.2	1.5	1.6	1.8	4.1	3.8	2.1	1.6
	i-C ₈ H ₁₈	0.84	0.73		0.95	1.4	0.67	0.99			0.83	1.3	0.74	0.66	
	i-C ₈ H ₁₈ *	0.75	0.88		0.63	1.1	0.54	0.84	0.57		0.62	1.5	0.83	0.55	
n-C ₈ H ₁₈	2.5	1.9	1.5	3.1	2.1	1.9	2.7	1.9	1.3	1.5	4.5	3.3	1.9	1.1	
Aromatics	C ₆ H ₆	780	820	390	1500	1600	3200	1500	770	250	520	1600	690	5900	6600
	C ₇ H ₈	5.6	7.7	3.2	18	29	51	35	6.1	1.5	3.5	33	7.7	230	470
	C ₈ H ₈	2	3.1	0.8	5.5	12	29	14	2.9		1.1	12	2.1	150	270
	C ₈ H ₁₀	2.2	3.5	1.1	5.4	15	26	17	3.3		1.5	14	2.1	170	450
	m,p-C ₈ H ₁₀	2.9	4.6	2.3	7.7	13	31	22	5.4	0.67	2.5	18	3.1	210	360
	o-C ₈ H ₁₀	1.1	2.1	1.2	2.4	5.4	13	8.8	2.3		1.5	7.7	1.4	100	140
	C ₉ H ₁₂		0.73			1.9	2.1	2.3				1.7		21	17
	C ₉ H ₁₂ *		0.55			1.1	1.5	2.5				0.76		18	19
	C ₉ H ₁₂ **					0.63	1.7	2.1				0.85		11	16
	C ₉ H ₁₂ ***							0.58						2.8	2.5

(To be continued)

		29	30	31	32	33	34	35	36	37	38	39	40	41	42
	C ₁₀ H ₈	0.76												3.5	4.1
	C ₁₀ H ₁₄													0.64	
	C ₁₀ H ₁₄ *													0.56	
Cyclics	C ₅ H ₁₀	15	14	5.7	18	17	21	17	14	6.5	5.8	21	11	8.5	15
	C ₆ H ₁₀	0.55		0.94	1.1	1.5	2.4	2.8	1.5	1.4	0.83		1.5	1.6	1.9
	C ₆ H ₁₂	2.6	3.3	2.1	2.8	2.9	3.4	5.1	3.1	2.9	2.5	5.1	2.8	6.2	4.7
	C ₆ H ₁₂ *	3.8	3.5	2.9	4.8	4.5	4.7	5.6	3.5	3.1	2.9	6.7	5.4	5.8	8.7
	C ₇ H ₁₄	1.4	1.7	1.5	2.6	2.1	2.7	2.9	2.1	1.6	1.5	3.8	2.1	2.6	3.4
	C ₇ H ₁₄ *	1.6	0.94	1.2	2.6	2.1	2.1	2.6	1.7	1.2	0.76	2.6	1.3	1.9	2.1
	C ₈ H ₁₆	1.5	0.55	0.64	1.7	2.6	1.4	0.85	1.7	1.9	2.3	2.8	1.9	1.6	2.8
	C ₈ H ₁₆ *	1.7			2.1	2.1	1.1	1	1.6	1.5	2.1	2.5	1.7	1.7	2.6
	C ₈ H ₁₆ **	0.82	0.74	0.86	1.6	1.6	1.6	1.1	1.7	1.4	1.5	3.8	2.9	1.5	2.1
	C ₉ H ₁₈												0.88		0.64
	C ₉ H ₁₈ *								0.54	0.67			1.1	0.88	0.53
C ₉ H ₁₈ **				0.53					0.79		0.78			0.76	
Alkenes	C ₃ H ₆	4.1	3.5	1.9	5.4	4.9	6.7	5.4	3.1	0.72	2.3	7.7	4.5	11	23
	C ₄ H ₈	4.5	3.3	1.5	5.1	3.3	5.5	4.3	2.5	0.57	2.1	6.6	3.4	8.7	12
	C ₅ H ₁₀	1.5	1.6		1.9	0.94	2.1	1.8				1.5	2.1	2.3	4.5
	C ₆ H ₁₂						0.53					0.65			1.1
	C ₆ H ₁₂ *	1.3	0.94		1.1		1.5	1.3				1.1	1.2	1.1	2.3
	C ₇ H ₁₄														0.57
	C ₇ H ₁₄ *														
	C ₈ H ₁₈														
S-bearing	CS ₂	12	11	4.4	10	12	45	10	11	3.2	13	47	10	71	215

(To be continued)

		29	30	31	32	33	34	35	36	37	38	39	40	41	42
	C ₄ H ₄ S	4.1	4.5	2.9	6.8	9.1	15	19	15	1.3	2.8	15	5.1	26	41
	C ₄ H ₆ S	3.9	3.7	2.4	5.6	6.3	8.5	23	15	2.7	3.1	10	1.7	19	33
	C ₅ H ₆ S	1.7	3.2	2.6	5.1	4.9	8.1	4.1	3.6		2.7	6.8	2.3	11	17
	C ₆ H ₈ S	2.1	2.8	1.7	3.4	2.7	5.8	1.6	1.9		2.8	2.9	2.1	17	38
	C ₂ H ₆ OS	2.6	2.4	1.8	1.5	1.9	1.1	0.76	3.4	2.1	1.7	0.55	2.2	6.6	7.1
	C ₂ H ₆ O ₂ S	1.6	2.7	1.9	1.6	2.8	1.6	1.7	3.9	2.4	1.5	0.87	1.7	1.1	1.3
	C ₇ H ₅ NS	1.6			1.5		0.82	1.3		0.65			0.83	0.77	0.54
O-bearing	C ₄ H ₄ O	0.65			0.73		0.64					0.54		0.84	1.1
	C ₄ H ₈ O	1.2	0.53		1.6	0.66	1.7		0.62		0.54	0.96		0.65	1.5
	C ₅ H ₆ O	0.83			0.95	0.62	1.3		1.1					1.1	1.5
	C ₄ H ₈ O ₂	2.7	2.5	2.9	2.7	2.6	3.3	3.1	2.6	2.7	2.8	1.9	1.6	1.1	1.8
	C ₅ H ₁₂ O		0.89	0.23				0.54	0.55		0.66	0.42	0.15	0.13	0.85
	C ₅ H ₁₂ O*		1.1	0.95				1.1	0.54		0.65	0.62	0.72	0.74	1.6
	C ₆ H ₁₄ O	0.64	1.5	1.1	0.92	0.53	0.65	1.7	0.84	0.86	1.2	1.5	1.7	1.1	3.1
	C ₆ H ₆ O	3.9	5.1	5.6	2.7	2.6	3.8	2.7	2.6	2.8	2.9	2.7	2.5	1.6	7.7
	C ₆ H ₁₄ O*	0.82		0.63	0.85		1.5	1.9	0.66	0.75		1.6	1.3	0.67	0.85
	C ₃ H ₆ O ₂	2.1	1.3	1.6	1.5	2.4	2.6	2.8	2.1	4.1	3.5	3.3	2.9	1.8	1.1
	C ₆ H ₁₂ O ₂	1.6	0.63	1.3	1.1	0.64	0.72	0.65	0.23	0.15		0.75	1.1		
	C ₆ H ₁₂ O ₂ *	1.7	0.66	1.7	0.68		0.97	0.75	0.11	0.26	1.3	1.1	0.75		0.67
	C ₆ H ₁₆ O ₂	0.53		1.1		0.96						0.76	0.67		
	C ₄ H ₁₀ O ₂	0.77		0.68		0.59	0.66		0.74			1.1		0.7	
	C ₅ H ₁₂ O ₂	0.66		0.51		0.22	0.64		0.43			0.55		0.77	
	C ₆ H ₁₄ O ₂	1.8	2.4	2.6	2.1	2.9	3.1	2	0.9		1.6	1.2	0.9	0.8	0.7
	C ₇ H ₁₆ O	2.4	0.8	1.1	1.7	1.6	2.1	2.5	2.8	3.1	3.6	2.9	5.2	1.6	2.1

(To be continued)

		29	30	31	32	33	34	35	36	37	38	39	40	41	42
	C ₄ H ₈ O*	4.7	4.6	0.8	1.2	1.3	5.1	5.4	2.6	1.8	4.5	4.6	1.7	1.1	1.3
	C ₆ H ₁₂ O	3.1	3.7	1.7	1.6	1.5	4.5	2.6	4.1	2.2	5.6	5.1	1.5	0.74	0.38
	C ₈ H ₈ O	1.7	0.94	1.6	0.83		0.64	0.52	1.1	1.3		0.64	0.71	0.21	
	C ₄ H ₈ O**	6.7	6.5	4.6	4.5	5.5	3.4	2.8	2.9	1.9	2.7	3.5	3.7	1.6	1.8
	C ₅ H ₁₀ O	5.1	5.7	4.5	4.3	4.1	2.8	2.4	2.1	1.5	1.6	4.2	2.6	0.91	0.47
	C ₆ H ₁₂ O*	6.8	6.6	6.1	4.7	4.4	3.3	3.1	2.5	2.6	2.2	4.7	3.1	0.56	0.41
	C ₇ H ₁₄ O	2.6	2.6	2.4	2.1	2.6	2.9	2.4	2	2.2	1.6	3.3	0.77	0.66	0.35
	C ₈ H ₁₆ O	1.5	1.9	1.7	1.6	1.3	0.8	0.5	1.5	1	0.62	1.7		0.41	
	C ₇ H ₆ O	1.1	1.6	1.5	2.4	2.5			2.2	1.6	0.87	0.65		0.24	
Halocarbons	CCl ₃ F			0.09		0.06		0.08	0.09	0.15	0.05		0.12		
	CCl ₂ F ₂	0.08	0.15	0.23		0.13		0.19	0.22	0.4	0.15		0.25		
	CClF ₃												0.06		
	CH ₃ Cl	0.09	0.15	0.2		0.13		0.19	0.22	0.4	0.15		0.25		
	CCl ₄			0.17		0.11		0.08	0.16	0.19	0.11		0.17	0.08	0.16
	C ₂ H ₂ Cl ₂			0.09		0.06				0.07			0.11	0.08	
	C ₂ HCl ₃					0.05			0.11	0.05			0.13	0.05	
	C ₂ H ₃ Cl	0.06	0.14	0.07		0.09		0.06	0.13	0.11			0.07		
	C ₆ H ₅ Cl	0.11	0.12	0.16		0.14		0.15	0.21	0.33	0.16		0.24		

(To be continued)

		43	44	45	46	47	48	49	50	51	52
Alkanes	C ₂ H ₆	5100	4600	4800	6100	3800	4900	4700	1800	3800	1300
	C ₃ H ₈	660	550	610	470	370	390	340	260	310	170
	C ₄ H ₁₀	13	14	17	12	12	15	14	12	13	8.7
	n-C ₄ H ₁₀	37	39	43	37	28	31	29	18	27	14
	i-C ₅ H ₁₂	6.6	6.4	7.8	5.7	5.9	7.7	6.9	6.2	6.5	4.2
	n-C ₅ H ₁₂	8.7	7.6	8.1	6.8	7.4	8.9	7.7	7.7	7.8	5.4
	i-C ₆ H ₁₄	9.9	9.1	8.7	4.8	6.2	7.7	7.9	7.6	7.8	3.1
	n-C ₆ H ₁₄	14	12	16	11	13	19	17	14	15	6.7
	i-C ₇ H ₁₆	0.72		0.53			0.61	0.84	0.68	0.57	
	n-C ₇ H ₁₆	1.4	0.96	1.1	0.77	1.1	1.3	1.4	1.4	1.4	0.92
	i-C ₈ H ₁₈										
	i-C ₈ H ₁₈ *										
n-C ₈ H ₁₈	1.1		0.55		0.53	0.69	0.55	0.96	0.65		
Aromatics	C ₆ H ₆	4700	4200	4500	5100	3300	3900	4100	1500	3300	1100
	C ₇ H ₈	150	120	140	190	98	95	150	31	79	23
	C ₈ H ₈	45	41	52	98	27	25	49	12	19	5.9
	C ₈ H ₁₀	170	88	110	120	55	57	130	15	31	13
	m,p-C ₈ H ₁₀	130	160	150	220	67	73	110	25	56	17
	o-C ₈ H ₁₀	65	48	69	110	25	34	44	6.7	21	3.3
	C ₉ H ₁₂	5.4	6.7	9.9	19	2.1	2.9	3.4	2.3	2.1	0.9
	C ₉ H ₁₂ *	6.6	7.1	7.8	16	3.5	4.4	3.3	1.5	2.3	1.1
	C ₉ H ₁₂ **	6.1	7.5	7.9	19	4.4	6.6	4.3	2.2	2.5	1.5
	C ₉ H ₁₂ ***	3.1	2.3	1.1	5.6	2.1	1.5	1.6	1	0.77	

(To be continued)

		43	44	45	46	47	48	49	50	51	52
	C ₁₀ H ₈	3.5	3.1	2.7	4.4	2.3	1.1	1.9	1.2	1.1	0.66
	C ₁₀ H ₁₄	0.73			1.2			0.75	0.53		
	C ₁₀ H ₁₄ *	0.84		1.1							
Cyclics	C ₅ H ₁₀	11	13	17	16	12	14	13	11	11	5.6
	C ₆ H ₁₀	1.1		0.83			0.94	0.64		0.56	
	C ₆ H ₁₂	6.1	4.8	3.3	3.8	3.6	3.1	2.6	3.6	2.7	2.8
	C ₆ H ₁₂ *	7.5	6.9	7.1	8.6	7.5	9.7	11	7.4	8.5	7.8
	C ₇ H ₁₄	2.1	2.7	2.1	2.9	2.2	3.1	4.5	3.1	2.6	4.5
	C ₇ H ₁₄ *	2.6	2.7	2.6	2.5	1.8	2.6	3.1	2.6	2.1	3.1
	C ₈ H ₁₆	2.6	1.7	1.5	1.8	2.1	2.8	3.4	2.1	2.2	4.1
	C ₈ H ₁₆ *	2.5	2.1	1.9	1.6	1.9	1.8	3.9	2.7	3.9	2.7
	C ₈ H ₁₆ **	2.2	2.6	2.7	2.5	3.1	3.4	3.3	2.7	3.1	5.1
	C ₉ H ₁₈		0.76	1.1	1.7	0.97		0.55	0.82		0.83
	C ₉ H ₁₈ *	0.86	1.3	1.6	1.5	1.1			0.78		0.57
C ₉ H ₁₈ **	0.69	1.5	1.8	1.8	1.2			0.77	0.64	1.1	
Alkenes	C ₃ H ₆	19	12	16	12	10	11	9.5	7.8	11	5.5
	C ₄ H ₈	16	9.9	15	11	9.8	13	12	8.8	14	6.6
	C ₅ H ₁₀	3.2	2.5	6.1	3.4	5.5	5.5	4.7	1.9	6.7	1.5
	C ₆ H ₁₂	1.3	1.5	1.2	0.56	1.2	1.6	1.2		1.2	
	C ₆ H ₁₂ *	2.1	1.9	2.5	2	3.3	3.1	2.4	0.93	3.5	0.96
	C ₇ H ₁₄	0.55		0.96		1.1	0.95	1.2		0.93	
	C ₇ H ₁₄ *	0.53		1.1		1.2	0.88	0.54		1.1	
	C ₈ H ₁₈	0.69		0.87		1.1	0.56	0.65		0.74	
S-bearing	CS ₂	254	256	271	266	378	255	305	240	210	187

(To be continued)

		43	44	45	46	47	48	49	50	51	52
	C ₄ H ₄ S	47	68	48	64	82	66	81	54	77	71
	C ₄ H ₆ S	25	41	30	38	69	54	36	43	61	53
	C ₅ H ₆ S	16	30	16	21	34	28	21	33	44	37
	C ₆ H ₈ S	54	56	21	35	19	23	22	28	21	16
	C ₂ H ₆ OS	5.6	6.9	7.8	5.4	3.8	6.6	8.1	4.9	4.3	6.3
	C ₂ H ₆ O ₂ S	1.8	1.1	0.65	0.73		0.65	0.76	0.83	1.1	1.5
	C ₇ H ₅ NS	0.78		1.2	1.1		0.96		1.5		0.87
O-bearing	C ₄ H ₄ O	0.82		1.2	1.1		0.75		0.75	0.54	0.84
	C ₄ H ₈ O	0.93		1.3	1.5	0.86	0.75	0.62	0.57	0.99	1.1
	C ₅ H ₆ O	0.51		0.83	1.5		0.87		1.1	0.75	1.1
	C ₄ H ₈ O ₂	3.1	2.8	2.7	3.5	1.9	0.86	1.9	4.5	3.1	2.3
	C ₅ H ₁₂ O	0.27	0.66	0.74	0.22	0.25	0.21	0.66	0.93	0.76	0.21
	C ₅ H ₁₂ O*	1.2	1.3	1.5	0.52	0.75	0.64	1.6	1.6	1.5	0.83
	C ₆ H ₁₄ O	2.8	1.9	1.6	1.1	1.5	2.4	2.7	2.2	2.7	1.5
	C ₆ H ₆ O	5.6	5.4	8.4	4.6	4.5	4.1	6.1	4.6	5.5	5.1
	C ₆ H ₁₄ O*	1.6	1.4	0.82	0.65	1.3	1.1		1.5	2.1	2.2
	C ₃ H ₆ O ₂	1.5	3.1	2.6	2.7	2.7	2.8	2.9	5.1	2.6	2.6
	C ₆ H ₁₂ O ₂	1.6	1.2			1.7	0.98		0.78	0.98	1.5
	C ₆ H ₁₂ O ₂ *		0.85		0.76	1.6	0.83		1.5	2.7	2.1
	C ₆ H ₁₆ O ₂		0.58			0.76			1.1	0.55	0.53
	C ₄ H ₁₀ O ₂		0.89	0.65		1.1				1.6	
	C ₅ H ₁₂ O ₂		0.66	0.41			0.56			1.2	
	C ₆ H ₁₄ O ₂		1.8	0.6	0.8	1.1	0.56		1.4	1.6	0.83
	C ₇ H ₁₆ O	1.8	1.4	1.9	1.6	1.7	1.5	2	1.8	0.1	1.6

(To be continued)

		43	44	45	46	47	48	49	50	51	52
	C ₄ H ₈ O*	1.5	1.8	0.87	1.1	1.3	1.5	0.56	0.98	2.2	0.71
	C ₆ H ₁₂ O	0.66	0.55	0.36	0.81	0.69	1.1	0.41	0.55	0.66	0.56
	C ₈ H ₈ O	0.51		0.46	0.87		1.1	0.26		0.27	0.71
	C ₄ H ₈ O**	1.1	1.6	0.89	1.3	1.1	0.65	0.84	1.1	1.3	1.1
	C ₅ H ₁₀ O	0.38	0.58	0.29	0.33	0.37	0.47	0.76	0.66	0.71	0.87
	C ₆ H ₁₂ O*	0.25	0.44	0.15	0.15	0.31	0.33	0.51	0.44	0.71	0.74
	C ₇ H ₁₄ O	0.14	0.36	0.11	0.12	0.26	0.26	0.43	0.32	0.54	0.51
	C ₈ H ₁₆ O	0.11	0.21		0.05	0.18	0.21	0.15			0.23
	C ₇ H ₆ O	0.19	0.16	0.53		2.2	1.8	1.2		0.57	0.93
Halocarbons	CCl ₃ F										
	CCl ₂ F ₂										
	CClF ₃										
	CH ₃ Cl										
	CCl ₄	0.13	0.14	0.16	0.11		0.06	0.17	0.18	0.07	0.09
	C ₂ H ₂ Cl ₂	0.07	0.11	0.13			0.06				0.07
	C ₂ HCl ₃	0.06	0.06	0.08			0.07				0.09
	C ₂ H ₃ Cl		0.11	0.015			0.06				0.11
	C ₆ H ₅ Cl						0.06	0.05			0.06

Table 6.4: Chemical composition (in nmol/mol) of VOCs in soil gases from the Solfatara Crater.

Alkanes

The relative abundances of alkanes of the Solfatara Crater interstitial soil gases were relatively consistent for the three groups, i.e. (i) 48-56 % Σ VOCs in group A, (ii) 43-55 % Σ VOCs in group B, and (iii) 29-51 % Σ VOCs in group C. Ethane (C_2H_6) was the most abundant compound, with concentrations ranging (i) from 1,300 to 7,300 nmol/mol (up to 48 % Σ VOCs) in group A, (ii) from 789 to 3,789 nmol/mol (up to 46 % Σ VOCs) in group B, and (iii) from 60 to 390 nmol/mol (up to 40 % Σ VOCs) in group C (Table 6.4; Figure 6.6). Propane was the second most abundant alkane, with contents

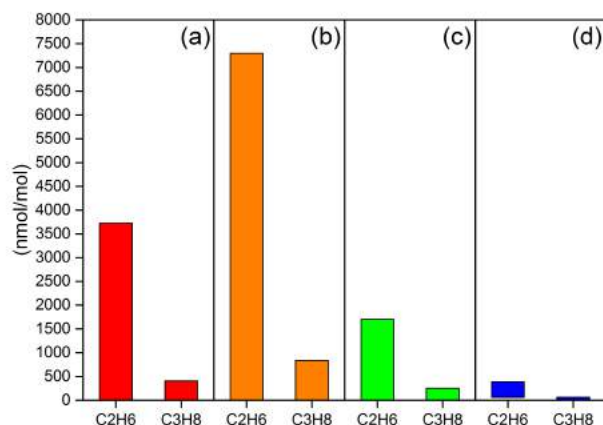


Figure 6.6: Floating column diagram for the concentrations (in nmol/mol) of ethane and propane in (a) BG and BN fumaroles (red), and in soil gases of type (b) A (orange), (c) B (green), and (d) C (blue).

(i) ≥ 170 nmol/mol (group A), (ii) from 33 to 250 nmol/mol (group B), and (iii) ≤ 65 nmol/mol (group C) (Table 6.4; Figure 6.6). The ethane/propane ratios were ranging from 4 to 15, i.e. similar to the values measured in the fumarolic gas samples (from 7 to 10).

As observed in the BG and BN fumaroles, the abundances of n-alkanes decreased with increasing molecular weight (Figure 6.7), with the exception of n-hexane, displaying concentrations higher than those measured for n-pentane. The n-hexane/n-pentane ratios in the soil gases ranged from 1.08

6. Results

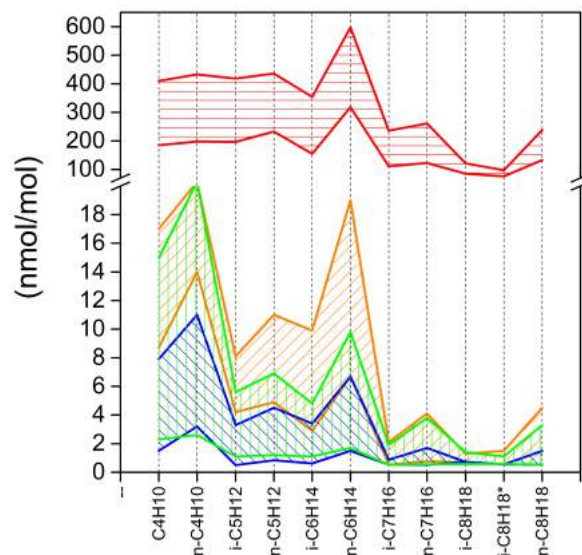


Figure 6.7: Area chart depicting the concentration ranges (in nmol/mol) of C_{4+} alkanes in fumaroles (red), and in soil gases of type A (orange), B (green), and C (blue).

to 3.35, i.e. comparable with the values measured in the fumarolic gases (from 1.32 to 1.91).

Branched alkanes were mostly present at concentrations lower than those of the corresponding linear alkanes (Table 6.4), the normal-/iso-alkanes ratios being from 0.84 to 3.33 and showing no relevant variations among the three groups of soil gases. The abundances of iso-alkanes relative to normal-alkanes were generally lower in soil gases with respect to those measured in the fumarolic gas samples (Figure 6.8).

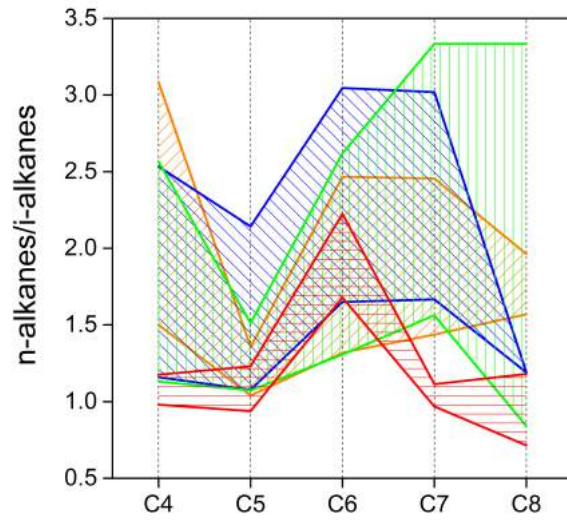


Figure 6.8: Area chart showing the range of normal- to iso-alkane ratios for of C₄₋₈ saturated hydrocarbons in fumaroles (red), and in soil gases of type A (orange), B (green), and C (blue).

6. Results

Aromatics

Aromatics in the soil gas samples ranged from 37 to 51 % of Σ VOCs. Benzene was the most abundant compound, with concentrations ranging from (i) 1,100 to 6,600 nmol/mol (up to 42 % Σ VOCs), group A, (ii) 360 to 1,600 nmol/mol (up to 47 % Σ VOCs), group B, and (iii) 120 to 380 nmol/mol (up to 50 % Σ VOCs), group C (Table 6.4).

Toluene, ethylbenzenes, xylenes and styrene were comprised between (i) 2.53 to 20.2 % Σ aromatics, group A, (ii) 1.33 to 6.65 % Σ aromatics, group B, and (iii) 0.57 to 3 % Σ aromatics, group C. Other species, including branched aromatics and naphthalene, accounted for ≤ 1.10 % Σ aromatics in group A and ≤ 0.51 % Σ aromatics in group B, whereas they were not detected in the soil gas samples pertaining to group C (Figure 6.9).

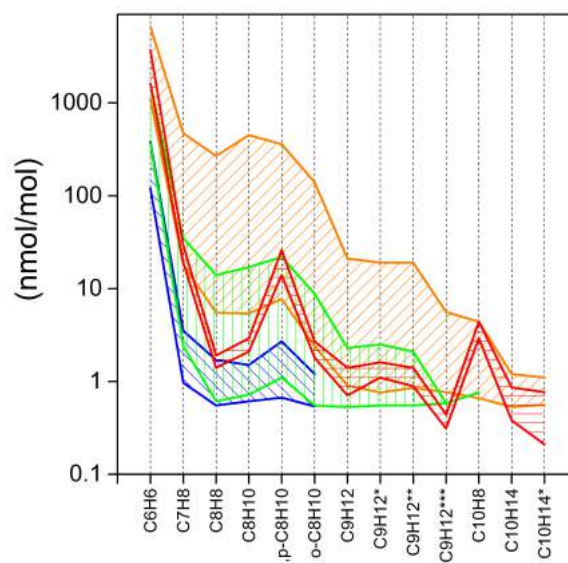


Figure 6.9: Area chart depicting the concentration ranges (in nmol/mol) of aromatic compounds in fumaroles (red), and in soil gases of type A (orange), B (green), and C (blue).

Alkenes

Alkenes were dominated by propene and butene, systematically present in all the analyzed soil gases (Table 6.4). Soil gases from group A were characterized by propene (from 5.4 to 23 nmol/mol) and butene (from 5.1 to 16 nmol/mol), followed by pentene (from 1.4 to 6.7 nmol/mol) and hexene (from 0.93 to 3.5 nmol/mol), whereas heptene and branched alkenes accounted for less than 4.6 nmol/mol (Table 6.4; Figure 6.10). The latter species were

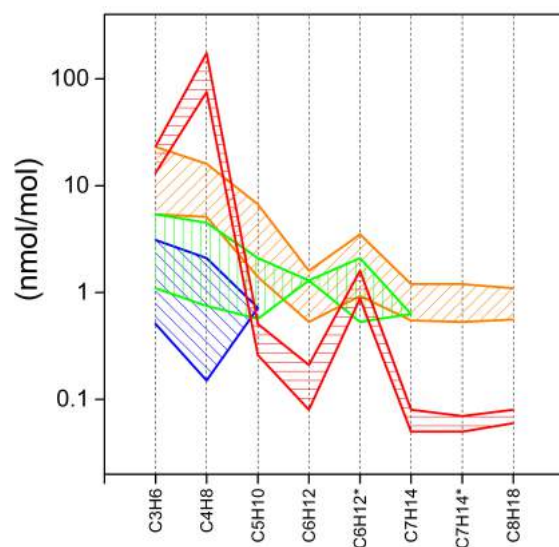


Figure 6.10: Area chart showing the concentration ranges (in nmol/mol) of alkenes in fumaroles (red), and in soil gases of type A (orange), B (green), and C (blue).

only detected in one sample (site 7) among the soil gases from group B, which showed pentene and hexene at concentrations ≤ 2.10 nmol/mol and propene and butene ranging from 1.10 to 5.40 nmol/mol and from 0.75 to 4.50 nmol/mol, respectively (Table 6.4; Figure 6.10). Alkenes in group C were only represented by propene (from 0.51 to 3.10 nmol/mol) and butene (from 0.15 to 2.10 nmol/mol), with pentene being only detected in one sample (site 22; Table 6.4).

Generally, alkenes were ranging from (*i*) 0.16 to 0.48 % Σ VOCs, group A,

6. Results

(ii) 0.21 to 0.67 % Σ VOCs, group B, and (iii) 0.10 to 0.73 % Σ VOCs, group C.

S-bearing compounds

S-bearing species in interstitial soil gases were mostly represented by carbon disulphide and thiophenes. Soil gases of group A were characterized by S-bearing compounds up to 12 % Σ VOCs, with carbon disulphide ranging from 10 to 378 nmol/mol and thiophene from 6.8 to 82 nmol/mol (Table 6.4). Methylated thiophenes, i.e. methylthiophene and dimethylthiophene, were present at concentrations up to 44 and 56 nmol/mol, respectively (Table 6.4). Dimethylsulphide ranged from 5.6 to 69 nmol/mol, whereas dimethylsulphoxide and dimethylsulphone were up to 8.1 and 3.9 nmol/mol, respectively (Table 6.4). Benzothiazole was present at concentrations up to 1.3 nmol/mol.

S-bearing compounds in the soil gases of group B accounted from 0.77 to 2.75 % Σ VOCs. Carbon disulphide was ranging from 3.20 to 16 nmol/mol and thiophene from 1.10 to 19 nmol/mol, whereas methylthiophene and dimethylthiophene were up to 4.90 and 2.80 nmol/mol, respectively (Table 6.4). Dimethylsulphide was measured at concentrations ranging from 0.8 to 23 nmol/mol, whereas dimethylsulphoxide and dimethylsulphone were detected at comparable concentrations (from 0.76 to 3.70 nmol/mol and from 0.85 to 3.90 nmol/mol, respectively; Table 6.4).

In the soil gases of group C, S-bearing species were ranging from 1.08 to 2.90 % Σ VOCs. Carbon disulphide was characterized by concentrations varying from 1.10 to 5.60 nmol/mol, whereas thiophene (up to 3.40 nmol/mol) was not detected in all the analyzed samples (Table 6.4). Among methylated thiophenes, methylthiophene was only recorded in three samples (sites 5, 8 and 22), with concentrations \leq 1.11 nmol/mol, whereas dimethylthiophene was not detected (Table 6.4). Dimethylsulphide, dimethylsulphoxide and dimethylsulphone were present at comparable concentrations (up to 4.50, 5.70 and 4.10 nmol/mol; Table 6.4).

Benzothiazole was occasionally present at similar concentrations (up to 1.90 nmol/mol) in all the three groups (Table 6.4).

O-bearing compounds

O-bearing compounds represented (i) ≤ 1.29 % Σ VOCs in the soil gases of group A (from 20 to 50 nmol/mol), (ii) from 1.04 to 5.35 % Σ VOCs in the soil gases of group B (from 33 to 56 nmol/mol), and (iii) ≥ 4.79 and up to 19 % Σ VOCs in the soil gases of group C (from 31 to 55 nmol/mol).

Soil gases of group B and C were dominated by aldehydes (up to 52 and 42 % Σ O-bearing compounds, respectively), ketones (up to 26 and 23 % Σ O-bearing compounds, respectively), and esters (up to 30 and 24 % Σ O-bearing compounds, respectively). Phenol, alcohols, ethers, glycol ethers and carboxylic acids showed no relevant differences for the soil gases of groups B and C (Figure 6.11). On the contrary, furans, which were not detected in

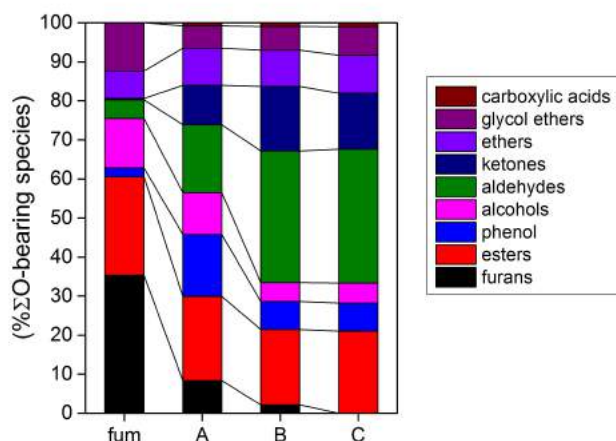


Figure 6.11: Average relative abundances (in % Σ O-bearing compounds) of furans, esters, phenol, alcohols, aldehydes, ketones, ethers, glycol ethers and carboxylic acids in fumarolic gases (fum) and in soil gases of groups A, B and C.

the soil gases of group C (Table 6.4), were measured up to 8 % Σ O-bearing compounds in the soil gases of group B.

In the group A, aldehydes, esters, phenol, ketones and alcohols (up to 47, 35, 29, 22, 21% Σ O-bearing compounds, respectively) were the main species of the O-bearing compounds, with furans representing up to 16 % Σ O-bearing

6. Results

compounds (Figure 6.11).

Cyclics

Cyclic compounds in interstitial soil gases included C₅ to C₈ structures measured at concentrations from (i) 0.23 to 1.29 % Σ VOCs, group A (from 23 to 50 nmol/mol), (ii) 0.91 to 2.22 % Σ VOCs, group B (from 14 to 39 nmol/mol), and (iii) 1.53 to 4.93 % Σ VOCs, group C (from 10 to 24 nmol/mol). Cyclopentane was the most abundant compound (up to 52, 57 and 36 % Σ cyclics in groups A, B and C, respectively), followed by cyclohexane (up to 24, 27 and 20 % Σ cyclics in groups A, B and C, respectively). Cyclooctane was measured at lower concentrations (up to 13, 10 and 15 % Σ cyclics in groups A, B and C, respectively), whereas no cycloheptane was detected (Table 6.4). Methylated, dimethylated and trimethylated C₅ and C₆ cycloalkanes were present at concentrations up to 53, 63 and 62 % Σ cyclics in groups A, B and C, respectively. Among methylated cycloalkanes, methylcyclopentane was the most abundant compound (up to 25, 24 and 24 % Σ cyclics in groups A, B and C, respectively). Methylcyclopentene was the only cycloalkene detected, showing concentrations up to 6, 23 and 17 % Σ cyclics in groups A, B and C, respectively.

Halocarbons

Halocarbons represented a very low fraction of the interstitial soil gases (Figure 6.5). In the group A, they accounted for ≤ 0.01 % of the total organic gas fraction, consisting of carbon tetrachloride, dichloroethane, trichloroethene, vinylchloride and chlorobenzene (up to 0.18 nmol/mol). Halocarbons in the soil gases of group B ranged from 0.02 to 0.19 % Σ VOCs. Carbon tetrachloride was the dominant compound (up to 39 % Σ halocarbons and 0.22 nmol/mol), followed by CFCs (ranging from 17 to 36 % Σ halocarbons and mainly represented by CFC12), chloromethane (up to 33 % Σ halocarbons), chlorobenzene (up to 32 % Σ halocarbons) and vinylchloride (up to 25 % Σ halocarbons). Dichloroethene and trichloroethene accounted for up to 13 and 10 % Σ halocarbons, respectively.

In the group C, halocarbons ranged from 0.14 to 0.76 % Σ VOCs. CFCs, mainly represented by CFC12 (up to 0.47 nmol/mol), were the most abundant compounds (from 31 to 39 % Σ halocarbons), followed by chlorobenzene (up to 30 % Σ halocarbons), chloromethane (up to 24 % Σ halocarbons), carbon tetrachloride (up to 13 % Σ halocarbons) and vinylchloride (up to 12 % Σ halocarbons). Dichloromethane and trichloromethane were detected at concentrations ≤ 6 % Σ halocarbons.

6.2.3 Soil flux measurements

The ΦCO_2 , ΦCH_4 and $\Phi\text{C}_6\text{H}_6$ values measured at each soil gas sampling point are reported in Table 6.5, with the exception of sites 41 to 52 where the CO_2 fluxes were too high ($>25,000 \text{ g m}^{-2}\text{day}^{-1}$) to be measured using the accumulation chamber method. The CO_2 fluxes ranged from 24 to 21,875 $\text{g m}^{-2}\text{day}^{-1}$, i.e. up to 6 orders of magnitude higher than those measured for CH_4 (from 0.000015 to 0.56 $\text{g m}^{-2}\text{day}^{-1}$) and C_6H_6 (from 0.000045 to 0.038 $\text{g m}^{-2}\text{day}^{-1}$). A clear positive correlation among CO_2 , CH_4 and C_6H_6 fluxes was recognized (Figure 6.12). The lowest values were measured where

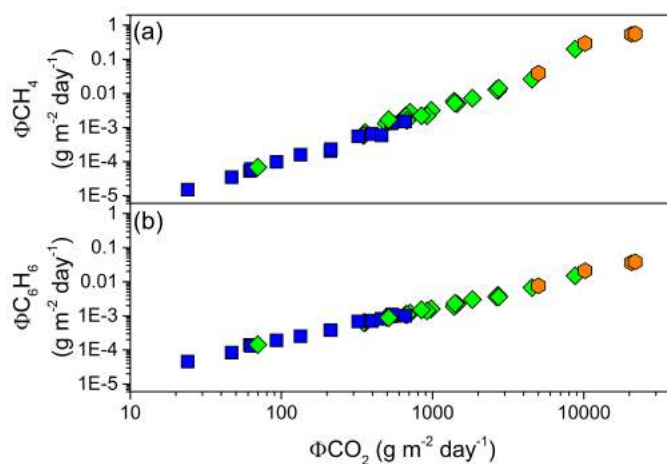


Figure 6.12: (a) ΦCH_4 and (b) $\Phi\text{C}_6\text{H}_6$ vs. ΦCO_2 values (in $\text{g m}^{-2} \text{day}^{-1}$). Symbols and colours as in Figure 6.2.

soil gases of type C were sampled, whereas the highest values corresponded

6. Results

to type A soil gases. Accordingly, ΦCO_2 increased at increasing CO_2/N_2 ratios (Figure 6.13), supporting the hypothesis of an increasing contribution by uprising hydrothermal fluids from the soil gases belonging to group C to those of group B and A.

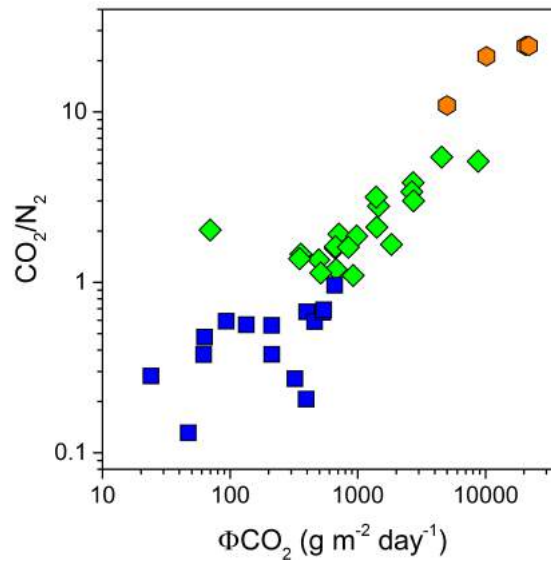


Figure 6.13: CO_2/N_2 ratios vs. ΦCO_2 values (in $\text{gm}^{-2}\text{day}^{-1}$). Symbols and colours as in Figure 6.2.

6.2 Solfatara Crater

Table 6.5: The ΦCO_2 , ΦCH_4 and $\Phi\text{C}_6\text{H}_6$ values (in $\text{gm}^{-2}\text{day}^{-1}$) are reported for each site.

ID	ΦCO_2	ΦCH_4	$\Phi\text{C}_6\text{H}_6$
1	134	0.00016	0.00025
2	62	0.000053	0.00014
3	24	0.000015	0.000045
4	358	0.00071	0.00063
5	93	0.000098	0.00019
6	495	0.0013	0.0009
7	665	0.0022	0.0011
8	63	0.000061	0.00013
9	710	0.0028	0.0012
10	350	0.00058	0.00063
11	668	0.0021	0.0011
12	8770	0.2	0.015
13	395	0.00066	0.00072
14	979	0.0032	0.0016
15	20664	0.54	0.036
16	70	0.000069	0.00014
17	322	0.00055	0.00068
18	397	0.00063	0.0007
19	211	0.0002	0.00038
20	919	0.0022	0.0014
21	677	0.0016	0.0011
22	660	0.0015	0.001
23	1452	0.005	0.0022
24	460	0.00058	0.00081
25	533	0.0013	0.00096
26	47	0.000035	0.000083
27	541	0.0014	0.0011
28	2706	0.012	0.004
29	4534	0.026	0.0067
30	1390	0.0059	0.0019
31	844	0.0022	0.0015
32	5007	0.039	0.0076
33	2649	0.013	0.0036
34	21875	0.56	0.038
35	1407	0.0052	0.0023

(To be continued)

6. Results

ID	ΦCO_2	ΦCH_4	$\Phi\text{C}_6\text{H}_6$
36	1834	0.0072	0.003
37	212	0.00023	0.00038
38	2736	0.014	0.0036
39	10188	0.29	0.021
40	512	0.0017	0.00087

Table 6.5: The ΦCO_2 , ΦCH_4 and $\Phi\text{C}_6\text{H}_6$ values (in $\text{gm}^{-2}\text{day}^{-1}$) are reported for each site.

6.2.4 Soil gases depth profiles

The concentrations (in mmol/mol) of the main inorganic gas constituents (CO₂, H₂S, CH₄, N₂, O₂, Ar) in interstitial soil gas samples collected in January 2016 at 10 and 30 cm depth along 5 vertical profiles within the Solfatara Crater are reported in Table 6.6, along with geographical coordinates (in UTM), temperature (in °C), ΦCO_2 (in gm⁻²day⁻¹) and $\delta^{13}\text{C-CO}_2$ values (expressed in ‰ vs. V-PDB).

Sites 1, 2 and 3 were characterized by temperature gradients $\geq 1.1^\circ\text{C}/\text{cm}$, with temperatures at 30 cm depth up to 57.6, 60.1 and 50.6 °C, respectively (Table 6.6), whereas sites 4 and 5 displayed temperature gradients $\leq 0.1^\circ\text{C}/\text{cm}$ and temperatures at 30 cm of 12.4 and 17.4 °C, respectively (Table 6.6). Similarly, the CO₂ fluxes in the latter sites were relatively low (161 and 110 gm⁻²day⁻¹ in sites 4 and 5, respectively), whereas ΦCO_2 values ranging from 557 to 3,350 gm⁻²day⁻¹ were measured in sites 1, 2, and 3 (Table 6.6). The chemical composition of interstitial soil gases at both 10 and 30 cm depth changed accordingly among the selected sites. Soil gases collected at sites 1, 2 and 3 were dominated by CO₂ (ranging from 804 to 943 mmol/mol; Table 6.6), followed by N₂ (from 54 to 147 mmol/mol; Table 6.6) and H₂S (from 1.2 to 1.9 mmol/mol; Table 6.6). CH₄ was present at minor concentrations (from 0.021 to 0.091 mmol/mol; Table 6.6). According to the classification adopted in Section 6.2.2 for soil gases collected at 30 cm depth, site 1 is pertaining to group A (CO₂/N₂ ratio of 17), whereas sites 2 and 3 can be referred to group B (CO₂/N₂ ratios of 9.3 and 8.6, respectively). O₂ and Ar generally showed increasing concentrations moving from site 1 to 2 and 3, with values at 30 cm depth ranging between 0.32 and 6.1 mmol/mol and from 0.68 to 1.3 mmol/mol (Table 6.6). While CO₂, H₂S and CH₄ decreased at decreasing depth, atmospheric components (N₂, O₂ and Ar) increased from 30 to 10 cm depth (Table 6.6), suggesting, as expected, an increasing air dilution at shallower depths. The same trend was observed in sites 4 and 5. The soil gases collected from these sites were generally dominated by N₂ (from 390 to 741 mmol/mol), with relatively high O₂ and Ar contents (up to 163 and 91 mmol/mol, respectively; Table 6.6) and CO₂/N₂ ratios at 30 cm depth of 1.5

6. Results

and 0.04, respectively. The CO₂ contents largely differed among sites 4 and 5, the former being characterized by concentrations ≥ 330 mmol/mol, while the latter had lower CO₂ contents (≤ 30 mmol/mol; Table 6.6). Similarly, H₂S and CH₄ showed higher concentrations in site 4 (up to 0.56 and 0.015 mmol/mol, respectively) than those recorded in site 5 (≤ 0.06 and ≤ 0.0039 mmol/mol, respectively; Table 6.6).

ID	East	North	ΦCO_2	depth	T	CO_2	H_2S	CH_4	N_2	O_2	Ar	$\delta^{13}\text{C-CO}_2$
1	427588	4519913	3350	0	24	887	1.6	0.064	109	0.88	1.4	-1.42
				10	37.2							
				30	57.6							
2	427539	4519923	557	0	23	887	1.3	0.021	107	3.3	1.4	-1.10
				10	42.9							
				30	60.1							
3	427352	4519984	896	0	19.4	804	1.2	0.047	147	46	1.8	-1.25
				10	26.3							
				30	50.6							
4	427571	4520048	161	0	9.8	330	0.31	0.0078	591	71	7.7	0.60
				10	10.5							
				30	12.4							
5	427388	4520113	110	0	13.7	15	0.05	0.0033	733	163	89	-0.07
				10	14.4							
				30	17.4							

Table 6.6: Location (in UTM), sampling depth (in cm), soil temperature (in $^{\circ}\text{C}$) and chemical composition (in mmol/mol) of the main gas species (CO_2 , H_2S , CH_4 , N_2 , O_2 , Ar) in soil gases collected along the 5 vertical profiles at Solfatara Crater. The isotopic composition of CO_2 ($\delta^{13}\text{C-CO}_2$, in $\%$ vs. V-PDB) and ΦCO_2 values (in $\text{gm}^{-2}\text{day}^{-1}$) measured at each sampling site are also reported.

6. Results

The $\delta^{13}\text{C-CO}_2$ values (Table 6.6) were ranging from -1.86 to -1.10 ‰ in sites 1, 2 and 3, consistently with the isotopic signature of soil gases collected in September 2013, with slightly higher values in site 4 (from -0.07 to 0.60 ‰). A decreasing trend in $\delta^{13}\text{C-CO}_2$ values with increasing depth was observed in each site.

The composition of VOCs (in nmol/mol) in soil gases from the 5 vertical profiles is reported in Table 6.7. No organic compounds were detected in gas samples from site 5 (Table 6.6). In the other sites, the organic fraction of soil gases at both 10 and 30 cm was dominated by alkanes (from 51 to 73 % ΣVOCs) and aromatics (from 21 to 27 % ΣVOCs). While alkanes, aromatics, alkenes, cyclics and S-bearing compounds increased at increasing depth, O-substituted species showed an opposite trend, i.e. increased at decreasing depth (Table 6.7). The highest concentrations of aldehydes, ketones and carboxylic acids (up to 16, 9.5 and 7.8 nmol/mol) were measured in site 4, which was characterized by the lowest T, low ΦCO_2 value and relatively high O_2 contents (Table 6.6).

ID	depth	C_2H_6	C_3H_8	nC_4H_{10}	iC_4H_{10}	C_6H_6	C_{5+} alkanes	alkenes	branched aromatics	ketones	aldehydes	carboxyl acids	cyclics	S-substituted
1	0													
	10	180	60	30	50	130	6.0	1.4	3.1	3.2	4.1	3.8	15	5.5
	30	310	90	50	70	170	11.0	1.8	4.5	1.2	2.4	2.6	34	7.8
2	10	220	90	60	50	150	7.3	1.6	2.8	4.1	5.5	4.7	21	6.6
	30	250	110	80	50	160	9.0	2.1	3.6	2.6	3.1	3.5	29	7.4
3	0													
	10	250	120	60	80	150	9.0	1.4	4.8	7.4	9.1	6.9	31	6.1
	30	290	150	90	110	180	12.0	1.7	6.9	3.7	4.4	3.1	39	7.1
4	0													
	10	50	10	10	0	30	2.0	0.2	0.7	9.5	16	7.8	4	0.7
	30	110	30	20	20	70	4.0	0.6	2.2	7.8	11	6.1	15	2.5

Table 6.7: Chemical composition (in nmol/mol) of VOCs in soil gases collected along the 5 vertical profiles at Solfatara Crater.

6.3 Nisyros Island

6.3.1 Fumarolic gases

The chemical composition of main inorganic (in mmol/mol) species in the dry fraction of fumarolic gases from Nisyros Island is reported in Table 6.8, together with $\delta^{13}\text{C-CO}_2$ values (expressed in ‰ vs. V-PDB).

The outlet temperatures ranged from 98.7 to 100.3 °C, i.e. close to the boiling point of water. The chemical composition of fumarolic gases was typically hydrothermal, dominated by CO_2 (from 784 to 905 mmol/mol) and H_2S (from 78 to 200 mmol/mol), with minor concentrations of CH_4 (from 1.8 to 9.8 mmol/mol) and H_2 (from 5.4 to 11 mmol/mol). Highly acidic gases were not detected, suggesting that gas discharges originated from boiling aquifers. N_2 , O_2 and Ar were present at low concentrations (up to 2.9, 0.010 and 0.011 mmol/mol, respectively; Table 6.8).

6. Results

ID	Site	Type	Date	East	North	depth	T
Kam	Kaminakia	fumarolic gas	Jun15	515458	4047998	-	98.7
MicP	Micros Polybotes	fumarolic gas	Jun15	514847	4048672	-	99.6
Ph	Phlegethon	fumarolic gas	Jun15	514605	4048519	-	99.5
Lof	Lofos	fumarolic gas	Jun15	515162	4048630	-	99.4
St	Stephanos	fumarolic gas	Jun15	515017	4048118	-	100.3
K	Kaminakia	soil gas	Jun15	515522	4048153	40	70
M	Micros Polybotes	soil gas	Jun15	514856	4048684	20	60.8
P	Phlegethon	soil gas	Jun15	514670	4048551	40	63.1
L	Lofos	soil gas	Jun15	515159	4048640	20	53
S	Stephanos	soil gas	Jun15	515101	4048181	40	69.6

ID	ΦCO_2	CO_2	H_2S	CH_4	N_2	O_2	Ar	H_2	$\delta^{13}\text{C-CO}_2$
Kam	-	905	78	9.8	1.8	0.0053	0.0053	5.4	-1.40
MicP	-	784	200	2.8	2.8	0.0082	0.011	11	-1.00
Ph	-	856	134	1.8	2.9	0.0083	0.0064	5.8	-1.10
Lof	-	828	162	2.9	2.4	0.010	0.011	5.4	-1.30
St	-	832	155	2.3	2.1	0.0057	0.011	7.9	-1.10
K	54.3	411	3.6	0.81	579	0.55	5.1	0.23	-1.11
M	111	841	37	2.30	118	0.51	0.91	0.65	-0.87
P	73.3	311	0.9	0.78	666	15	5.7	0.18	-1.14
L	129	411	2.3	1.10	577	3.1	5.2	0.31	-1.33
S	94.1	304	7.7	0.88	680	0.92	6.3	0.22	-1.11

Table 6.8: Location (in UTM), outlet temperature (in $^{\circ}\text{C}$), sampling depth (in cm) and chemical composition (in mmol/mol) of the main gas species (CO_2 , H_2S , CH_4 , N_2 , O_2 , Ar, H_2) for fumaroles and soil gases from Nisyros Island. The isotopic composition of CO_2 ($\delta^{13}\text{C-CO}_2$, in ‰ vs. V-PDB) and the ΦCO_2 values (in $\text{gm}^{-2}\text{day}^{-1}$) measured at each soil gas sampling site are also reported.

The isotopic composition of CO_2 (Table 6.8) ranged from -1.40 to -1.00 ‰ , i.e. consistently with the $\delta^{13}\text{C-CO}_2$ values reported in literature (Kavouridis et al., 1999: $-2.2 \pm 0.4 \text{‰}$; Brombach et al., 2003: from -0.4 to -4.1 ‰). These values, higher than the typical isotopic signature of magmatic derived CO_2 (ca. -6 ‰ ; Rollinson, 1993; Sano and Marty, 1995; Hoefs, 2009), were interpreted as related to mixing between the magmatic source and CO_2 from thermometamorphic reactions on limestone (typically characterized by $\delta^{13}\text{C-CO}_2$ values around $0 \pm 2 \text{‰}$; Sano and Marty, 1995; Clark, 2015) hosting the deep hydrothermal aquifer (Kavouridis et al., 1999; Brombach et al., 2003).

The Σ VOCs (Table 6.9) were ranging from 6,058 to 10,078 nmol/mol, corresponding to ≤ 0.54 % of the CH_4 concentration. The most abundant organic species were represented by alkanes (up to 6,427 nmol/mol) and aromatics (up to 4,563 nmol/mol). Ethane was the most abundant saturated hydrocarbon (≥ 71 % Σ alkanes), with concentrations ranging from 2,402 to 5,128 nmol/mol, i.e. one order of magnitude higher than those measured for the other alkanes (Table 6.9). Propane was the second most abundant alkane, with contents ranging from 343 to 730 nmol/mol. As observed in the Solfatara Crater fumaroles, the concentrations of normal-alkanes showed decreasing trend at increasing chain length (from C_2 to C_8), with normal-hexane being slightly enriched relative to normal-pentane in samples from Kaminakia, Micros Polybotes and Lofos dome. C_{4-8} branched-alkanes were present at concentrations systematically lower than those measured for their linear isomers, the normal- to iso-alkane ratios varying from 1.0 to 2.4 (Table 6.9).

The saturated hydrocarbons dominated the organic fraction, representing from 52 to 64 % Σ VOCs in fumarolic gas samples from Kaminakia, Micros Polybotes, Phlegethon and Stefanos (Table 6.9; Figure 4.7), with aromatics ranging from 28 to 39 % Σ VOCs. Contrarily, aromatics were predominant (52 % Σ VOCs) in the fumarolic gas sample from Lofos dome, where alkanes were 39 % Σ VOCs. Aromatics were largely dominated by benzene (from 2,016 to 4,194 nmol/mol), followed by toluene, m,p-xylene, ethylbenzene and styrene (up to 280, 150, 120 and 110 nmol/mol, respectively; Table 6.3.2). Minor amounts of naphthalene and o-xylene (up to 1.6 and 1.2 nmol/mol, respectively) were also detected.

Alkenes were the third most abundant compounds (from 4.8 to 6.2 % Σ VOCs), largely consisting of iso-butene (from 290 to 620 nmol/mol), with minor amounts of propene (from 0.7 to 1.5 nmol/mol; Table 6.9).

Among S-bearing compounds (from 2.0 to 3.7 % Σ VOCs), carbon disulphide was the most abundant species (from 150 to 270 nmol/mol), followed by thiophene, methylthiophene and dimethylsulphide (up to 16, 13 and 6.9 nmol/mol, respectively; Table 6.9).

O-bearing compounds and cyclics represented a relatively low fraction of the

6. Results

total VOCs (up to 0.09 and 0.05 % Σ VOCs, respectively). Cyclopentane and cyclohexane (≤ 1.5 and ≤ 1.6 nmol/mol, respectively) were the only detected cyclic compounds. Furans (furan, tetrahydrofuran and methylfuran) and esters (methyl-, ethyl- and butyl-acetate) were the most abundant O-bearing species (from 19 to 86 and from 11 to 68 % Σ O-bearing compounds, respectively). Hexanone was the only ketone detected in the analyzed fumarolic gas samples (≤ 13 % Σ O-bearing compounds), whereas the corresponding aldehyde, i.e. hexanal, was only found in Lof and St samples representing 10 and 8 % Σ O-bearing compounds (Table 6.9).

Table 6.9: Chemical composition (in nmol/mol) of VOCs in fumarolic (Kam, MicP, Ph, Lof, St) and soil gases (K, M, P, L, S) from Nisyros Island.

			Kam	MicP	Ph	Lof	St	K	M	P	L	S
Alkanes	ethane	C ₂ H ₆	2402	3823	4741	2459	5128	515	2380	690	890	1260
	propane	C ₃ H ₈	343	496	637	608	730	55	270	64	110	150
	normalbutane	n-C ₄ H ₁₀	75	110	140	130	160	11	55	13	1.8	28
	isobutane	i-C ₄ H ₁₀	57	85	110	87	110	8.1	44	11	1.5	29
	normalpentane	n-C ₅ H ₁₂	41	41	97	35	88	7.8	42	8.9	1.2	21
	isopentane	i-C ₅ H ₁₂	33	21	66	19	44	6.8	31	5.5	1.1	15
	normalhexane	n-C ₆ H ₁₄	69	45	85	36	74	9.5	56	8.7	1.6	26
	isohexane	i-C ₆ H ₁₄	55	25	74	22	37	4.1	23	6.4	1.1	22
	normalheptane	n-C ₇ H ₁₆	44	12	51	15	21	1.1	5.6	1.5	0.4	4.4
	isoheptane	i-C ₇ H ₁₆	21	12	26	11	11	0.8	1.3	1.1	0.2	3.1
	normaloctane	n-C ₈ H ₁₈	16	17	33	12	13	0.8	0.9	0.7		1.3
isooctane	i-C ₈ H ₁₈	11	15	14	11	11	0.5	0.7	0.5		1.1	
Aromatics	benzene	C ₆ H ₆	2016	2159	2375	4194	2603	65	350	85	140	210
	toluene	C ₇ H ₈	150	150	260	280	130	1.5	9.5	1.2	8.7	8.5
	styrene	C ₈ H ₈	56	15	110	16	17	1.1	4.2	0.6	2.9	0.8
	ethylbenzene	C ₈ H ₁₀	69	26	120	33	28	1.3	5.6	1.5	6.6	5.1
	m,p-xylene	m,p-C ₈ H ₁₀	78	33	150	38	36	1.5	6.6	1.8	7.5	5.6
	o-xylene	o-C ₈ H ₁₀	0.6	0.8	1.1	0.6	1.2	0.4	0.9		0.3	0.2
	naphtalene	C ₁₀ H ₈	1.3	1.6	1.5	0.7	1.4		1.1			
Cyclics	cyclopentane	C ₅ H ₁₀	1.5	1.3	1.2	1.3	0.7	0.2	0.7			0.3
	cyclohexane	C ₆ H ₁₂	1.6	1.5	1.4	1.4	0.9	0.4	1.1			0.5

(To be continued)

			Kam	MicP	Ph	Lof	St	K	M	P	L	S
Alkenes	propene	C ₃ H ₆	1.5	2.5	3.1	2.8	2.3	0.3	1.5	0.6	0.7	0.5
	isobutene	i-C ₄ H ₈	290	440	510	530	620	42	220	47	110	120
S-bearing compounds	carbon disulphide	CS ₂	210	150	230	270	180	89	150	56	41	39
	dimethylsulphide	C ₂ H ₆ S	2.5	6.1	6.9	5.8	4.8	0.6	3.1	0.8	1.1	1.9
	thiophene	C ₄ H ₄ S	5.1	14	15	16	9.9	3.6	19	4.9	6.1	12
	methylthiophene	C ₅ H ₆ S	3.6	8.6	11	13	8.7	4.1	15	3.1	5.5	8.4
	dimethylsulphoxide	C ₂ H ₆ OS						3.2	2.8	3.9	6.8	7.1
O-bearing compounds	furan	C ₄ H ₄ O	0.5	2.1	1.3	1.7	1.9	0.3	1.1	0.7	0.5	0.4
	tetrahydrofuran	C ₄ H ₈ O	0.5	2.8	1.7	2.4	2.3	0.5	1.2	0.8	0.6	0.7
	methylfuran	C ₅ H ₆ O		0.5	0.7	0.6	1.2		0.4			
	ethylacetate	C ₄ H ₈ O ₂	1.4	0.7	0.7	0.5	0.3	2.1	0.5	2.8	1.7	1.3
	methylacetate	C ₃ H ₆ O ₂	0.9	0	0.4	0.4	0.2	3.8	0.4	7.8	5.5	4.6
	buthylacetate	C ₆ H ₁₂ O ₂	1.3	0.2	0.5	0.6	0.3	4.4	0.6	4.7	3.9	3.1
	butanone	C ₄ H ₈ O						0.6		0.8	1.5	1.3
	hexanone	C ₆ H ₁₂ O	0.7	0	0.5	0.3	0.4	1.4	0.7	1.3	1.3	0.6
	acetophenone	C ₄ H ₈ O						0.8		1.4	0.7	0.8
	hexanal	C ₆ H ₁₂ O				0.7	0.6	1.5	0.5	1.8	1.1	1.2
	benzaldehyde	C ₇ H ₆ O						0.6		1.2	0.4	0.7

Table 6.9: Chemical composition (in nmol/mol) of VOCs in fumarolic (Kam, MicP, Ph, Lof, St) and soil gases (K, M, P, L, S) from Nisyros Island.

6.3.2 Interstitial soil gases and soil flux measurements

The concentrations of main inorganic gas species (CO_2 , H_2S , CH_4 , N_2 , O_2 , Ar and H_2 ; in mmol/mol) of interstitial soil gases collected at 20 or 40 cm depth in Nisyros Island from 5 sites located within Kaminakia, Micros Polybotes, Phlegethon and Stefanos craters and Lofos dome (Figure 4.7) is reported in Table 6.8 together with soil CO_2 flux measurements (in $\text{gm}^{-2}\text{day}^{-1}$).

The chemical composition of soil gases was dominated by N_2 , spanning 118 to 680 mmol/mol (Table 6.8), followed by CO_2 (from 304 to 841 mmol/mol). The CO_2/N_2 ratios ranged from 0.45 to 0.71 in K, P, L and S samples, whereas the composition of the soil gas collected within the Micros Polybotes crater was CO_2 -dominated, the CO_2/N_2 ratio being 7.1. The latter sample was also characterized by H_2S , CH_4 and H_2 contents of 37, 2.3 and 0.65 nmol/mol, respectively, i.e. significantly higher than those measured in the other analyzed soil gases (from 0.9 to 3.6, from 0.81 to 1.10 and from 0.18 to 0.31 nmol/mol, respectively; Table 6.8), suggesting a strong contribution from deep hydrothermal fluids. The isotopic composition of CO_2 of the analyzed samples ranged from -1.33 to -0.87 ‰ (Table 6.8), i.e. similar to the $\delta^{13}\text{C}-\text{CO}_2$ values measured in the fumarolic gases (Table 6.8), confirming a dominant hydrothermal component in the collected soil gases, as expected on the basis of the relatively high ΦCO_2 values (from 54.3 to 129 $\text{gm}^{-2}\text{day}^{-1}$) and soil temperatures (from 53 to 70 °C). Accordingly, atmospheric gases, i.e. O_2 and Ar, were measured at relatively low concentrations (up to 15 and 6.3 mmol/mol; Table 6.8).

The ΣVOCs ranged from 851 to 3,706 nmol/mol (Table 6.9), the highest concentrations being measured in the gas sample collected from Micros Polybotes crater. The organic fraction of interstitial soil gases was largely dominated by alkanes, ranging from 73 to 79 % ΣVOCs and mainly consisting of ethane (from 515 to 2,380 nmol/mol) and propane (from 55 to 270 nmol/mol). As observed for the fumarolic gases, the concentrations of normal-alkanes decreased at increasing molecular weight, with the exception of the soil gases from Kaminakia, Micros Polybotes and Lofos, which showed concentrations of normal-hexane higher than those measured for normal-pentane (Table 6.9).

6. Results

The normal- to iso-alkane ratios were from 0.97 to 4.31.

Aromatics ranged from 8 to 12 % Σ VOCs. Benzene was the most abundant compound (from 65 to 350 nmol/mol), whereas alkylated aromatics (toluene, styrene, ethylbenzene, and xylenes) were measured at concentrations ≤ 9.5 . Naphtalene was only detected in the soil gas sample from Micros Polybotes (Table 6.9).

Alkenes (from 5 to 8 % Σ VOCs) consisted of iso-butene (from 42 to 220 nmol/mol) and minor amounts of propene (≤ 1.5 nmol/mol), whereas cyclics (cyclopentene and cyclohexane) were only detected in the soil gas samples from Kaminakia, Micros Polybotes and Stefanos craters (≤ 1.1 nmol/mol and ≤ 0.7 % Σ VOCs; Table 6.9).

S-bearing and O-substituted compounds amounted to larger fractions of VOCs in soil gases (up to 12 and 2.2 % Σ VOCs, respectively) relative to the fumarolic samples.

S-bearing compounds were dominated by carbon disulphide and thiophenes (up to 150 and 19 nmol/mol, respectively). DMSO was detected in concentrations (up to 71 nmol/mol) generally higher than those of DMS (Table 6.9), except for the soil gas sample from Micros Polybotes (with DMS and DMSO contents of 3.1 and 2.8 nmol/mol, respectively).

O-bearing compounds were dominated by esters (from 28 to 66 % Σ O-bearing compounds), with concentrations (up to 7.8 nmol/mol) higher than those measured in the fumarolic samples (≤ 1.4 nmol/mol), whereas furans were the most abundant compounds in the Micros Polybotes sample (50 % Σ O-bearing compounds), representing less than 7.5 % Σ O-bearing compounds in the other soil gases (Table 6.9). Ketones (butanone and acetophenone) and aldehydes (hexanal and benzaldehyde) were enriched in soil gases (up to 20 and 13 % Σ O-bearing compounds, respectively) relative to the fumarolic discharges.

6.4 Poggio dell'Olivo

6.4.1 Vezza Creek bubbling gas

The chemical composition of the gas sample (VC) collected from the bubbling pool close to the Vezza Creek was dominated by CO₂ (980 mmol/mol), followed by N₂ (11.1 mmol/mol), CH₄ (6.80 mmol/mol) and H₂S (2.56 mmol/mol; Table 6.10). Minor amounts of O₂ and Ar (0.33 and 0.26 mmol/L, respectively) were also measured.

The isotopic composition of CO₂ ($\delta^{13}\text{C-CO}_2$; Table 6.10) was slightly positive (0.59 ‰), whereas the isotopic signature of CH₄ ($\delta^{13}\text{C-CH}_4$; Table 6.10) was of -26.1 ‰, consistent with the isotopic values measured in the hydrothermal discharges from the VCVD area (Cinti et al., 2014).

6. Results

ID	Date	East	North	CO ₂	H ₂ S	N ₂	O ₂	Ar	CH ₄	$\delta^{13}\text{C-CO}_2$	$\delta^{13}\text{C-CH}_4$
VC	Jun14	4709750	264776	980	2.56	11.1	0.33	0.26	6.80	0.59	-26.1
G1	Jun14	4709903	264768	948	0.20	46.6	2.37	1.13	2.09	0.42	-26.1
G2	Jun14	4709913	264784	952	0.21	43.1	1.04	1.06	2.15	0.50	-25.9
G3	Jun14	4709895	264752	921	0.11	66.4	10.5	1.56	0.75	1.07	-23.2
G4	Jun14	4709906	264743	935	0.11	57.4	5.78	1.32	0.78	0.53	-22.7
G5	Jun14	4709962	264744	982	0.20	14.4	0.21	0.21	3.22	0.47	-25.8
G6	Jun14	4709953	264737	917	0.09	71.2	8.05	1.61	1.84	0.51	-25.6
G7	Jun14	4709953	264730	781	0.025	181	34.4	3.65	0.32	0.93	-22.1
G8	Jun14	4709943	264716	925	0.056	61.6	10.9	1.44	0.81	0.51	-21.5
G9	Jun14	4709958	264755	978	0.47	16.1	0.25	0.41	4.53	0.59	-25.9
G10	Jun14	4709945	264748	978	0.52	17.1	0.34	0.43	4.31	0.53	-26.1
G11	Jun14	4709926	264746	978	0.46	16.6	0.47	0.41	4.17	0.42	-26.4
G12	Jun14	4709927	264740	936	0.35	53.9	1.48	1.32	6.49	0.39	-26.3
G13	Jun14	4709917	264752	954	0.33	38.8	2.91	0.74	2.51	0.52	-25.2
G14	Jun14	4709934	264768	961	0.11	33.3	1.01	0.81	4.26	0.55	-26.6
G15	Jun14	4709908	264778	876	0.031	98.8	22.2	2.01	0.87	0.38	-21.8
G16	Jun14	4709907	264793	968	0.088	23.7	2.29	0.52	5.39	0.61	-26.3
G17	Jun14	4709885	264777	863	0.029	109	25.2	2.11	0.71	0.38	-22.8
G18	Jun14	4709962	264731	848	0.031	115	33.2	2.31	0.65	0.61	-23.2
G19	Jun14	4709958	264753	967	0.32	26.9	0.35	0.65	5.14	0.87	-25.9
G20	Jun14	4709937	264781	941	0.051	50.3	4.14	1.25	2.99	0.55	-24.5

Table 6.10: Location (in UTM) and chemical composition (in mmol/mol) of the main gas species (CO₂, H₂S, N₂, O₂, Ar, CH₄) for VC and soil gas (G1-G20) samples from Poggio dell’Olivo. The isotopic composition of CO₂ and CH₄ ($\delta^{13}\text{C-CO}_2$ and $\delta^{13}\text{C-CH}_4$, respectively, in ‰ vs. V-PDB) are also reported.

The total amount of VOCs was of 14,525 nmol/mol (Table 6.11), corresponding to 0.21 % of the CH₄ content. The organic gas fraction was largely dominated by saturated hydrocarbons, whose sum was of 13,850 nmol/mol, i.e. 95 % Σ VOCs. Alkanes were mainly represented by ethane (11,000 nmol/mol), followed by propane (1,300 nmol/mol) and normalbutane (310 nmol/mol; Table 6.11). The concentrations of C₅ and C₆ normal-alkanes were 170 and 250 nmol/mol, respectively. Iso-alkanes showed concentrations slightly lower than the corresponding normal-alkanes (Table 6.11), the normal- to iso- ratios for C₄, C₅ and C₆ isomers being 1.15, 1.31 and 1.09, respectively. The second most abundant homologous series in the VC gas sample was that of alkenes (616 nmol/mol, i.e. 4.24 % Σ VOCs), largely constituted by methylpropene (610 nmol/mol; Table 6.11), with minor amounts of normalhexene, normalpentene and methylpentene (2.6, 2.3 and 1.1 nmol/mol; Table 6.11). Aromatics were 0.26 % Σ VOCs and were consisting of benzene (31 nmol/mol) and toluene (6.3 nmol/mol; Table 6.11). Other homologous series, i.e. cyclics, O-bearing compounds and halocarbons, were present at relatively low amounts (up to 12.8, 4.8 and 3.6 nmol/mol; Table 6.11), corresponding to ≤ 0.088 % Σ VOCs. Cyclics were only represented by C₅ and C₆ compounds, i.e. methylcyclopentane, cyclopentane, methylcyclohexane, dimethylcyclohexane and cyclohexane (Table 6.11), whereas chlorohexane and trichloromethylpropane were the only halocarbons detected (Table 6.11). Among O-substituted compounds, alcohols (hexanol, dimethylbutanol and methylhexanol) were the most abundant species (63 % Σ O-bearing compounds). Aldehydes (ethanal), carboxylic acids (acetic acid) and ketones (propanone) were present at extremely low concentrations (0.7, 0.6 and 0.5 nmol/mol; Table 6.11), corresponding to 15, 13 and 10 % Σ O-bearing compounds.

Table 6.11: Chemical composition (in nmol/mol) of VOCs in the VC gas vent and related soil gases (G1-G20) from Poggio dell'Olivo.

	Formula	Name	VC	G1	G2	G3	G4	G5	G6
Alkanes	C ₂ H ₆	Ethane	11000	5600	6800	3500	4100	8600	8100
	C ₃ H ₈	Propane	1300	450	510	380	350	690	880
	i-C ₄ H ₁₀	Methylpropane	270						80
	n-C ₄ H ₁₀	n-Butane	310					60	90
	n-C ₅ H ₁₂	n-Pentane	170	95	87	120	110	150	95
	3i-C ₅ H ₁₂	3-Methylbutane	130	66	61	83	76	95	83
	n-C ₆ H ₁₄	n-Hexane	250	150	130	190	210	250	91
	i-C ₆ H ₁₄	3-Methylpentane	230	130	140	160	210	240	83
	i-C ₇ H ₁₆	3-Methylhexane	190	91	88	120	130	160	77
Alkenes	i-C ₄ H ₈	Methylpropene	610	230	210	150	170	260	370
	n-C ₅ H ₁₀	n-Pentene	2.3	2.3	1.8	1.4	1.5	2.4	2.4
	i-C ₆ H ₁₂	2-Methylpentene	1.1	1.4	1.1	0.5	0.6	0.8	0.6
	n-C ₆ H ₁₂	n-Hexene	2.6	1.7	1.3	1.1	1.2	1.5	1.7
Cyclics	c-C ₅ H ₁₀	Cyclopentane	2.6	1.1	1.1	0.9	1.4	2.8	2.5
	c-C ₅ H ₉ CH ₃	3-Methylcyclopentane	3.2	1.2	1.5	0.9	1.2	2.7	2.9
	c-C ₆ H ₁₂	Cyclohexane	2.1	1.1	1.4	0.6	1.1	2.1	2.1
	c-C ₆ H ₁₁ CH ₃	3-Methylcyclohexane	2.6	1.1	1.3	0.7	1.3	2.5	2.2
	c-C ₆ H ₁₁ CH ₃ CH ₃	2,3-Dimethylcyclohexane	2.3	1.2	0.8	0.5	1.1	2.1	1.6
Aromatics	C ₆ H ₆	Benzene	31	23	29	21	19	22	25
	C ₇ H ₈	Toluene	6.3	0.8	0.7	0.8		0.6	0.7
Cl-bearing	C ₆ H ₁₃ Cl	Chlorohexane	1.9	1.1	1.3	0.7	1.5	1.7	1.6

(To be continued)

	Formula	Name	VC	G1	G2	G3	G4	G5	G6
	C ₃ H ₄ Cl ₃ CH ₃	1,1,1-Trichloromethylpropane	1.7	0.9	1.1	1.1	1.3	1.5	1.6
Alcohols	C ₆ H ₁₃ OH	Hexanol	1.2	0.9	1.2	0.9	0.7	0.9	1.1
	C ₆ H ₁₄ O	Dimethylbutanol	0.9	0.8	1.1	0.5	0.8	0.9	1.1
	C ₇ H ₁₆ O	Methylhexanol	0.9	0.9	1.4	0.6	0.7	1.1	1.3
Carboxylic Acids	HCOOH	Formic acid					0.8		
	CH ₃ COOH	Acetic acid	0.6	0.7	0.9	0.7	0.8	0.6	0.7
Esters	C ₃ H ₆ O ₂	Ethyl formate		0.5		0.5			
Ketones	C ₃ H ₆ O	Propanone	0.5	0.8	0.9	1.1	1.3	0.7	0.5
Aldehydes	C ₂ H ₄ O	Ethanal	0.7	0.6	0.7	0.9	1.1	0.7	0.5
	C ₃ H ₆ O	Propanal		0.5		0.7	1.2	0.5	0.6
N-bearing	C ₄ H ₉ N	Pyrrolidine					0.8		
	C ₅ H ₁₁ NO	Methylbutanamide				0.9	1.1		
Terpenes	C ₁₀ H ₆	α-pinene				0.6			

(To be continued)

	Formula	Name	G7	G8	G9	G10	G11	G12	G13
Alkanes	C ₂ H ₆	Ethane	1500	2900	9600	8300	9300	19000	8500
	C ₃ H ₈	Propane	130	260	910	870	890	1900	660
	i-C ₄ H ₁₀	Methylpropane			110	120	130	250	110
	n-C ₄ H ₁₀	n-Butane			160	130	150	290	120
	n-C ₅ H ₁₂	n-Pentane	21	110	150	95	120	190	110
	3i-C ₅ H ₁₂	3-Methylbutane	12	75	120	72	110	160	88
	n-C ₆ H ₁₄	n-Hexane	13	130	250	120	180	330	160
	i-C ₆ H ₁₄	3-Methylpentane	8.2	120	230	86	140	320	120
	i-C ₇ H ₁₆	3-Methylhexane	6.1	72	180	77	180	290	110
Alkenes	i-C ₄ H ₈	Methylpropene		180	390	450	390	1100	240
	n-C ₅ H ₁₀	n-Pentene	0.7	1.2	1.9	2.3	2.1	2.6	2.2
	i-C ₆ H ₁₂	2-Methylpentene		0.7	0.8	1.1	1.1	1.3	0.8
	n-C ₆ H ₁₂	n-Hexene	0.6	0.8	1.6	2.4	1.8	3.1	1.9
Cyclics	c-C ₅ H ₁₀	Cyclopentane	0.6	1.1	2.5	2.6	2.1	2.5	1.7
	c-C ₅ H ₉ CH ₃	3-Methylcyclopentane	0.7	0.6	1.9	2.1	2.3	2.7	2.1
	c-C ₆ H ₁₂	Cyclohexane		0.5	2.1	1.9	1.6	1.9	1.6
	c-C ₆ H ₁₁ CH ₃	3-Methylcyclohexane	0.5	1.2	2.3	2.3	2.1	2.4	1.9
	c-C ₆ H ₁₁ CH ₃ CH ₃	2,3-Dimethylcyclohexane		0.6	1.7	2.1	2.3	2.6	1.8
Aromatics	C ₆ H ₆	Benzene	7.5	15	24	22	17	25	26
	C ₇ H ₈	Toluene			0.9	0.7		0.8	0.6
Cl-bearing	C ₆ H ₁₃ Cl	Chlorohexane	0.6	0.6	1.7	1.8	2.1	2.5	1.7
	C ₃ H ₄ Cl ₃ CH ₃	1,1,1-Trichloromethylpropane	0.7	0.8	1.9	1.5	2.3	2.1	1.8
Alcohols	C ₆ H ₁₃ OH	Hexanol	0.6	0.8	1.2	1.4	1.1	1.6	1.4

(To be continued)

	Formula	Name	G7	G8	G9	G10	G11	G12	G13
	C ₆ H ₁₄ O	Dimethylbutanol	0.5	0.6	0.7	1.1	0.8	1.1	1.2
	C ₇ H ₁₆ O	Methylhexanol	0.7	0.8	0.9	1.3	1.1	1.4	1.5
Carboxylic Acids	HCOOH	Formic acid	0.5						
	CH ₃ COOH	Acetic acid	1.1	1	0.6	0.7	0.5		0.8
Esters	C ₃ H ₆ O ₂	Ethyl formate	0.8	0.7					
Ketones	C ₃ H ₆ O	Propanone	1.3	1.6	0.7	0.8		0.6	0.7
Aldehydes	C ₂ H ₄ O	Ethanal	1.1	1.2	0.8	0.9	0.6	0.7	0.8
	C ₃ H ₆ O	Propanal	1.3	1.1	0.7	0.6		0.5	0.7
N-bearing	C ₄ H ₉ N	Pyrrolidine	1.8	1.2					
	C ₅ H ₁₁ NO	Methylbutanamide	2.4	0.9					
Terpenes	C ₁₀ H ₁₆	α -pinene	0.9						

(To be continued)

	Formula	Name	G14	G15	G16	G17	G18	G19	G20
Alkanes	C ₂ H ₆	Ethane	9100	3900	9800	2900	2700	9100	8100
	C ₃ H ₈	Propane	880	330	940	230	260	970	660
	i-C ₄ H ₁₀	Methylpropane	90		130			150	120
	n-C ₄ H ₁₀	n-Butane	110		170			190	130
	n-C ₅ H ₁₂	n-Pentane	130	36	140	43	21	160	110
	3i-C ₅ H ₁₂	3-Methylbutane	110	31	91	36	16	120	87
	n-C ₆ H ₁₄	n-Hexane	270	55	250	65	36	260	130
	i-C ₆ H ₁₄	3-Methylpentane	210	48	230	57	31	210	120
	i-C ₇ H ₁₆	3-Methylhexane	160	35	150	42	22	160	86
Alkenes	i-C ₄ H ₈	Methylpropene	290	130	340	110	110	310	260
	n-C ₅ H ₁₀	n-Pentene	2.4	0.9	1.8	1.1	1.1	2.6	2.1
	i-C ₆ H ₁₂	2-Methylpentene	1.2		1.1	0.5	0.5	0.7	1.2
	n-C ₆ H ₁₂	n-Hexene	2.6	0.6	1.9	0.8	1.1	2.5	2.9
Cyclics	c-C ₅ H ₁₀	Cyclopentane	1.9	0.9	1.8	0.6	0.8	2.6	2.3
	c-C ₅ H ₉ CH ₃	3-Methylcyclopentane	2.2	0.7	1.9	0.7	0.9	3.1	3.5
	c-C ₆ H ₁₂	Cyclohexane	1.5	0.6	2.1	0.5	0.5	2.7	2.5
	c-C ₆ H ₁₁ CH ₃	3-Methylcyclohexane	1.8	1.1	1.5	0.7	0.6	3.1	2.7
	c-C ₆ H ₁₁ CH ₃ CH ₃	2,3-Dimethylcyclohexane	1.7	0.8	1.6	0.9		2.6	2.4
Aromatics	C ₆ H ₆	Benzene	20	15	24	16	14	22	26
	C ₇ H ₈	Toluene	0.7		0.7			1.1	0.8
Cl-bearing	C ₆ H ₁₃ Cl	Chlorohexane	1.5	0.8	1.8	0.5	0.8	1.5	1.7
	C ₃ H ₄ Cl ₃ CH ₃	1,1,1-Trichloromethylpropane	1.6	1.1	1.6	0.7	0.6	1.6	1.8
Alcohols	C ₆ H ₁₃ OH	Hexanol	1.5	0.8	1.6	1.1	0.7	1.2	1.1

(To be continued)

	Formula	Name	G14	G15	G16	G17	G18	G19	G20
	C ₆ H ₁₄ O	Dimethylbutanol	1.2	0.5	1.5	0.7	0.5	1.3	0.8
	C ₇ H ₁₆ O	Methylhexanol	1.7	0.6	1.7	0.8	0.8	1.1	1.3
Carboxylic Acids	HCOOH	Formic acid				0.6			
	CH ₃ COOH	Acetic acid	0.6	0.9	0.6	1.4	1.2	0.7	0.9
Esters	C ₃ H ₆ O ₂	Ethyl formate				0.8	0.6		
Ketones	C ₃ H ₆ O	Propanone	0.7	1.6	0.7	1.3	1.1	0.9	0.7
Aldehydes	C ₂ H ₄ O	Ethanal	0.6	1.4	0.6	1.2	1.3	0.8	0.7
	C ₃ H ₆ O	Propanal	0.5	1.2	0.5	0.9	1.1	0.6	0.5
N-bearing	C ₄ H ₉ N	Pyrrolidine		1.2		1.1	2.4		
	C ₅ H ₁₁ NO	Methylbutanamide		1.1		0.9	2.1		
Terpenes	C ₁₀ H ₆	α-pinene		0.7			0.6		

Table 6.11: Chemical composition (in nmol/mol) of VOCs in the VC gas vent and related soil gases (G1-G20) from Poggio dell'Olivo.

6. Results

6.4.2 Interstitial soil gases

The chemical composition (in mmol/mol) of the inorganic fraction (CO_2 , H_2S , N_2 , O_2 , Ar and CH_4) in the interstitial soil gas samples collected at 40 cm depth from 20 sites within the Poggio dell'Olivo area is reported in Table 6.10. CO_2 (from 781 to 982 mmol/mol) was the most abundant compound, followed by N_2 (from 14.4 to 181 mmol/mol) and O_2 (from 0.21 to 34.4 mmol/mol). Minor contents of Ar (≤ 6.49 mmol/mol), CH_4 (≤ 3.65 mmol/mol) and H_2S (≤ 0.52 mmol/mol) were also detected (Table 6.10). The $\delta^{13}\text{C}\text{-CO}_2$ and $\delta^{13}\text{C}\text{-CH}_4$ values (Table 6.10) were ranging from -0.39 to 1.07 ‰ and from -26.6 to -21.5 ‰, respectively, i.e. consistent with the isotopic signature of CO_2 and CH_4 in the VC bubbling gas sample (Table 6.10). The N_2/Ar ratios ranged from 39.3 to 68.6, i.e. between air and ASW values (Figure 6.14), suggesting an atmospheric origin of N_2 related to air contribution to the gas samples. At increasing CO_2/N_2 ratios (ranging from 4.3 to 68.2), i.e. decreasing air fraction, reduced gas species (H_2S and CH_4) increased, whereas the contents of the atmospheric components (O_2 and Ar) decreased (Table 6.10).

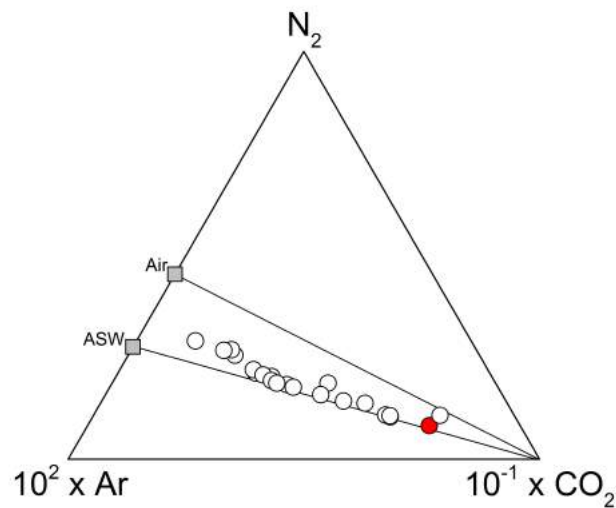


Figure 6.14: $\text{CO}_2\text{-N}_2\text{-Ar}$ ternary diagram for VC (red circle) and G1-G20 soil gas (white circles) samples.

The total concentrations of VOCs were from 1,715 to 23,885 nmol/mol (Table 6.11), representing from 0.07 to 3.63 % of the CH₄ contents. The composition of the organic gas fraction was largely dominated by alkanes, ranging from 95 to 99 % Σ VOCs, followed by alkenes (from 0.08 to 4.71 % Σ VOCs). Aromatics and O-bearing compounds ranged from 0.11 to 0.46 and from 0.03 to 0.46 % Σ VOCs, respectively. Minor amounts of cyclics (from 0.05 to 0.14 % Σ VOCs) and halocarbons (from 0.02 to 0.08 % Σ VOCs) were measured. N-substituted compounds (methylbutanamide and pyrrolidine) and terpenes (α -pinene) were occasionally detected (≤ 0.25 and ≤ 0.05 % Σ VOCs, respectively).

Alkanes

Ethane was by far the most abundant alkane in soil gases, with concentrations ranging from 1,500 to 19,000 nmol/mol, followed by propane (from 130 to 1,900 nmol/mol; Table 6.11). The ethane/propane ratio values ranged from 9.2 to 13.3, higher than that measured in VC sample (i.e. 8.5). C₄ alkanes were occasionally measured, with concentrations up to 290 nmol/mol (Table 6.11). Normalhexane was the third most abundant compound (ranging from 13 to 330 nmol/mol; Table 6.11), whereas normalpentane was measured at lower concentrations (from 21 to 190 nmol/mol; Table 6.11). The iso-alkanes were generally detected at lower amounts relative to the corresponding normal-alkanes, the normal- to iso- ratios ranging from 0.93 to 1.75.

Alkenes

Alkenes were mainly dominated by iso-butene, ranging from 110 to 1,100 nmol/mol (Table 6.11). Minor amounts of normal-pentene, methyl-pentene and normal-hexene were up to 2.6, 1.4 and 3.1 nmol/mol, respectively.

Aromatics

Aromatics were mainly represented by benzene, ranging from 7.5 to 29 nmol/mol (Table 6.11). Toluene was occasionally detected at concentrations ≤ 1.1

6. Results

nmol/mol.

O-bearing compounds

The detected O-bearing compounds (ranging from 4.1 to 8.8 nmol/mol) included alcohols, ketones, aldehydes, carboxylic acids and esters (Table 6.11). Alcohols were generally the most abundant oxygenated compounds constituting from 23 to 73 % Σ O-bearing species, equally represented by dimethylbutanol, hexanol and methylhexanol. Aldehydes (ethanal, propanal) and ketones (propanone) were present at relative abundances ≤ 37 and ≤ 23 % Σ O-bearing compounds, respectively. Among carboxylic acids, which were up to 23 % Σ O-bearing compounds, acetic acid was detected in almost all the analyzed soil gas samples (up to 1.4 nmol/mol), whereas formic acid was only found in few samples (Table 6.11). Ethyl formate was the only ester measured, detected only in few samples (≤ 10 % Σ O-bearing compounds).

Cyclics

Cyclics in soil gases consisted of C₅ and C₆ structures, with and without methyl groups (Table 6.11), i.e. cyclopentane, methylcyclopentane, cyclohexane, methylcyclohexane and dimethylcyclohexane, with concentrations up to 3.5 nmol/mol.

Halocarbons

Halocarbons in the soil gases were consisting of chlorohexane and trichloroisobutane (up to 2.5 nmol/mol; Table 6.11). They represented a minor component of the organic fraction of soil gases, with relative amounts from 0.02 to 0.08 % Σ VOCs (≤ 4.6 nmol/mol).

6.4.3 Soil gases depth profiles

The chemical inorganic composition of interstitial soil gases collected along the 5 vertical profiles (Table 6.12) showed significant changes with depth.

The P1 and P2 profiles were characterized by relatively high CO₂ concentrations, slightly increasing with depth up to 981 and 977 mmol/mol, and $\delta^{13}\text{C-CO}_2$ values ranging from 0.38 to 0.54 ‰ (Table 6.12). H₂S and CH₄ showed increasing concentrations with depth, ranging from 0.14 to 0.61 mmol/mol and from 2.91 to 5.16 mmol/mol along P1 profile and from 0.078 to 0.485 mmol/mol and from 0.36 to 4.21 mmol/mol along P2 profile, respectively (Table 6.12). The $\delta^{13}\text{C-CH}_4$ values decreased at increasing CH₄ contents, i.e. increasing depth, ranging from -24.1 to -26.1 ‰ and from -18.6 to -26.2 ‰ in P1 and P2, respectively. N₂, O₂ and Ar contents showed decreasing trends with increasing depth, the maximum concentrations (70.1, 4.61 and 0.95 mmol/mol in P1 and 73.9, 20.7 and 1.58 mmol/mol in P2, respectively) being mostly measured at 10 cm depth.

The P3 and P4 profiles were characterized by sharply increasing CO₂ concentrations with depth (from 49 to 575 mmol/mol and from 69 to 808 mmol/mol in P3 and P4, respectively) and relatively low H₂S concentrations, being below the detection limit at shallow depth and increasing between 25 and 50 cm depth up to 0.021 and 0.094 mmol/mol in P3 and P4, respectively (Table 6.12). CH₄ also showed a strong increase with depth (from 0.006 to 0.69 and from 0.031 to 2.76 mmol/mol in P3 and P4, respectively), whereas N₂, O₂ and Ar concentrations were characterized by decreasing vertical trends (767 to 413, 174 to 3.45 and 10.1 to 7.05 mmol/mol in P3 and 755 to 184, 167 to 0.09 and 9.46 to 4.68 mmol/mol in P4, respectively). The $\delta^{13}\text{C-CO}_2$ values showed no evident variation trend along the two profiles, ranging from 3.02 to 3.51 ‰ in P3 and from 1.36 to 2.70 ‰ in P4 (Table 6.12). Contrarily, the isotopic signature of CH₄ clearly showed a decreasing trend varying from -12.9 ‰ at 25 cm to -20.3 ‰ at 50 cm in P3 and from -11.0 ‰ at 15 cm to -24.7 ‰ at 50 cm in P4 (Table 6.12).

Table 6.12: Location (in UTM) and chemical composition (in mmol/mol) of the main gas species (CO_2 , H_2S , N_2 , O_2 , Ar, CH_4) in soil gas samples collected from 10 to 50 cm depth along P1-P5 vertical profiles at Poggio dell'Olivo. The isotopic composition of CO_2 and CH_4 ($\delta^{13}\text{C}-\text{CO}_2$ and $\delta^{13}\text{C}-\text{CH}_4$, respectively, in ‰ vs. V-PDB) is also reported.

ID	East	North	Depth	CO_2	H_2S	N_2	O_2	Ar	CH_4	$\delta^{13}\text{C}-\text{CO}_2$	$\delta^{13}\text{C}-\text{CH}_4$
P1	4709962	264744	10	922	0.14	70.1	4.61	0.95	2.91	0.50	-24.1
			15	934	0.17	59.6	2.81	0.73	3.75	0.51	-24.4
			20	946	0.21	50.2	0.71	0.65	3.66	0.46	-24.7
			25	951	0.26	44.7	0.67	0.55	3.64	0.52	-25.0
			30	959	0.27	36.6	0.54	0.51	3.51	0.48	-25.1
			35	963	0.39	31.4	0.05	0.52	4.36	0.50	-25.5
			40	974	0.56	20.5	0.04	0.43	4.77	0.52	-25.7
			45	979	0.59	15.2	0.03	0.38	5.11	0.51	-26.0
			50	981	0.61	13.3	0.02	0.29	5.16	0.49	-26.1
P2	4709962	264731	10	903	0.078	73.9	20.7	1.46	0.36	0.40	-18.6
			15	911	0.111	71.2	15.8	1.58	0.55	0.39	-20.2
			20	916	0.156	69.7	11.7	1.51	0.94	0.54	-22.1
			25	937	0.233	52.7	7.49	1.26	1.21	0.38	-23.5
			30	949	0.246	43.5	4.35	1.06	1.87	0.39	-24.7
			35	959	0.301	35.5	1.88	0.78	2.55	0.38	-25.5
			40	973	0.315	22.3	0.65	0.51	3.04	0.42	-25.9
			45	977	0.361	19.1	0.04	0.42	3.26	0.40	-26.3
			50	977	0.485	17.6	0.03	0.39	4.21	0.41	-26.2
P3	4709910	264728	10	49		767	174	10.1	0.006	3.25	

(To be continued)

ID	East	North	Depth	CO ₂	H ₂ S	N ₂	O ₂	Ar	CH ₄	$\delta^{13}\text{C-CO}_2$	$\delta^{13}\text{C-CH}_4$
			15	63		754	173	9.55	0.025	3.51	
			20	124		712	155	9.15	0.057	3.43	
			25	114	0.008	751	126	9.31	0.13	3.51	-12.9
			30	233	0.011	678	79.7	8.84	0.21	3.35	-14.6
			35	342	0.012	611	47.6	8.55	0.35	3.28	-16.7
			40	445	0.015	515	31.3	7.31	0.45	3.20	-18.5
			45	510	0.018	457	24.2	7.15	0.52	3.18	-18.8
			50	575	0.021	413	3.45	7.05	0.69	3.02	-20.3
P4	4709898	264737	10	69		755	167	9.46	0.031	2.70	
			15	128		721	142	9.15	0.11	2.53	-11.0
			20	192		669	130	8.64	0.12	2.44	-12.1
			25	302	0.005	623	67	8.44	0.14	1.99	-13.6
			30	402	0.005	555	34.2	8.15	0.23	1.87	-15.1
			35	633	0.011	351	7.8	7.46	0.54	1.93	-17.7
			40	723	0.023	265	4.8	6.67	0.95	1.71	-18.5
			45	780	0.048	211	1.0	5.26	1.71	1.65	-20.6
			50	808	0.094	184	0.09	4.68	2.76	1.36	-24.7
P5	4709976	264764	10	32		772	186	9.95		-7.68	
			15	51		764	185	9.91		-6.57	
			20	57		752	181	9.55		-5.98	
			25	61		796	133	10.4		-6.62	
			30	88		841	60.7	10.3	0.016	-12.9	
			35	97		866	25.9	11.2	0.051	-0.76	
			40	85	0.005	901	2.87	11.1	0.11	-0.44	-49.5

(To be continued)

ID	East	North	Depth	CO ₂	H ₂ S	N ₂	O ₂	Ar	CH ₄	$\delta^{13}\text{C-CO}_2$	$\delta^{13}\text{C-CH}_4$
			45	102	0.011	889	1.2	11.7	0.18	-0.38	-53.7
			50	120	0.012	871	0.9	11.6	0.49	-0.45	-58.9

Table 6.12: Location (in UTM) and chemical composition (in mmol/mol) of the main gas species (CO₂, H₂S, N₂, O₂, Ar, CH₄) in soil gas samples collected from 10 to 50 cm depth along P1-P5 vertical profiles at Poggio dell'Olivo. The isotopic composition of CO₂ and CH₄ ($\delta^{13}\text{C-CO}_2$ and $\delta^{13}\text{C-CH}_4$, respectively, in ‰ vs. V-PDB) is also reported.

The P5 profile displayed the lowest CO₂ concentrations (ranging from 32 to 120 mmol/mol and increasing with depth), with $\delta^{13}\text{C-CO}_2$ values ranging over a relatively wide range (from -12.9 to -0.38 ‰; Table 6.12). H₂S and CH₄ were only detected at depths ≥ 40 cm and ≥ 30 cm, with concentrations increasing with depth up to 0.012 and 0.49 mmol/mol at 50 cm. The $\delta^{13}\text{C-CH}_4$ values were strongly negative (from -58.9 to -49.5 ‰; Table 6.12). N₂ and Ar concentrations were relatively high, with minor variations along the profile (from 752 to 901 mmol/mol and from 9.55 to 11.7 mmol/mol, respectively), whereas O₂ showed decreasing concentrations ranging from 186 mmol/mol at 10 cm to 0.9 mmol/mol at 50 cm (Table 6.12).

The variations in the inorganic gas composition were associated with changes in the VOCs distribution. The total amount of VOCs showed an increasing trend with depth along the five profiles, although the respective concentrations resulted to be relatively variable (Table 6.13).

The P1 and P2 profiles were characterized by the highest ΣVOCs values, ranging from 9,089 to 14,363 nmol/mol and from 3,275 to 13,637 nmol/mol in P1 and P2, respectively. Alkanes were the most abundant VOC group (>94 % ΣVOCs), being mainly constituted of ethane (up to 11,000 nmol/mol) and propane (up to 1,700 and 1,200 nmol/mol in P1 and P2, respectively), followed by n-pentane (up to 610 nmol/mol). Both normal and iso C₄₋₆ alkanes were detected, with concentrations and normal/iso ratios generally increasing with depth (Table 6.13). Among C₇ alkanes, only iso-heptane was detected, showing increasing concentrations with depth. Alkenes represented the second most abundant homologous family (up to 4.6 and 5.6 % ΣVOCs in P1 and P2, respectively) with a clear increasing trend with depth (from 110 to 615 nmol/mol and from 80 to 613 nmol/mol in P1 and P2, respectively). Iso-butene was the dominant alkene with concentrations up to 610 nmol/mol in both P1 and P2. Normal-pentene, normal-hexene and iso-hexene were only detected at ≥ 30 cm in P1 and ≥ 35 cm in P2 with concentrations up to 2.1 and 2.6 nmol/mol, respectively (Table 6.13). Similarly, aromatics showed increasing concentrations with depth, up to 23.8 and 24.8 nmol/mol in P1 and P2, respectively (≤ 0.21 % ΣVOCs), being exclusively represented by benzene at shallow depths, with toluene being detected only at ≥ 35 and ≥ 40 cm

6. Results

depths in P1 and P2, respectively. Cyclics, although present at relatively low concentrations (≤ 10.2 and ≤ 14.2 nmol/mol in P1 and P2, respectively), were detected along the whole P1 and P2 profiles. They were only consisting of C₅ and C₆ compounds, eventually methylated. Similarly, halocarbons (chlorohexane and trichloroisobutane) were similarly detected along the whole P1 profile (up to 3.1 nmol/mol), whereas they were occurring at ≥ 25 cm depth in P2 profile (up to 2.4 nmol/mol). Alcohols (hexanol, dimethylbutanol and methylhexanol) were the only O-bearing compounds detected along the whole P1 and P2 profiles with concentrations spanning 1.1 to 2.9 nmol/mol and 3.0 to 4.4 nmol/mol, respectively (Table 6.13). Among carboxylic acids, whose maximum concentrations were of 1.1 and 1.3 nmol/mol in P1 and P2, respectively, were represented by formic acid at very shallow depths (≤ 15 cm) and acetic acid (or ethanoic acid) over a wide depth range (Table 6.13). Formic acid ethyl ester was occasionally detected (up to 0.9 nmol/mol) between 15 and 40 cm depth (Table 6.13). The highest concentrations of propanone (0.9 and 1.1 nmol/mol in P1 and P2, respectively) were measured at 10 cm in both P1 and P2, whereas generally decreasing values were measured at increasing depths. Similarly, aldehydes, which were occasionally found in P1, showed decreasing contents at increasing depths in P2, with maximum concentrations of 1.2 (ethanal) and 1.0 (propanal) at 15 cm (Table 6.13). N-bearing compounds (pyrrolidine and methylbutanamide) and α -pinene were only detected in the P2 profile at 10 and 15 cm depth (Table 6.13).

In the P3 and P4 profiles, the total amount of VOCs ranged from 120 to 2,863 and from 473 to 8,155 nmol/mol, respectively. Alkanes were ≥ 87 % Σ VOCs, mainly consisting of ethane (up to 2,100 and 5,800 nmol/mol in P3 and P4, respectively) and propane (up to 560 and 710 nmol/mol in P3 and P4, respectively). Both ethane and propane showed increasing trends along the P3 and P4 profiles, together with heavier alkanes (Table 6.13). Normal- and iso-butane were not detected in P3, whereas they were measured at ≥ 35 cm depth in P4 (up to 470 and 450 nmol/mol, respectively). Normal-pentane was the most abundant alkane after propane (up to 120 and 510 nmol/mol at 50 cm depth in P3 and P4, respectively), but it was only recorded at depths ≥ 40 cm in P3 and ≥ 15 cm in P4 (Table 6.13). Similarly, iso-pentane,

normal-hexane and iso-hexane were detected at depths ≥ 20 cm in P3 (up to 13, 9.3 and 32 nmol/mol) and ≥ 15 cm in P4 (up to 56, 41 and 67 nmol/mol). Isoheptane was measured at ≥ 40 cm in P3 and ≥ 35 cm in P4 (up to 5.6 and 11 nmol/mol, respectively).

Alkenes were not detected along the P3 profile, whereas in P4 iso-butene was measured at ≥ 40 cm (up to 5.2 nmol/mol) and normal-pentene and n-hexene at 50 cm (0.6 and 0.8 nmol/mol, respectively). Benzene was the only aromatic compound detected in both P3 and P4, with concentrations increasing with depth up to 8.7 and 13 nmol/mol, respectively. Cyclics showed increasing concentrations from 30 to 50 cm depth in P4, with concentrations up to 2.9 nmol/mol, whereas only cyclopentane and methylcyclopentane were detected in P3 at 50 cm depth (0.6 and 0.7 nmol/mol, respectively; Table 6.13). Similarly, halocarbons were only measured at 50 cm depth in P3 (chlorohexane 0.6 nmol/mol) and at ≥ 40 cm depth in P4 (chlorohexane and chloroisobutane up to 0.9 and 0.81 nmol/mol, respectively). Differently, alcohols were present along the whole P3 and P4 profiles with concentrations ≤ 1.2 and ≤ 1.9 nmol/mol, respectively, depicting no clear trend with depth (Table 6.13). Among carboxylic acids, formic acid was detected between 15 and 30 cm (up to 0.9 nmol/mol) in P3 and at ≤ 15 cm (up to 0.6 nmol/mol) in P4, whereas acetic acid was found at ≥ 15 cm depth with concentrations up to 1.3 nmol/mol in both P3 and P4 (Table 6.13). Ester was occasionally found in P3 and P4, up to 1.3 and 0.7 nmol/mol, respectively. Differently, ketones and aldehydes were recovered along the whole profiles with decreasing concentrations at increasing depth. In particular, the highest concentration of propanone was measured at 10 and 25 cm in P3 (2.1 nmol/mol) and at 10 cm in P4 (1.9 nmol/mol), whereas ethanal and propanal were up to 2.3 and 1.8 nmol/mol at 20 cm in P3 and 2.3 and 2.1 nmol/mol at 10 cm in P4, respectively (Table 6.13). Almost all the profiles showed the presence of N-bearing compounds, with a slightly increasing trend with depth in P3 (pyrrolidine and methylbutanamide up to 2.1 and 1.6 nmol/mol), whereas the P4 profile did not evidence a clear trend. Terpene was found at shallow depths (≤ 30 cm), with maximum concentrations of 1.0 nmol/mol at 20 cm in P3 and 1.2 nmol/mol at 10 cm in P4 (Table 6.13).

6. Results

The P5 profile displayed the lowest Σ VOCs values, varying between 8 and 9 nmol/mol from 10 to 30 cm and increasing from 69 to 254 nmol/mol between 35 and 50 cm. Alkanes were only detected at ≥ 35 cm depth, being represented by ethane (up to 170 nmol/mol), propane (60 nmol/mol at 50 cm) and iso-hexane (up to 11 nmol/mol at ≥ 40 cm). No alkenes, aromatics, cyclics, halocarbons or N-bearing compounds were detected. O-bearing compounds largely dominated the organic fraction of soil gases collected up to 30 cm depth, ranging from 76 and 93 % Σ VOCs, i.e. as long as alkanes were below the detection limit. In particular, aldehydes and ketones were the most abundant O-bearing compounds up to 40 cm depth. Propanone (from 1.7 to 3.1 nmol/mol) and ethanal and propanal (from 1.6 to 2.4 and from 1.2 to 2.3 nmol/mol, respectively) were characterized by decreasing concentrations with increasing depth. Alcohols were only detected at ≥ 40 cm with concentrations ≤ 1.7 nmol/mol (Table 6.13). Similarly, formic acid, acetic acid and formic acid ethyl ester were detected at ≥ 20 cm, ≥ 40 cm and ≥ 30 cm with concentrations up to 1.4, 0.9 and 1.8 nmol/mol, respectively (Table 6.13). Differently from the other profiles, α -pinene was detected along the entire profile, with concentrations ranging from 0.5 and 2.1 nmol/mol and displaying a sharp decrease with depth between 10 and 25 cm (Table 6.13).

Table 6.13: Chemical composition (in nmol/mol) of VOCs in soil gas samples collected from 10 to 50 cm depth along P1-P5 vertical profiles at Poggio dell'Olivo.

	Formula	P1 10	P1 15	P1 20	P1 25	P1 30	P1 35	P1 40	P1 45	P1 50
Alkanes	C ₂ H ₆	8200	8800	11000	11000	9900	9800	9700	11000	9700
	C ₃ H ₈	560	610	730	780	960	1200	1600	1700	1600
	i-C ₄ H ₁₀	30	40	60	70	110	120	130	150	160
	n-C ₄ H ₁₀	30	60	90	120	120	150	160	190	210
	n-C ₅ H ₁₂	31	36	44	51	76	85	96	95	110
	3i-C ₅ H ₁₂	11	15	22	33	51	66	71	85	130
	n-C ₆ H ₁₄	65	71	84	110	110	140	180	220	250
	i-C ₆ H ₁₄	19	35	41	55	68	87	150	180	210
i-C ₇ H ₁₆	13	23	39	66	78	96	170	210	230	
Alkenes	i-C ₄ H ₈	110	150	210	250	330	350	440	490	610
	n-C ₅ H ₁₀					0.6	1.3	1.5	1.9	2.1
	i-C ₆ H ₁₂						0.5	0.7	0.8	0.9
	n-C ₆ H ₁₂					0.9	1.2	1.4	1.7	1.8
Cyclics	c-C ₅ H ₁₀	1.5	1.9	1.7	2.1	1.9	2.2	2.4	2.3	2.1
	c-C ₅ H ₉ CH ₃	1.3	1.8	2.1	2.2	1.7	1.8	2.1	2.2	2.5
	c-C ₆ H ₁₂	1.2	1.7	1.8	2.1	1.9	2.1	1.9	1.8	1.6
	c-C ₆ H ₁₁ CH ₃	1.5	2.1	2.2	1.9	2.2	2.3	2.1	1.9	1.8
	c-C ₆ H ₁₁ CH ₃ CH ₃	1.2	1.7	2.1	1.9	1.7	1.6	1.5	1.3	1.5
Aromatics	C ₆ H ₆	7.5	8.1	10	12	13	16	19	22	23
	C ₇ H ₈						0.5	0.6	0.6	0.8
Cl-bearing	C ₆ H ₁₃ Cl	1.2	1.7	1.5	1.6	1.4	1.8	1.8	1.6	1.7

(To be continued)

	Formula	P1 10	P1 15	P1 20	P1 25	P1 30	P1 35	P1 40	P1 45	P1 50
	$C_3H_4Cl_3CH_3$	1.1	1.4	1.5	1.3	1.7	1.1	1.5	1.4	1.3
Alcohols	$C_6H_{13}OH$		0.7	0.8	1.1	0.9	0.8	0.9	1.1	0.8
	$C_6H_{14}O$	0.5	0.8	1.1	0.7	0.9	0.8	0.9	0.6	0.9
	$C_7H_{16}O$	0.6	0.7	0.9	0.8	0.7	0.9	1.1	0.8	1.1
Carboxylic Acids	HCOOH	0.5	0.5							
	CH_3COOH		0.6	0.7	0.9	0.5	0.7	0.5		
Esters	$C_3H_6O_2$		0.5			0.8		0.7		
Ketones	C_3H_6O	0.9	0.8	0.7	0.5	0.6		0.7		0.5
Aldehydes	C_2H_4O	0.6		0.7	0.6		0.5			
	C_3H_6O	0.5		0.9	0.8		0.5		0.6	
N-bearing	C_4H_9N									
	$C_5H_{11}NO$									
Terpenes	$C_{10}H_6$									

(To be continued)

	Formula	P2 10	P2 15	P2 20	P2 25	P2 30	P2 35	P2 40	P2 45	P2 50
Alkanes	C ₂ H ₆	2900	3700	3400	4800	6100	8100	8800	8400	11000
	C ₃ H ₈	190	260	410	460	730	920	1000	1200	1100
	i-C ₄ H ₁₀					60	80	90	90	100
	n-C ₄ H ₁₀					60	90	110	130	120
	n-C ₅ H ₁₂	16	21	33	49	61	77	88	96	99
	3i-C ₅ H ₁₂	7.6	11	15	26	38	51	63	71	85
	n-C ₆ H ₁₄	51	66	75	88	96	110	130	150	180
	i-C ₆ H ₁₄	11	22	39	41	55	81	94	110	150
	i-C ₇ H ₁₆	7.0	9	19	35	55	77	110	130	170
Alkenes	i-C ₄ H ₈	80	120	190	240	350	450	520	610	580
	n-C ₅ H ₁₀						0.8	0.9	1.5	2.6
	i-C ₆ H ₁₂								0.5	0.7
	n-C ₆ H ₁₂						0.8	1.1	1.3	2.3
Cyclics	c-C ₅ H ₁₀	0.5	0.7	1.2	1.9	2.1	2.5	2.7	3.3	3.6
	c-C ₅ H ₉ CH ₃		0.5	1.1	1.4	1.7	2.2	2.5	2.8	3.1
	c-C ₆ H ₁₂		0.6	0.9	1.2	1.6	2	2.1	2.3	2.5
	c-C ₆ H ₁₁ CH ₃	0.5	0.6	0.7	1.5	1.8	2.1	2.3	2.7	2.7
	c-C ₆ H ₁₁ CH ₃ CH ₃		0.7	0.9	1.4	1.8	1.7	2.1	2.4	2.3
Aromatics	C ₆ H ₆	2.1	7.1	8.8	10	11	15	20	20	24
	C ₇ H ₈							0.5	0.5	0.8
Cl-bearing	C ₆ H ₁₃ Cl				0.5	0.8	1.2	1.1	1.3	1.1
	C ₃ H ₄ Cl ₃ CH ₃					0.7	0.9	0.9	1.1	1.3
Alcohols	C ₆ H ₁₃ OH	1.2	1.4	1.2	1.3	1.1	0.8	1.1	0.9	1.5

(To be continued)

	Formula	P2 10	P2 15	P2 20	P2 25	P2 30	P2 35	P2 40	P2 45	P2 50
	C ₆ H ₁₄ O	1.1	0.9	1.2	1.3	0.8	1.1	0.9	0.8	1.6
	C ₇ H ₁₆ O	0.9	0.8	1.4	1.5	1.3	1.1	1.2	1.4	1.3
Carboxylic Acids	HCOOH	0.5								
	CH ₃ COOH	0.8	0.7	0.9	0.7	0.8	0.5	0.5		0.6
Esters	C ₃ H ₆ O ₂		0.5	0.5	0.7	0.9				
Ketones	C ₃ H ₆ O	1.1	0.5	0.8	0.7	0.6	0.5			
Aldehydes	C ₂ H ₄ O	1	1.2	1.1	0.9	0.8	0.5	0.7	0.6	
	C ₃ H ₆ O	0.8	1	0.9	0.7	0.6	0.6	0.6	0.5	0.5
N-bearing	C ₄ H ₉ N	0.7								
	C ₅ H ₁₁ NO		6							
Terpenes	C ₁₀ H ₆	0.7								

(To be continued)

	Formula	P3 10	P3 15	P3 20	P3 25	P3 30	P3 35	P3 40	P3 45	P3 50
Alkanes	C ₂ H ₆	110	230	410	900	1400	1600	1700	1900	2100
	C ₃ H ₈		50	90	180	360	410	450	510	560
	i-C ₄ H ₁₀									
	n-C ₄ H ₁₀									
	n-C ₅ H ₁₂						1.6	5.1	9.0	13
	3i-C ₅ H ₁₂					0.6	1.9	4.2	7.1	9.3
	n-C ₆ H ₁₄			0.8	3.1	5.4	8.3	14	26	32
	i-C ₆ H ₁₄							0.9	2.1	5.6
	i-C ₇ H ₁₆									
Alkenes	i-C ₄ H ₈							60	110	120
	n-C ₅ H ₁₀									
	i-C ₆ H ₁₂									
	n-C ₆ H ₁₂									
Cyclics	c-C ₅ H ₁₀									0.6
	c-C ₅ H ₉ CH ₃									0.7
	c-C ₆ H ₁₂									
	c-C ₆ H ₁₁ CH ₃									
	c-C ₆ H ₁₁ CH ₃ CH ₃									
Aromatics	C ₆ H ₆	1.1	1.9	3.5	4.2	5.1	6.2	6.6	7.5	8.7
	C ₇ H ₈									
Cl-bearing	C ₆ H ₁₃ Cl									0.6
	C ₃ H ₄ Cl ₃ CH ₃									
Alcohols	C ₆ H ₁₃ OH	0.5		0.5	0.7	1.1	0.9	0.7	0.6	0.9

(To be continued)

	Formula	P3 10	P3 15	P3 20	P3 25	P3 30	P3 35	P3 40	P3 45	P3 50
	C ₆ H ₁₄ O	0.7	0.5		0.6	0.9	0.7	0.8	0.9	0.7
	C ₇ H ₁₆ O	0.6	0.7	0.6	0.8	1.2	0.9	1.2	1.1	0.8
Carboxylic Acids	HCOOH		0.7		0.9	0.8			0.8	0.6
	CH ₃ COOH		0.6	0.5	0.7	1.1	1.3	1.2	0.9	1.7
Esters	C ₃ H ₆ O ₂		0.8		0.7		0.7			1.3
Ketones	C ₃ H ₆ O	2.1	1.8	1.9	2.1	1.7	1.5	1.3	1.1	1.2
Aldehydes	C ₂ H ₄ O	1.9	2.1	2.3	1.7	1.5	1.5	1.3	1.1	1.2
	C ₃ H ₆ O	1.5	1.7	1.8	1.3	1.1	1.2	1.1	0.9	1.3
N-bearing	C ₄ H ₉ N	0.5	0.8	0.6	0.8	1.6	1.5	1.2	2.1	1.9
	C ₅ H ₁₁ NO		0.7	1.1	0.9	1.2	1.5	1.1	1.6	1.2
Terpenes	C ₁₀ H ₆	0.9	0.8	1	0.6	0.5				

(To be continued)

	Formula	P4 10	P4 15	P4 20	P4 25	P4 30	P4 35	P4 40	P4 45	P4 50
Alkanes	C ₂ H ₆	350	530	660	610	860	1900	2900	3700	5800
	C ₃ H ₈	110	130	150	190	210	430	530	650	710
	i-C ₄ H ₁₀						70	150	360	450
	n-C ₄ H ₁₀						80	110	390	470
	n-C ₅ H ₁₂				0.8	1.7	5.4	11	28	56
	3i-C ₅ H ₁₂			0.5	1.1	1.6	3.2	7.3	17	41
	n-C ₆ H ₁₄		0.6	2.1	7.3	12	19	21	55	67
	i-C ₆ H ₁₄						0.8	3.1	6.5	11
	i-C ₇ H ₁₆							0.7	1.4	5.2
Alkenes	i-C ₄ H ₈		60	90	110	150	260	350	440	510
	n-C ₅ H ₁₀									0.6
	i-C ₆ H ₁₂									
	n-C ₆ H ₁₂									0.8
Cyclics	c-C ₅ H ₁₀						0.5	0.9	1.5	2.9
	c-C ₅ H ₉ CH ₃					0.8	1.1	1.6	2.1	2.7
	c-C ₆ H ₁₂							0.8	1.4	2.2
	c-C ₆ H ₁₁ CH ₃					0.5	0.8	1.1	1.7	2.3
	c-C ₆ H ₁₁ CH ₃ CH ₃							0.6	1.3	1.9
Aromatics	C ₆ H ₆	1.6	2.6	4.4	5.1	7.3	7.9	10	12	13
	C ₇ H ₈									
Cl-bearing	C ₆ H ₁₃ Cl							0.5	0.7	0.9
	C ₃ H ₄ Cl ₃ CH ₃								0.5	0.8
Alcohols	C ₆ H ₁₃ OH	0.8	1.1	1.3	1.1	0.8	0.9	1.1	0.7	0.6

(To be continued)

	Formula	P4 10	P4 15	P4 20	P4 25	P4 30	P4 35	P4 40	P4 45	P4 50
	C ₆ H ₁₄ O	1.1	1.2	1.5	1.6	1.1	1.3	0.8	0.5	0.8
	C ₇ H ₁₆ O	0.9	1.5	1.9	1.8	1.4	1.2	0.8	0.9	0.7
Carboxylic Acids	HCOOH	0.6	0.5							
	CH ₃ COOH			0.8	0.9	1.1	1.3	1.1	1.2	0.9
Esters	C ₃ H ₆ O ₂		0.6		0.7					
Ketones	C ₃ H ₆ O	1.9	1.8	1.1	0.8	0.7	0.8	0.6	0.8	0.7
Aldehydes	C ₂ H ₄ O	2.3	1.7	1.2	0.9	1	1.1	1.3	1.2	0.8
	C ₃ H ₆ O	2.1	1.8	1.4	1.1	0.8	0.9	1.1	0.9	0.7
N-bearing	C ₄ H ₉ N			0.6	0.8	1.2	1.3	1.1	0.8	0.8
	C ₅ H ₁₁ NO	0.5		0.9	1.4	1.1	1.6	1.1	0.8	0.9
Terpenes	C ₁₀ H ₆	1.2	0.8	0.8	0.7	0.6				

(To be continued)

	Formula	P5 10	P5 15	P5 20	P5 25	P5 30	P5 35	P5 40	P5 45	P5 50
Alkanes	C ₂ H ₆						60	70	80	170
	C ₃ H ₈									60
	i-C ₄ H ₁₀									
	n-C ₄ H ₁₀									
	n-C ₅ H ₁₂									
	3i-C ₅ H ₁₂									
	n-C ₆ H ₁₄							2.1	6.3	11
	i-C ₆ H ₁₄									
i-C ₇ H ₁₆										
Alkenes	i-C ₄ H ₈									
	n-C ₅ H ₁₀									
	i-C ₆ H ₁₂									
	n-C ₆ H ₁₂									
Cyclics	c-C ₅ H ₁₀									
	c-C ₅ H ₉ CH ₃									
	c-C ₆ H ₁₂									
	c-C ₆ H ₁₁ CH ₃									
	c-C ₆ H ₁₁ CH ₃ CH ₃									
Aromatics	C ₆ H ₆									
	C ₇ H ₈									
Cl-bearing	C ₆ H ₁₃ Cl									
	C ₃ H ₄ Cl ₃ CH ₃									
Alcohols	C ₆ H ₁₃ OH							0.6	1.3	1.5

(To be continued)

	Formula	P5 10	P5 15	P5 20	P5 25	P5 30	P5 35	P5 40	P5 45	P5 50
	C ₆ H ₁₄ O								0.8	1.1
	C ₇ H ₁₆ O							0.7	1.2	1.7
Carboxylic Acids	HCOOH			0.7	0.8		0.7	0.9	1.4	1.2
	CH ₃ COOH							0.8	0.9	0.6
Esters	C ₃ H ₆ O ₂					0.8	1.8	1.2	1.4	0.9
Ketones	C ₃ H ₆ O	2.6	2.5	3.1	2.7	2.1	1.8	2.6	1.7	1.9
Aldehydes	C ₂ H ₄ O	2.3	2.1	2.2	2.4	2.1	1.8	1.7	1.6	1.8
	C ₃ H ₆ O	1.7	1.8	2.3	2.1	1.8	1.5	1.3	1.2	1.5
N-bearing	C ₄ H ₉ N									
	C ₅ H ₁₁ NO									
Terpenes	C ₁₀ H ₆	2.1	1.4	1.1	0.6	0.8	0.9	0.5	0.7	0.7

Table 6.13: Chemical composition (in nmol/mol) of VOCs in soil gas samples collected from 10 to 50 cm depth along P1-P5 vertical profiles at Poggio dell'Olivo.

6.5 Cava dei Selci

6.5.1 Gas vents

The chemical composition (in mmol/mol) of the main gas compounds (CO₂, H₂S, CH₄, N₂, O₂, Ar, H₂, CO) in the dry fraction of two gas vents (CS1 and CS2) collected from the main gas emission area of Cava dei Selci is reported in Table 6.14. CO₂ was the largely dominant gas compound (up to 985 mmol/mol), followed by H₂S, N₂ and CH₄ (up to 11, 5.6 and 0.91 mmol/mol, respectively). Minor concentrations of O₂, H₂, Ar and CO (up to 0.13, 0.056, 0.051 and 0.0033 mmol/mol) were also measured (Table 6.14). The isotopic composition of CO₂ ($\delta^{13}\text{C-CO}_2$; Table 6.14) was of 1.08 and 0.9 ‰ in CS1 and CS2, respectively. These values are in the variation range of $\delta^{13}\text{C-CO}_2$ values of both the Cava dei Selci gas vents (from 0.75 to 1.39 ‰; Carapezza and Tarchini, 2007; Carapezza et al., 2012) and the main gas manifestations from the Alban Hills region (from -3.5 to 1.39 ‰; Chiodini and Frondini, 2001; Carapezza et al., 2012). The isotopic signature of CH₄ (Table 6.14) was of -29 and -30 ‰ in CS1 and CS2, respectively, i.e. similar to the value reported by Tassi et al. (2012d) for gas vent at Solfatara di Pomezia (i.e. -29.3 ‰).

The organic fraction amounted to 4,882 and 5,313 nmol/mol in CS1 and CS2, respectively (0.58 and 0.60 % of the CH₄ content; Table 6.14), largely consisting of alkanes (87 and 88 % ΣVOCs) and aromatics (13 and 12 % ΣVOCs). Ethane was the most abundant alkane (up to 3,600 nmol/mol), followed by propane (up to 660 nmol/mol) and normal-butane (up to 220 nmol/mol), whereas C₅₊ alkanes were measured at lower concentrations (up to 69 nmol/mol). Iso-butane was detected at concentrations (up to 160 nmol/mol) lower than those of its normal isomer (Table 6.14). Benzene concentrations (up to 640 nmol/mol) were two orders of magnitude higher than those measured for branched aromatics (up to 7.8 nmol/mol). O-bearing compounds were mainly consisting of esters and acids (up to 2.4 nmol/mol), with minor amounts of ketones, aldehydes and other non-identified compounds (up to 0.60, 0.13 and 0.39, respectively). S-bearing compounds were

6. Results

detected at concentrations of 1.70 and 2.50 nmol/mol in CS1 and CS2, respectively (Table 6.14).

ID	CS1	CS2
Date	Apr16	Apr16
East	301685	301700
North	4628022	4628010
CO₂	985	982
H₂S	9.2	11
N₂	4.3	5.6
O₂	0.13	0.087
Ar	0.032	0.051
H₂	0.036	0.056
CO	0.0033	0.0009
CH₄	0.82	0.91
$\delta^{13}\text{C-CO}_2$	1.08	0.9
$\delta^{13}\text{C-CH}_4$	-29	-30
C₂H₆	3300	3600
C₃H₈	510	660
iC₄H₁₀	160	150
nC₄H₁₀	220	180
C₆H₆	610	640
C₅₊ alkanes	71	69
branched aromatics	6.1	7.8
kenotes	0.15	0.60
aldehydes	0.15	0.13
esters+acids	2.40	2.10
S-substituted	1.70	2.50
others	0.24	0.39

Table 6.14: Location (in UTM) and chemical composition of the main gas species (CO₂, H₂S, N₂, O₂, Ar, H₂, CO, CH₄; in mmol/mol) and VOCs (in nmol/mol) from the CS1 and CS2 gas vents at Cava dei Selci. The isotopic composition of CO₂ and CH₄ ($\delta^{13}\text{C-CO}_2$ and $\delta^{13}\text{C-CH}_4$, respectively, in ‰ vs. V-PDB) is also reported.

6.5.2 Interstitial soil gases and soil flux measurements

The chemical composition (in mmol/mol) of the inorganic fraction (CO_2 , H_2S , N_2 , O_2 , Ar and CH_4) of interstitial soil gas samples collected at 20 cm depth from 30 sites within the main gas emission area of Cava dei Selci is reported in Table 6.15. CO_2 (from 272 to 962 mmol/mol), N_2 (from 36 to 551 mmol/mol) and O_2 (from 0.51 to 218 mmol/mol) were the most abundant compounds. Relatively low contents of Ar, H_2S and CH_4 (up to 12, 3.3 and 0.13 mmol/mol, respectively) were also measured (Table 6.15). The N_2/Ar ratios ranged from 34 to 50, i.e. close to the ASW values (Figure 6.15), pointing to a prevailing shallow origin of N_2 . According to CO_2/N_2 ratios and soil CO_2 fluxes (Figure 6.16), four groups of soil gases were distinguished: (i) soil gases (A type) characterized by high CO_2/N_2 ratios (from 11 to 19) and ΦCO_2 (from 4,373 to 13,638 $\text{gm}^{-2}\text{day}^{-1}$), (ii) soil gases (B type) with high CO_2/N_2 ratios (from 6.3 to 27) and lower ΦCO_2 values (from 833 to 2,109 $\text{gm}^{-2}\text{day}^{-1}$), (iii) soil gases (C type) with CO_2/N_2 ratios from 1.6 to 4.1 and ΦCO_2 values from 194 to 1,223 $\text{gm}^{-2}\text{day}^{-1}$, and (iv) soil gases (D type) with low CO_2/N_2 ratios (from 0.6 to 1.3) and ΦCO_2 values (from 83 to 344 $\text{gm}^{-2}\text{day}^{-1}$). The contribution from deep fluids was expected to increase at increasing CO_2/N_2 ratios and ΦCO_2 values, although the diffuse degassing could be affected by variations in the soil permeability. Accordingly, hydrothermal-related gases (H_2S and CH_4) increased at increasing CO_2/N_2 ratios, whereas air-derived species (Ar and O_2) showed an opposite trend.

6. Results

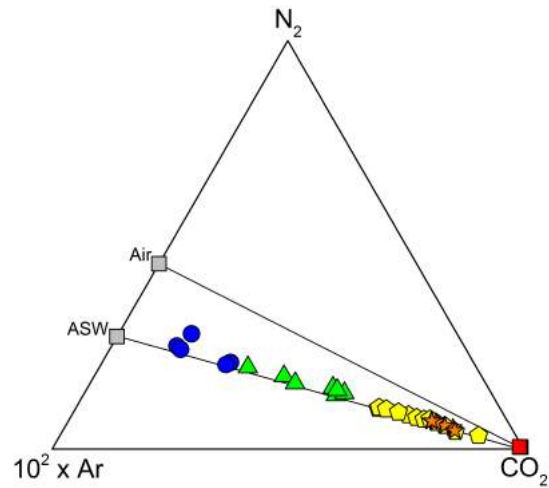


Figure 6.15: CO_2 - N_2 -Ar ternary diagram for (i) gas vents (red squares) and soil gases of type (ii) A (orange stars), (iii) B (yellow pentagons), (iv) C (green triangles) and (v) D (blue circles) collected from Cava dei Selci.

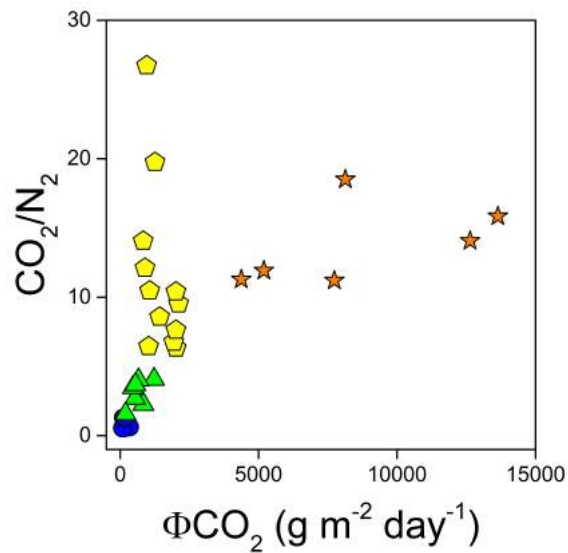


Figure 6.16: CO_2/N_2 ratios vs. ΦCO_2 values (in $gm^{-2}day^{-1}$) for gas vents and soil gases from Cava dei Selci. Symbols and colors as in Figure 6.15.

6.5 Cava dei Selci

ID	Date	East	North	CO ₂	H ₂ S	N ₂	O ₂	Ar	CH ₄	ΦCO ₂
C1	Apr16	301691	4628013	272		498	218	12	0.023	122
C2	Apr16	301695	4628027	935	3.3	59	1.6	1.4	0.075	13638
C3	Apr16	301687	4628022	928	3.2	66	1.2	1.6	0.044	12640
C4	Apr16	301684	4628018	908	2.6	81	6.8	1.9	0.075	7734
C5	Apr16	301683	4628013	843	0.13	131	22	3.4	0.019	1030
C6	Apr16	301679	4628024	917	2.4	77	1.4	1.8	0.055	5191
C7	Apr16	301684	4628028	914	1.9	81	1.5	1.9	0.13	4373
C8	Apr16	301684	4628032	928	0.88	66	3.6	1.6	0.036	833
C9	Apr16	301677	4628025	944	1.9	51	1.5	1.4	0.11	8134
C10	Apr16	301676	4628023	948	0.64	48	2.1	1.4	0.022	1257
C11	Apr16	301671	4628028	920	0.14	76	2.3	1.8	0.025	895
C12	Apr16	301673	4628031	299		484	205	12	0.011	344
C13	Apr16	301679	4628035	962	0.39	36	0.51	0.85	0.098	956
C14	Apr16	301680	4628041	302		551	136	11	0.021	83
C15	Apr16	301678	4628044	508		395	87	9.6	0.018	114
C16	Apr16	301674	4628039	498		388	104	9.9	0.015	159
C17	Apr16	301671	4628034	831	0.056	131	35	3.3	0.041	2022
C18	Apr16	301663	4628030	846	0.22	125	26	3.1	0.034	1939
C19	Apr16	301658	4628035	759	0.12	187	49	4.7	0.023	1223
C20	Apr16	301667	4628040	640	0.13	284	69	6.7	0.021	842
C21	Apr16	301673	4628046	882	0.056	103	12	2.5	0.026	1425
C22	Apr16	301665	4628053	896	0.12	94	7.8	2.3	0.014	2109
C23	Apr16	301661	4628049	690	0.069	256	48	6.4	0.011	541
C24	Apr16	301655	4628042	904	0.056	87	6.6	2.1	0.046	2011
C25	Apr16	301653	4628044	877	0.46	115	5.1	2.8	0.054	2012
C26	Apr16	301653	4628048	900	0.29	86	12	1.9	0.024	1063
C27	Apr16	301659	4628054	745	0.095	185	66	4.2	0.019	661
C28	Apr16	301649	4628051	599	0.087	381	11	9.2	0.023	194
C29	Apr16	301657	4628029	744	0.11	215	36	4.7	0.021	461
C30	Apr16	301657	4628024	742	0.12	202	51	4.5	0.022	550

Table 6.15: Location (in UTM) and chemical composition (in mmol/mol) of the main gas species (CO₂, H₂S, N₂, O₂, Ar, CH₄; in mmol/mol) in soil gas samples from Cava dei Selci. The ΦCO₂ values (in gm⁻²day⁻¹) measured at each soil gas sampling site are also reported.

6. Results

Similarly, Σ VOCs (from 47 to 1,148 nmol/mol) increased with the CO_2/N_2 ratio, the highest concentrations being measured in the A type soil gases (Figure 6.17). The organic fraction was largely dominated by alkanes (from 78

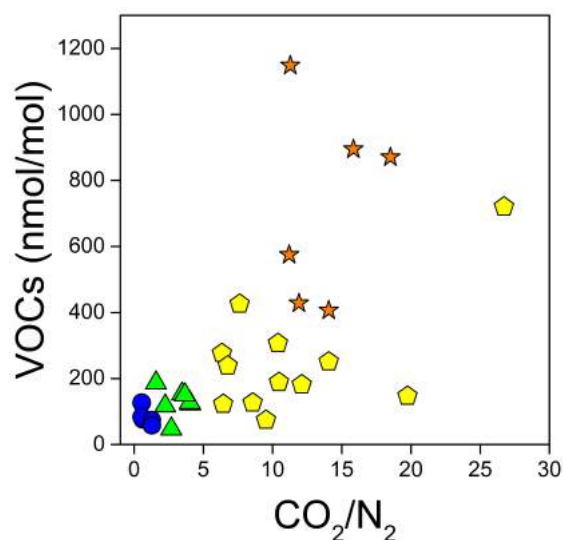


Figure 6.17: VOCs concentrations (in nmol/mol) vs. CO_2/N_2 ratios for gas vents and soil gases from Cava dei Selci. Symbols and colors as in Figure 6.15.

to 97 % Σ VOCs), mainly ethane (from 36 to 610 nmol/mol) and propane (from 3 to 150 nmol/mol), with minor amounts of iso-butane (from 0.5 to 26 nmol/mol), normal-butane (from 0.2 to 15 nmol/mol) and C_{5+} alkanes (from 1.1 to 160 nmol/mol; Table 6.16). The highest concentrations of alkanes were measured in the A type soil gases, which were also enriched in cyclics, alkenes and aromatics (up to 12, 110 and 13 nmol/mol, respectively) relative to the other soil gas groups (up to 6.9, 55 and 7.0 nmol/mol, respectively). Moreover, S-bearing compounds were only detected in the A type soil gases (from 0.5 to 1.2 nmol/mol; Table 6.16). O-bearing compounds (from 1.8 to 51 nmol/mol), representing ≤ 14 % Σ VOCs, showed no significant correlation with the CO_2/N_2 ratios. Specifically, ketones, aldehydes and carboxylic acids were detected at concentrations up to 16, 23 and 12 nmol/mol (Table 6.16).

Table 6.16: Chemical composition (in nmol/mol) of VOCs in soil gas samples from Cava dei Selci.

ID	C ₂ H ₆	C ₃ H ₈	i-C ₄ H ₁₀	n-C ₄ H ₁₀	C ₆ H ₆	C ₅₊	alkanes	alkenes	branched aromatics
C1	85	11	2.3	1.5	1.4	8		11	
C2	440	110	26	15	11	150		87	1.2
C3	210	61	11	6.7	6.9	45		48	0.28
C4	390	61	10	5.5	6	41		44	0.26
C5	77	12	2.1	1.4	1.2	8.4		7.1	
C6	230	75	13	7.7	6.6	51		33	0.27
C7	610	150	26	15	12	160		110	1.1
C8	180	32	4.1	1.6	1.2	11		12	
C9	560	96	12	8.5	7.8	88		76	0.31
C10	91	15	2.3	2.1	1.5	12		15	0.17
C11	110	23	3.6	4.1	2.5	15		14	0.19
C12	56	9.5	1.5	1.1	1.2	1.1		1.6	
C13	470	86	9.1	7.5	6.8	67		55	0.23
C14	74	5	0.5	0.2	0.2				
C15	66	4	0.6	0.4	0.3				
C16	52	3	0.5	0.3	0.2				
C17	140	45	9.4	6.6	4.5	33		25	0.18
C18	130	42	8.4	5.1	4.4	25		11	0.15
C19	88	12	1.8	0.9	0.5	7.7		5.5	
C20	87	10	1.6	0.8	0.7	6.1		3.3	
C21	96	11	1.5	0.9	0.8	4.8		2.5	

(To be continued)

ID	C ₂ H ₆	C ₃ H ₈	i-C ₄ H ₁₀	n-C ₄ H ₁₀	C ₆ H ₆	C ₅₊	alkanes	alkenes	branched aromatics
C22	57	8	0.9	0.7	0.6		1.1	1.6	
C23	36	5	0.7	0.5	0.6				
C24	210	35	6.6	2.7	3.9		26	12	0.25
C25	280	49	8.1	3.5	4.4		45	16	0.39
C26	120	25	5.1	2.1	3.6		14	8.7	0.11
C27	94	11	1.6	2.6	2.1		5.8	1.1	
C28	110	21	6.6	4.4	3.5		16	12	0.12
C29	85	15	4.5	3.9	2.9		11	7.6	0.08
C30	91	17	5.1	4.4	3.5		12	7.8	0.09

(To be continued)

ID	kenotes	aldehydes	carboxylic acids	cyclics	S-substituted	others
C1	1.5	1.1	1.6	1.8		
C2	16	13	11	12	1.2	1.1
C3	2.6	2.9	3.3	7.5	1.1	
C4	3.3	2.1	3.6	6.6	0.6	0.8
C5	3.8	3.6	4.5	1.5		
C6	1.6	1.1	2.3	5.4	0.8	
C7	15	23	12	12	0.5	1.2
C8	2.6	1.8	3.4	1.4		
C9	5.5	2.6	5.8	5.5	0.7	1.3
C10	2.1	1.4	2.5	1.6		
C11	2.3	1.5	2.6	2.7		
C12	0.8	0.6	1.1	1.5		
C13	4.4	2.1	4.6	6.9		0.7
C14	1.3	0.5	0.7	0.5		
C15	0.7	0.5	0.6	0.4		
C16	1.1	0.5	0.4	0.6		
C17	4.1	0.26	5.4	3.1		
C18	3.2	1.7	3.6	3.9		
C19	2.3	1.2	2.9	0.6		
C20	2.5	1.7	2.8	0.8		
C21	3.1	1.6	3.3	0.7		
C22	1.3	0.6	1.5	0.5		
C23	1.5	0.8	1.6	0.3		

(To be continued)

ID	kenotes	aldehydes	carboxylic acids	cyclics	S-substituted	others
C24	2.4	1.4	2.1	4.1		
C25	6.1	3.8	6.5	2.6		0.6
C26	2.3	1.2	3.3	3.5		
C27	2.4	1.3	2.7	2.6		
C28	3.6	2.2	3.3	3.9		
C29	2.1	16	2.5	2.5		
C30	2.2	1.5	2.5	3.7		

Table 6.16: Chemical composition (in nmol/mol) of VOCs in soil gas samples from Cava dei Selci.

Chapter 7

Distribution of VOCs from hydrothermal gas discharges: insights on primary processes

7.1 Introduction

While laboratory experiments give hints on the possible reactions occurring on VOCs under hydrothermal conditions, the actual processes governing the chemical features of organics in natural hydrothermal environments can only be assessed on the basis of empirical data.

In volcanic and hydrothermal systems, deep hydrothermal reservoirs feed several typologies of fluid emissions at the surface. Among them, punctual gas emissions, especially those having high outlet temperatures, are generally considered compositionally similar to deep fluids within the hydrothermal reservoirs, whose temperature and redox conditions can accordingly be predicted on the basis of the chemical features of gases discharged at the surface through a thermodynamic approach (e.g. Giggenbach, 1980, 1987, 1997).

Due to their rapid ascent through highly permeable pathways, the composition of fluids emitted from high flow rate gas discharges (e.g. fumaroles) remains mostly unaffected by secondary processes, these being induced by the abruptly changing physicochemical conditions at shallow depths, and the

7. Distribution of VOCs from hydrothermal gas discharges

chemical features related to the primary processes occurring at depth are preserved almost unmodified at the surface.

Accordingly, in this chapter, the chemical composition of punctual gas discharges (fumaroles, bubbling gases, gas vents) collected from the four study areas is discussed to investigate the control exerted by physicochemical conditions of the deep hydrothermal systems on the chemical reactions involving the organic gas species by (i) highlighting similarities and differences in the VOCs distribution in gas emissions from active volcanoes and low-to-medium enthalpy hydrothermal systems and (ii) comparing the analytical results with those gathered from experimental runs. An exhaustive characterization of the organic fraction occurring in punctual gas vents, an essential prerequisite for the recognition of the occurrence of secondary processes on VOCs emitted diffusively from the soil in hydrothermal systems, will be described in detail in the next chapter section.

7.2 General features of volcanic-hydrothermal systems

From the point of view of fluid geochemistry, an actively degassing volcano can be modeled, as follows (Figure 7.1): a magma degassing at depth releases

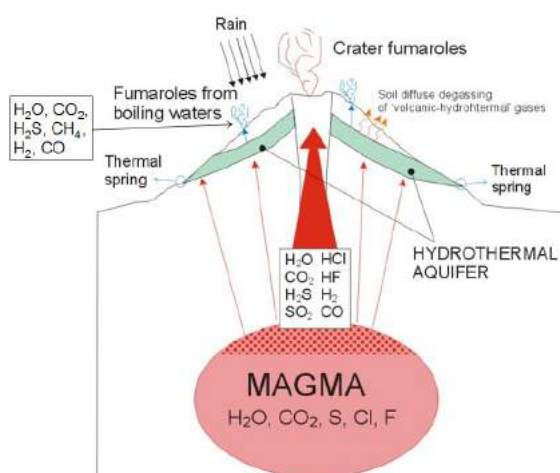


Figure 7.1: Schematic model of a typical volcanic-hydrothermal system.

7.2 General features of volcanic-hydrothermal systems

hot magmatic fluids that can either (i) arrive directly at the surface feeding high temperature fumaroles (crater fumaroles in Figure 7.1), or (ii) interact with groundwater producing a hot and boiling aquifer that may feed another type of fumaroles (fumaroles from boiling waters in Figure 7.1). The hot magmatic fluids interacting with the aquifer not only supply thermal energy to the hydrothermal reservoir through H₂O condensation but also undergo “magmatic gas scrubbing” processes (Giggenbach, 1996; Symonds et al., 2001), resulting in significant differences in the physicochemical characteristics with respect to those of high-T and boiling-derived fumaroles. Marini and Gambardella (2005) simulated the changes in temperature during the progressive addition of hot (915 °C) magmatic gas into 1000 g of pure water at 25 °C and at fixed pressure (0.1 MPa). By adding relatively low amounts of magmatic gas (<0.4 mol), the gas completely dissolved in water (liquid field) and no significant changes in temperature were observed (Figure 7.2).

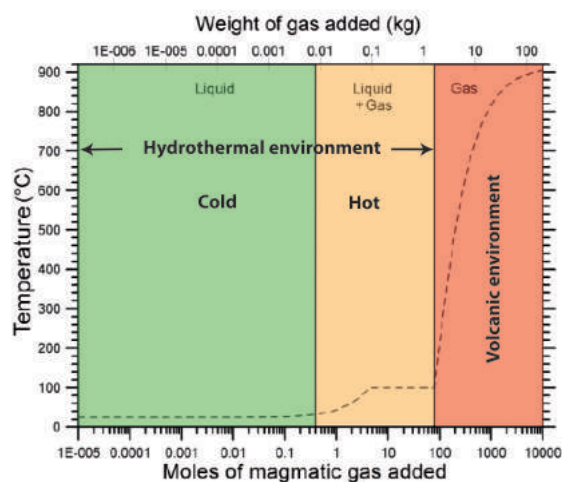


Figure 7.2: Temperature changes associated with the progressive addition of magmatic gas at 915 °C into 1000 g of pure water initially at 25 °C (modified from Marini and Gambardella, 2005).

Further additions of magmatic gas led to the formation of a bi-phase system (liquid+gas; under the imposed conditions, the transition occurred at a temperature of 32.4 °C only) and an increment in temperature up to the boiling point of water (100 °C; i.e. saturation temperature at 0.1 MPa; Figure 7.2).

7. Distribution of VOCs from hydrothermal gas discharges

The boiling temperature was maintained constant through the addition of increasing amounts of magmatic gas (from 4.29 up to 79.3 moles) by the coexistence of liquid and gaseous water (Figure 7.2). As the dry conditions were attained, temperature sharply increased from the boiling point to the original temperature of the magmatic gas (915 °C; Figure 7.2). Accordingly, the fluids emitted from hydrothermal and volcanic environments show significant differences in the discharge temperatures, as well as in the chemical composition of the main inorganic gas species (Symonds et al., 2001; Marini and Gambardella, 2005), as briefly described below.

Volcanic fumaroles are characterized by high temperatures (higher than the boiling point of water and up to >800 °C), high contents of acidic gases (SO₂, HCl, HF) and CO (Figure 7.3). Hydrothermal fluids, produced by boiling of hot aquifers, generally show temperatures close to the boiling point of water, no highly acidic gases and high contents of H₂S and CH₄ (Figure 7.3). The presence of methane is related to the reducing conditions of the hydrothermal environment whereas high temperature fluids in volcanic areas are characterized by more oxidizing conditions (Marini and Gambardella, 2005), which prevent the formation of CH₄. In both volcanic and hot hydrothermal fumaroles the chemical composition is dominated by H₂O followed by CO₂ (Figure 7.3). Differently, cold gas emissions display temperatures ≪100 °C and compositions dominated by CO₂, with minor amounts of H₂S and CH₄, whereas H₂O is not present (Figure 7.3). Air-derived gases (O₂, N₂, Ar) in both volcanic/hydrothermal and cold fluid discharges result from atmospheric contribution or meteoric waters involved in the hydrothermal system, N₂ and Ar possibly being also related to mantle/crustal sources (Sigurdsson et al., 2015).

7.2 General features of volcanic-hydrothermal systems

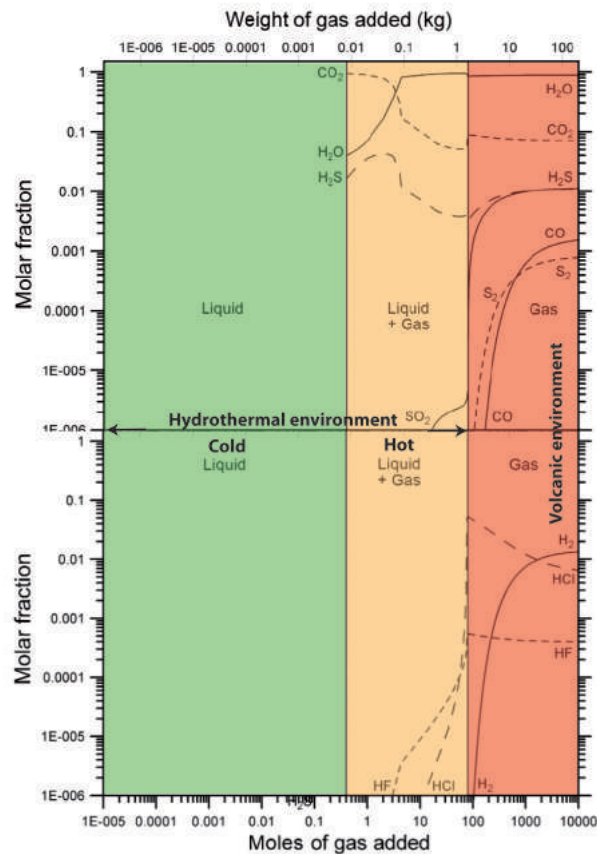


Figure 7.3: Variations in the molar fractions of gaseous inorganic species (H₂O, CO₂, H₂S, CO, S₂, SO₂, H₂, HCl, HF) during progressive addition of hot (915 °C) magmatic gas into 1000 g of pure water initially at 25 °C (pressure fixed at 0.1 MPa) (modified from Marini and Gambardella, 2005).

7.3 Thermal features

The fluid emissions collected in the four study areas can be classified, as follows: (i) steam-saturated fumaroles, (ii) boiling fumaroles, (iii) cold gas bubbling pool and (iv) dry CO₂ emissions.

The steam-saturated fumaroles are defined as fumaroles whose outlet temperatures are around 160 °C. Both Bocca Nuova and Bocca Grande at Solfatara Crater are classified as steam-heated fumaroles (which accordingly are also called “solfatara” type fumaroles; Minissale, 2014), with discharge temperatures from 150 to 164 °C. The chemical features of these fumaroles has been interpreted as related to the boiling of a hydrothermal aquifer thermally close to the point of maximum enthalpy of saturated steam, i.e. about 235 °C and 30.6 bar (e.g. Cioni et al., 1984; Minissale, 2014). The enthalpy-entropy (or Mollier) diagram for water is shown in Figure 7.4. According to the

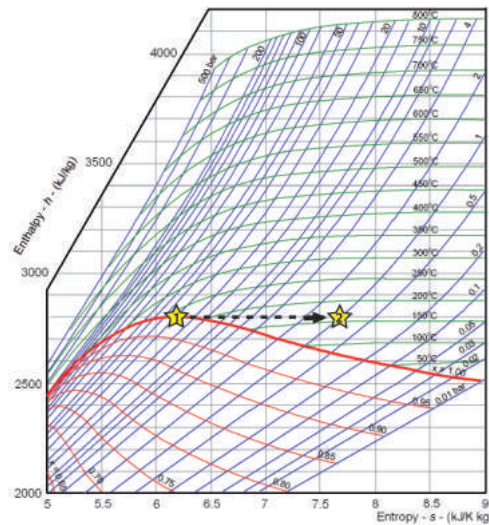


Figure 7.4: Enthalpy vs. entropy (or Mollier) diagram for water. The yellow star labelled 1 corresponds to the maximum enthalpy point (i.e. 235 °C and 30.6 bar) on the steam saturation line. The dashed arrow depicts the isenthalpic pressure loss due to steam uprising to the surface. The yellow star labelled 2 corresponds to the resulting fumarolic discharge at 1 bar, displaying an outlet temperature of 160 °C.

First Law of thermodynamics, the expansion of steam without heat or work

transfer occurs at constant enthalpy (DiPippo, 2008). Hence, as the deep saturated steam at 235 °C and 30.6 bar rises toward the surface, it experiences isenthalpic pressure loss that, at atmospheric pressure, would result in a gas discharge at 160 °C (process 1 to 2 in Figure 7.4).

Fumaroles from Nisyros caldera are typical boiling fumaroles at atmospheric pressure, characterized by outlet temperatures ranging from 98.7 to 100.3 °C (i.e. boiling point of water according to elevation). This type of fumaroles is related to steam generally derived by secondary boiling of aquifers at relatively shallow depths, located between the deep hydrothermal reservoir and the surface (Minissale, 2002).

The fluid emissions collected from the low-to-medium enthalpy hydrothermal systems of Central Italy consisted of (i) cold gas bubbling pool (VC) at Poggio dell'Olivo and (ii) dry gas vents (CS1 and CS2) at Cava dei Selci. These gas emissions were characterized by low temperatures, i.e. 25-36 °C at Poggio dell'Olivo (Chiodini et al., 1995) and 24 °C at Cava dei Selci (Giggenbach, 1998).

7.4 Inorganic constituents

Before discussing the specific features of VOCs in deep-sourced gases discharged from the selected active volcanic-hydrothermal systems and low-to-medium enthalpy hydrothermal areas, it is useful to illustrate the general compositional characteristics of the inorganic fraction that may provide information about the prevailing physicochemical conditions at depth.

As summarized above, inorganic gas species in hydrothermal fluid emissions are the results of the overall settings of the deep hydrothermal system and mainly depend on the composition of the deep hydrothermal fluid, with possible (i) magmatic and/or crustal contributions, (ii) gas scrubbing processes, and/or (iii) secondary boiling of shallow aquifers. Accordingly, the relative abundances of the main inorganic constituents (CO₂, N₂, H₂S and CH₄) showed remarkable changes among the collected samples.

The CO₂-N₂-H₂S and the CO₂-N₂-CH₄ ternary diagrams are reported in Figure 7.5 and Figure 7.6. Among active volcanic-hydrothermal systems,

7. Distribution of VOCs from hydrothermal gas discharges

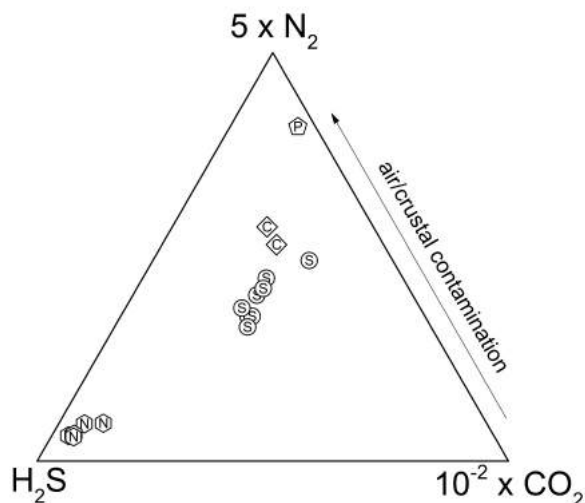


Figure 7.5: CO_2 - N_2 - H_2S ternary diagram for (a) hydrothermal gases from active volcanoes (S = Solfatara Crater; N = Nisyros Island) and (b) cold gas discharges from low-to-medium enthalpy systems (P = Poggio dell’Olivo; C = Cava dei Selci).

the steam-saturated fumaroles from Solfatara Crater were characterized by higher CO_2/CH_4 and CO_2/H_2S ratios than those measured in boiling fumaroles from Nisyros caldera. According to Chiodini et al. (2003, 2010a, 2012 and 2015), the CO_2/CH_4 ratios in gas discharges from Campi Flegrei progressively increased in the last 20 years, being associated to an accelerating process of ground deformation. This trend was interpreted as related to repeated injections of magmatic fluids into the hydrothermal system (Chiodini et al., 2012). Such process would result in both (i) changes in redox conditions, due to the input of the relatively oxidizing magmatic gases, and (ii) increase of temperature at depth because of the condensation of magmatic vapours within the hydrothermal aquifer. The latter effect would produce an increase in fumarolic CO and H_2 , whose fugacities are controlled by temperature and less affected by changes in redox conditions than CH_4 (Chiodini and Marini, 1998). Accordingly, in the H_2 -CO- CH_4 ternary diagram (Figure 7.7) the Solfatara fumaroles plot close to the field of high-temperature volcanic gases (Chiodini et al., 1993). Contrarily, boiling fumaroles from

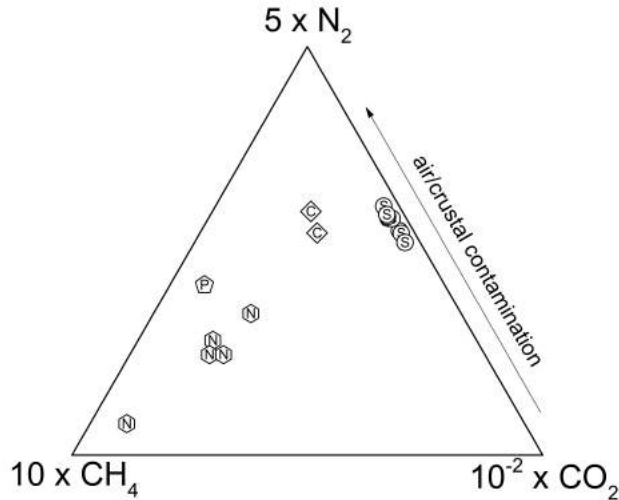


Figure 7.6: $\text{CO}_2\text{-N}_2\text{-CH}_4$ ternary diagram for the deep-sourced hydrothermal gases. Symbols as in Figure 7.5.

Nisyros Island fall in the field of typical hydrothermal gases (Figure 7.7). CO was not detected (although reported by previous authors; e.g. Chiodini and Marini, 1998; Fiebig et al., 2004), whereas CH_4 and H_2S showed relatively high concentrations (Figure 7.5 and Figure 7.6), as expected for fluids derived from reducing hydrothermal reservoirs. However, Brombach et al. (2003) recognized the occurrence of magmatic inputs, especially below the Stephanos and Micros Polybotes craters and to a smaller degree below the marginal fumarolic areas of Phlegethon and Megalos Polybotes craters.

Among the gas emissions from Central Italy, the cold dry gas vents from Cava dei Selci were largely dominated by CO_2 and H_2S . The relatively low CH_4 and H_2 concentrations (Figure 7.7) were likely due to a prolonged residence of the gases at shallow oxidizing and low-T ($<150\text{ }^\circ\text{C}$) conditions (Giggenbach et al., 1988). CO was detected at very low amounts.

Similarly, the chemical composition of the bubbling gas from Poggio dell'Olivo was similarly dominated by CO_2 , whereas H_2S was detected at low concentrations (Figure 7.5) and N_2 was the second most abundant inorganic constituent. Differently, CH_4 concentrations were higher with respect to those

7. Distribution of VOCs from hydrothermal gas discharges

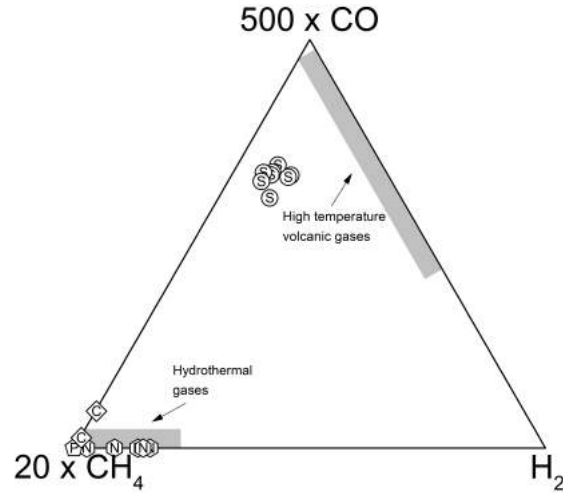


Figure 7.7: H_2 - CO - CH_4 ternary diagram for the deep-sourced hydrothermal gases. Symbols as in Figure 7.5. The grey fields indicate the typical composition of high-temperature volcanic gases and hydrothermal fluids, as reported by Chiodini et al. (1993).

of the dry gas samples from Cava dei Selci (Figure 7.6). The relatively high CH_4/CO_2 and low $\text{H}_2\text{S}/\text{CO}_2$ ratios were a likely consequence of gas-water interaction, as the solubility in water of these gas species vary, as follows: $\text{H}_2\text{S} > \text{CO}_2 > \text{CH}_4$. Accordingly, the N_2/Ar ratio (43) was close to that of ASW (38).

7.5 Volatile organic compounds

The Σ VOCs values in gases collected from hydrothermal systems associated with active volcanoes were comparable to those from low-to-medium enthalpy hydrothermal systems, ranging from 5,935 to 12,070 nmol/mol and from 4,882 to 14,524 nmol/mol, respectively (Table 7.1). Up to 95 different VOCs pertaining to 7 homologues series (alkanes, aromatics, cyclics, alkenes, S-bearing compounds, O-substituted species and halocarbons) were identified among the collected gas samples. The relative percentages (mean values) of the different groups of VOCs are shown in Figure 7.8 and reported in Table 7.1.

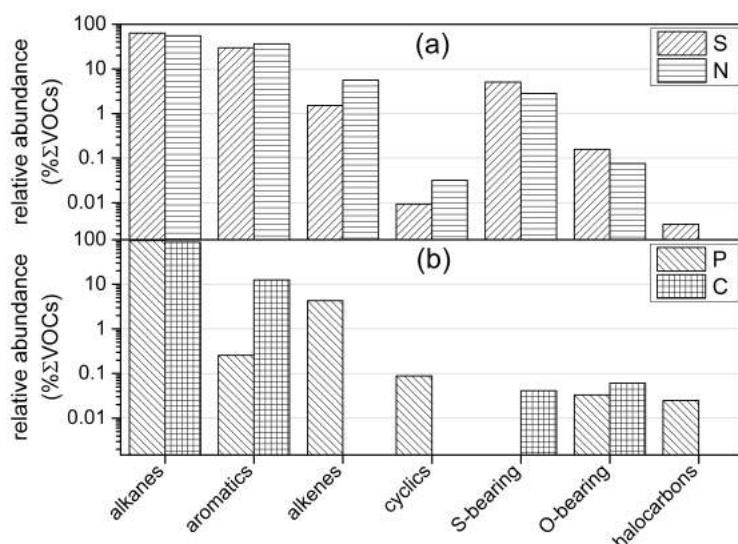


Figure 7.8: Relative abundances (expressed as % Σ VOCs; logarithmic scale) of the main organic groups in hydrothermal gases collected from (a) active volcanic systems (S = Solfatara Crater; N = Nisyros Island) and (b) low-to-medium enthalpy systems (P = Poggio dell'Olivo; C = Cava dei Selci) are shown.

The organic fraction of hydrothermal gases discharged from active volcanic areas was largely dominated by alkanes (mainly ethane and propane) and aromatics (mainly benzene), whose sum was >90 % of total VOCs, whereas alkanes alone represented almost the total organic fraction of cold gas emis-

7. Distribution of VOCs from hydrothermal gas discharges

	Solfatara Crater		Nisyros Island		Poggio dell'Olivo		Cava dei Selci	
	nmol/mol	% Σ VOCs	nmol/mol	% Σ VOCs	nmol/mol	% Σ VOCs	nmol/mol	% Σ VOCs
alkanes	3,749-7,643	61-67	3,166-6,427	39-64	13,850	95	4,261-4,659	87-88
aromatics	1,667-3,759	29-33	2,371-4,563	28-52	37	-	616-648	12-13
alkenes	94-196	0.91-1.9	292-622	4.8-6.2	616	4.2	-	-
cydics	0.66-0.9	0.006-0.012	1.6-3.1	0.016-0.051	13	0.088	-	-
S-bearing	310-561	3.9-6.7	179-305	2.0-3.7	-	-	1.7-2.5	0.03-0.05
O-bearing	10-16	0.10-0.27	5.3-7.2	0.06-0.09	4.8	0.03	2.9-3.2	0.060-0.061
halocarbons	≤ 0.48	≤ 0.006	-	-	3.6	0.025	-	-
Σ VOCs	5,935-12,070		6,058-10,078		14,524		4,882-5,313	

Table 7.1: The concentration range (min-max) of VOCs (in nmol/mol) and of the main homologues series (in nmol/mol and in % Σ VOCs) are reported for the gas samples collected from punctual vents in the four study areas.

7.5 Volatile organic compounds

sions from Poggio dell'Olivo and Cava dei Selci (95 and ≥ 87 % Σ VOCs, respectively; Table 7.1 and Figure 7.9).

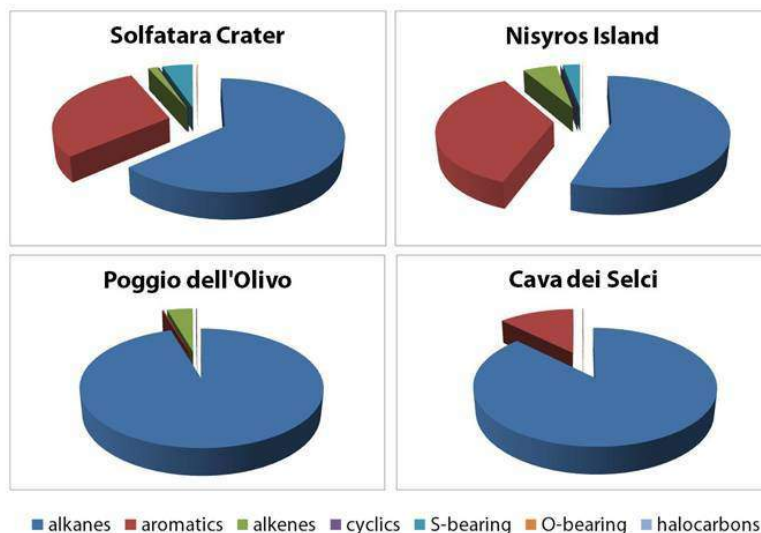


Figure 7.9: Pie charts of mean VOCs composition in hydrothermal gases from Solfatara Crater, Nisyros Island, Poggio dell'Olivo and Cava dei Selci.

Among alkanes, C_2 to C_8 linear and branched chain compounds were detected in the analyzed samples, the former showing higher concentrations than the corresponding isomers (the normal- to iso-ratios ranged from 0.7 to 2.4 for C_{4-8} alkanes in gases from both active volcanoes and low-to-medium enthalpy systems). The relatively high concentrations of the linear chain saturated hydrocarbons, commonly found in gases from hydrothermal systems (e.g. Tassi, 2004; Capecchiacci, 2012), are likely the result of the high thermal stability of these compounds. Ethane was the most abundant alkane, after CH_4 , in all the analyzed gas samples (Figure 7.10), spanning from 40 to 54 % Σ alkanes in fumaroles from Solfatara Crater and from 71 to 81 % Σ alkanes in gas emissions from Nisyros Island, Poggio dell'Olivo and Cava dei Selci (Figure 7.11). As previously seen in Chapter 2, this compound is the most stable hydrocarbon after CH_4 at temperatures up to around 580 °C (Figure 2.4), whereas the stability of C_{3+} alkanes generally decreases at increasing number of carbon atoms in the chain. Accordingly, the concentrations of linear saturated hydrocarbons generally decreased at increasing

7. Distribution of VOCs from hydrothermal gas discharges

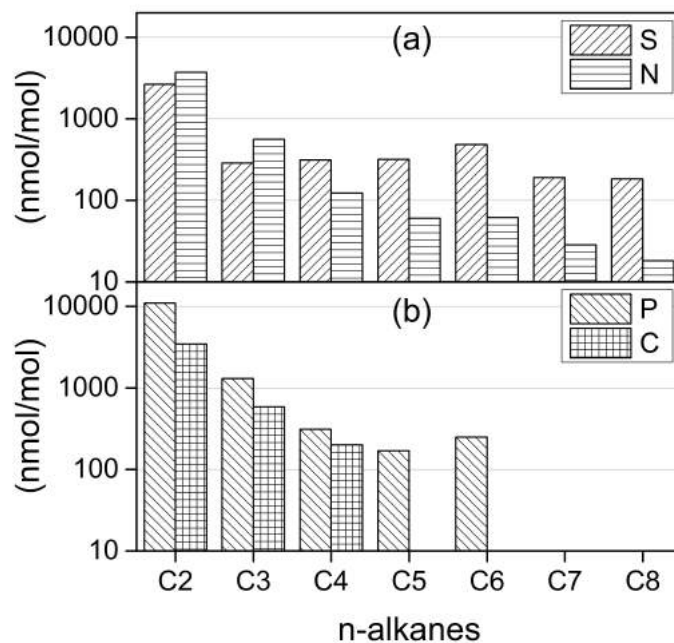


Figure 7.10: Average concentrations (in nmol/mol) of C₂₋₈ normal-alkanes in (a) hydrothermal gases from active volcanoes (S = Solfatarata Crater; N = Nisyros Island) and (b) cold gas discharges from low-to-medium enthalpy systems (P = Poggio dell'Olivo; C = Cava dei Selci).

chain length in the homologues series in both hydrothermal gases from active volcanoes (Figure 7.10a) and cold gas discharges from low-to-medium enthalpy systems (Figure 7.10b). A similar pattern was also recognized in natural gases from both sedimentary basin gas fields and hydrothermal systems, and interpreted as related to thermal degradation (pyrolysis) of organic matter (Darling, 1998). However, by comparing the composition of fumarolic gas discharges and geothermal fluids from deep production wells from three different geothermal fields in El Salvador, Tassi et al. (2007) observed a significant depletion in organic gases due to scrubbing processes at relatively shallow depths. In particular, the observed progressive decrease in relative abundances of normal-alkanes at increasing chain length was ascribed to the diverse mobility of these compounds during their uprising towards the surface, which in turn depends on the molecular volume of each gas species (Tassi

7.5 Volatile organic compounds

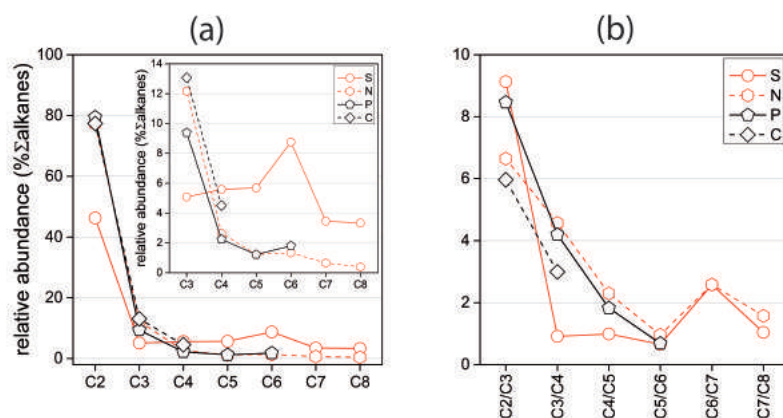


Figure 7.11: **(a)** Average relative abundances (in % Σ alkanes) of C_{2-8} normal-alkanes and **(b)** C_2/C_3 , C_3/C_4 , C_4/C_5 , C_5/C_6 , C_6/C_7 and C_7/C_8 mean ratios among normal-alkanes in gas emissions from active volcanoes (red), i.e. Solfatara Crater (S; circles and straight line) and Nisyros Island (N; hexagons and dashed line) and low-to-medium enthalpy systems (black), i.e. Poggio dell’Olivo (P; pentagons and straight line) and Cava dei Selci (C; diamonds and dashed lines).

et al., 2007 and references therein). Processes occurring at shallow depths, such as gas-aquifers interaction and condensation processes, are expected to be strongly affected by local geological features (e.g. rocks permeability, hydrogeological setting). However, gas samples from both Nisyros Island and Central Italy were characterized by similar distribution of C_{2-8} normal-alkanes in terms of *(i)* relative abundances with respect to total alkanes (Figure 7.11a), and *(ii)* C_i/C_{i+1} ratios, where i is the number of carbon atoms in the alkane chain (Figure 7.11b). Hence, it seems more likely that processes occurring at depth within the hydrothermal system (thermal degradation), rather than during fluids uprising (gas scrubbing and condensation), regulate the relative abundances of n-alkanes distribution. A thermogenic origin from decomposition of organic matter for n-alkanes in fumarolic emissions from Nisyros Island was postulated by Fiebig et al. (2015) on the basis of *(i)* the carbon isotope distribution pattern of light hydrocarbons, *(ii)* the $CH_4/(C_2H_6+C_3H_8)$ ratios and *(iii)* the $\delta^{13}C-CH_4$ values. The hydrothermal gases from Nisyros Island and Central Italy showed C_i/C_{i+1} ratios generally

7. Distribution of VOCs from hydrothermal gas discharges

higher than 1, except for the C_5/C_6 ratio (Figure 7.11b). Normal-hexane was present at higher concentrations than normal-pentane also in gases from Solfatara Crater (Figure 7.11b), where it was the second most abundant alkane after ethane (Figure 7.11a). Relatively higher contents of C_6 , when compared to those of other n-alkanes, were also recognized by Darling (1998) and Tassi (2004) in volcanic and hydrothermal fluids from several systems and ascribed to the stability of the hexane structure (Tassi, 2004). Fumarolic gases from Solfatara Crater displayed a different pattern in the relative abundances of alkanes with respect to samples collected at Nisyros, Poggio dell'Olivo and Cava dei Selci (Figure 7.11a). In particular, C_{5+} compounds accounted for a larger fraction of alkanes, whereas the relative abundances of ethane and propane were lower than those measured in gases from the other study areas (Figure 7.11a).

As evidenced on the basis of the inorganic constituents (Section 7.4), the fumarolic discharges at Solfatara Crater were related to higher temperatures and more oxidizing conditions at depth relative to the other investigated systems. At these conditions, the production of unsaturated compounds from alkanes through a well-known reversible reaction is favoured (Seewald, 1994; Capaccioni et al., 1995, 2004; Taran and Giggenbach, 2003, 2004; Tassi et al., 2012c). Accordingly, alkenes were found to generally dominate the organic fraction in magmatic gases, representing about 40 % Σ VOCs (Capecchiacci, 2012), whereas they are present at significantly lower concentrations (around 7 % Σ VOCs) in hydrothermal gases (Capecchiacci, 2012) and almost absent (except for iso-butene; Tassi, 2004) in cold gas emissions. Among the analyzed samples, alkenes represented ≤ 1.9 % Σ VOCs in fumarolic gases from Solfatara Crater, whereas they were up to 6.2 and 4.2 % Σ VOCs in gas samples from Nisyros Island and Poggio dell'Olivo, respectively. No alkenes were detected at Cava dei Selci. However, different unsaturated hydrocarbons were detected in the analyzed systems. Normal-butene and propene dominated the alkenes homologous series in gas discharges from Solfatara Crater, whereas iso-butene was almost the only alkene detected in gas samples from Nisyros Island (with low contents of propene) and Poggio dell'Olivo. While the presence of iso-butene in hydrothermal gases originated at variable temperature

7.5 Volatile organic compounds

conditions was suggested to be related to the involvement of this compound as a by-product of several organic reaction pathways (Tassi, 2004), the concentrations of alkenes are generally expected to be particularly sensitive to the temperature of the hydrothermal system, as the thermal instability of the unsaturated hydrocarbons increases at decreasing temperature (Figure 2.4). Accordingly, propane/propene ratios in the steam-saturated fumaroles from Solfatara Crater were ranging from 13 to 19, i.e. significantly lower than those measured in the boiling fumaroles from Nisyros Island (from 199 to 317). Therefore, the existence of a thermodynamic drive toward the dehydrogenation to alkene, enhanced by the high temperatures and relatively oxidizing conditions in the deep reservoir, could contribute to the relatively low abundance of C₂₋₄ alkanes observed in the Solfatara Crater gas samples. While short chain alkanes undergo reequilibration with the corresponding alkenes as a function of temperature, longer alkanes may alternatively undergo dehydrocyclization reactions under hydrothermal conditions, forming cyclics and, successively, aromatics (see Chapter 3). For instance, as seen in Chapter 3, cyclohexane was quite readily produced after the reaction of both hexane and dodecane in water at 300 °C and 85 bar. Although hexane was not detected, it is a likely intermediate product of the conversion of dodecane to cyclohexane. Accordingly, the relative enrichment in normal-hexane observed in the analyzed samples (Figure 7.11) could be indicative of the ongoing dehydrocyclization and aromatization of medium-long chain alkanes. Moreover, cyclic compounds, though present at relatively low concentrations (Table 7.1), were mostly consisting of C₅ and C₆ compounds. While methyl-cyclopentanes can easily be formed through isomerization of cyclic C₆ hydrocarbons, the latter readily undergo dehydrogenation under hydrothermal conditions, yielding aromatics (see Chapter 3).

Aromatics were up to 52 % Σ VOCs in the fumarolic gas discharges from Solfatara Crater and Nisyros Island and \leq 37 % in the cold gas emissions from Poggio dell’Olivo and Cava dei Selci (Table 7.1; Figure 7.8). Benzene was the main aromatic compound and the second most abundant VOC after ethane at both Solfatara Crater and Nisyros Island. The benzene/ethane ratios were close to 1 or even higher (up to 1.7), in agreement with the val-

7. Distribution of VOCs from hydrothermal gas discharges

ues observed by Capaccioni et al. (1995, 2004) in hydrothermal gases from active volcanoes, whereas lower ratios (from 0.003 to 0.19) were measured in cold gas emissions from Central Italy. In general, aromatics to alkanes ratios increased moving from cold gas emissions to hydrothermal fluids from active volcanoes, together with H_2 concentrations (Figure 7.12), as a consequence of (i) increasing stability of the aromatic ring at increasing temperatures (Figure 2.4), and (ii) increasing availability of catalytic agents (e.g. acid species, sulphur gases, Al-silicates, iron oxides and sulphide minerals) enhancing “reforming” processes (Capaccioni et al., 1993, 1995; Tassi et al., 2010) and dehydrogenation reactions. The normal-hexane, cyclohexane and

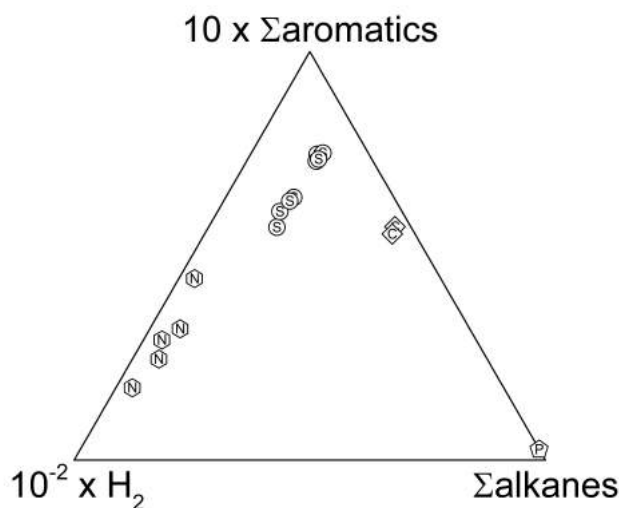


Figure 7.12: $\Sigma \text{alkanes}$, $\Sigma \text{aromatics}$ and H_2 ternary diagram. Symbols as in Figure 7.5.

benzene ternary diagram is shown in Figure 7.13. While fumarolic gases from Solfatara Crater were largely dominated by benzene and normal-hexane, the benzene/cyclohexane ratios gradually decreased moving from high-T systems (Solfatara) to medium (Nisyros) and low-T systems (Poggio dell’Olivo). This trend is in agreement with the strong dependence of the equilibrium constant of the dehydrogenation reaction of cyclohexane to benzene (see Chapter 3; Figure 3.1). On the other hand, the faster kinetics of organic reactions at

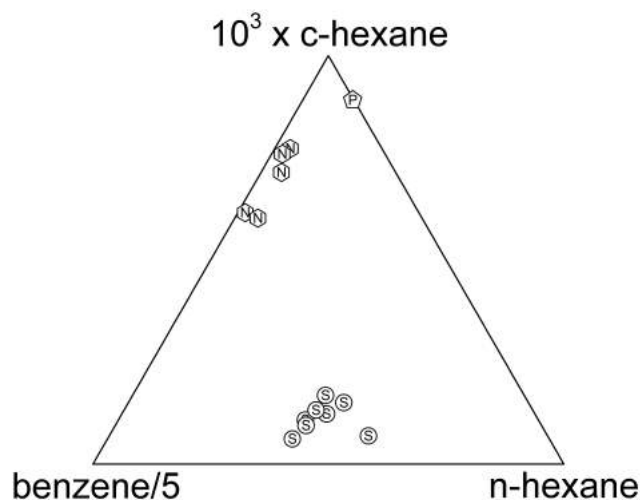


Figure 7.13: Normal-hexane, cyclohexane and benzene ternary diagram. Symbols as in Figure 7.5.

increased temperatures could be at the origin of the low concentrations of cyclics in the hydrothermal gases from Solfatara Crater. Thus, in a system rich in alkanes and characterized by high temperatures, cyclohexane, once formed, is quickly converted into benzene.

Among aromatics, methylated compounds were detected at markedly lower concentrations than benzene, the benzene/ $(\Sigma$ branched aromatics) ratio ranging from 3.7 to 64 in hydrothermal gases from active volcanoes and from 5 to 100 in gases from low-to-medium enthalpy systems. The most abundant branched aromatic was toluene. McCollom et al. (2001) experimentally observed that this compound readily degraded to benzene at high temperatures (300-330 °C). The thermal decomposition of toluene (and other alkylated aromatics) in water under hydrothermal conditions was found to proceed by either demethylation to benzene (7.1), as follows:



7. Distribution of VOCs from hydrothermal gas discharges

or oxidative decarboxylation pathway (7.2), as follows:



The process may generate not only benzene, but also PAHs such as naphthalene, as supported by the occurrence in the fumarolic gases from both Solfatara Crater and Nisyros Island. According to McCollom et al. (2001), toluene decarboxylation occurs in oxidizing environments containing high concentrations of dissolved sulphur compounds yielding benzaldehyde and phenol as intermediate products (Figure 7.14). Accordingly, the latter O-

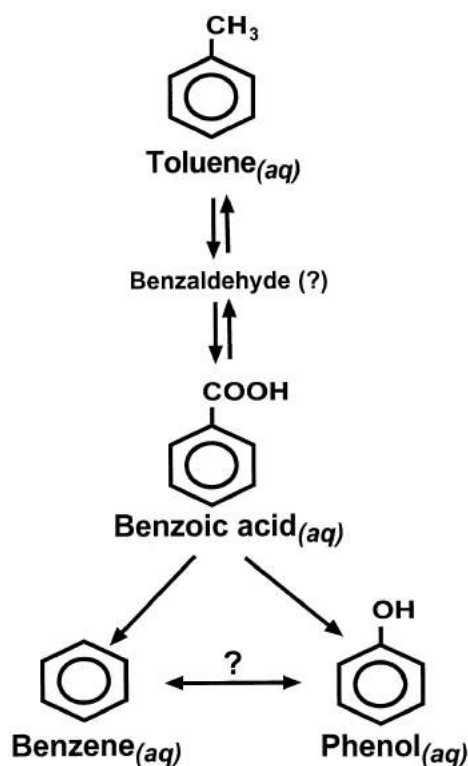


Figure 7.14: Reaction scheme for the conversion of toluene to benzoic acid, benzene and phenol (after McCollom et al., 2001).

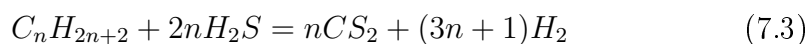
substituted aromatic compounds were detected in the fumarolic gases from Solfatara Crater.

Besides hydrocarbons, heteroatomic organic compounds were generally ≤ 6.7

7.5 Volatile organic compounds

and ≤ 4.2 % Σ VOCs in gases from active volcanoes and low-to-medium enthalpy systems, respectively (Table 7.1; Figure 7.8). The heteroatomic compounds detected in the analyzed samples included S-bearing species, O-substituted compounds and halocarbons.

S-bearing compounds were mainly found in hydrothermal gas samples from active volcanic areas, with relative abundances ranging from 2.0 to 6.7 % Σ VOCs, whereas, among cold gas emissions, they were measured at Cava dei Selci, although at low concentrations (≤ 0.05 % Σ VOCs). The main abundant S-bearing species in gases from active volcanic systems was carbon disulphide, followed by thiophenes and DMS. These compounds are typical of hydrothermal environments, where their formation is enhanced by reducing conditions and high sulphur fugacity (Tassi et al., 2010 and references therein). Tassi et al. (2010) suggested that the production of thiophenes in a natural environment might proceed through the addition of H_2S to dienes in the presence of H^+ and metal catalysts (Paal-Knorr synthesis). Results from experimental runs carried out on hexane and dodecane at 300 °C in water (see Chapter 3) revealed that thiophenes can quite readily be produced from normal-alkanes in the presence of sphalerite. Analogously, thiols were observed among the products of experiments on cyclic C_6 hydrocarbons at 300 °C in the presence of sulphide minerals (sphalerite and pyrite; Chapter 3). Moreover, Heinen and Lauwers (1996) found that both thiols and carbon disulphide were produced during experiments involving iron sulphide (FeS), H_2S and CO_2 in water under anaerobic conditions even at relatively low temperatures (≤ 90 °C). In natural hydrothermal environments, characterized by reducing conditions, $T < 400$ °C and relatively high H_2S concentrations, the production of carbon disulphide may take place from the combination of alkanes and H_2S (7.3) (e.g. Petherbridge et al., 2002; Schwandner et al., 2013), as follows:



O-bearing compounds were present at low amounts in both hydrothermal gases from active volcanoes and those from low-to-medium enthalpy hydrothermal systems (≤ 0.27 % Σ VOCs and ≤ 0.03 % Σ VOCs, respectively;

7. Distribution of VOCs from hydrothermal gas discharges

Table 7.1). The production of these compounds likely occurred (*i*) at shallow depths in the presence of oxidizing conditions and available oxygen or (*ii*) by mixing with air at fumarolic emission vents (Schwandner et al., 2013). However, oxygenation of organic compounds also occurs under hydrothermal conditions. As proved experimentally by e.g. Seewald (2001, 2003) and Shipp et al. (2013), and confirmed by the results of the experiments carried out in the framework of the current PhD project (Chapter 3), alcohols production can proceed via addition reaction on alkenes and by subsequently oxidizing alcohols to aldehydes or ketones. Similarly, oxygenation to O-bearing cyclic compounds may also occur through ring closure of oxygenated alkenes on the site of the double bond (Schwandner et al., 2013). A similar process was also suggested by Tassi et al. (2010) for furans production through catalytic hydrogenation of oxygenated alkenes (Paal-Knorr synthesis). Furans are typically associated with magmatic gases (Capecchiacci, 2012), suggesting that these compounds are thermodynamically favoured by high temperatures and oxidizing conditions at depth (Tassi et al., 2010). Accordingly, among the collected samples, furans were almost exclusively detected in fluids from medium-to-high temperature volcanic emissions (Figure 7.15), ranging from 23 to 46 % Σ O-bearing species and from 19 to 86 % Σ O-bearing species in gases from Solfatara Crater and Nisyros Island, respectively. At Solfatara Crater, the sum of furans and alcohols (mainly phenol) represented from 53 to 70 % Σ O-bearing species, while aldehydes, esters, ketones, ethers and glycol ethers were up to 18, 17, 9, 8 and 1 % Σ O-bearing species. Alcohols are easily produced through hydration of alkenes, a reaction step included in the general reaction scheme proposed by Seewald (2001, 2003) for organic functional group interconversions (Figure 2.6). The hydration reaction is thermodynamically enhanced at decreasing temperatures (Shock et al., 2013), supporting the hypothesis that alcohols (as well as the other O-substituted species, except for furans) are mainly produced at shallow depths during the fluids uprising (Schwandner et al., 2013). Under hydrothermal conditions, the reactivity of alcohols was experimentally observed to be even higher than that of alkenes (Shipp et al., 2013). Hence, unless a rapid uprising of volcanic/hydrothermal fluids is able to quench their

7.5 Volatile organic compounds

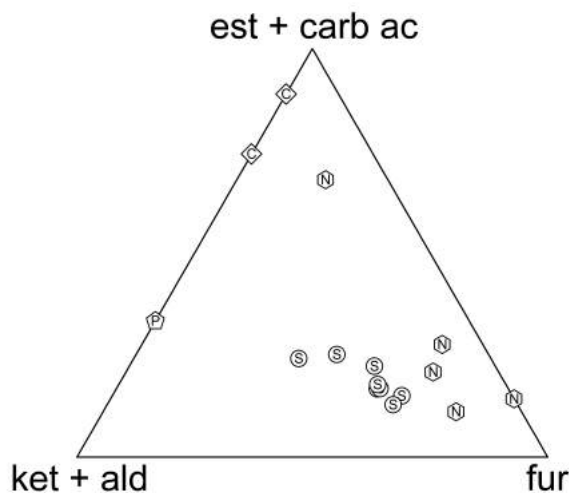


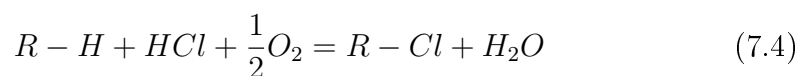
Figure 7.15: Furans (fur), esters plus carboxylic acids (est + carb ac) and ketones plus aldehydes (ket + ald) ternary diagram. Symbols as in Figure 7.5.

concentrations characterizing the deep reservoirs up to the emission at the surface, alcohols are expected to undergo secondary processes, such as dehydrogenation to aldehydes and ketones, or reactions with carboxylic acids forming esters. Accordingly, alcohols were detected at very low concentrations in gas samples from both Solfatara Crater and Poggio dell'Olivo. At Nisyros Island, alcohols were not detected, whereas esters (from 11 to 68 % Σ O-bearing species) were the second most abundant compounds after furans, followed by ketones and aldehydes (up to 13 and 10 % Σ O-bearing species). Among cold gas emissions, alcohols (63 % Σ O-bearing species) and esters and carboxylic acids (from 65 to 82 % Σ O-bearing species) dominated the composition of O-bearing VOCs at Poggio dell'Olivo and Cava dei Selci, whereas aldehydes and ketones were detected at lower amounts.

Halocarbons were only detected in hydrothermal fluids discharged from Solfatara Crater and Poggio dell'Olivo, with abundances ≤ 0.48 and of 0.025 % Σ VOCs, respectively, being exclusively represented by Cl-substituted compounds. Stoiber et al. (1971) first identified halocarbons in volcanic gases, interpreting them as related to air contamination. An atmospheric origin

7. Distribution of VOCs from hydrothermal gas discharges

for CFCs in volcanic fluids was confirmed by other authors (e.g. Frische et al., 2006; Tassi et al., 2012c). A volcanogenic origin of organohalogens was instead proposed by Jordan et al. (2000). By analyzing fumarolic gas emissions from Vulcano Island and Mt. Etna (Italy), Tassi et al. (2012c) confirmed that most hydrogenated halocarbons and CCl_4 have a geogenic origin. Different reactions have been proposed for halocarbons production in volcanic gases, such as hydrous thermal halogenation (7.4), as follows:



or gas-phase reaction (7.5) consisting in free radical substitution of elemental chlorine for hydrogen in methane (Schwandner et al., 2013 and references therein), as follows:



While the bubbling gas from Poggio dell'Olivo was characterized by C_3 and C_6 chloroalkanes, fumarolic gases from Solfatara Crater showed the presence of unsaturated C_2 chlorohydrocarbons (vinylchloride, dichloroethene and trichloroethene) and chlorobenzene, compounds that were previously recognized in volcanic gases (e.g. Jordan et al., 2000; Tassi et al., 2009; Schwandner et al., 2013). According to Jordan et al. (2000), the production of vinylchloride, dichloroethene and trichloroethene likely occurs via subsequent halogenation reactions of ethene.

Chapter 8

Distribution of VOCs in interstitial soil gases: evidences of secondary processes

8.1 Introduction

While the uprising of gases through fumarolic conduits was assumed to be fast enough to keep the compositional features of VOCs almost unaltered with respect to those released from the deep hydrothermal reservoirs, allowing to gain information on primary processes occurring at depth from fumarolic gas composition (as discussed in the previous chapter), an analogous assumption cannot be considered valid when gases diffusively released from the soil are taken into account. Since the gas flow rate of diffused degassing is orders of magnitude lower than that of fumarolic vents, the slowly uprising fluids permeating the soil likely undergo compositional rearrangements in response to abruptly changing physicochemical conditions. Thermogenic processes are expected to be replaced by microbial activity theoretically capable of deeply modify the composition of the gas organic fraction, although their influence on hydrothermal-derived VOCs in areas of intense diffused degassing is still almost unexplored.

In this chapter, the compositional features of the analyzed interstitial soil

8. Distribution of VOCs in interstitial soil gases

gases are discussed for each study area. The VOCs composition in soil gases from sites affected by different hydrothermal contributions are compared with that in hydrothermal fluids discharged from punctual high flow rate gas vents with the aim of understanding the role of shallow secondary processes on controlling the diffused emissions of VOCs from volcanic and hydrothermal areas.

8.2 Solfatara Crater

At Solfatara Crater hydrothermal fluids are largely released through not only fumarolic discharges, but also via intense diffuse degassing (Tedesco and Scarsi, 1999; Chiodini et al., 2001, 2005; Caliro et al., 2007; Granieri et al., 2003, 2010; Tassi et al., 2013b). Accordingly, high soil CO₂ fluxes were measured throughout the crater floor, with values up to >25,000 g m⁻² day⁻¹. Both (i) the strict positive correlation between soil CO₂ and CH₄ fluxes and (ii) the increasing concentrations of hydrothermal-related gas species (CO₂, CH₄, H₂S and H₂) and decreasing contents of atmospheric compounds (N₂, O₂ and Ar) at increasing ΦCO₂ values, highlighted the contribution from ascending fluids released from the deep hydrothermal reservoir. Similarly, the emission of VOCs is not expected to be restricted to the fumarolic vents. Accordingly, soil C₆H₆ fluxes were positively correlated with ΦCO₂ values, benzene representing one of the most abundant organic compounds in fumarolic gases. Similarly, the total amount of VOCs showed an increasing trend at increasing ΦCO₂ and CO₂/N₂ ratio values (Figure 8.1), suggesting that (i) most organic compounds are derived from the uprising deep-originated gases, and (ii) the composition of soil gases could be explained in terms of mixing of deep-sourced hydrothermal fluids with air.

As a first approximation, the origin of organic compounds (hydrothermal vs. shallow environment) can be assessed on the basis of the correlation with the CO₂/N₂ ratio values and the comparison with fumarolic gases. The various VOC families identified in the soil gas samples showed different trends. Alkanes, alkenes, aromatics and S-substituted compounds showed increasing trends at increasing CO₂/N₂ ratios (Figure 8.2), pointing to a deep origin of these species, mainly associated with the uprising hydrothermal fluids. Accordingly, alkanes, alkenes, aromatics and S-substituted compounds dominated the chemical composition of the organic fraction in fumarolic gases (Figure 6.1). Differently, the concentrations of O-substituted compounds and halocarbons in soil gases decreased at increasing CO₂/N₂ ratios (Figure 8.3), suggesting they have a shallow origin. Cyclics showed a peculiar trend. Although the contents of these compounds increased at increasing

8. Distribution of VOCs in interstitial soil gases

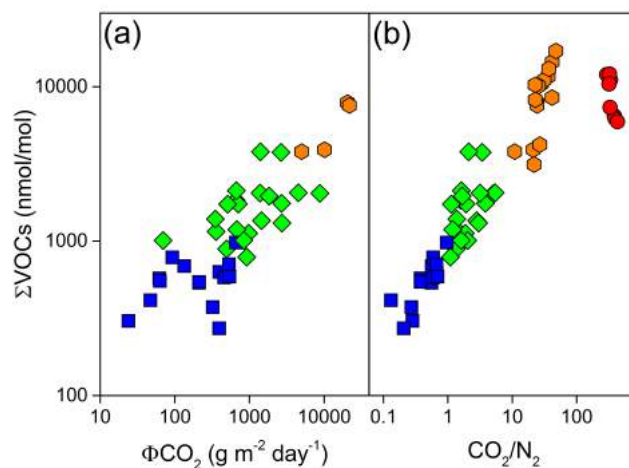


Figure 8.1: Total concentrations of VOCs (in nmol/mol) vs. **(a)** ΦCO_2 values (in $\text{g m}^{-2} \text{day}^{-1}$) and **(b)** CO_2/N_2 ratios for fumarolic gases (red circles) and soil gases of type A (orange hexagons), B (green diamonds) and C (blue squares) from Solfatara Crater.

CO_2/N_2 ratios (Figure 8.3), suggesting a deep origin, the concentrations of cyclics in soil gases were remarkably higher than those measured in the fumarolic gas samples pointing to the occurrence of chemical reactions enhancing cyclic production at depth during hydrothermal fluid uprising and/or within the shallow environment. Chemical reactions occurring during the relatively slow uprising of the hydrothermal fluid through the crater soil (i.e. at decreasing temperature and rapidly changing redox conditions), including abiotic and biogenic secondary processes at both depth and shallow levels, are expected to contribute to the distribution of VOCs in interstitial soil gases. Accordingly, different behaviours of organic species were observed among the homologues series. Among alkanes, the positive correlation with CO_2/N_2 ratios was particularly evident for ethane, propane, normal-butane and, to a lower extent, normal-pentane and normal-hexane, whereas normal- C_{7-8} and iso-alkanes showed a more scattered trend. BTEX and styrene clearly increased at increasing CO_2/N_2 ratios, whereas more complex alkylated aromatics showed no clear trend. Contrarily, the correlation with the CO_2/N_2 ratios was evident for all the alkenes. Among S-

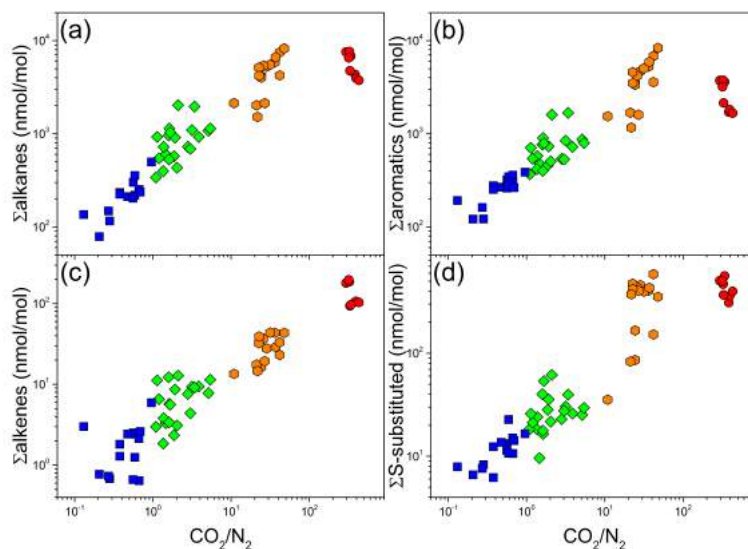


Figure 8.2: Total concentrations of (a) alkanes, (b) aromatics, (c) alkenes, and (d) S-substituted compounds (in nmol/mol) vs. CO_2/N_2 ratios for fumarolic gases and soil gases from Solfatara Crater. Symbols as in Figure 8.1.

bearing compounds, benzothiazole showed no correlation with the CO_2/N_2 ratios, whereas the DMSO and DMSO_2 concentrations decreased at increasing CO_2/N_2 ratios. Cyclohexane was the only cyclic compound showing a clear correlation with the CO_2/N_2 ratios. Among halocarbons, CFCs, chlorobenzene and chloromethane showed increasing concentrations at decreasing CO_2/N_2 ratios, whereas chloroethenes and carbon tetrachloride displayed no trend. Although the different O-bearing functional groups had no clear distribution relative to the CO_2/N_2 ratios, soil gases of type A were enriched in alcohols and furans, which were the most abundant O-bearing species in BG and BN fumaroles, and depleted in ketones and alcohols relative to soil gases of types B and C.

The occurrence of secondary processes affecting VOCs can be highlighted on the basis of changes in the ratios of selected organic compounds or homologous series (*i*) between soil gases and fumaroles, and (*ii*) among soil gases collected from sites with different ΦCO_2 values, i.e. corresponding to differ-

8. Distribution of VOCs in interstitial soil gases

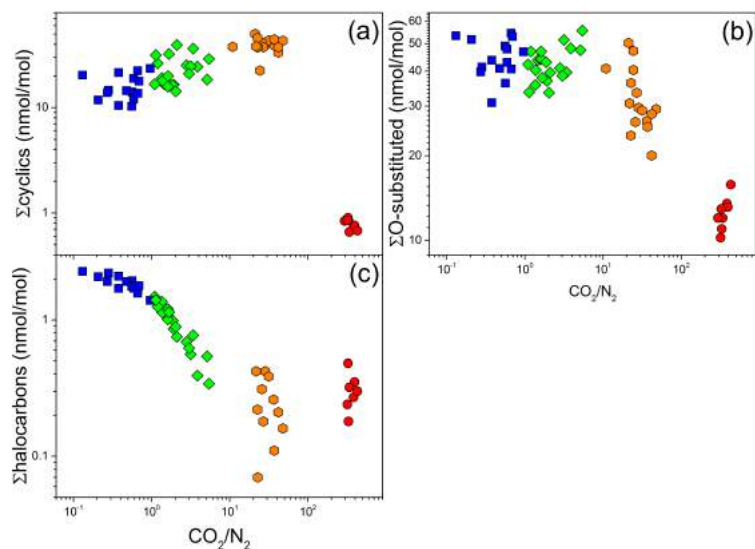


Figure 8.3: Total concentrations of (a) cyclics, (b) O-bearing species, and (c) halocarbons (in nmol/mol) vs. CO_2/N_2 ratios for fumarolic gases and soil gases from Solfatara Crater. Symbols as in Figure 8.1.

ent fluid uprising velocities.

Significant differences among fumaroles and soil gases were observed in the ratios between the two dominant organic families, i.e. alkanes and aromatics (Figure 8.4). Soil gases were characterized by a strong enrichment in aromatics with respect to fumarolic gases, the alkanes/aromatics ratios decreasing at decreasing CO_2/N_2 values. The lowest alkanes/aromatics ratios were thus measured in the type C soil gases, for which a stronger influence of secondary processes was expected. The trend in Figure 8.4 could be caused by either (i) degradation of alkanes or (ii) production of aromatics.

It is worth noting that soil gases of type A were characterized by (i) alkanes concentrations comparable to, and (ii) aromatics contents higher than, those found in fumarolic gases (Figure 8.2). Similarly, enrichments of aromatics in soil gases relative to fumarolic discharges were observed in fluids from Vulcano Island by Schwandner et al. (2004) when soil gas samples collected from crater flanks characterized by diffuse degassing were compared with the

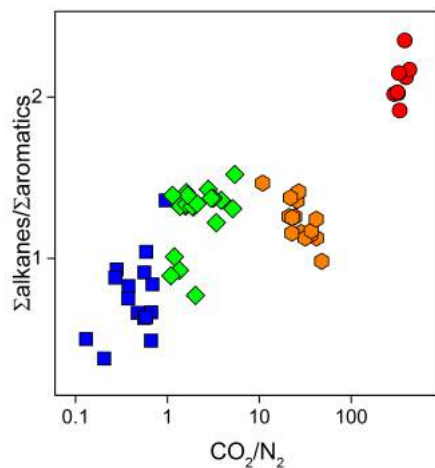


Figure 8.4: Alkanes/aromatics ratios vs. CO_2/N_2 ratios for fumarolic gases and soil gases from Solfatara Crater. Symbols as in Figure 8.1.

La Fossa crater fumaroles. This suggests that aromatic production may be enhanced during fluids uprising through diffuse degassing with respect to the faster rise along fumarolic conduits, although contribution from sorption of aromatics in the soil cannot be excluded. As reported in Chapter 3, the production of aromatics from saturated hydrocarbons through a stepwise dehydrogenation process is favoured at oxidizing conditions and in the presence of catalytic agents. Both (*i*) the increasingly oxidizing conditions encountered by hydrothermal fluids diffusively moving toward the surface and (*ii*) the interaction with minerals favoured by the relatively slow rise of deep gases, may enhance the production of cyclohexane and benzene from normal-hexane via dehydrogenation (Figure 3.2). Accordingly, the benzene/normal-hexane ratios, which may provide hints on how the overall dehydrocyclization process proceeds, showed higher values in soil gases of type A with respect to the fumarolic gas samples (Figure 8.5). Moreover, while the correlation of cyclohexane with the CO_2/N_2 ratios confirmed an origin related to the deep hydrothermal fluids for this substance, the significant enrichment in the cyclic compound observed in soil gases (Figure 8.5) pointed to an enhanced dehydrogenation in soil gases relative to fumarolic discharges. Nevertheless,

8. Distribution of VOCs in interstitial soil gases

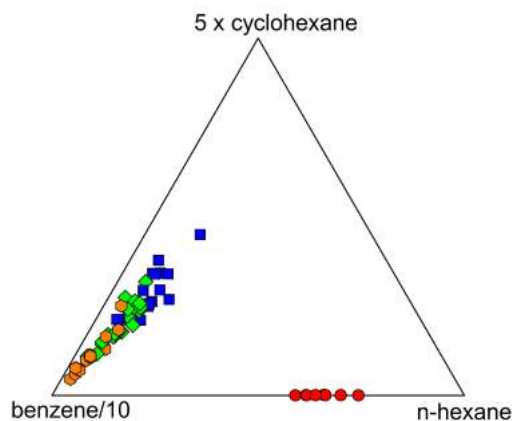


Figure 8.5: Normal-hexane, cyclohexane and benzene ternary diagram for fumarolic gases and soil gases from Solfatara Crater. Symbols as in Figure 8.1.

the decreasing benzene/cyclohexane ratios measured at decreasing CO_2/N_2 values (Figure 8.5) may be related to (i) dearomatization of benzene to cyclohexane, consistent with the thermodynamic drive toward hydrogenation at decreasing temperatures (Figure 3.2), or (ii) incomplete conversion of cyclohexane to benzene. The latter hypothesis was invoked by Tassi et al. (2012a) who ascribed the enrichment in cyclic compounds observed in gases discharged from mud volcanoes in Central and Southern Italy and fed by reservoirs in the 100-120 °C temperature range to incomplete aromatization of alkanes. On the other hand, dearomatization of benzene to cyclohexane seems to be unlikely considering the high stability of the aromatic ring. Once formed, the aromatic ring is extremely stable and persists in many geologic environments, even at high temperatures (McCollom et al., 2001). Hence, benzene is considered rather recalcitrant to both biotic and abiotic decomposition processes. However, the presence of substituent groups, particularly methyl groups, on the aromatic ring may significantly increase the reactivity of the aromatic compound (McCollom et al., 2001). Accordingly, as the CO_2/N_2 ratios decreased, the benzene/ Σ (alkylated aromatics) ratios sharply increased among soil gases (Figure 8.6), suggesting that alkylated aromatic compounds readily undergo degradation processes at shallow depths. Ac-

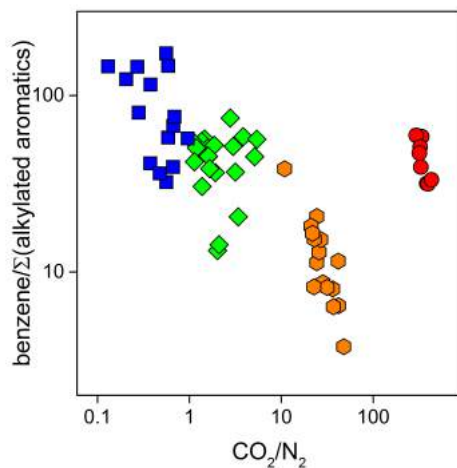


Figure 8.6: Benzene/alkylated aromatics ratios vs. CO_2/N_2 ratios for fumarolic gases and soil gases from Solfatara Crater. Symbols as in Figure 8.1.

cordingly, the benzene/branched aromatics ratios showed increasing trends at decreasing depths in soil gases from the 1-4 vertical profiles, indicating that degradation processes on branched aromatics were efficient at 10-30 cm depth, being likely associated with microbial activity. Accordingly, toluene is promptly degraded at both aerobic and anaerobic conditions by microbial communities (e.g. Spormann and Widdel, 2000; Fritsche and Hofrichter, 2008; Fuchs et al., 2011).

On the other hand, the trend observed in Figure 8.4 may be related not only to aromatic production but also to alkanes degradation. While the concentrations of ethane and propane in soil gases of type A were comparable to those measured in fumarolic gases, the contents of C_{4+} alkanes were markedly lower. In particular, a significant depletion in C_7 and C_8 alkanes was observed in soil gases with respect to fumarolic samples. Condensation processes and gas-water interactions at shallow depth could be responsible for the observed trend (Tassi et al., 2007 and references therein). Moreover, alkanes may undergo both biogenic and abiotic degradation, participating to a series of reactions involving functional group interconversions. The scattered trend of iso-alkanes with respect to the CO_2/N_2 values and the normal-/iso-alkanes

8. Distribution of VOCs in interstitial soil gases

ratios displaying comparable values in soil and fumarolic gases indicated the apparently random occurrence of isomerization processes, which did not seem to be controlled by the physicochemical conditions. On the contrary, functional group interconversions consisting of hydrogenation/dehydrogenation, hydration/dehydration and other substitution or addition reactions are expected to be affected by environmental parameters, such as redox and temperature.

The occurrence of abiotic functional groups interconversions during fluids uprising can be investigated comparing the distribution of minor VOCs families in soil gases of type A with respect to fumarolic gases.

Following the scheme proposed by Seewald (2001, 2003; Figure 2.6), the alkane/alkene pairs are expected to interconvert through hydrogenation/dehydrogenation reactions under hydrothermal conditions. The alkenes/alkanes ratios in soil gases of type A were significantly lower than those measured in fumarolic gas samples. As discussed in Chapter 2, at fixed redox conditions, hydrogenation of alkenes to alkanes is thermodynamically favoured at decreasing temperatures. However, the hydrogenation rate is expected to be slower at shallow depths, where the increasingly oxidizing conditions enhance the reverse reaction instead. Unless a rapid hydrothermal fluid uprising, able to quench the concentrations of alkenes characterizing the deep reservoirs up to the surface emission (which is not the case for diffuse degassing), occurs, the high reactivity of the double C=C bond may lead alkenes to undergo addition reactions, such as hydration. Hydration of alkenes to alcohols is indeed thermodynamically favoured at decreasing temperatures and may compete with hydrogenation of alkenes to alkanes (Shock et al., 2013) as fluids cool slowly down approaching the surface. Accordingly, soil gases of type A were characterized by alkanes/alcohols ratios lower than those measured in fumarolic gases, suggesting that hydration reactions played a major role in the degradation of alkenes during fluids uprising through the soil. At decreasing CO₂/N₂ values in soil gases, the alkanes/alcohols ratios progressively decreased whereas the overall concentrations of O-bearing compounds generally increased. In particular, a progressive enrichment in ketones and aldehydes relative to alcohols was observed at decreasing CO₂/N₂ ratios. Similarly, an

increment of phenol and benzaldehyde relative to benzene was recognized. The increment in O-bearing compounds is consistent with the increasing availability of O₂. The increasingly oxidizing conditions are expected to favour the abiotic dehydrogenation reaction of alcohols to ketones. Moreover, alcohols, ketones, aldehydes, and other O-substituted compounds are common by-products of the metabolic pathways of microorganisms (Chapter 2), being involved in both cellular respiration and fermentative processes. Microbial activity is expected to play a major role in the production of O-bearing VOCs at shallow depths. Accordingly, an increase in the concentrations of O-bearing compounds, associated with an increment in O₂ contents, was observed in soil gases collected at 10 cm depth with respect to those sampled at 30 cm depth along the same vertical profile in the Solfatara Crater, confirming that the production of oxygenated compounds was related to processes mostly occurring at aerobic conditions. Similarly, the CH₄/CO₂ ratios decreased along the five vertical profiles approaching the surface, pointing to the possible occurrence of oxidative processes related, for example, to methanotrophic activity. As discussed in Chapter 2, methanotrophic microorganisms are known to cometabolize a variety of VOCs, including halocarbons, leading to the production of O-bearing compounds. Moreover, halocarbons may be used as electron acceptors for microbial respiration under anaerobic conditions. In reductive dechlorination, hydrogen atoms sequentially replace those of chlorine in the halocarbon, hence trichloroethene may be producing dichloroethene and, subsequently, vinylchloride, or carbon tetrachloride may yield chloromethane. Similarly, abiotic halogenation reactions occurring at depth cannot be excluded. No particular trend was observed in soil gases, except for chlorobenzene and chloromethane. The latter, however, was only detected in soil gases of type B and C, together with CFCs, suggesting that these compounds mainly derived from air contribution. Accordingly, CFCs and CH₃Cl were not detected in the BG and BN fumarolic gas samples. Although increasing air contribution (i.e. increasing Ar/CO₂ ratios; soil gases of groups B and C) corresponded to CFCs+CH₃Cl/other halocarbons ratios approaching the value measured in local air (Figure 8.7), the concentrations of other halocarbons in soil gases at increasing contribution from the hy-

8. Distribution of VOCs in interstitial soil gases

drothermal source were significantly higher with respect to those expected for these compounds assuming air as their sole source. This implies that

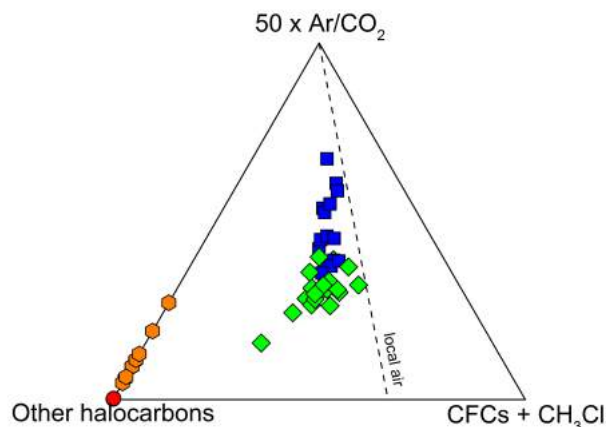


Figure 8.7: CFCs+CH₃Cl, Ar/CO₂ and other halocarbons ternary diagram for fumarolic gases and soil gases from Solfatara Crater. Symbols as in Figure 8.1. The dashed line indicates CFCs+CH₃Cl/ other halocarbons ratio in local air (unpublished data).

most halocarbons had a geogenic origin, as also observed by Schwandner et al. (2004) in soil gases from Vulcano Island.

S-bearing compounds were clearly related to deep contribution from hydrothermal fluids (Figure 8.2). The only exceptions were DMSO and DMSO₂, which were inversely correlated with the CO₂/N₂ ratios. In particular, the concentrations of the more oxidized compound (DMSO₂) increased relative to both DMS and DMSO at decreasing CO₂/N₂ values (Figure 8.8), indicating the occurrence of oxidative processes involving S-bearing compounds in soil gases. Accordingly, a variety of DMS-degrading microorganisms are reported in literature (e.g. Schäfer et al., 2010; Eyice et al., 2015), including methanotrophs and nitrifying bacteria, capable to oxidize DMS to DMSO and DMSO₂ under aerobic conditions.

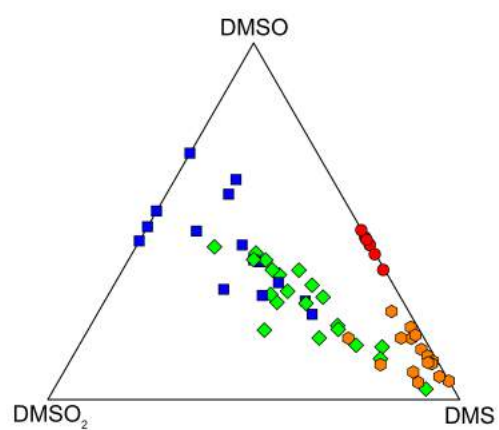


Figure 8.8: DMS, DMSO and DMSO₂ ternary diagram for fumarolic gases and soil gases from Solfatara Crater. Symbols as in Figure 8.1.

8. Distribution of VOCs in interstitial soil gases

8.3 Nisyros Island

At Nisyros Island, soil gas samples were collected within the hydrothermal craters of the Lakki Plain, in sites characterized by thermal anomalies, hydrothermally altered terrains, lack of vegetation, and relatively high soil CO_2 fluxes, i.e. up to $129 \text{ g m}^{-2} \text{ day}^{-1}$. Although the ΦCO_2 values were markedly lower than those observed at Solfatara Crater, they were remarkably higher than the local biological background ΦCO_2 value of $8 \text{ g m}^{-2} \text{ day}^{-1}$ reported by Cardellini et al. (2003). Hence, in these soil gases a relevant hydrothermal contribution was expected. Accordingly, relatively high concentrations of CO_2 , CH_4 and H_2S were detected. The $\delta^{13}\text{C}\text{-CO}_2$ values, similar to those measured in the fumarolic gases, confirmed a relevant input of deep hydrothermal fluids.

Although the total amounts of VOCs were lower in soil gases relative to fumaroles, as expected considering air dilution at very shallow depths, different behaviours were observed in the relative abundances of the different homologous series (Figure 8.9), pointing to the occurrence of secondary processes during the uprising of deep fluids. Among alkanes, the relative abundances

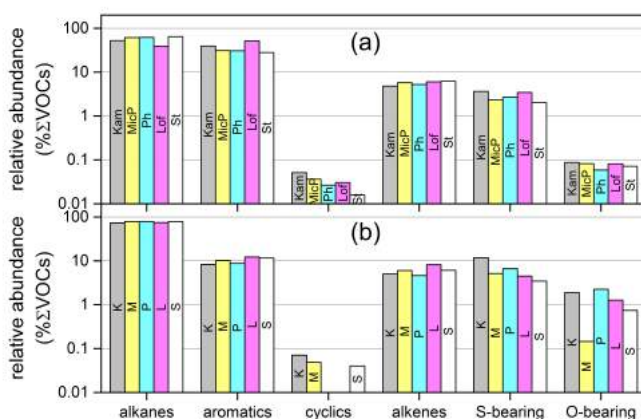


Figure 8.9: Relative abundances (in % ΣVOCs) of the different families of VOCs (alkanes, aromatics, cyclics, alkenes, S-bearing and O-bearing compounds) in (a) fumarolic and (b) soil gas samples from Nisyros Island.

of C₂ to C₆ saturated hydrocarbons with respect to the sum of alkanes (Figure 8.10) followed approximately the same pattern in both fumaroles and soil gases, suggesting that these compounds (*i*) were mainly controlled by reactions occurring within the deep hydrothermal reservoir, and (*ii*) displayed analogous behaviour relative to secondary processes during fluids uprising.

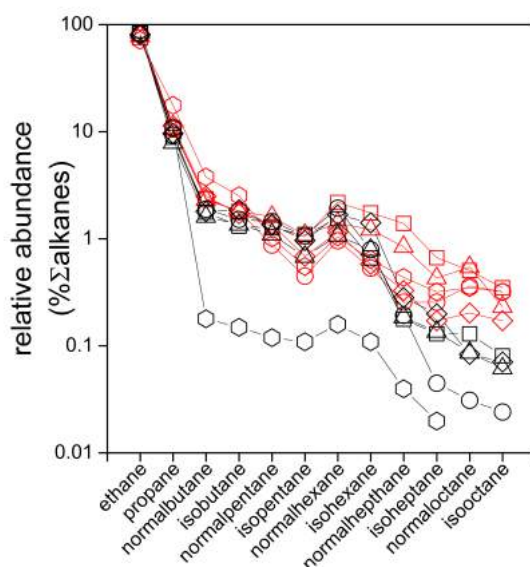


Figure 8.10: Relative abundances (in % Σ alkanes) of alkanes in **(a)** fumarolic (red symbols) and **(b)** soil gas (black symbols) samples collected in Kaminakia (squares), Micros Polybotes (circles), Phlegethon (triangles) and Stephanos (diamonds) craters and Lofos dome (hexagons) in Nisyros Island.

Differently, C₇₋₈ alkanes in soil gases had lower abundances with respect to the fumarolic discharges (Figure 8.10), likely due to the increasing instability of saturated hydrocarbons at increasing structural complexity. However, the enrichment of alkanes in soil gases (from 73 to 79 % Σ VOCs) with respect to fumarolic samples (from 39 to 64 % Σ VOCs) indicates that these compounds were, as expected, almost unaffected by secondary processes occurring at shallow depths, considering the relatively high soil CO₂ fluxes measured in the selected soil gas sampling sites.

Aromatics, the second most abundant organic homologues series in fumarolic discharges (from 28 to 52 % Σ VOCs), were significantly depleted in soil gases,

8. Distribution of VOCs in interstitial soil gases

representing from 8 to 12 % Σ VOCs. The decrease in abundance was particularly pronounced for toluene, the benzene/toluene ratios ranging from 16 to 71 in soil gases, i.e. markedly lower than the values measured in fumarolic gases (from 9 to 20). The highest benzene/toluene ratios were associated with the highest concentrations of O-substituted aromatics, i.e. acetophenone and benzaldehyde. McCollom et al. (2001) recognized benzaldehyde as a likely short-lived intermediate of the toluene decarboxylation to benzoic acid and benzene (Figure 7.14), a process that was proven to be favoured in the presence of high concentrations of dissolved sulphur compounds (McCollom et al., 2001). Microbial activity may also contribute to degradation of alkylated aromatics. For instance, ethylbenzene may be oxidized to acetophenone by e.g. denitrifying bacteria, while toluene is known to be degraded by numerous anaerobes (Widdel et al., 2006; Fuchs et al., 2011).

The overall enrichment in O-bearing compounds observed in soil gases relative to fumarolic vents may be related to the oxidative metabolic activity of microorganisms. Not only O-bearing compounds represented a larger portion of the organic fraction, but esters, ketones and aldehydes also showed higher concentrations in soil gases than those of fumarolic gases, with esters representing up to 66 % Σ O-bearing compounds. This confirms that these compounds had a shallow origin. The lowest concentrations of O-bearing compounds were found in the soil gas sample from Micros Polybotes crater, where furans were 50 % Σ O-bearing compounds, indicating a higher contribution from deep hydrothermal fluids (fumarolic gases displayed furans contents up to 86 % Σ O-bearing compounds).

Similarly to O-bearing compounds, S-substituted species represented a larger fraction of VOCs in soil gases (from 3 to 12 % Σ VOCs) than in the fumaroles (≤ 4 % Σ VOCs). In particular, whilst the relative abundances of DMS, thiophenes and carbon disulphide were comparable to those in fumarolic gases, DMSO was only present in soil gases and, thus, was likely produced by shallow oxidative processes. Moreover, the DMSO/DMS ratios were ranging from 3.7 to 6.2 in soil gases, whereas in Micros Polybotes DMSO was slightly depleted with respect to DMS (DMSO/DMS ratio of 0.9), further supporting the shallow origin of DMSO.

8.4 Poggio dell'Olivo

At Poggio dell'Olivo, the intense diffuse degassing was highlighted by the lack of vegetation in the Solfatara Secca area. Accordingly, Cardellini et al. (2003) reported a total output of CO₂ and CH₄ from this area of 22.5 t day⁻¹ and 43 kg day⁻¹, respectively. The uprising of deep hydrothermal fluids is also responsible for the vigorous gas bubbling in the Vezza Creek, which is imposed along a fault that allows a rapid rising of a large amount of deep fluids with negligible air dilution. Hence, the composition of the VC sample can be considered to represent that of the deep fluid source, i.e. a CO₂-dominated gas with minor amounts of CH₄ and H₂S.

Although the chemistry and the CO₂ isotopic signature of G1-G20 soil gas samples resembled that of VC indicating relevant hydrothermal fluids contribution, soil gases were characterized by significantly lower CO₂/N₂ ratios with respect to the bubbling gas, likely due to air dilution. Moreover, the relative abundances of both inorganic and organic species in soil gases showed variations relative to VC sample that cannot be caused by air dilution only. In Figure 8.11, the ratios of CH₄ and H₂S, i.e. hydrothermal fluid-related species, to Ar are plotted vs. CO₂/N₂, which is assumed to be inversely correlated to air fraction. Although both H₂S/Ar and CH₄/Ar ratios showed decreasing trends at decreasing CO₂/N₂ ratios, their values were significantly lower than those expected for simple mixing between air and hydrothermal fluids (Figure 8.11). These trends can be explained by the occurrence of oxidation processes related to chemical reactions and/or microbial activity, able to exert a strong influence on the composition of fluids diffusively released from soils. Accordingly, evidences of methane microbial uptake were provided by isotopic data (Figure 8.12). While soil gases with relatively high CO₂/N₂ ratios were characterized by δ¹³C-CH₄ values similar to that measured in VC sample (-26.1 ‰), a progressive enrichment in the heavier isotope (¹³C) was observed at increasingly aerobic conditions, up to δ¹³C-CH₄ values of -21.5 ‰. Accordingly, microbial oxidation of CH₄ is known to be typically associated with a kinetic isotopic effect that enriches the residual CH₄ in the heavier isotope whereas ¹²C is preferentially consumed by methane oxidizing

8. Distribution of VOCs in interstitial soil gases

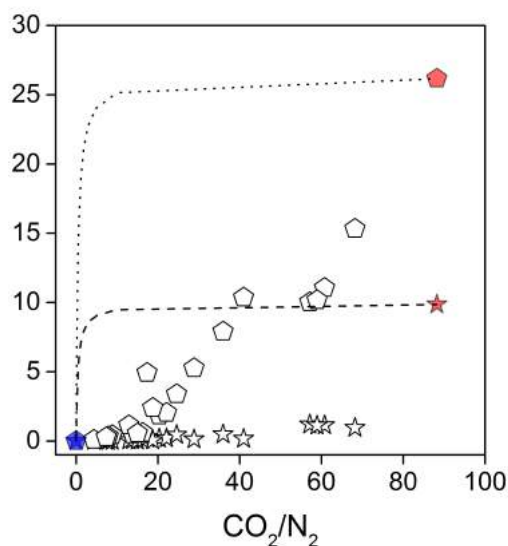


Figure 8.11: CH₄/Ar (pentagons) and H₂S/Ar (stars) vs. CO₂/N₂ ratios in G1-G20 soil gases (white) and VC sample (red) from Poggio dell'Olivo and air (blue). The mixing lines (dashed lines) between hydrothermal fluids (VC sample) and air are shown.

bacteria, i.e. methanotrophs (Whiticar, 1999). Methanotrophs are aerobic bacteria that use CH₄ as a sole carbon and energy source. The metabolic pathway is shown in Figure 8.13: methane is oxidized to methanol that is subsequently converted to formaldehyde and then to formic acid. The carboxylic acid can be converted to CO₂ or assimilated for biomass production through several pathways, depending on the microorganism (Hanson and Hanson, 1996; Rojo, 2009). The oxidation of methane to methanol is catalyzed by methane monooxygenase enzymes (MMOs) that exhibit a striking lack of substrate specificity, resulting in the cometabolism of a very large number of organic compounds (Hanson and Hanson, 1996; Fritsche and Hofrichter, 2008 and references therein). Accordingly, whilst the Σ VOCs values in soil gases generally increased at increasing CO₂/N₂ ratios, suggesting that these compounds were mainly related to the deep hydrothermal contribution, the different families of organics displayed different behaviours. The concentrations of alkanes, alkenes, cyclics, aromatics and Cl-substituted compounds

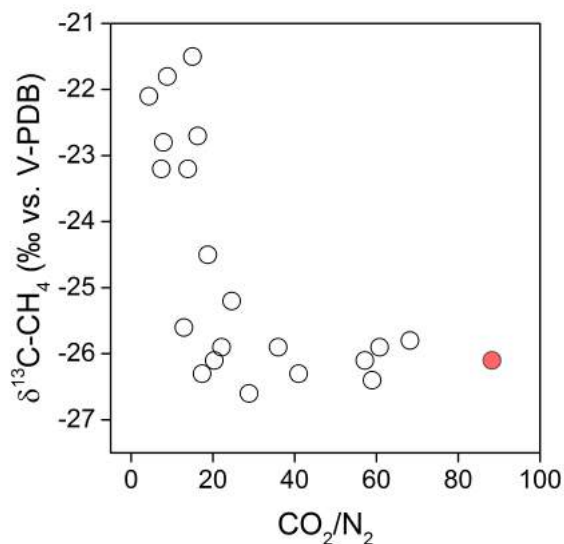


Figure 8.12: $\delta^{13}\text{C-CH}_4$ (in ‰ vs. V-PDB) vs. CO_2/N_2 ratios in G1-G20 soil gases (white circles) and VC sample (red circle) from Poggio dell'Olivo.

increased as the hydrothermal fluid contribution increased, showing a trend toward the VC gas composition (Figure 8.14). Differently, N-substituted compounds and terpenes were only detected in few soil gas samples (G3, G4, G7, G8, G15, G17, G18) characterized by low CO_2/N_2 ratios and located in marginal and partially vegetated portions of Solfatara Secca (Figure 4.11), suggesting that these species may represent vegetation-derived volatile organic trace compounds. Accordingly, α -pinene is one of the principal terpenes emitted by plants (e.g. Owen et al., 2001; Asensio et al., 2008). These soil gas samples also displayed the highest contents of O-bearing compounds, which were progressively more enriched in soil gases with decreasing CO_2/N_2 ratios (Figure 8.14), where oxidative processes are expected to be increasingly favoured. Accordingly, samples G3, G4, G7, G8, G15, G17 and G18 were characterized by the highest $\delta^{13}\text{C-CH}_4$ values (≥ -23.2 ‰).

The influence of biodegradation within the soil on hydrothermal-derived VOCs can be investigated in more detail on the basis of chemical and isotopic features of soil gases collected from 10 to 50 cm along the 5 vertical profiles

8. Distribution of VOCs in interstitial soil gases

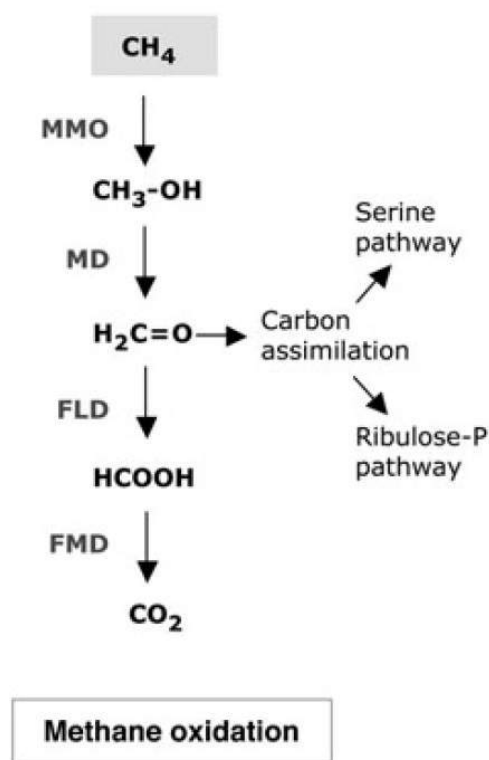


Figure 8.13: Aerobic pathway for the degradation of methane. MMO, methane monooxygenase; MD, methanol dehydrogenase; FLD, formaldehyde dehydrogenase; FMD, formate dehydrogenase (after Rojo, 2009).

in the Solfatara Secca (Figure 4.11).

The trends depicted by CO_2/N_2 , CH_4/Ar and $\text{H}_2\text{S}/\text{Ar}$ ratios in Figure 8.15 indicate increasing hydrothermal fluid contribution at increasing sampling depth, whereas the inverse trend of O_2/Ar ratios suggested (i) air dilution and (ii) increasingly aerobic conditions towards the soil-atmosphere interface. In particular, the relatively low N_2 , Ar and O_2 contents and the high CO_2 concentrations measured in the P1 and P2 profiles pointed to a relevant hydrothermal fluids input in these two sites. Accordingly, the $\delta^{13}\text{C}\text{-CO}_2$ values were similar to that measured in VC sample (Figure 8.16). The $\delta^{13}\text{C}\text{-CH}_4$ values were comparable to the isotopic signature of the VC sample along the entire P1 profile, consistently with the relatively low decrease in CH_4 contents observed at decreasing gas sampling depths, suggesting negligible oxidation

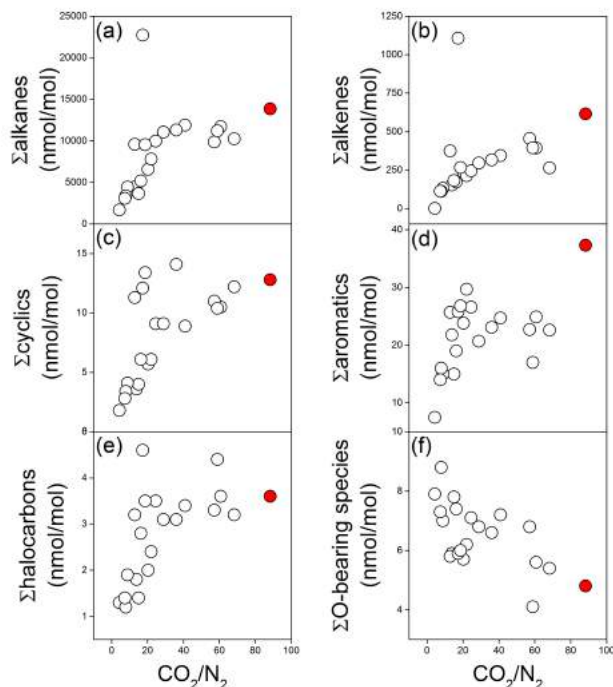


Figure 8.14: Contents of (a) alkanes, (b) alkenes, (c) cyclics, (d) aromatics, (e) halocarbons, and (f) O-bearing compounds (in nmol/mol) vs. CO₂/N₂ ratios in G1-G20 soil gases (white circles) and VC sample (red circle) from Poggio dell'Olivo.

effects at shallow depths and primarily thermogenic origin of CH₄. Similarly, no relevant variations in the composition of the organic fraction, generally resembling that of VC, were recognized along P1, except for a slight decrease in the relative abundances of alkenes (only represented by iso-butene at ≤ 25 cm) and aromatics (toluene was detected only at ≥ 30 cm) at decreasing depths (Figure 8.17). In the P2 profile a slightly increasing trend of the $\delta^{13}\text{C-CH}_4$ values was recognized at ≤ 30 cm (Figure 8.16), corresponding to an increasing CH₄ depletion (Figure 8.15), pointing to the occurrence of microbial oxidative processes. In the same depth range, an increase in the relative amounts of O-bearing compounds was observed (Figure 8.17). While

8. Distribution of VOCs in interstitial soil gases

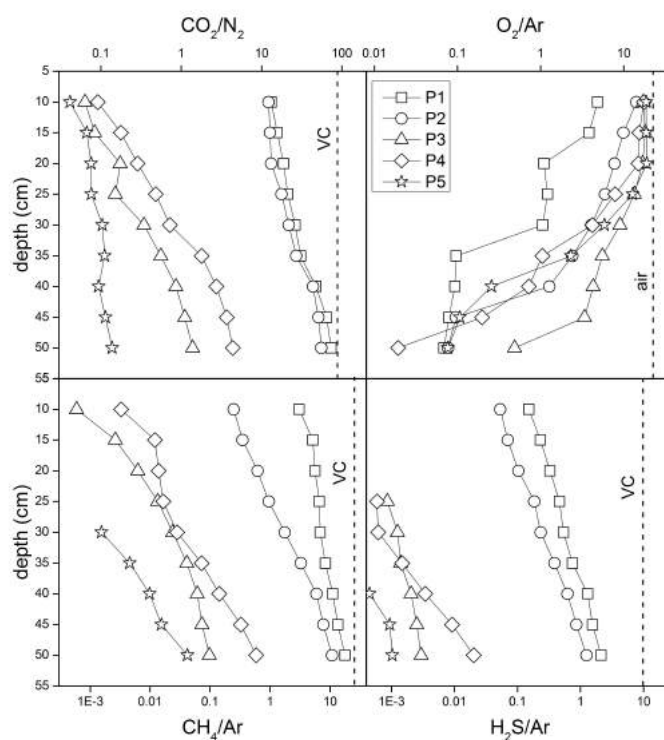


Figure 8.15: CO_2/N_2 , O_2/Ar , CH_4/Ar and $\text{H}_2\text{S}/\text{Ar}$ ratios vs. depth (in cm) in soil gases from P1-P5 profiles at Poggio dell'Olivo. The dashed lines indicate the CO_2/N_2 , CH_4/Ar and $\text{H}_2\text{S}/\text{Ar}$ ratios in VC sample and O_2/Ar in air.

the relative abundances of alcohols progressively decreased, aldehydes, ketones and esters increased, with propanone and ethyl formate being only detected in this depth interval (Figure 8.18). On the contrary, alkenes (except for iso-butene), toluene, and normal- and iso-butane were not detected at depths lower than about 30 cm, whereas Cl-substituted compounds were only found at ≥ 25 cm (Figure 8.17). The variations in both $\delta^{13}\text{C}-\text{CH}_4$ values and VOC composition were sharper along the P3 and P4 profiles. These two sites were affected by less hydrothermal fluids contribution, as testified by the significantly lower CO_2/N_2 , CH_4/Ar and $\text{H}_2\text{S}/\text{Ar}$ ratios relative to those of the P1 and P2 profiles (Figure 8.15), with H_2S being only detected at ≥ 25 cm depths. The deep hydrothermal contribution was slightly higher in P4,

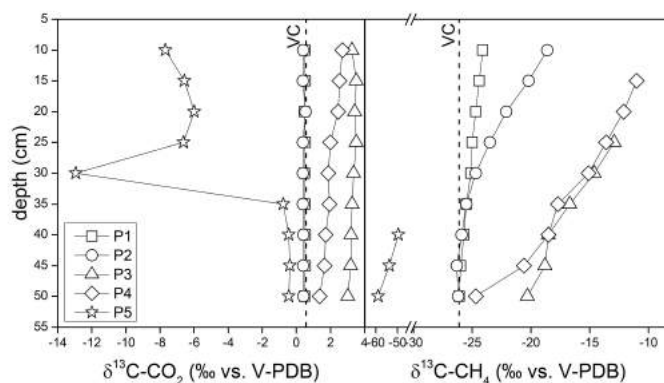


Figure 8.16: $\delta^{13}\text{C-CO}_2$ and $\delta^{13}\text{C-CH}_4$ (in ‰ vs. V-PDB) vs. depth (in cm) in soil gases from P1-P5 profiles at Poggio dell'Olivo. The dashed lines indicate the isotopic values in VC sample.

where the isotopic signature of CH_4 at 50 cm was similar to that measured at the bottom of the P1 and P2 profiles (Figure 8.16). However, $\delta^{13}\text{C-CH}_4$ values rapidly increased at decreasing depths (Figure 8.16). The decrease in VOCs concentrations approaching the surface was particularly abrupt below 30 cm depth, where the contents of alkanes, benzene, cyclics, alkenes (mainly iso-butene, with C_{5-6} alkenes only at 50 cm depth) and halocarbons rapidly decreased. Among alkanes, normal- and iso-butane and iso- C_{7-8} compounds were only detected at ≥ 35 cm depth. Toluene was not detected along the P4 profile, while halocarbons and cyclics were only measured at ≥ 40 and ≥ 30 cm depths. Contrarily, terpenes were detected at shallower depths (≤ 30 cm). A sharp increase in relative abundances of aromatics and O-bearing compounds and a decrease in alkanes were observed between 35 and 30 cm depth, where a carbon isotopic fractionation of 2.6 ‰ in CH_4 was measured. No relevant changes in the relative abundances of alcohols, carboxylic acids, ketones and aldehydes were observed in this depth interval, whereas the decrease in concentrations of normal- and iso-butane and iso- C_{7-8} compounds below the detection limit might suggest the occurrence of particularly efficient biodegradative processes able to oxidize C_4 and medium-long chain

8. Distribution of VOCs in interstitial soil gases

alkanes. The enrichment in benzene may be ascribed to the high stability of the aromatic ring under aerobic conditions. Similar trends were observed along the P3 profile. At this site, a less sharp decrease in CH₄ concentrations was observed at decreasing depths (Figure 8.15), although the isotopic signature of CH₄ values evidenced the occurrence of methanotrophic activity. The relatively high $\delta^{13}\text{C-CH}_4$ value at 50 cm may suggest that CH₄ oxidation was likely efficient at higher depths. Halocarbons and cyclics were only detected at 50 cm, alkenes (except iso-butene) were found at ≥ 40 cm, alkanes C₅₊ were occasionally measured at ≥ 25 cm and C₄ alkanes were lacking along the whole profiles, suggesting that these compounds, associated with hydrothermal input, were efficiently degraded by processes within the soil. O-bearing compounds, rapidly increasing at shallow depths, were mainly represented by aldehydes and ketones.

O-bearing compounds, together with terpenes, represented the totality of VOCs in soil gas samples collected at ≤ 30 cm depth along the P5 profile (Figure 8.19). At ≤ 25 cm depth, no CH₄ or H₂S were detected, indicating negligible contribution from hydrothermal fluids. Accordingly, the $\delta^{13}\text{C-CO}_2$ values were ranging from -7.68 to -5.98 ‰, i.e. close to the isotopic signature of atmospheric CO₂ (ca. -8 ‰; Scripps CO₂ Program, <http://scrippsco2.ucsd.edu>). Air contribution was also highlighted by the low CO₂/N₂ ratios and high O₂/Ar values (Figure 8.15). However, the chemical and isotopic composition of soil gases abruptly changed at ≥ 35 cm. $\delta^{13}\text{C-CO}_2$ sharply shifted to higher values (from -0.76 to -0.38 ‰; Figure 8.16), while CH₄ and H₂S were detected at concentrations progressively increasing with depth, pointing to some contribution from deep hydrothermal fluids. Nevertheless, the markedly negative $\delta^{13}\text{C-CH}_4$ values (from -58.9 to -49.5 ‰; Figure 8.16) suggested a mainly biogenic origin of methane. Accordingly, the VOCs detected along the P5 profile likely represent either (*i*) the compounds most recalcitrant to biodegradation, or (*ii*) the products of shallow secondary processes. At ≥ 35 cm alkanes were the most abundant VOCs (Figure 8.19), although their concentrations were strikingly lower than those measured in the other sites. Alkanes were mainly constituted by ethane, with normal-hexane and propane being present at ≥ 40 cm and at 50 cm

depth, respectively. Besides α -pinene, which was detected along the whole profile, O-bearing compounds at ≥ 35 cm were composed not only of aldehydes and ketones, but also by esters, carboxylic acids and alcohols, the latter compounds clearly increasing in abundance with depth (Figure 8.18).

8. Distribution of VOCs in interstitial soil gases

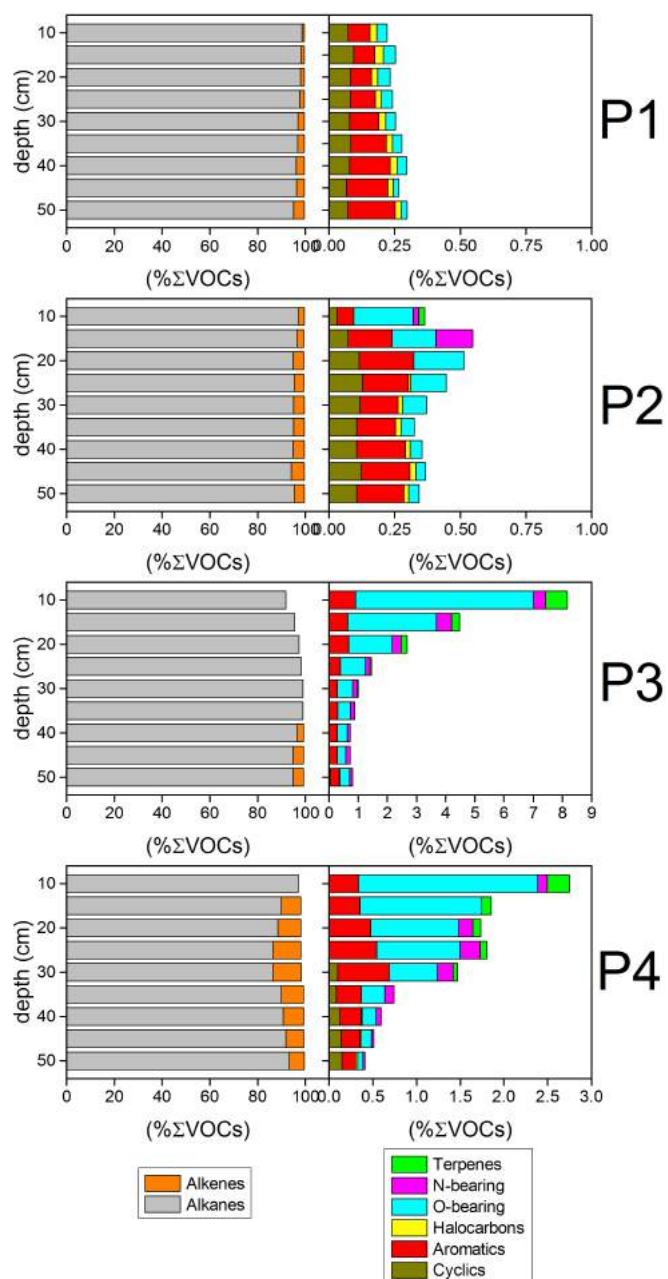


Figure 8.17: Relative abundances (in % Σ VOCs) of different families of VOCs (alkanes, alkenes, cyclics, aromatics, halocarbons, O-bearing and N-bearing compounds, and terpenes) vs. depth (in cm) in soil gases from P1-P4 profiles at Poggio dell'Olivo.

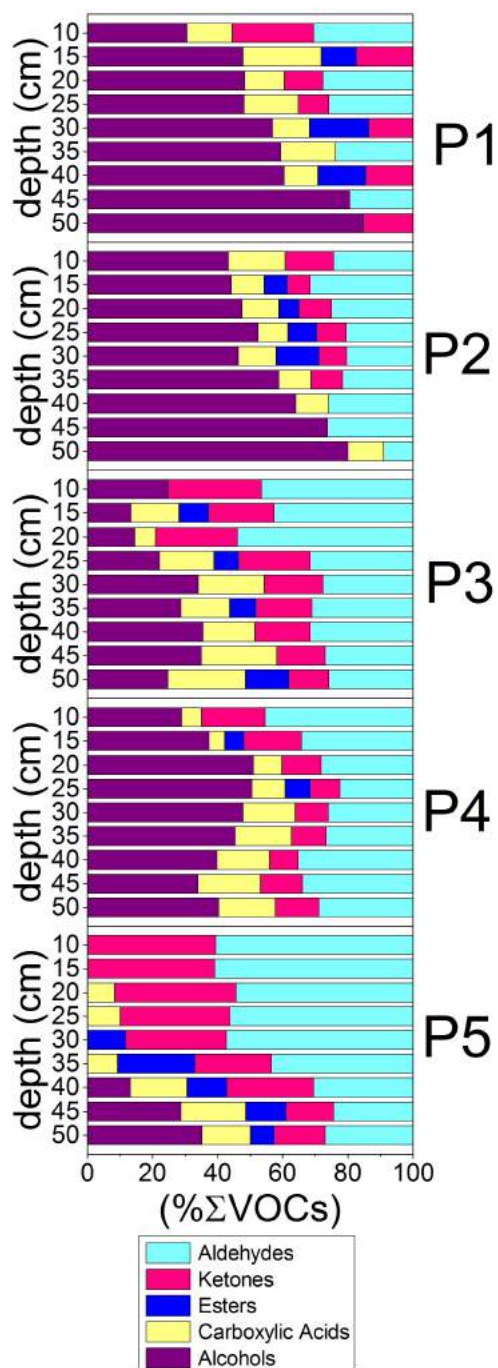


Figure 8.18: Relative abundances (in % Σ O-bearing compounds) of alcohols, carboxylic acids, esters, ketones and aldehydes vs. depth (in cm) in soil gases from P1-P5 profiles at Poggio dell'Olivo.

8. Distribution of VOCs in interstitial soil gases

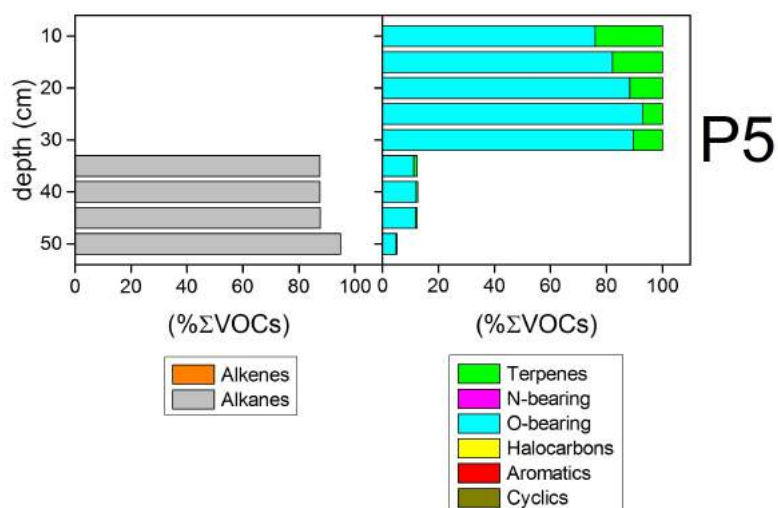


Figure 8.19: Relative abundances (in % Σ VOCs) of different families of VOCs (alkanes, alkenes, cyclics, aromatics, halocarbons, O-bearing and N-bearing compounds, and terpenes) vs. depth (in cm) in soil gases from P5 profile at Poggio dell'Olivo.

8.5 Cava dei Selci

Cava dei Selci is site of a very huge degassing activity due to endogenous deep originated CO_2 , with ΦCO_2 values up to 2 orders of magnitude higher than those measured at Nisyros Island. Soil gases collected from sites characterized by the highest ΦCO_2 values (type A) showed relatively high H_2S and CH_4 contents, pointing to a relevant contribution from deep-sourced hydrothermal fluids as those discharged from the CS1 and CS2 gas vents. However, relevant differences were observed in the relative abundances of the various families of VOCs in soil gases of type A with respect to those measured in the CS1 and CS2 gas vents (Figure 8.20), indicating that strong modifications affected the deep fluids during their uprising toward the surface, even when high soil CO_2 fluxes were present. In agreement with the

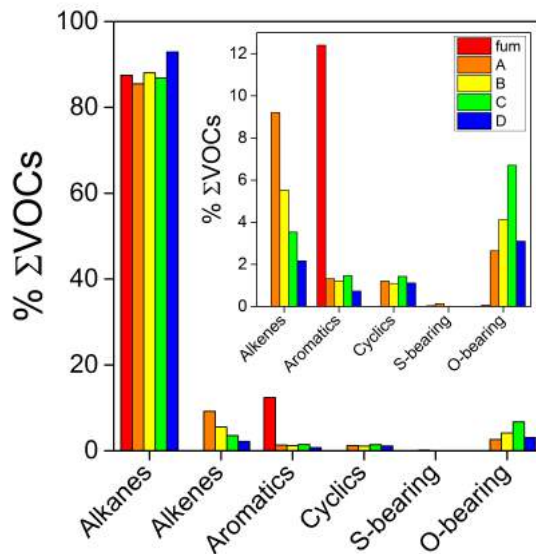


Figure 8.20: Relative abundances (mean values; in % ΣVOCs) of different families of VOCs (alkanes, alkenes, aromatics, cyclics, S-bearing and O-bearing compounds) in gas vents (red) and soil gases of type A (orange), B (yellow), C (green) and D (blue).

results from the other study areas, cyclics and O-bearing compounds (particularly ketones and aldehydes) were enriched in soil gases relative to fumarolic

8. Distribution of VOCs in interstitial soil gases

samples (Figure 8.20), possibly suggesting (i) incomplete aromatization and (ii) oxidation processes. Differently, aromatics were strongly depleted, the branched aromatics/benzene ratios being higher in soil gases of type A with respect to the CS1 and CS2 samples (Figure 8.20), whereas alkenes, which were not detected in the CS1 and CS2 samples, were up to 12 % Σ VOCs in the type A soil gases. Moreover, although both the relative abundances of alkanes and the C_3/C_2 and C_4/C_3 ratios were comparable in soil and fumarolic gases (Figure 8.20 and Figure 8.21), the C_{5+}/C_4 ratios in the type A soil gases were significantly higher than those measured in the CS1 and CS2 samples (Figure 8.21), indicating a strong enrichment in long-chain saturated hydrocarbons. Hence, these results may indicate (i) the occurrence of

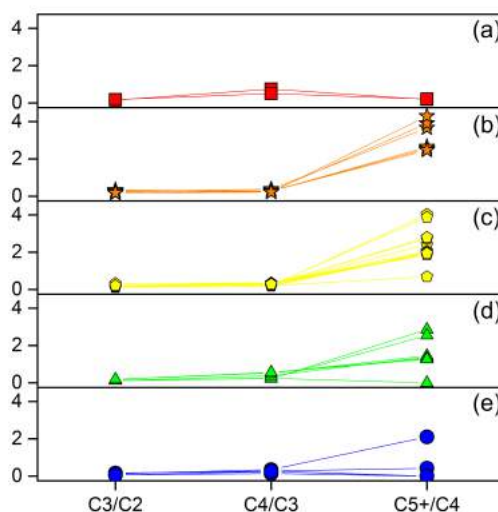


Figure 8.21: C_3/C_2 , C_4/C_3 and C_{5+}/C_4 ratios among alkanes in (a) gas vents (red squares) and soil gases of type (b) A (orange stars), (c) B (yellow pentagons), (d) C (green triangles) and (e) D (blue circles).

secondary processes, possibly consisting in the reformation of deep-sourced fluids represented by the CS1 and CS2 gases (e.g. alkylation reactions on aromatic compounds, or metathesis reactions able to convert short alkanes into longer chain analogues), favoured by the slower uprising of fluids dif-

fusively passing through the soil relative to the high flow rate gas vents, and/or (ii) the presence of a secondary source of VOCs affecting soil gases, such as thermal degradation of organic matter at shallower depths relative to the source feeding the main gas discharges. As the ΦCO_2 values decreased, and then the uprising of the hydrothermal fluids progressively decreased, the most relevant changes in the soil gas composition were a decrease in the relative abundances of alkenes, as expected on the basis of the high reactivity of the C=C double bond, and a sharp increase in the content of O-bearing compounds, according to the longer residence time of fluids at progressively oxidizing conditions and to the occurrence of microbially-driven oxidative processes at shallow depths. However, contrarily to what expected on the basis of the higher availability of molecular oxygen, a decrease in the relative abundances of O-bearing compounds was observed in the soil gases of type D with respect to those of samples collected from sites at higher ΦCO_2 values, together with an increase in alkanes (Figure 8.20). It has to be considered that the presence of a shallow water table (at ca. 40 cm depth) was recognized during the sampling campaign throughout the gas emission area that likely complicated the soil system with respect to the other study areas, enhancing the occurrence of different secondary processes. Accordingly, gas-water interaction may be responsible for the observed decrease in the polar, and hence soluble, O-bearing compounds and the increase in the abundance of the apolar and insoluble saturated hydrocarbons.

Chapter 9

Conclusions

The ongoing increase of airborne pollutant and greenhouse gas concentrations at a global scale is giving a strong pulse to initiatives aimed to develop reliable models to simulate present and future climate and air quality, including accurate estimates of both anthropogenic and natural contaminant emissions. Once emitted to the atmosphere, VOCs may act as both greenhouse gases and tropospheric ozone and secondary organic aerosol (SOA) producers, affecting climate, air quality and human health. Besides their presence in fumarolic fluids is documented since the 1960s-70s, emissions from volcanic and hydrothermal systems are still not exhaustively enumerated among natural sources in the estimation of global budgets of atmospheric VOCs (e.g. Kansal, 2009 and references therein). This is partly due to the scanty information on the composition of the organic fraction of fluids emitted from volcanic and hydrothermal systems. VOCs are indeed rarely analyzed in such environments, the published data being generally limited to light hydrocarbons in fumarolic emissions, whereas few studies include heteroatomic compounds and VOCs diffuse emissions from soils. Moreover, in order to carry out a reliable estimation of the global output of VOCs from volcanic and hydrothermal systems, it is of paramount importance to verify that the composition of organic compounds in hydrothermal fluids is not randomly dependent on the starting material and/or secondary processes, but strictly controlled by the physicochemical conditions of the deep fluid reser-

9. Conclusions

voirs. Although recurrent patterns in the relative abundances of VOCs were found in hydrothermal/volcanic gases that originated at similar temperature and redox conditions (Capaccioni et al., 1993, 1995), suggesting that these compounds can be used as geoindicators for processes occurring at the fluid source(s), the mechanisms responsible for the production of most VOCs in natural environments are still poorly understood.

Hence, the overriding purpose of this thesis was to increase the scientific knowledge on the composition and behaviour of VOCs in volcanic and hydrothermal fluids. To accomplish this goal, both experimental and empirical methods were applied, the experimental, sampling and analytical efforts being specifically aimed to investigate (*i*) primary processes affecting VOCs within hydrothermal reservoirs at depth, and (*ii*) secondary processes, causing chemical modifications in the organic fraction of hydrothermal fluids during their uprising toward the surface.

Primary processes were investigated through laboratory experiments and analyzing VOCs composition in gases naturally discharged from low-to-high temperature fumaroles, boiling and bubbling pools and dry gas, mainly CO₂, emissions. The study sites are located in the Mediterranean area, as follows: (*i*) high-enthalpy hydrothermal systems associated with active volcanoes (Solfatara Crater, Italy, and Nisyros Island, Greece) and (*ii*) low-to-medium enthalpy hydrothermal systems (Poggio dell'Olivo and Cava dei Selci, Italy).

The empirical data confirmed the strong dependence of VOCs composition on the physicochemical conditions of the deep feeding environment, providing indications of primary processes that were supported by the results of laboratory experiments carried out at hydrothermal conditions. The latter allowed to verify the production of benzene from linear (normal-hexane and normal-dodecane) and cyclic (cyclohexane and cyclohexene) aliphatic compounds at 300 °C and 85 bar, i.e. resembling the industrial catalytic reforming process, as suggested by Capaccioni et al. (1993). In detail, benzene was readily produced in water at the experimental conditions via (*i*) cyclization of normal alkanes and subsequent (*ii*) dehydrogenation of cyclic aliphatics, although isomerization and hydration reactions were found to eventually com-

pete with the aromatization pathway. Benzene production was favoured by experiments performed in the presence of sulphides (sphalerite and pyrite) and iron oxides (magnetite and hematite), indicating that these minerals may act as catalysts for organic reactions. An increase in the reactivity of the C-H bonds was observed in the presence of sphalerite, as confirmed by experimental runs carried out in heavy water, suggesting that ZnS may be an efficient catalytic agent for hydrogenation/dehydrogenation reactions. It is worth noting the potential industrial applications of these results. The production of S-bearing compounds (thiophenes and cyclohexanethiol) during experiments performed on both linear and cyclic aliphatic in the presence of sulphide minerals revealed that minerals may participate to organic reactions.

The results from the experiments were compared with the measured composition of VOCs in hydrothermal fluids from the four selected study areas. The concentrations of VOCs in natural samples were in the order of 10^3 - 10^4 nmol/mol, including up to 95 different compounds. Hydrocarbons, in particular alkanes and aromatics, largely dominated the composition of the organic compounds. Aromatics were more abundant in fumarolic gases from active volcanoes, where relatively high concentrations of alkenes were also recognized, likely due to the higher temperatures of these systems. The composition of normal-alkanes showed a rapid decrease of the concentrations of species having increasing molecular weight, as expected by considering their stability at such thermodynamic conditions. At relatively high temperatures, alkanes may indeed undergo both (*i*) dehydrogenation to alkenes, and (*ii*) dehydrocyclization and subsequent aromatization, as demonstrated by the laboratory experiments. The latter pathway, particularly affecting C_{6+} alkanes, was evidenced by the peculiarly high relative abundance of normal-hexane in the analyzed samples and by the increasing aromatics/alkanes ratios and H_2 concentrations moving from low-to-medium enthalpy hydrothermal systems to active volcanoes, in agreement with thermodynamic data. On the other hand, the relative enrichment in cyclics in fluids from low-to-medium enthalpy hydrothermal systems likely indicates an incomplete aromatization process. The higher sulphur fugacity in hydrothermal systems associated

9. Conclusions

with active volcanoes was likely responsible for the relatively high concentrations of S-bearing organic compounds, in particular thiophenes, carbon disulphide and DMS, the latter being a potential climate-cooling gas (Liss and Lovelock, 2007 and references therein). Among the O-bearing compounds, furans were associated with high temperatures and oxidizing conditions related to magmatic fluid inputs into deep hydrothermal reservoirs, whilst alcohols, aldehydes, ketones, esters, etc. were likely produced as hydrothermal fluids cooled down approaching the surface and encountered oxidizing conditions. Among halocarbons, only Cl-substituted compounds were measured, although they occurred at very low amounts. CFCs and CH₃Cl, which are well-known stratospheric ozone-depleting chemicals, were not detected.

Secondary processes were investigated by comparing the composition of fumarolic gases with that of interstitial soil gases sampled from hydrothermalized soils within the same study areas. The strong differences shown by interstitial vs. fumarolic gases were not consistent with the diluting effect of air typically occurring in soils, indicating that secondary processes were able to significantly modify the composition of VOCs released from the hydrothermal source. Secondary processes may include both (i) thermogenic processes occurring at depth during fluids uprising, such as dehydrocyclization reactions of alkanes, likely responsible for the enrichment in cyclic compounds in soil gases relative to fumaroles, and (ii) shallow oxidative processes, mainly driven by microbial activity, affecting hydrocarbons and producing O-bearing compounds. The relatively low alkanes/aromatics ratios recorded in the soil gases were also likely related to the high stability of the aromatic ring even in presence of free O₂. The effects of secondary processes were also evident for the S-bearing compounds, such as DMS, a compound that was found in the fumarolic gases, although approaching the surface it resulted to be oxidized to DMSO and DMSO₂. The VOC composition in the interstitial soil gases collected at regular depths along vertical profiles suggested that microbial communities play a pivotal role in controlling the composition of VOCs in uprising hydrothermal fluids prior to their release into the atmosphere through diffuse degassing. VOCs can be involved in the metabolic processes of aerobic and anaerobic microorganisms, for instance, being cometabolized

by methanotrophs, whose presence in hydrothermal and volcanic areas is well documented (D'Alessandro et al., 2011 and references therein). The study of the interplay between VOCs and microbial life in harsh conditions, such as those characterizing volcanic and hydrothermal environments, is an intriguing research topic due to its relevant implications for both purely scientific biogeochemical research field (origin of life, astrobiology) and bioremediation applications. Understanding how microbial activity impacts VOCs in soils from volcanic and hydrothermal systems may lead to the development of innovative bio-techniques for the abatement of pollutant emissions. Moreover, the analysis of VOCs in soils from extreme environments combined with microbiological studies may significantly contribute to the discovery of extremophiles able to produce novel antibacterial and anticancer agents. These aspects are matter of study of ongoing research projects and collaborations, started during the PhD program, involving biologists from CNR-IRSA (Rome, Italy) and the Department of Biology of the University of Florence.

References

- Acocella V., Funicello R., 2006. *Transverse systems along the extensional Tyrrhenian margin of central Italy and their influence on volcanism*. *Tectonics*, 25, TC2003, doi: 10.1029/2005TC001845.
- Agusto M., Tassi F., Caselli A.T., Vaselli O., Rouwet D., Capaccioni B., Caliro S., Chiodini G., Darrah T., 2013. *Gas geochemistry of the magmatic-hydrothermal fluid reservoir in the Copahue-Caviahue Volcanic Complex (Argentina)*. *Journal of Volcanology and Geothermal Research*, 257, 44-56, doi: 10.1016/j.jvolgeores.2013.03.003.
- Aiuppa A., Tamburello G., Di Napoli R., Cardellini C., Chiodini G., Giudice G., Grassa F., Pedone M., 2013. *First observations of the fumarolic gas output from a restless caldera: Implications for the current period of unrest (2005-2013) at Campi Flegrei*. *Geochem. Geophys. Geosyst.*, 14(10), 4153-4169, doi: 10.1002/ggge.20261.
- Akiya N., Savage P.E., 2001. *Kinetics and mechanism of cyclohexanol dehydration in high-temperature water*. *Ind. Eng. Chem. Res.*, 40, 1822-1831, doi: 10.1021/ie000964z.
- Alexander M., 1994. *Biodegradation and bioremediation*. Academic Press Inc., San Diego, USA, pp. 302.
- Amato A., Chiarabba C., 1995. *Recent uplift of the Alban Hills volcano (Italy), evidence for magmatic inflation?*. *Geophys. Res. Lett.*, 22, 1985-1988, 1995.
- Ambrosio M., Doveri M., Fagioli M.T., Marini L., Principe C., Raco B., 2010. *Water-rock interaction in the magmatic-hydrothermal system of Nisyros Island (Greece)*. *J. Volcanol. Geoth. Res.*, 192, 57-68, doi: 10.1016/j.jvolgeores.2010.02.005.
- Amend J.P., Shock E.L., 1998. *Energetics of amino acid synthesis in hydrothermal ecosystems*. *Science*, 281, 1659-1662.
- Amend J.P., Shock E.L., 2001. *Energetics of overall metabolic reactions of thermophilic and hyperthermophilic Archaea and Bacteria*. *FEMS Microbiol. Rev.*, 25, 175-243.
- Amend J.P., Rogers K.L., Shock E.L., Gurrieri S., Inguaggiato S., 2003. *Energetics of chemolithoautotrophy in the hydrothermal system of Vulcano Island, southern Italy*. *Geobiology*, 1, 37-58.

References

- Anderson G., 2005. *Thermodynamics of natural systems, Second Edition*. Cambridge University Press, Cambridge, United Kingdom, pp. 648.
- Annunziatellis A., Ciotoli G., Lombardi S., Nolasco F., 2003. *Short- and long-term gas hazard: the release of toxic gases in the Alban Hills volcanic area (central Italy)*. J. Geochem. Explor., 77, 93-108, doi: 10.1016/S0375-6742(02)00272-8.
- Arthur C.L., Pawliszyn J., 1990. *Solid phase microextraction with thermal desorption using fused silica optical fibers*. Anal. Chem., 62, 2145-2148.
- Asensio D., Owen S.M., Llusia J., Peñuelas J., 2008. *The distribution of volatile isoprenoids in the soil horizons around Pinus halepensis trees*. Soil Biol. Biochem., 40, 2937-2947, doi: 10.1016/j.soilbio.2008.08.008.
- Baiocchi A., Dragoni W., Lotti F., Luzzi G., Piscopo V., 2006. *Outline of the hydrogeology of the Cimino and Vico volcanic area and of the interaction between groundwater and Lake Vico (Lazio Region, Central Italy)*. Boll. Soc. Geol. It., 125, 187-202.
- Baiocchi A., Lotti F., Piscopo V., 2012. *Conceptual hydrogeological model and groundwater resource estimation in a complex hydrothermal area: the case of the Viterbo geothermal area (Central Italy)*. J. Water Resource Prot., 4, 231-247, doi: 10.4236/jwarp.2012.44026.
- Barberi F., Buonasorte G., Cioni R., Fiordalisi A., Foresi L., Iaccarino S., Laurenzi M.A., Sbrana A., Vernia L., Villa I.M., 1994. *Plio-Pleistocene geological evolution of the geothermal area of Tuscany and Latium*. Memorie Descrittive della Carta Geologica d'Italia, 49, 77-134.
- Barberi F., Innocenti F., Ricci C.A., 1971. *Il magmatismo nell'Appennino centro-settentrionale*. La Toscana Meridionale. Rendiconti della Società Italiana di Mineralogia e Petrologia, 27, 169-210.
- Barbieri R., Cavalazzi B., 2014. *How do modern extreme hydrothermal environments inform the identification of Martian habitability? The case of the El Tatio Geyser Field*. Challenges, 5, 430-443, doi: 10.3390/challe5020430.
- Battaglia M., Troise C., Obrizzo F., Pingue F., De Natale G., 2006. *Evidence for fluid migration as the source of deformation at Campi Flegrei caldera (Italy)*. Geophys. Res. Lett., 33, L01307, doi: 10.1029/2005GL024904.
- Beaubien S.E., Ciotoli G., Lombardi S., 2003. *Carbon dioxide and radon gas hazard in the Alban Hills area (central Italy)*. J. Volcanol. Geotherm. Res., 123, 63-80, doi: 10.1016/S0377-0273(03)00028-3.
- Berg I.A., 2011. *Ecological aspects of the distribution of different autotrophic CO₂ fixation pathways*. Appl. Environ. Microbiol., 77, 6, 1925-1936, doi: 10.1128/AEM.02473-10.
- Bergfeld D., Evans W.C., Howle J.F., Farrar C.D., 2006. *Carbon dioxide emissions from vegetation-kill zones around the resurgent dome of Long Valley caldera, eastern California, USA*. J. Volcanol. Geotherm. Res., 152, 140-156, doi: 10.1016/j.jvolgeores.2005.11.003.
- Berrino G., Corrado G., Luongo G., Toro B. *Ground deformation and gravity changes accompanying the 1982 Pozzuoli uplift*. Bull. Volcanol., 47(2), 187-

200.

- Berrino G., 1994. *Gravity changes induced by height-mass variations at the Campi Flegrei Caldera*. J. Volcanol. Geoth. Res., 61(3-4), 293-309.
- Bonafede M., Mazzanti M., 1998. *Modelling gravity variations consistent with ground deformation in the Campi Flegrei caldera (Italy)*. J. Volcanol. Geoth. Res., 81, 137-157.
- Bondarev V.B., Porshnev N.V., Nenarokov D.F., 1982. *Gas chromatographic analysis of the vapours and gases discharged from the thermal fields of Kamchatka*. J. Chromatogr., 247, 347-351.
- Botta O., Bada J.L., 2002. *Extraterrestrial organic compounds in meteorites*. Surv. Geophys., 23, 411-467.
- Brock T.D., 1967. *Life at high temperatures*. Science, 158, 1012-1019.
- Brombach T., Cardellini C., Marini L., 2001. *Soil diffuse degassing and thermal energy fluxes from the southern Lakki plain, Nisyros (Greece)*. Geophys. Res. Lett., 28(1), 69-72.
- Brombach T., Caliro S., Chiodini G., Fiebig J., Hunziker J.C., Raco B., 2003. *Geochemical evidence for mixing of magmatic fluids with seawater, Nisyros hydrothermal system, Greece*. Bull. Volcanol., 65, 505-516, doi: 10.1007/s00445-003-0278-x.
- Brown T.E., LeMay H.E., Bursten B.E., Murphy C., Woodward P., 2012. *Chemistry: The Central Science, 12th Edition*. Prentice Hall, New Jersey, pp. 1200.
- Bruno P.P.G., Ricciardi G. P., Petrillo Z., Di Fiore V., Troiano A., Chiodini G., 2007. *Geophysical and hydrogeological experiments from a shallow hydrothermal system at Solfatara Volcano, Campi Flegrei, Italy: Response to caldera unrest*. J. Geophys. Res., 112, B06201, doi:10.1029/2006JB004383.
- Caliro S., Chiodini G., Galluzzo D., Granieri D., La Rocca M., Saccorotti G., Ventura G., 2005. *Recent activity of Nisyros volcano (Greece) inferred from structural, geochemical and seismological data*. Bull. Volcanol., 67, 358-369, doi: 10.1007/s00445-004-0381-7.
- Caliro S., Chiodini G., Moretti R., Avino R., Granieri D., Russo M., Fiebig J., 2007. *The origin of the fumaroles of La Solfatara (Campi Flegrei, South Italy)*. Geochim. Cosmochim. Ac., 71, 3040-3055, doi: 10.1016/j.gca.2007.04.007.
- Capaccioni B., Martini M., Mangani F., Giannini L., Nappi G., Prati F., 1993. *Light hydrocarbons in gas-emissions from volcanic areas and geothermal fields*. Geochem. J., 27, 7-17.
- Capaccioni B., Martini M., Mangani F., 1995. *Light hydrocarbons in hydrothermal and magmatic fumaroles: hints of catalytic and thermal reactions*. B. Volcanol., 56, 593-600.
- Capaccioni B., Mangani F., 2001. *Monitoring of active but quiescent volcanoes using light hydrocarbon distribution in volcanic gases: the results of 4 years of discontinuous monitoring in the Campi Flegrei (Italy)*. Earth Planet. Sci. Lett., 188, 543-555.

References

- Capaccioni B., Tassi F., Vaselli O., 2001. *Organic and inorganic geochemistry of low temperature gas discharges at the Baia di Levante beach, Vulcano Island, Italy*. J. J. Volcanol. Geoth. Res., 108, 173-185.
- Capaccioni B., Taran Y., Tassi F., Vaselli O., Mangani G., Macias J.L., 2004. *Source conditions and degradation processes of light hydrocarbons in volcanic gases: an example from El Chichón volcano (Chiapas State, Mexico)*. Chem. Geol., 206, 81-96, doi: 10.1016/j.chemgeo.2004.01.011.
- Capecchiacci F., 2012. *Geochemica dei fluidi vulcanici e idrotermali: origine delle componenti organiche e loro impatto ambientale*. Ph.D. Thesis, Univ. of Florence: Florence, Italy.
- Carapezza M.L., Badalamenti B., Cavarra L., Scalzo A., 2003. *Gas hazard assessment in a densely inhabited area of Colli Albani Volcano (Cava dei Selci, Roma)*. J. Volcanol. Geotherm. Res., 123, 81-94, doi: 10.1016/S0377-0273(03)00029-5.
- Carapezza M.L., Tarchini L., 2007. *Accidental gas emission from shallow pressurized aquifers at Alban Hills volcano (Rome, Italy): Geochemical evidence of magmatic degassing?*. J. Volcanol. Geotherm. Res., 165, 5-16, doi: 10.1016/j.jvolgeores.2007.04.008.
- Carapezza M.L., Barberi F., Ranaldi M., Ricci T., Tarchini L., Barrancos J., Fischer C., Granieri D., Lucchetti C., Melian G., Perez N., Tuccimei P., Vogel A., Weber K., 2012. *Hazardous gas emissions from the flanks of the quiescent Colli Albani volcano (Rome, Italy)*. Appl. Geochem., 27, 1767-1782, doi: 10.1016/j.apgeochem.2012.02.012.
- Cardellini C., Chiodini G., Frondini F., Granieri D., Lewicki J., Peruzzi L., 2003. *Accumulation chamber measurements of methane fluxes: application to volcanic-geothermal areas and landfills*. Appl. Geochem., 18, 45-54.
- Castaldi S., Tedesco D., 2005. *Methane production and consumption in an active volcanic environment of Southern Italy*. Chemosphere, 58, 131-139, doi: 10.1016/j.chemosphere.2004.08.023.
- Chaigneau M., Conrad K., 1970. *Volcanic gas from Vulcano (Lipari Islands)*. Adad. Sci. Comptes Rendus, Ser. D, 271(2), 165-167.
- Chiarabba C., Amato A., Delaney P.T., 1997. *Crustal structure, evolution and volcanic unrest of the Alban Hills, Central Italy*. Bull. Volcanol., 59, 161-170.
- Chikere C.B., Okpokwasili G.C., Chikere B.O., 2011. *Monitoring of microbial hydrocarbon remediation in the soil*. 3 Biotech, 1, 117-138, doi: 10.1007/s13205-011-0014-8.
- Chiodini G., Cioni R., Leonis C., Marini L., Raco B., 1993. *Fluid geochemistry of Nisyros island, Dodecanese, Greece*. J. Volcanol. Geoth. Res., 56(1-2), 95-112.
- Chiodini G., 1994. *Temperature, pressure and redox conditions governing the composition of the cold CO₂ gases discharged in north Latium (Central Italy)*. Appl. Geochem., 9, 287-295.
- Chiodini G., Frondini F., Ponziani F., 1995. *Deep structures and carbon dioxide degassing in Central Italy*. Geothermics, 24(1), 81-94.

-
- Chiodini G., Cioni R., Guidi M., Raco B., Marini L., 1998. *Soil CO₂ flux measurements in volcanic and geothermal areas*. Appl. Geochem., 13(5), 543-552.
- Chiodini G., Marini L., 1998. *Hydrothermal gas equilibria: The H₂O-H₂-CO₂-CO-CH₄ system*. Geochim. Cosmochim. Ac., 62(15), 2673-2687.
- Chiodini G., Frondini F., Kerrick D.M., Rogie J., Parello F., Peruzzi L., Zanzari A.R., 1999. *Quantification of deep CO₂ fluxes from Central Italy. Examples of carbon balance for regional aquifers and of soil diffuse degassing*. Chem. Geol., 159, 205-222.
- Chiodini G., Frondini F., Cardellini C., Parello F., Peruzzi L., 2000. *Rate of diffuse carbon dioxide Earth degassing estimated from carbon balance of regional aquifers: The case of central Apennine, Italy*. J. Geophys. Res., 105(B4), 8423-8434.
- Chiodini G., Frondini F., 2001. *Carbon dioxide degassing from the Albani Hills volcanic region, Central Italy*. Chem. Geol., 177, 97-83.
- Chiodini G., Frondini F., Cardellini C., Granieri D., Marini L., Ventura G., 2001. *CO₂ degassing and energy release at Solfatara volcano, Campi Flegrei, Italy*. J. Geophys. Res., 106(B8), 16,213-16,221.
- Chiodini G., Brombach T., Caliro S., Cardellini C., 2002. *Geochemical indicators of possible ongoing volcanic unrest at Nisyros Island (Greece)*. Geophys. Res. Lett., 29(16), 1759, doi: 10.1029/2001GL014355.
- Chiodini G., Todesco M., Caliro S., Del Gaudio C., Macedonio G., Russo M., 2003. *Magma degassing as a trigger of bradyseismic events: The case of Phlegrean Fields (Italy)*. Geophys. Res. Lett., 30(8), 1434, doi: 10.1029/2002GL016790.
- Chiodini G., Avino R., Brombach T., Caliro S., Cardellini C., De Vita S., Frondini F., Granieri D., Marotta E., Ventura G., 2004a. *Fumarolic and diffuse soil degassing west of Mount Epomeo, Ischia, Italy*. J. Volcanol. Geoth. Res., 133, 291-309, doi: 10.1016/S0377-0273(03)00403-7.
- Chiodini G., Cardellini C., Amato A., Boschi E., Caliro S., Frondini F., Ventura G., 2004b. *Carbon dioxide Earth degassing and seismogenesis in central and southern Italy*. Geophys. Res. Lett., 31, L07615, doi: 10.1029/2004GL019480.
- Chiodini G., Granieri D., Avino R., Caliro S., Costa A., 2005. *Carbon dioxide diffuse degassing and estimation of heat release from volcanic and hydrothermal systems*. J. Geophys. Res., 110, B08204, doi:10.1029/2004JB003542.
- Chiodini G., 2008. *A new web-based catalog of Earth degassing sites in Italy*. Eos, 89(37), 341-342.
- Chiodini G., Caliro S., Cardellini C., Granieri D., Avino R., Baldini A., Donnini M., Minopoli C., 2010a. *Long-term variations of the Campi Flegrei, Italy, volcanic system as revealed by the monitoring of hydrothermal activity*. J. Geophys. Res., 115, B03205, doi:10.1029/2008JB006258.
- Chiodini G., Cioni R., Guidi M., Raco B., Marini L., 2010b. *Soil CO₂ flux measurements in volcanic and geothermal areas*. Appl. Geochem., 13(5), 543-552.
- Chiodini G., Caliro S., De Martino P., Avino R., Gherardi F., 2012. *Early signals of new volcanic unrest at Campi Flegrei caldera? Insights from geochemical*
-

References

- data and physical simulations*. *Geology*, 40, 943-946, doi: 10.1130/G33251.1.
- Chiodini G., Cardellini C., Caliro S., Chiarabba C., Frondini F., 2013. *Advective heat transport associated with regional Earth degassing in central Apennine (Italy)*. *Earth Planet. Sc. Lett.*, 373, 65-74, doi: 10.1016/j.epsl.2013.04.009.
- Chiodini G., Vandemeulebrouck J., Caliro S., D'Auria L., De Martino P., Mangiacapra A., Petrillo Z., 2015. *Evidence of thermal-driven processes triggering the 2005-2014 unrest at Campi Flegrei caldera*. *Earth Planet. Sci. Lett.*, 414, 58-67, doi: 10.1016/j.epsl.2015.01.012.
- Cimarelli C., De Rita D., 2006. *Structural evolution of the Pleistocene Cimini trachytic volcanic complex (central Italy)*. *Bull. Volcanol.*, 68, 538-548, doi: 10.1007/s00445-005-0028-3.
- Cinti D., Tassi F., Procesi M., Bonini M., Capecchiacci F., Voltattorni N., Vaselli O., Quattrocchi F., 2014. *Fluid geochemistry and geothermometry in the unexploited geothermal field of the Vicano-Cimino Volcanic District (Central Italy)*. *Chem. Geol.*, 371, 96-114, doi: 10.1016/j.chemgeo.2014.02.005.
- Cioni R., Corazza E., Marini L., 1984. *The gas/steam ratio as indicator of heat transfer at the Solfatara fumaroles, Phlegrean Fields (Italy)*. *Bull. Volcanol.*, 47(2), 295-302.
- Cioni R., Corazza E., Fratta M., Guidi M., Magro G., Marini L., 1989. *Geochemical precursors at Solfatara volcano, Pozzuoli (Italy)*. In: . Latter J. H. (ed.), *Volcanic Hazard*, Springer Verlag, Berlin, pp. 384-398.
- Civetta L., Orsi G., Scandone P., Pece R., 1978. *Eastwards migrations of the Tuscan anatectic magmatism due to anticlock wise rotation of the Apennines*. *Nature*, 276, 604-606.
- Clark I., 2015. *Groundwater geochemistry and isotopes*. CRC Press, Boca Raton (FL), p. 456.
- Cody G.D., Boctor N.Z., Brandes J.A., Filley T.R., Hazen R.M., Yoder H.S.Jr., 2004. *Assaying the catalytic potential of transition metal sulfides for abiotic carbon fixation*. *Geochim. Cosmochim. Ac.*, 68(10), 2185-2196.
- Corrado G., Guerra I., Lo Bascio A., Luongo G., Rampoldi R., 1977. *Inflation and microearthquake activity of Phlegrean Fields, Italy*. *Bull. Volcanol.*, 40(3), 169-188.
- Corrado, G., De Lorenzo S., Mongelli F., Tramacere A., Zito G., 1998. *Surface heat flow density at the Phlegraean Fields Caldera (Southern Italy)*. *Geothermics*, 27, 469-484.
- Crittendon R.C., Parsons E.J., 1994. *Transformations of cyclohexane derivatives in supercritical water*. *Organometallics*, 13, 2587-2591.
- D'Alessandro W., Brusca L., Kyriakopoulos K., Martelli M., Michas G., Papadakis G., Salerno F., 2011. *Diffuse hydrothermal methane output and evidence of methanotrophic activity within the soils at Sousaki (Greece)*. *Geofluids*, 11, 97-107, doi: 10.1111/j.1468-8123.2010.00322.x.
- Dale Ortego J., Kowalska M., Cocke D.L., 1991. *Interactions of montmorillonite with organic compounds - adsorptive and catalytic properties*. *Chemosphere*,

-
- 22(8), 769-798.
- Darling W.G., 1998. *Hydrothermal hydrocarbon gases: 1, Genesis and geothermometry*. Appl. Geochem., 13(7), 815-824.
- De Vivo B., Rolandi G., Gans P.B., Calvert A., Bohrson W.A., Spera F.J., Belkin H.E., 2001. *New constraints on the pyroclastic eruptive history of the Campanian volcanic Plain (Italy)*. Miner. Petrol., 73, 47-65, doi: 10.1007/s0071001700-10.
- Deino A.L., Orsi G., de Vita S., Piochi M., 2004. *The age of the Neapolitan Yellow Tuff caldera-forming eruption (Campi Flegrei caldera - Italy) assessed by $^{40}\text{Ar}/^{39}\text{Ar}$ dating method*. J. Volcanol. Geoth. Res., 133, 157-170, 10.1016/S03-77-0273(03)00396-2.
- Derwent R.G., 1995. *Source, distribution and fate of VOCs in the atmosphere*. Environ. Sci. Technol., 4, 1-15.
- Des Marais D.J., Donchin J.N., Nehring N.L., Truesdell A.H., 1981. *Molecular carbon isotopic evidence for the origin of geothermal hydrocarbons*. Nature, 292, 826-828.
- Di Filippo M., Toro B., 1995. *Gravity features. Stratigraphy and volcano-tectonics*. In: Trigila R. (Ed.), *The Volcano of the Alban Hills, Rome*, pp. 213-219.
- DiPippo R., 2008. *Geothermal Power Plants: Principles, Applications, Case Studies and Environmental Impact, 2nd Edition*, Butterworth-Heinemann (Elsevier), Oxford, pp. 520.
- Di Vito M., Lirer L., Mastrolorenzo G., Rolandi G., 1987. *The 1538 Monte Nuovo eruption (Campi Flegrei, Italy)*. Bull. Volcanol., 49, 608-615.
- Doğan T., Sumino H., Nagao K., Notsu K., Tuncer M.K., Çelik C., 2009. *Adjacent releases of mantle helium and soil CO₂ from active faults: Observations from the Marmara region of the North Anatolian Fault zone, Turkey*. Geochem. Geophys. Geos., 10(11), Q11009, doi: 10.1029/2009GC002745.
- Dvorak J.J., Berrino G., 1991. *Recent ground movement and seismic activity in Campi Flegrei, Southern Italy: Episodic growth of a resurgent dome*. J. Geophys. Res., 96(B2), 2309-2323.
- Etiope G., Fridriksson T., Italiano F., Winiwarter W., Theloke J., 2007. *Natural emissions of methane from geothermal and volcanic sources in Europe*. J. Volcanol. Geoth. Res., 165, 76-86, doi: 10.1016/j.jvolgeores.2007.04.014.
- Etiope G., Ciccioli P., 2009. *Earth's degassing: a missing ethane and propane source*. Science, 323, 478, doi: 10.1126/science.1165904.
- Evans, W.C., White, L.D., Rapp, J.B., 1998. *Geochemistry of some gases in hydrothermal fluids from the southern Juan de Fuca ridge*. J. Geophys. Res., 15, 305-313.
- Evans W.C., Sorey M.L., Cook A.C., Kennedy B.M., Shuster D.L., Colvard E.M., White L.D., Huebner M.A., 2002. *Tracing and quantifying magmatic carbon discharge in cold groundwaters: lessons learned from Mammoth Mountain, USA*. J. Volcanol. Geotherm. Res., 114, 291-312.
-

References

- Eyice Ö., Namura M., Chen Y., Mead A., Samavedam S., Schäfer H., 2015. *SIP metagenomics identifies uncultivated Methylophilaceae as dimethylsulphide degrading bacteria in soil and lake sediment*. ISME J., 9(11), 2336-2348, doi: 10.1038/ismej.2015.37.
- Ferris J.P., 2005. *Mineral catalysis and prebiotic synthesis: montmorillonite-catalyzed formation of RNA*. Elements, 1, 145-149.
- Fiebig J., Chiodini G., Caliro S., Rizzo A., Spangenberg J., Hunziker J.C., 2004. *Chemical and isotopic equilibrium between CO₂ and CH₄ in fumarolic gas discharges: generation of CH₄ in arc magmatic-hydrothermal systems*. Geochim. Cosmochim. Ac., 68(10), 2321-2334, doi: 10.1016/j.gca.2003.10.035.
- Fiebig J., Woodland A.B., Spangenberg J., Oschmann W., 2007. *Natural evidence for rapid abiogenic hydrothermal generation of CH₄*. Geochim. Cosmochim. Ac., 71, 3028-3039, doi: 10.1016/j.gca.2007.04.010.
- Fiebig J., Woodland A.B., D'Alessandro W., Püttmann W., 2009. *Excess methane in continental hydrothermal emissions is abiogenic*. Geology, 37(6), 495-498, doi: 10.1130/G25598A.1.
- Fiebig J., Tassi F., D'Alessandro W., Vaselli O., Woodland A.B., 2013. *Carbon-bearing gas geothermometers for volcanic-hydrothermal systems*. Chem. Geol., 351, 66-75, doi: 10.1016/j.chemgeo.2013.05.006.
- Fiebig J., Hofmann S., Tassi F., D'Alessandro W., Vaselli O., Woodland A.B., 2015. *Isotopic patterns of hydrothermal hydrocarbons emitted from Mediterranean volcanoes*. Chem. Geol., 396, 152-163, doi: 10.1016/j.chemgeo.2014.12.030.
- Findlayson J.B., Barnes I.L., Naughton J.J., 1968. *Developments in volcanic gas research in Hawaii*. In: Knopoff L., Drake C.L., Hart P.J. (eds.), *The crust and mantle of the Pacific Basin*, Am. Geophys. Union Geophys. Mon., 12, pp. 428-439.
- Fischer F., Tropsch H., 1923. *The preparation of synthetic oil mixtures (synthol) from carbon monoxide and hydrogen*. Brennst. Chem., 4, 276-285.
- Fischer F., Tropsch H., 1926. *The synthesis of petroleum at atmospheric pressure from gasification products of coal*. Brennst. Chem., 7, 97-104.
- Foght J., 2008. *Anaerobic biodegradation of aromatic hydrocarbons: pathways and prospects*. J. Mol. Microbiol. Biotechnol., 15, 93-120, doi: 10.1159/000121324.
- Francalanci L., Vougioukalakis G.E., Perini G., Manetti P., 2005. *A West-East Traverse along the magmatism of the south Aegean volcanic arc in the light of volcanological, chemical and isotope data*. In: Fytikas M., Vougioukalakis G.E. (eds.), *The South Aegean Active Volcanic Arc, present knowledge and future perspectives*. Developments in Volcanology, Elsevier, Amsterdam, 2005.
- Frepoli A., Amato A., 1997. *Contemporaneous extension and compression in the Northern Apennines from earthquake fault-plane solutions*. Geophys. J. Int., 129, 368-388.
- Frische M., Garofalo K., Hansteen T.H., Borchers R., Harnisch J., 2006. *The origin of stable halogenated compounds in volcanic gases*. Environ. Sci. Pollut. Res., 13(6), 406-413, doi: 10.1065/espr2006.01.291.

-
- Fritsche W., Hofrichter M., 2008. *Aerobic degradation by microorganisms*. In: Rehm H.J., Reed G. (eds.), *Biotechnology: Environmental Processes II, Volume 11b, Second Edition*, 144-167.
- Froncini F., Caliro S., Cardellini C., Chiodini G., Morgantini N., Parello F., 2008. *Carbon dioxide degassing from Tuscany and Northern Latium (Italy)*. *Global Planet. Change*, 61, 89-102, doi: 10.1016/j.gloplacha.2007.08.009.
- Fu Q., Foustoukos D.I., Seyfried W.E.Jr., 2008. *Mineral catalyzed organic synthesis in hydrothermal systems: An experimental study using time-of-flight secondary ion mass spectrometry*. *Geophys. Res. Lett.*, 35(L07612), doi: 10.1029/2008GL033389.
- Fuchs G., Boll M., Heider J., 2011. *Microbial degradation of aromatic compounds – from one strategy to four*. *Nat. Rev. Microbiol.*, 9, 803-816, doi: 10.1038/nrmicro2652.
- Gadd G.M., 2010. *Metals, minerals and microbes: geomicrobiology and bioremediation*. *Microbiology*, 156, 609-643, doi: 10.1099/mic.0.037143-0.
- Gagliano A.L., D'Alessandro W., Tagliavia M., Parello F., Quatrini P., 2014. *Methanotrophic activity and diversity of methanotrophs in volcanic geothermal soils at Pantelleria (Italy)*. *Biogeosciences*, 11, 5865-5875, doi: 10.5194/bg-11-5865-2014.
- Gagliano A.L., Tagliavia M., D'Alessandro W., Franzetti A., Parello F., Quatrini P., 2015. *So close, so different: geothermal flux shapes divergent soil microbial communities at neighbouring sites*. *Geobiology*, 14(2), 150-162, doi: 10.1111/gbi.12167.
- Gal F., Gadalia A., 2011. *Soil gas measurements around the most recent volcanic system of metropolitan France (Lake Pavin, Massif Central)*. *C. R. Geosci.*, 343, 43-54, doi: 10.1016/j.crte.2010.11.008.
- Galbraith D., Gross S.A., Paustenbach D., 2010. *Benzene and human health: A historical review and appraisal of associations with various diseases*. *Crit. Rev. Toxicol.*, 40(2), 1-46, doi: 10.3109/10408444.2010.508162.
- Gambardella B., Cardellini C., Chiodini G., Froncini F., Marini L., Ottonello G., Vetuschi Zuccolini M., 2004. *Fluxes of deep CO₂ in the volcanic areas of central-southern Italy*. *J. Volcanol. Geotherm. Res.*, 136, 31-52, doi: 10.1016/j.jvolgeores.2004.03.018.
- Gennadiev A.N., Pikovskii Y.I., Tsibart A.S., Smirnova M.A., 2015. *Hydrocarbons in soils: origin, composition, and behavior (review)*. *Eurasian Soil Sci+*, 48(10), 1076-1089, doi: 10.1134/S1064229315100026.
- Geotermica Italiana, 1983. *Nisyros 1 geothermal well*. Unpublished PPC-EEC report, pp. 106.
- Geotermica Italiana, 1984. *Nisyros 2 geothermal well*. Unpublished PPC-EEC report, pp. 44.
- Giggenbach W.F., 1975. *A simple method for collection and analysis of volcanic gases*. *Bull. Volcanol.*, 39(1), 132-145.
-

References

- Giggenbach W.F., 1980. *Geothermal gas equilibria*. *Geochim. Cosmochim. Ac.*, 44, 2021-2032.
- Giggenbach W.F., Martini M., Corazza E., 1986. *The effects of hydrothermal processes on the chemistry of some recent volcanic gas discharges*. *Per. Mineral.*, 55, 15-28.
- Giggenbach W.F., 1987. *Redox processes governing the chemistry of fumarolic gas discharges from White Island, New Zealand*. *Appl. Geochem.*, 2, 143-161.
- Giggenbach W.F., Minissale A.A., Scandiffio G., 1988. *Isotopic and chemical assessment of geothermal potential of the Colli Albani area, Latium region, Italy*. *Appl. Geochem.*, 3, 475-486.
- Giggenbach W.F., 1996. *Chemical Composition of Volcanic Gases*. In: Scarpa R., Tilling R.I. (eds), *Monitoring and Mitigation of Volcano Hazards*, Springer, Berlin, Heidelberg, pp. 221-256.
- Giggenbach W.F., 1997. *Relative importance of thermodynamic and kinetic processes in governing the chemical and isotopic composition of carbon gases in high-heatflow sedimentary basins*. *Geochim. Cosmochim. Ac.*, 16(17), 3763-3785.
- Giordano G., De Benedetti A.A., Diana A., Diano G., Gaudioso F., Marasco F., Miceli M., Mollo S., Cas R.A.F., Funicello R., 2006. *The Colli Albani mafic caldera (Roma, Italy): Stratigraphy, structure and petrology*. *J. Volcanol. Geotherm. Res.*, 155, 49-80, doi: 10.1016/j.jvolgeores.2006.02.009.
- Girelli A., 1969. *Petrolio e Petrochimica*. In: *Trattato di Chimica Industriale ed Applicata*, Zanichelli N. (Ed.), Bologna, 2, 929-1126.
- Glamoclija M., Garrel L., Berthon J., López-García P., 2004. *Biosignatures and bacterial diversity in hydrothermal deposits of Solfatara crater, Italy*. *Geomicrobiol. J.*, 21, 529-541, doi: 10.1080/01490450490888235.
- Goesmann F., Rosenbauer H., Bredehöft J.H., Cabane M., Ehrenfreund P., Gautier T., Giri C., Krüger H., Le Roy L., MacDermott A.J., McKenna-Lawlor S., Meierhenrich U.J., Muñoz Caro G.M., Raulin F., Roll R., Steele A., Steininger H., Sternberg R., Szopa C., Thiemann W., Ulamec S., 2015. *Organic compounds on comet 67P/Churyumov-Gerasimenko revealed by COSAC mass spectrometry*. *Science*, 349(6247), doi: 10.1126/science.aab0689.
- Gottsmann J., Rymer H., Berrino G., 2006. *Unrest at the Campi Flegrei caldera (Italy): A critical evaluation of source parameters from geodetic data inversion*. *J. Volcanol. Geoth. Res.*, 150, 132-145, doi: 10.1016/j.jvolgeores.2005.07.002.
- Granieri D., Chiodini G., Marzocchi W., Avino R., 2003. *Continuous monitoring of CO₂ soil diffuse degassing at Phlegrean Fields (Italy): influence of environmental and volcanic parameters*. *Earth Planet. Sc. Lett.*, 212, 167-179, doi: 10.1016/S0012-821X(03)00232-2.
- Granieri D., Avino R., Chiodini G., 2010. *Carbon dioxide diffuse emission from the soil: ten years of observations at Vesuvio and Campi Flegrei (Pozzuoli), and linkages with volcanic activity*. *Bull. Volcanol.*, 72, 103-118, doi: 10.1007/s00445-009-0304-8.

-
- Guéret C., Daroux M., Billaud F., 1997. *Methane pyrolysis: thermodynamics*. Chem. Eng. Sci., 52(2), 815-827.
- Gunter B.D., 1978. *C₁-C₄ hydrocarbons in hydrothermal gases*. Geochim. Cosmochim. Ac., 42, 137-139.
- Hand E., 2015. *Mars rover finds long-chain organic compounds*. Science, 347(6229), 1402-1403, doi: 10.1126/science.347.6229.1402.
- Hanson R.S., Hanson T.E., 1996. *Methanotrophic bacteria*. Microbiol. Rev., 60(2), 439-471.
- Hazen R.M., Papineau D., Bleeker W., Downs R.T., Ferry J.M., McCoy T.J., Sverjensky D.A., Yang H., 2008. *Mineral evolution*. Am. Mineral., 93, 1693-1720, doi: 10.2138/am.2008.2955.
- He H., Zhong Y., Liang X., Tan W., Zhu J., Wang C.Y., 2015. *Natural magnetite: an efficient catalyst for the degradation of organic contaminant*. Sci. Rep., 5:10139, doi: 10.1038/srep10139.
- Heinen W., Lauwers A.M., 1996. *Organic sulfur compounds resulting from the interaction of iron sulfide, hydrogen sulfide and carbon dioxide in an anaerobic aqueous environment*. Orig. Life Evol. Biosph., 26, 131-150.
- Heinicke J., Martinelli G., Telesca L., 2012. *Geodynamically induced variations in the emission of CO₂ gas at San Faustino (Central Apennines, Italy)*. Geofluids, 12(2), 123-132, doi: 10.1111/j.1468-8123.2011.00345.x.
- Helgeson H.C., Owens C.E., Knox A.M., Richard L., 1998. *Calculation of the standard molal thermodynamic properties of crystalline, liquid, and gas organic molecules at high temperatures and pressures*. Geochim. Cosmochim. Ac., 62(6), 985-1081.
- Henson J., Redman R., Rodriguez R., Stout R., 2005. *Fungi in Yellowstone's geothermal soils and plants*. Yellowstone Science, 13(4), 25-30.
- Hoefs J., 2009. *Stable isotope geochemistry, 6th Edition*. Springer, Berlin, p. 285.
- Holliger C., Wohlfarth G., Diekert G., 1999. *Reductive dechlorination in the energy metabolism of anaerobic bacteria*. FEMS Microbiol. Rev., 22, 383-398.
- Holmen A., Olsvik O., Rokstad O.A., 1995. *Pyrolysis of natural gas: chemistry and process concepts*. Fuel Process. Technol., 42, 249-267.
- Hooker P.J., Bertrami R., Lombardi S., O'Nions R.K., Oxburgh E.R., 1985. *Helium-3 anomalies and crust-mantle interaction in Italy*. Geochim. Cosmochim. Ac., 49, 2505-2513.
- HSDB, *Hazardous Substances Data Bank*, web site: <<http://toxnet.nlm.nih.gov/cgi-bin/sis/htmlgen?HSDB>>.
- Huber R., Sacher M., Vollmann A., Huber H., Rose D., 2000. *Respiration of arsenate and selenate by hyperthermophilic Archaea*. System. Appl. Microbiol., 23, 305-314.
- Huff J., 2007. *Benzene-induced cancers: abridged history and occupational health impact*. Int. J. Occup. Environ. Health, 13(2), 213-221, doi: 10.1179/oeh.2007-13.2.213.
-

References

- Hunt J.M., 1979. *Petroleum Geochemistry and Geology*. W.H. Freeman Publishing Co., San Francisco, pp. 617.
- Hunt J.M., 1984. *Generation and migration of light hydrocarbons*. Science, 226, 1265-1270.
- Hurni L., Jenny B., Gogu R., Freimark H., Terribilini A., Dietrich V., 2005. *Geowarn: a web-based atlas information system for volcanic monitoring*. Proceedings of the 21st International Cartographic Conference ICC 2005, A Coruña, Spain.
- Iacono Marziano G., Gaillard F., Pichavant M., 2007. *Limestone assimilation and the origin of CO₂ emissions at the Alban Hills (Central Italy): Constraints from experimental petrology*. J. Volcanol. Geotherm. Res., 166(2), 91-105, doi: 10.1016/j.jvolgeores.2007.07.001.
- Ingmanson D.E., Dowler M.J., 1977. *Chemical evolution and the evolution of the Earth's crust*. Orig. Life, 8(3), 221-224.
- Insam H., Seewald M.S.A., 2010. *Volatile organic compounds (VOCs) in soils*. Biol. Fertil. Soils, 46, 199-213, doi: 10.1007/s00374-010-0442-3.
- Isidorov V.A., Zenkevich I.G., Ioffe B.V., 1990. *Volatile Organic Compounds in Solfataric Gases*. J. Atmos. Chem., 10, 329-340.
- IPCC, 2007. *Climate Change 2007: The Physical Science Basis*. In: Solomon S., Qin D., Manning M., Chen Z., Marquis M., Averyt K.B., Tignor M., Miller H.L. (eds.), *Contribution of Working Group I to the Fourth Assessment Report of the Intergovernmental Panel on Climate Change*, Cambridge University Press. Cambridge, United Kingdom, pp. 996.
- Johnson J.W., Oelkers E.H., Helgeson H.C., 1992. *SUPCRT92: A software package for calculating the standard molal thermodynamic properties of minerals, gases, aqueous species, and reactions from 1 to 5000 bar and 0 to 1000 C*. Comput. Geosci., 18, 899-947.
- Jordan A., Harnisch J., Borchers R., Le Guern F., Shinohara H., 2000. *Volcanogenic Halocarbons*. Environ. Sci. Technol., 34(6), 1122-1124, doi: 10.1021/es990838q.
- Kämpf H., Bräuer K., Schumann J., Hahne K., Strauch G., 2013. *CO₂ discharge in an active, non-volcanic continental rift area (Czech Republic): Characterisation ($\delta^{13}C$, $^3He/^4He$) and quantification of diffuse and vent CO₂ emissions*. Chem. Geol., 339, 71-83, doi: 10.1016/j.chemgeo.2012.08.005.
- Kansal A., 2009. *Sources and reactivity of NMHCs and VOCs in the atmosphere: A review*. J. Hazard. Mater., 166, 17-26, doi: 10.1016/j.jhazmat.2008.11.048.
- Kaschke M., Russell M.J., Cole W.J., 1994. *[FeS/FeS₂], a redox system for the origin of life*. Origins Life Evol. Biosphere, 24, 43-56.
- Katritzky A.R., Balasubramanian M., Siskin M., 1990. *Aqueous high-temperature chemistry of carbo- and heterocycles. 2. Monosubstituted benzenes: benzyl alcohol, benzaldehyde, and benzoic acid*. Energ. Fuel., 4, 449-505.
- Katritzky A.R., Allin S.M., Siskin M., 1996. *Aquathermolysis: Reactions of organic compounds with superheated water*. Acc. Chem. Res., 29(8), 399-406.

-
- Kaur N., Kishore D., 2012. *Montmorillonite: An efficient, heterogeneous and green catalyst for organic synthesis*. J. Chem. Pharm. Res., 4(2), 991-1015.
- Kavouridis T., Kuris D., Leonis C., Liberopoulou V., Leontiadis J., Panichi C., La Ruffa G., Caprai A., 1999. *Isotope and chemical studies for a geothermal assessment of the island of Nisyros (Greece)*. Geothermics, 28, 219-239.
- Kerrick D.M., McKibben M.A., Seward T.M., Caldeira K., 1995. *Convective hydrothermal CO₂ emission from high heat flow regions*. Chem. Geol., 121, 285-293.
- Killops S., Killops V., 2005. *Introduction to organic geochemistry, Second Edition*. Blackwell Publ., Malden, MA, pp. 393.
- Kinwig H.S., Winson A., Gottsmann J., 2010. *Analysis of volcanic threat from Nisyros Island, Greece, with implications for aviation and population exposure*. Nat. Hazards Earth Syst. Sci., 10, 1101-1113, doi: 10.5194/nhess-10-1101-2010.
- Konn C., Charlou J.L., Donval J.P., Holm N.G., Dehairs F., Bouillon S., 2009. *Hydrocarbons and oxidized organic compounds in hydrothermal fluids from Rainbow and Lost City ultramafic-hosted vents*. Chem. Geol., 258, 299-314, doi: 10.1016/j.chemgeo.2008.10.034.
- Konn C., Testemale D., Querellou J., Holm N.G., Charlou J.L., 2011. *New insight into the contributions of thermogenic processes and biogenic sources to the generation of organic compounds in hydrothermal fluids*. Geobiology, 9(1), 79-93, doi: 10.1111/j.1472-4669.2010.00260.x.
- Konn C., Charlou J.L., Holm N.G., Mousis O., 2015. *The production of methane, hydrogen and organic compounds in ultramafic-hosted hydrothermal vents of the Mid-Atlantic Ridge*. Astrobiology, 15(5), 381-399, doi: 10.1089/ast.2014.1198.
- Lagios E., Sakkas V., Parcharidis Is., Dletrich V., 2005. *Ground deformation of Nisyros Volcano (Greece) for the period 1995-2002: Results from DInSAR and DGPS observations*. Bull. Volcanol., 68, 201-214, doi: 10.1007/s00445-005-0004-y.
- Lardini D., Nappi G., 1987. *I cicli eruttivi del Complesso Vulcanico Cimino*. Rendiconti Società Italiana di Mineralogia e Petrologia, 42, 141-153.
- Laurenzi A.M., Villa I.M., 1987. ⁴⁰Ar/³⁹Ar chronostratigraphy of Vico ignimbrites. Period. Mineral., 56, 285-293.
- Lebedev M.M., Dekusar Z.B., 1980. *Hydrocarbons in geothermal water on South Kamchatka*. Vulcanol. i Seismol., 5, 93-97.
- Leff J.W., Fierer N., 2008. *Volatile organic compound (VOC) emissions from soil and litter samples*. Soil Biol. Biochem., 40, 1629-1636, doi: 10.1016/j.soilbio.2008.01.018.
- Leif R.N., Simoneit B.R.T., 1995. *Ketones in hydrothermal petroleum and sediment extracts from Guaymas Basin, Gulf of California*. Org. Geochem., 23(10), 889-904.
- Lewicki J.L., Evans W.C., Hilley G.E., Sorey M.L., Rogie J.D., Brantley S.L., 2003. *Shallow soil CO₂ flow along the San Andreas and Calaveras Faults, California*.
-

References

- J. Geophys. Res., 108(B4), 2187, doi: 10.1029/2002JB002141.
- Lien P.J., Yang Z.H., Chang Y.M., Tu Y.T., Kao C.M., 2016. *Enhanced bioremediation of TCE-contaminated groundwater with coexistence of fuel oil: Effectiveness and mechanism study*. Chem. Eng. J., 289, 525-536, doi: 10.1016/j.cej.2016.01.011.
- Lineweaver C.H., Schwartzman D., 2003. *Cosmic thermobiology: Thermal constraints on the origin and evolution of life in the universe*. Cell. Origin Life Ext., 6, 223-248.
- Liss P.S., Lovelock J.E., 2007. *Climate change: the effect of DMS emissions*. Environ. Chem., 4, 377-378, doi: 10.1071/EN07072.
- Little C.D., Palumbo A.Y., Herbes S.E., Lidstrom M.E., Tyndall R.L., Gilmer P.J., 1988. *Trichloroethylene biodegradation by a methane-oxidizing bacterium*. Appl. Environ. Microbiol., 54(4), 951-956.
- Madigan M.T., Marris B.L., 1997. *Extremophiles*. Sci. Am., 276, 82-87.
- Mango F., Jarvie D., Herriman E., 2009. *Natural gas at thermodynamic equilibrium. Implications for the origin of natural gas*. Geochem. Trans., 10(6), doi: 10.1186/1467-4866-10-6.
- Marinelli G., 1975. *Magma evolution in Italy*. In: Squyres C.H. (Ed.), *Geology of Italy*. The Earth Science Society of the Libyan Arab Republic, Tripoli, pp. 165-219.
- Marini L., Fiebig J., 2005. *Fluid geochemistry of the magmatic-hydrothermal system of Nisyros (Greece)*. Mém. Géol., 44, 192.
- Marini L., Gambardella B., 2005. *Geochemical modeling of magmatic gas scrubbing*. Ann. Geophys., 48(4/5), 739-753.
- Marini L., Principe C., Chiodini G., Cioni R., Frytikas M., Marinelli G., 1993. *Hydrothermal eruptions of Nisyros (Dodecanese, Greece)*. Past events and present hazard. J. Volcanol. Geotherm. Res., 56, 71-95.
- Mariucci M.T., Amato A., Montone P., 1999. *Recent tectonic evolution and present stress in the Northern Apennines (Italy)*. Tectonics, 18(1), 108-118.
- Markhinin E.K., Podkletnov N.E., Zbrueva A.I., 1975. *Amino-acids, hydrocarbons and other organic compounds in juvenile volcanic ash*. RAS USSR, 222, 1438-1440.
- Martin W., Baross J., Kelley D., Russell M.J., 2008. *Hydrothermal vents and the origin of life*. Nat. Rev. Microbiol., 6, 805-814, doi: 10.1038/nrmicro1991.
- Martini M., Cellini Legittimo P., Piccardi G., Giannini L., 1986. *The fumaroles of Vulcano (Italy): differences in chemical compositions produced by the surface environment*. Geothermics, 15, 205-209.
- Matsuo S., 1961. *On the chemical nature of fumarolic gases of Vulcano Showashinzan, Hokkaido, Japan*. J. Earth Sci. Nagoya Univ., 8, 80-100.
- Matsuo S., 1988. *Activity report of Japanese Group for the chemical prediction of volcanic eruptions*. Per. Mineral., 55, 39-53.
- Mattei M., Conticelli S., Giordano G., 2010. *The Tyrrhenian margin geological setting: from the Apennine orogeny to the K-rich volcanism*. In: Funiciello R.,

-
- Giordano G. (eds.), *The Colli Albani Volcano*. Special Publications of IAVCEI, 3, 7-27.
- McCollom T.M., 2013. *Laboratory simulations of abiotic hydrocarbon formation in Earth's deep subsurface*. Rev. Mineral. Geochem., 75, 467-494, doi: 10.2138/rmg.2013.75.15.
- McCollom T.M., Seewald J.S., Simoneit B.R.T., 2001. *Reactivity of monocyclic aromatic compounds under hydrothermal conditions*. Geochim. Cosmochim. Ac., 65(3), 455-468.
- McCollom T.M., Seewald J.S., 2003. *Experimental constraints on the hydrothermal reactivity of organic acids and acid anions: I. Formic acid and formate*. Geochim. Cosmochim. Ac., 67(19), 3625-3644, doi: 10.1016/S0016-7037(03)00136-4.
- McCollom T.M., Seewald J.S., 2007. *Abiotic synthesis of organic compounds in deep-sea hydrothermal environments*. Chem. Rev., 107, 382-401, doi: 10.1021/cr0503660.
- McSween H.Y., Richardson S.M., Uhle M.E., 2003. *Geochemistry: Pathways and Processes, Second Edition*. Columbia University Press, New York, pp. 363.
- Megharaj M., Ramakrishnan B., Venkateswarlu K., Sethunathan N., Naidu R., 2011. *Bioremediation approaches for organic pollutants: A critical perspective*. Environ. Int., 37(8), 1362-1375, doi: 10.1016/j.envint.2011.06.003.
- Mendes R., Garbeva P., Raaijmakers J.M., 2013. *The rhizosphere microbiome: significance of plant beneficial, plant pathogenic, and human pathogenic microorganisms*. FEMS Microbiol. Rev., 37, 634-663, doi: 10.1111/1574-6976.12028.
- Meyer-Dombard D.R., Shock E.L., Amend J.P., 2005. *Archaeal and bacterial communities in geochemically diverse hot springs of Yellowstone National Park, USA*. Geobiology, 3, 211-217.
- Miller S.L., Urey H.C., 1959. *Organic compound synthesis on the Primitive Earth*. Science, 130(3370), 245-251.
- Minissale A., 2000. *Origin, transport and discharge of CO₂ in central Italy*. Earth-Sci. Rev., 66, 89-141, doi: 10.1016/j.earscirev.2003.09.001.
- Minissale A., Magro G., Martinelli G., Vaselli O., Tassi F., 2000. *Fluid geochemical transect in the Northern Apennines (central-northern Italy): fluid genesis and migration and tectonic implications*. Tectonophysics, 319, 199-222.
- Minissale A., 2002. *Geochemical and geophysical methods in geothermal exploration*. In: Chandrasekharam D., Bundschuh J. (eds.), *Geothermal energy resources for developing countries*, Swets & Zeitlinger, Lisse, The Netherlands, pp. 179-194.
- Minissale A., 2004. *Origin, transport and discharge of CO₂ in central Italy*. Earth-Sci. Rev., 66, 89-141, doi: 10.1016/j.earscirev.2003.09.001.
- Minissale A., 2014. *Chemical hierarchy of hydrothermal signals at surface and hierarchy of eventual geophysical investigations in geothermal exploration*. Proceedings 5th African Rift geothermal Conference, Arusha, Tanzania, 29-31 October 2014.
-

References

- Montegrossi G., Tassi F., Vaselli O., Buccianti A., Garofalo K., 2001. *Sulphur species in volcanic gases*. Anal. Chem., 73, 3709-3715, doi: 10.1021/ac001429b.
- Mukhin L. M., Bondarev V. B., and Safonova E. N., 1978. *The role of volcanic processes in the evolution of organic compounds on the primitive Earth*. Modern Geol., 6, 119-122.
- Mukhopadhyay A., 2015. *Tolerance engineering in bacteria for the production of advanced biofuels and chemicals*. Trends Microbiol., 23(8), 498-508, doi: 10.1016/j.tim.2015.04.008.
- Nelson D., Cox M., 2005. *Lehninger principles of biochemistry, Forth Edition*. W.H. Freeman and Company, New York, pp. 1216.
- Nicoletti M., 1969. *Datazioni argon-potassio di alcune vulcanite delle regioni vulcaniche Cimina e Vicana*. Period. Mineral., 38, 1-20.
- NIST, 2005. *NIST/EPA/NIH Mass Spectral Library, 2005*, web site: <<http://www.nist.gov/srd/nist1a.htm>>.
- Norris T.B., Wraith J.M., Castenholz R.W., McDermott T.R., 2002. *Soil microbial community structure across a thermal gradient following a geothermal heating event*. Appl. Environ. Microbiol., 68(12), 6300-6309, doi: 10.1128/AEM.68.12-6300-6309.2002.
- North F.K., 1995. *Petroleum geology*. Chapman & Hall (Ed.), Londra, pp. 631.
- Owen S.M., Boissard C., Hewitt C.N., 2001. *Volatile organic compounds (VOCs) emitted from 40 Mediterranean plant species: VOC speciation and extrapolation to habitat scale*. Atmos. Environ., 35, 5393-5409.
- Papadopoulos G.A., Sachpazi M., Panopoulou G., Stavrakakis G., 1998. *The volcanoseismic crisis of 1996-97 in Nisyros, SE Aegean Sea, Greece*. Terra Nova, 10(3), 151-154.
- Peccerillo A., 1999. *Multiple mantle metasomatism in central-southern Italy: geochemical effects, timing and geodynamic implications*. Geology, 27, 315-318.
- Peccerillo A., 2005. *Plio-Quaternary volcanism in Italy. Petrology, Geochemistry, Geodynamics*. Springer, Heidelberg, pp. 365.
- Pe-Piper G., Piper D.J.W., 2005. *The South Aegean active volcanic arc: relationships between magmatism and tectonics*. Developments in Volcanology, 7, 113-133, doi: 10.1016/S1871-644X(05)80034-8.
- Peñuelas J., Asensio D., Tholl D., Wenke K., Rosenkranz M., Piechulla B., Schnitzler J.P., 2014. *Biogenic volatile emissions from the soil*. Plant Cell Environ., doi: 10.1111/pce.12340.
- Perini G., Conticelli S., Francalanci L., Davidson J.P., 2000. *The relationship between potassic and calc-alkaline post-orogenic magmatism at Vico volcano, central Italy*. J. Volcanol. Geotherm. Res., 95, 247-272.
- Petherbridge J.R., May P.W., Fuge G.M., Rosser K.N., Ashfold M.N.R., 2002. *In situ plasma diagnostics of the chemistry behind sulfur doping of CVD diamond films*. Diam. Relat. Mat., 11, 301-306.
- Pieri M., 1988. *Petrolio: origine, ricerca, produzione, dati statistici, aspetti economici*. Zanichelli (Ed.), Bologna, pp. 410.

-
- Pizzarello S., Shock E.L., 2010. *The organic composition of carbonaceous meteorites: the evolutionary story ahead of biochemistry*. Cold Harb. Perspect. Biol., 2:a002105, doi: 10.1101/cshperspect.a002105.
- Plyasunov A.V., Shock E.L., 2000. *Standard state Gibbs energies of hydration of hydrocarbons at elevated temperatures as evaluated from experimental phase equilibria studies*. Geochim. Cosmochim. Ac., 64(16), 2811-2833.
- Plyasunov A.V., Shock E.L., 2003. *Prediction of the vapor-liquid distribution constants for volatile nonelectrolytes in water up to its critical temperature*. Geochim. Cosmochim. Ac., 67(24), 4981-5009, doi: 10.1016/j.gca.2003.08.003.
- Rahimpour M.R., Jafari M., Iranshahi D., 2013. *Progress in catalytic naphtha reforming process: a review*. Appl. Energ., 109, 79-93, doi: 10.1016/j.apenergy.2013.03.080.
- Rampelotto P.H., 2013. *Extremophiles and extreme environments*. Life, 3, 482-485, doi: 10.3390/life3030482.
- Riguzzi F., Pietrantonio G., Devoti R., Atzori S., Anzidei M., 2009. *Volcanic unrest of the Colli Albani (central Italy) detected by GPS monitoring test*. Phys. Earth Planet. In., 177(1-2), 79-87, doi: 10.1016/j.pepi.2009.07.012.
- Rogie J.D., Kerrick D.M., Chiadini G., Frondini F., 2000. *Flux measurements of nonvolcanic CO₂ emission from some vents in central Italy*. J. Geophys. Res., 105(B4), 8435-8445.
- Royo F., 2009. *Degradation of alkanes by bacteria*. Environ. Microbiol., 11(10), 2477-2490, doi: 10.1111/j.1462-2920.2009.01948.x.
- Rollinson H., 1993. *Using geochemical data*. Longman, London, UK, p. 352.
- Russell M.J., Martin W., 2004. *The rocky roots of the acetyl-CoA pathway*. Trends Biochem. Sci., 29(7), 358-363, doi: 10.1016/j.tibs.2004.05.007.
- Sano Y., Marty B., 1995. *Origin of carbon in fumarolic gas from island arcs*. Chem. Geol. (Isotope Geoscience Section), 119, 265-274.
- Schäfer H., Myronova N., Boden R., 2010. *Microbial degradation of dimethylsulphide and related C₁-sulphur compounds: organisms and pathways controlling fluxes of sulphur in the biosphere*. J. Exp. Bot., 61(2), 315-334, doi: 10.1093/jxb/erp355.
- Schmidt R., Cordovez V., de Boer W., Raaijmakers J., Garbeva P., 2015. *Volatile affairs in microbial interactions*. ISME J., 9, 2329-2335, doi: 10.1038/ismej.2015.42.
- Schmidt R., Etalo D.W., de Jager V., Gerards S., Zweers H., de Boer W., Garbeva P., 2016. *Microbial small talk: volatiles in fungal-bacterial interactions*. Front. Microbiol., 6, 1495, doi: 10.3389/fmicb.2015.01495.
- Schmitt-Kopplin P., Gabelica Z., Gougeon R.D., Fekete A., Kanawati B., Harir M., Gebefuegi I., Eckel G., Hertkorn N., 2010. *High molecular diversity of extraterrestrial organic matter in Murchison meteorite revealed 40 years after its fall*. PNAS, 107(7), 2763-2768, doi: 10.1073/pnas.0912157107.
- Schoell, M., 1980. *The hydrogen and carbon isotopic composition of methane from natural gases of various origins*. Geochim. Cosmochim. Ac., 44(5), 649-661.
-

References

- Schulz-Bohm K., Zweers H., de Boer W., Garbeva P., 2015. *A fragrant neighborhood: volatile mediated bacterial interactions in soil*. Front. Microbiol., 6, 1212, doi: 10.3389/fmicb.2015.01212.
- Schwandner F.M., Seward T.M., Gize A.P., Hall A., Dietrich V.J., 2004. *Diffuse emission of organic trace gases from the flank and crater of a quiescent active volcano (Vulcano, Aeolian Islands, Italy)*. J. Geophys. Res., 109, D04301, doi: 10.1029/2003JD003890.
- Schwandner F.M., Seward T.M., Gize A.P., Hall A., Dietrich V.J., 2013. *Halocarbons and other trace heteroatomic organic compounds in volcanic gases from Vulcano (Aeolian Islands, Italy)*. Geochim. Cosmochim. Ac., 101, 191-221, doi: 10.1016/j.gca.2012.10.004.
- Scripps CO₂ Program, Scripps Institution of Oceanography UC San Diego, <http://scrippsco2.ucsd.edu>.
- Scrocca D., Doglioni C., Innocenti F., 2003. *Constraints for an interpretation of the Italian geodynamics: a review*. Memorie Descrittive della Carta Geologica d'Italia, 62, 15-46.
- Seewald J.S., 1994. *Evidence for metastable equilibrium between hydrocarbons under hydrothermal conditions*. Nature, 370, 285-287.
- Seewald J.S., 2001. *Aqueous geochemistry of low molecular weight hydrocarbons at elevated temperatures and pressures: Constraints from mineral buffered laboratory experiments*. Geochim. Cosmochim. Ac., 65(10), 1641-1664.
- Seewald J.S., 2003. *Organic-inorganic interactions in petroleum-producing sedimentary basins*. Nature, 426, 327-333. Semrau J.D., 2011. *Bioremediation via methanotrophy: overview of recent findings and suggestions for future research*. Front. Microbiol., 2, 209, doi: 10.3389/fmicb.2011.00209.
- Sherwood Lollar B., 2004. *Life's Chemical Kitchen*. Science, 304, 972-973.
- Shipp J., Gould I.R., Herckes P., Shock E.L., Williams L.B., Hartnett H.E., 2013. *Organic functional group transformations in water at elevated temperature and pressure: Reversibility, reactivity, and mechanisms*. Geochim. Cosmochim. Ac., 104, 194-209, doi: 10.1016/j.gca.2012.11.014.
- Shipp J., Gould I.R., Shock E.L., Williams L.B., Hartnett H.E., 2014. *Sphalerite is a geochemical catalyst for carbon-hydrogen bond activation*. PNAS, 111(32), 11642-11645, doi: 10.1073/pnas.1324222111.
- Shock E.L., 1990a. *Do amino acids equilibrate in hydrothermal fluids?*. Geochim. Cosmochim. Ac., 54, 1185-1189.
- Shock E.L., 1990b. *Geochemical constraints on the origin of organic compounds in hydrothermal systems*. Orig. Life Evol. Biosph., 20, 331-367.
- Shock E.L., 1992. *Hydrothermal organic synthesis experiments*. Orig. Life Evol. Biosph., 22, 135-146.
- Shock E.L., Helgeson H.C., 1990. *Calculation of the thermodynamic and transport properties of aqueous species at high pressures and temperatures: Standard partial molal properties of organic species*. Geochim. Cosmochim. Ac., 54(4), 915-945.

-
- Shock E.L., Schulte M.D., 1998. *Organic synthesis during fluid mixing in hydrothermal systems*. J. Geophys. Res., 103(E12), 28,513-28,527.
- Shock E.L., Canovas P., Yang Z., Boyer G., Johnson K., Robinson K., Fecteau K., Windman T., Cox A., 2013. *Thermodynamics of organic transformations in hydrothermal fluids*. Rev. Mineral. Geochem., 76, 311-350, doi: 10.2138/rmg.2013.76.9.
- Shock E.L., Boyd E.S., 2015. *Principles of geobiochemistry*. Elements, 11, 395-401, doi: 10.2113/gselements.11.6.395.
- Sigurdsson H., Houghton B., McNutt S.R., Rymer H., Stix J., 2015. *The Encyclopedia of Volcanoes, 2nd Edition*. Academic Press, San Diego, pp.1456.
- Siskin M., Katritzky A.R., 2000. *A review of the reactivity of organic compounds with oxygen-containing functionality in superheated water*. J. Anal. Appl. Pyrolysis, 54, 193-214.
- Soma Y., Soma M., 1989. *Chemical reactions of organic compounds on clay surfaces*. Environ. Health Perspect., 83, 205-214.
- Spormann A.M., Widdel F., 2000. *Metabolism of alkylbenzenes, alkanes, and other hydrocarbons in anaerobic bacteria*. Biodegradation, 11, 85-105.
- Stefánsson A., Arnórsson S., 2002. *Gas pressures and redox reactions in geothermal fluids in Iceland*. Chem. Geol., 190, 251-271, doi: 10.1016/S0009-2541(02)00119-5.
- Stetter K.O., 1999. *Extremophiles and their adaptation to hot environments*. FEBS Letters, 452, 22-25.
- Stetter K.O., 2006. *Hyperthermophiles in the history of life*. Phil. Trans. R. Soc. B., 361, 1837-1843, doi: 10.1098/rstb.2006.1907.
- Stoiber R.E., Leggett D.C., Jenkins Th.F., Murrmann R.P., Rose W.I.Jr., 1971. *Organic compounds in volcanic gas from Santiaguito volcano, Guatemala*. Geol. Soc. Amer. Bull., 82, 2299-2302.
- Symonds R.B., Gerlach T.M., Reed M.H., 2001. *Magmatic gas scrubbing: implications for volcano monitoring*. J. Volcanol. Geoth. Res., 108, 303-341.
- Takai K., Nakamura K., Toki T., Tsunogai U., Miyazaki M., Miyazaki J., Hira-yama H., Nakagawa S., Nunoura T., Horikoshi K., 2008. *Cell proliferation at 122 °C and isotopically heavy CH₄ production by a hyperthermophilic methanogen under high-pressure cultivation*. PNAS, 105(31), 10949-10954, doi: 10.1073_pnas.0712334105.
- Taran Y.A., Pokrovsky B.G., Esikov A.D., 1989. *Deuterium and oxygen-18 in fumarolic steam and amphiboles from some Kamchatka volcanoes: "andesitic waters"*. Dokl. Akad. Nauk SSSR 304, 440-443.
- Taran Y.A., Giggenbach W.F., 2003. *Geochemistry of Light Hydrocarbons in Subduction-Related Volcanic and Hydrothermal Fluids*. Society of Economic Geologists Special Publication, 10, 61-74.
- Taran Y., Giggenbach W.F., 2004. *Evidence for metastable equilibrium between hydrocarbons in volcanic gases*. In: R.B. Wanty and R.R. Seal (eds.), *Water-Rock Interaction*, A.A. Balkema, Leiden, pp. 193-195.
-

References

- Tassi F., 2004. *Fluidi in ambiente vulcanico: evoluzione temporale dei parametri composizionali e distribuzione degli idrocarburi leggeri in fase gassosa*. Ph.D. Thesis, Univ. of Florence: Florence, Italy.
- Tassi F., Martinez C., Vaselli O., Capaccioni B., Viramonte J., 2005a. *Light hydrocarbons as redox and temperature indicators in the geothermal field of El Tatio (northern Chile)*. Appl. Geochem., 20, 2049-2062, doi: 10.1016/j.apgeochem.2005.07.013.
- Tassi F., Vaselli O., Capaccioni B., Giolito C., Duarte E., Fernandez E., Minissale A., Magro G., 2005b. *The hydrothermal-volcanic system of Rincon de la Veja volcano (Costa Rica): A combined (inorganic and organic) geochemical approach to understanding the origin of the fluid discharges and its possible application to volcanic surveillance*. J. Volcanol. Geoth. Res., 148, 315-333, doi: 10.1016/j.jvolgeores.2005.05.001.
- Tassi F., Vaselli O., Capaccioni B., Montegrossi G., Barahona F., Caprai A., 2007. *Scrubbing process and chemical equilibria controlling the composition of light hydrocarbons in natural gas discharges: An example from the geothermal field of El Salvador*. Geochem. Geophys. Geosys., 8(5), Q05008, doi: 10.1029/2006GC001487.
- Tassi F., Capaccioni B., Capecchiacci F., Vaselli O., 2009. *Non-methane Volatile Organic Compounds (VOCs) at El Chichón volcano (Chiapas, México): Geochemical features, origin and behavior*. Geof. Int., 48(1), 85-95.
- Tassi F., Montegrossi G., Capecchiacci F., Vaselli O., 2010. *Origin and distribution of thiophenes and furans in gas discharges from active volcanoes and geothermal systems*. Int. J. Mol. Sci., 11, 1434-1457, doi:10.3390/ijms11041434.
- Tassi F., Bonini M., Montegrossi G., Capecchiacci F., Capaccioni B., Vaselli O., 2012a. *Origin of light hydrocarbons in gases from mud volcanoes and CH₄-rich emissions*. Chem. Geol., 294-295, 113-126, doi: 10.1016/j.chemgeo.2011.12.004.
- Tassi F., Capecchiacci F., Buccianti A., Vaselli O., 2012b. *Sampling and analytical procedures for the determination of VOCs released into air from natural and anthropogenic sources: A comparison between SPME (Solid Phase Micro Extraction) and ST (Solid Trap) methods*. Appl. Geochem., 27, 115-123, doi: 10.1016/j.apgeochem.2011.09.023.
- Tassi F., Capecchiacci F., Cabassi J., Calabrese S., Vaselli O., Rouwet D., Pecoraino G., Chiodini G., 2012c. *Geogenic and atmospheric sources for volatile organic compounds in fumarolic emissions from Mt. Etna and Vulcano Island (Sicily, Italy)*. J. Geophys. Res., 117, D17305, doi: 10.1029/2012JD017642.
- Tassi F., Fiebig J., Vaselli O., Nocentini M., 2012d. *Origins of methane discharging from volcanic-hydrothermal, geothermal and cold emissions in Italy*. Chem. Geol., 310-311, 36-48, doi: 10.1016/j.chemgeo.2012.03.018.
- Tassi F., Capecchiacci F., Giannini L., Vougioukalakis G.E., Vaselli O., 2013a. *Volatile organic compounds (VOCs) in air from Nisyros Island (Dodecanese Archipelago, Greece): Natural versus anthropogenic sources*. Environ. Pollut., 180, 111-121, doi: 10.1016/j.envpol.2013.05.023.

-
- Tassi F., Nisi B., Cardellini C., Capecchiacci F., Donnini M., Vaselli O., Avino R., Chiodini G., 2013b. *Diffuse soil emission of hydrothermal gases (CO₂, CH₄, C₆H₆) at Solfatara crater (Campi Flegrei, southern Italy)*. Appl. Geochem., 35, 142-153, doi: 10.1016/j.apgeochem.2013.03.020.
- Tedesco D., Scarsi P., 1999. *Chemical (He, H₂, CH₄, Ne, Ar, Na) and isotopic (He, Ne, Ar, C) variations at the Solfatara crater (southern Italy): mixing of different sources in relation to seismic activity*. Earth Planet. Sci. Lett., 171(3), 465-480.
- Tibaldi A., Pasquarè F.A., Papanikolaou D., Nomikou P., 2008. *Tectonics of Nisyros Island, Greece, by field and offshore data, and analogue modelling*. J. Struct. Geol., 30, 1489-1506, doi: 10.1016/j.jsg.2008.08.003.
- Tissot B.P., Welte D.H., 1984. *Petroleum Formation and Occurrence, Second Revised and Enlarged Edition*. Springer-Verlag, Berlin Heidelberg, pp. 699.
- Todesco M., Chiodini G., Macedonio G., 2003. *Monitoring and modelling hydrothermal fluid emission at La Solfatara (Phlegrean Fields, Italy). An interdisciplinary approach to the study of diffuse degassing*. J. Volcanol. Geoth. Res., 125, 57-79, doi: 10.1016/S0377-0273(03)00089-1.
- Trigila R., Agosta E., Currado C., De Benedetti A.A., Freda C., Gaeta M., Palladino D.M., Rosa C., 1995. *Petrology*. In: Trigila R. (Ed.), *The Volcano of the Alban Hills*. Tipografia S.G.S., Roma, 95-165.
- Turata U.T., Ramanathan R., 2003. *Catalytic naphtha reforming: revisiting its importance in the modern refinery*. J. Sci. Res., 62, 963-978.
- Vaselli O., Tassi F., Montegrossi G., Capaccioni B., Giannini L., 2006. *Sampling and analysis of volcanic gases*. Acta Vulcanol., 18(1-2), 65-76.
- Vaselli O., Tassi F., Tedesco D., Poreda J.R., Caprai A., 2011. *Submarine and inland gas discharges from the Campi Flegrei (southern Italy) and the Pozzuoli Bay: geochemical clues for a common hydrothermal-magmatic source*. Procedia Earth Planet. Sci., 4, 57-73, doi: 10.1016/j.proeps.2011.11.007.
- Vieille C., Zeikus G.J., 2001. *Hyperthermophilic enzymes: sources, uses and molecular mechanisms for thermostability*. Microbiol. Mol. Biol. Rev., 65(1), 1-43, doi: 10.1128/MMBR.65.1.1-43.2001.
- Viveiros F., Cardellini C., Ferreira T., Caliro S., Chiodini G., Silva C., 2010. *Soil CO₂ emissions at Furnas Volcano, São Miguel Island, Azores archipelago: Volcano monitoring perspectives, geomorphologic studies, and land use planning application*. J. Geophys. Res., 115(B12208), doi: 10.1029/2010JB007555.
- Voltaggio M., Barbieri M., 1995. *Geochronology*. In: Trigila, R. (Ed.), *The Volcano of the Alban Hills, Rome*. pp. 167-192.
- Wächtershäuser G., 1988. *Before enzymes and templates: Theory of surface metabolism*. Microbiol. Rev., 52(4), 452-484.
- Watanabe M., Sato T., Inomata H., Smith R.L.Jr., Arai K., Kruse A., Dinjus E., 2004. *Chemical reactions of C₁ compounds in near-critical and supercritical water*. Chem. Rev., 104, 5803-5821, doi: 10.1021/cr020415y.
-

References

- Weiss M.c., Sousa F.L., Mrnjavac N., Neukirchen S., Roettger M., Nelson-Sathi S., Martin W.F., 2016. *The physiology and habitat of the last universal common ancestor*. Nat. Microbiol., 1, 16116, doi: 10.1038/nmicrobiol.2016.116.
- Welhan J.A., 1988. *Origins of methane in hydrothermal systems*. Chem. Geol., 71, 183-198.
- Wheatley R.E., 2002. *The consequences of volatile organic compound mediated bacterial and fungal interactions*. A. van Leeuw., 81, 357-364.
- White D.E., Waring G.A., 1963. *Volcanic emanations*. In: *Data of geochemistry (6th ed.)*, U.S. Geol. Survey Prof. Paper 440-K, pp. K1-K27.
- Whiticar M.J., 1999. *Carbon and hydrogen isotope systematics of bacterial formation and oxidation of methane*. Chem. Geol., 161, 291-314.
- WHO, 2000. *Air quality guidelines for Europe, 2nd ed.*, Copenhagen, WHO Regional Publications, European Series, No. 91, pp. 273.
- Widdel F., Rabus, 2001. *Anaerobic biodegradation of saturated and aromatic hydrocarbons*. Curr. Opin. Biotechnol., 12, 259-276.
- Widdel F., Boetius A., Rabus R., 2006. *Anaerobic biodegradation of hydrocarbons including methane*. In: Dworkin M., Falkow S., Rosenberg E., Schleifer K.-H., Stackebrandt E. (Eds.), *The Prokaryotes, Volume 2: Ecophysiology and Biochemistry, Third Edition*, Springer, Berlin, pp. 1028-1049.
- Williams L.B., Canfield B., Voglesonger K.M., Holloway J.R., 2005. *Organic molecules formed in a "primordial womb"*. Geology, 33(11), 913-916, doi: 10.1130/G21751.1.
- Wolicka D., Suszek A., Borkowski A., Bielecka A., 2009. *Application of aerobic microorganisms in bioremediation in situ of soil contaminated by petroleum products*. Bioresour. Technol., 100, 3221-3227, doi: 10.1016/j.biortech.2009.02.020.
- Wright I.P., Sherifan S., Barber S.J., Morgan G.H., Andrews D.J., Morse A.D., 2015. *CHO-bearing organic compounds at the surface of 67P/Churyumov-Gerasimenko revealed by Ptolemy*. Science, 349(6247), doi: 10.1126/science.aab-0673.
- Yang Z., Gould I.R., Williams L.B., Hartnett H.E., Shock E.L., 2012. *The central role of ketones in reversible and irreversible hydrothermal organic functional group transformations*. Geochim. Cosmochim. Ac., 98, 48-65, doi: 10.1016/j.gca.2012.08.031.

Appendix A

Published Papers



Contents lists available at ScienceDirect

Applied Geochemistry

journal homepage: www.elsevier.com/locate/apgeochem



Volatile organic compounds (VOCs) in soil gases from Solfatara crater (Campi Flegrei, southern Italy): Geogenic source(s) vs. biogeochemical processes



F. Tassi^{a,b,*}, S. Venturi^a, J. Cabassi^a, F. Capecchiacci^{a,b}, B. Nisi^c, O. Vaselli^{a,b}

^a Department of Earth Sciences, University of Florence, Via La Pira 4, 50121 Florence, Italy

^b CNR-IGG Institute of Geosciences and Earth Resources, Via La Pira 4, 50121 Florence, Italy

^c CNR-IGG Institute of Geosciences and Earth Resources, Via G. Moruzzi 1, 56124 Pisa, Italy

ARTICLE INFO

Article history:

Available online 19 February 2015

Editorial handling by M. Kersten

ABSTRACT

The chemical composition of volatile organic compounds (VOCs) in soil gases from the Solfatara crater (Campi Flegrei, Italy) was analyzed to investigate the effects of biogeochemical processes on gases discharged from the hydrothermal reservoir and released into the atmosphere through diffuse degassing. The chemistry of fluids from fumarolic vents, which represent preferential pathways for fluid uprising, was also reported for comparison. Oxidation–reduction and hydration–dehydration reactions, as well as microbial activity, strongly affected the composition of C₄–C₉ alkanes, alkenes, S-bearing compounds and alkylated aromatics, especially in those sites where the soil showed relatively low permeability to uprising fluids. Other endogenous organic compounds, such as benzene, phenol and hydrofluorocarbons were able to transit through the soil almost undisturbed, independently on the gas emission rate. Products of VOC degradation mainly consisted of aldehydes, ketones, esters, ethers and, subordinately, alcohols. Cyclic compounds revealed the occurrence of VOCs produced within sedimentary formations overlying the hydrothermal reservoir, whereas the presence of chlorofluorocarbons (CFCs) was likely related to air contamination. The results of the present study highlighted the strict control of biogeochemical processes on the behavior of hydrothermal VOCs that, at least at a local scale, may have a significant impact on air quality. This information could be improved by laboratory experiments conducted at specific chemical–physical conditions and in presence of different microbial populations.

© 2015 Elsevier Ltd. All rights reserved.

1. Introduction

Volatile organic compounds (VOCs), which can be defined as organic species with a vapor pressure <760 torr (101.3 kPa) and >1 torr (0.13 kPa) at 20 °C (Derwent, 1995), are commonly found at significant concentrations in geothermal and volcanic fluids (Shock et al., 2013, and references therein). In these environments, VOCs are mostly produced by degradation of organic material proceeding through (i) bacteria-driven reactions and (ii) thermogenic processes (Des Marais et al., 1981; Darling, 1998; Mango, 2000). However, the large availability of precursory molecules (CO, CO₂ and biogenic hydrocarbons) and the chemical–physical conditions characterizing hydrothermal–magmatic fluid reservoirs seem to favor VOC abiotic synthesis (Szatmari, 1989; Seewald, 1994; Sugisaki and Mimura, 1994; Sherwood Lollar et al., 2002; Taran

and Giggenbach, 2003; McCollom and Seewald, 2007; McCollom et al., 2010). VOCs typically recognized in volcanic and geothermal fluids (Inn et al., 1981; Isidorov et al., 1990, 1992; Capaccioni et al., 1995, 2001, 2004; Jordan et al., 2000; Schwandner et al., 2004; Tassi et al., 2005, 2009a; 2012a) may exert a considerable environmental burden. Light alkanes and CFCs are greenhouse gases (Shindell et al., 2009). Halogenated compounds play a key role as primary agents of tropospheric and stratospheric ozone depletion (Cicerone et al., 1974; Molina and Rowland, 1974; Rowland and Molina, 1994; Brune, 1996). Aromatics have carcinogenic, teratogenic and mutagenic effects to humans (Harkov et al., 1985; Mølhav et al., 1986; Wood and Porter, 1986; Assmuth and Kalevi, 1992; WHO, 2010; Kim et al., 2013). Notwithstanding the potential importance of VOCs for air quality, the effective hydrocarbon seepage from natural sources is poorly constrained and limited to the analysis of few species (Etioppe et al., 2007, 2008; Etioppe and Ciccio, 2009). Those VOCs that enter the atmospheric cycle from deep-seated fluid reservoirs are sensitive to changes in chemical–physical conditions, i.e., temperature and redox. Therefore,

* Corresponding author at: Department of Earth Sciences, University of Florence, Via La Pira 4, 50121 Florence, Italy. Tel.: +39 0552757477; fax: +39 055284571. E-mail address: franco.tassi@unifi.it (F. Tassi).



Contents lists available at ScienceDirect

Organic Geochemistry

journal homepage: www.elsevier.com/locate/orggeochem

Biodegradation of CO₂, CH₄ and volatile organic compounds (VOCs) in soil gas from the Vicano–Cimino hydrothermal system (central Italy)

F. Tassi^{a,b,*}, S. Venturi^{a,b}, J. Cabassi^{a,b}, O. Vaselli^{a,b}, I. Gelli^a, D. Cinti^c, F. Capecciacci^{a,b}^a Department of Earth Sciences, University of Florence, Via La Pira 4, 50121 Florence, Italy^b CNR-IGG Institute of Geosciences and Earth Resources, Via La Pira 4, 50121 Florence, Italy^c Istituto Nazionale di Geofisica e Vulcanologia (INGV), Via di Vigna Murata 605, 00143 Rome, Italy

ARTICLE INFO

Article history:

Received 20 February 2015

Received in revised form 15 June 2015

Accepted 23 June 2015

Available online 29 June 2015

Keywords:

Soil gas

VOCs

Degradation process

Microbial activity

Hydrothermal system

Vicano–Cimino volcanic system

ABSTRACT

We investigated the effect of microbial activity on the chemistry of hydrothermal fluids related to the Vicano–Cimino system, central Italy. The database included the composition and $\delta^{13}\text{C}$ CO₂ and $\delta^{13}\text{C}$ CH₄ values for soil gas from an area characterized by intense degassing of fluids having a deep origin. The $\delta^{13}\text{C}$ CH₄ values along vertical profiles in the soil indicated that CH₄ was controlled by microbial oxidation occurring at shallow (<50 cm) depth, where free O₂ was available. This was consistent with the vertical gradients of CH₄, H₂S and O₂ concentrations. The $\delta^{13}\text{C}$ CO₂ values in soil gas, characterized by a composition similar to that of the hydrothermal fluids, were not significantly influenced by biodegradation. On the contrary, gas strongly affected by air contamination showed a significant $\delta^{13}\text{C}$ CO₂ fractionation. Microbial activity caused strong consumption of hydrothermal alkanes, alkenes, cyclics and hydrogenated halocarbons, whereas benzene was recalcitrant. Oxygenated compounds from hydrocarbon degradation consisted of alcohols, with minor aldehydes, ketones and carboxylic acids. A predominance of alcohols at a high rate of degassing flux, corresponding to a short residence time of hydrothermal gas within the soil, indicated incomplete oxidation. N-bearing compounds were likely produced by humic substances in the soil and/or related to contamination by pesticides, whereas α -pinene traced air entering the soil. The study demonstrates that microbial communities in the soil play an important role for mitigating the release to the atmosphere of C-bearing gases, especially CH₄, through diffuse soil degassing, a mechanism that in central Italy significantly contributes to the discharge of CO₂-rich gas from deep sources.

© 2015 Elsevier Ltd. All rights reserved.

1. Introduction

CO₂, CH₄ and non-CH₄ volatile organic gases (hereafter VOCs), discharged from both anthropogenic and natural sources to the atmosphere, are a cause of environmental concern, since they are able to exert a strong impact on air quality, global climate and human health (e.g. Cicerone et al., 1974; Mølhav et al., 1986; Assmuth and Kalevi, 1992; Rowland and Molina, 1994; Brune, 1996; Kuran and Sojak, 1996; Harnisch et al., 2002). The amount of geogenic and anthropogenic gas input to the atmosphere depends on (i) gas production rate from the primary source and (ii) secondary processes, such as those occurring in soil, where the availability of O₂ permeating through the soil–air interface favors the degradation of gas originating under reducing conditions.

The capability of microbial communities to adapt to different environmental conditions likely explains the strong influence that their activity can have on the chemistry of underground circulating fluids. Thus, it is not surprising that the composition of gas from diffuse soil degassing is often significantly different with respect to that of the original deep fluid (Tassi et al., 2013). The behavior of CO₂, CH₄ and VOCs in soils is thus controlled by biotic and abiotic processes and constrained by a large number of physical–chemical parameters. The activity of soil microbes able to produce or consume carbon-bearing gas is indeed driven by different soil features, which include (i) microbial community composition and biomass, (ii) carbon substrate, (iii) redox conditions, (iv) temperature, (v) pH, (vi) nutrient availability and (vii) permeability (Insam and Seewald, 2010 and references therein). A reliable prediction of the fate of these gaseous compounds in soil is complicated by their distribution between gas–liquid (Henry's law coefficient) and solid–liquid (absorption partition coefficient) phases, as well as by gas transport mechanisms (e.g. diffusion, advection) at the soil pore

* Corresponding author at: Department of Earth Sciences, University of Florence, Via La Pira 4, 50121 Florence, Italy; Tel.: +39 0552757477; fax: +39 055290312. E-mail address: franco.tassi@unifi.it (F. Tassi).

A. Published Papers

Elsevier Editorial System(tm) for Journal of
Volcanology and Geothermal Research
Manuscript Draft

Manuscript Number:

Title: Mineral-assisted production of benzene under hydrothermal
conditions: insights from experimental studies on C6 cyclic hydrocarbons

Article Type: SI: VHSTaran

Keywords: hydrothermal gases; organic compounds; benzene; mineral
catalysts; catalytic reforming; laboratory experiments

Corresponding Author: Dr. Stefania Venturi,

Corresponding Author's Institution: University of Florence

First Author: Stefania Venturi

Order of Authors: Stefania Venturi; Franco Tassi; Ian R Gould; Everett L
Shock; Hilairy E Hartnett; Edward D Lorange; Christiana Bockisch;
Kristopher M Fecteau; Francesco Capecchiacci; Orlando Vaselli

Abstract: Volatile Organic Compounds (VOCs) are ubiquitously present at low but detectable concentrations in hydrothermal fluids from volcanic and geothermal systems. Although their behavior is strictly controlled by physical and chemical parameters, the mechanisms responsible for the production of most VOCs in natural environments are poorly understood. Among them, benzene, whose abundances were found to be relatively high in hydrothermal gases, can theoretically be originated from reversible catalytic reforming processes, i.e. multi-step dehydrogenation reactions, involving saturated hydrocarbons. However, this hypothesis and other hypotheses are difficult to definitively prove on the basis of compositional data obtained by natural gas discharges only. In this study, therefore, laboratory experiments were carried out to investigate the production of benzene from cyclic hydrocarbons at hydrothermal conditions, specifically 300 °C and 85 bar. The results of experiments carried out in the presence of water and selected powdered minerals, suggest that cyclohexane undergoes dehydrogenation to form benzene, with cyclohexene and cyclohexadiene as by-products, and also as likely reaction intermediates. This reaction is slow when carried out in water alone and competes with isomerization and hydration pathways. However, benzene formation was increased compared to these competing reactions in the presence of sulfide (sphalerite and pyrite) and iron oxide (magnetite and hematite) minerals, whereas no enhancement of any reaction products was observed in the presence of quartz. The production of thiols was observed in experiments involving sphalerite and pyrite, suggesting that sulfide minerals may act both to enhance reactivity and also as reactants after dissolution. These experiments demonstrate that benzene can be effectively produced at hydrothermal conditions through dehydrogenation of saturated cyclic organic structures and highlight the crucial role played by minerals in this process.

Appendix B

Conference Proceedings

B. Conference Proceedings

AGU FALL MEETING

San Francisco | 15–19 December 2014

Degradation Pathways for Geogenic Volatile Organic Compounds (VOCs) in Soil Gases from the Solfatara Crater (Campi Flegrei, Southern Italy).

Franco Tassi¹, **Stefania Venturi²**, **Jacopo Cabassi³**, **Francesco Capecchiacci²**, **Barbara Nisi Sr.²** and **Orlando Vaselli¹**, (1)University of Florence, Florence, Italy, (2)University of Florence, Dipartimento di Scienze della Terra, Florence, Italy, (3)University of Florence, Earth Sciences, Florence, Italy

Abstract:

The chemical composition of volatile organic compounds (VOCs) in soil gases from the Solfatara crater (Campi Flegrei, Southern Italy) was analyzed to investigate the effects of biogeochemical processes occurring within the crater soil on gases discharged from the hydrothermal reservoir and released into the atmosphere through diffuse degassing. In this system, two fumarolic vents (namely Bocca Grande and Bocca Nuova) are the preferential pathways for hydrothermal fluid uprising. For our goal, the chemistry of VOCs discharged from these sites were compared to that of soil gases. Our results highlighted that C₄-C₉ alkanes, alkenes, S-bearing compounds and alkylated aromatics produced at depth were the most prone to degradation processes, such as oxidation-reduction and hydration-dehydration reactions, as well as to microbial activity. Secondary products, which were enriched in sites characterized by low soil gas fluxes, mostly consisted of aldehydes, ketons, esters, ethers, organic acids and, subordinately, alcohols. Benzene, phenol and hydrofluorocarbons (HFCs) produced at depth were able to transit through the soil almost undisturbed, independently on the emission rate of diffuse degassing. The presence of cyclics was possibly related to an independent low-temperature VOC source, likely within sedimentary formations overlying the hydrothermal reservoir. Chlorofluorocarbons (CFCs) were possibly due to air contamination. This study demonstrated the strict control of biogeochemical processes on the behaviour of hydrothermal VOCs that, at least at a local scale, may have a significant impact on air quality. Laboratory experiments conducted at specific chemical-physical conditions and in presence of different microbial populations may provide useful information for the reconstruction of the degradation pathways controlling fate and behaviour of VOCs in the soil.

Experimental studies of mineral-catalyzed dehydrogenation of C₆ cyclic hydrocarbons under hydrothermal conditions

Venturi S.^{*1-2}, Tassi F.¹⁻², Gould I.R.³, Shock E.L.³⁻⁴, Lorange E.D.⁵, Bockisch C.³ & Fecteau K.³

1. Dipartimento di Scienze della Terra, Università di Firenze. 2. Istituto di Geoscienze e Georisorse, CNR, Firenze. 3. Department of Chemistry and Biochemistry, Arizona State University, Tempe, USA. 4. School of Earth and Space Exploration, Arizona State University, Tempe, USA. 5. Department of Chemistry, Vanguard University, Costa Mesa, USA.

Corresponding email: stefania.venturi@unifi.it

Keywords: Mineral-catalyzed organic reactions, hydrothermal fluids, catalytic reforming.

Hydrothermal gases are characterized by a complex mixture of organic volatiles. Patterns in the relative abundances of the main classes of organics are found in gases from natural systems (e.g. volcanoes, geothermal sites) characterized by similar T and redox, which suggests that the compositions of the gas mixtures are sensitive to physical and chemical conditions. The attainment of metastable equilibrium between organic compounds has been demonstrated experimentally (Seewald, 1994). Studies on fumarolic gases (Taran & Giggenbach, 2004) have shown that alkane/alkene interconversion can approach equilibrium in natural environments. Reversible catalytic reforming may be responsible for the high abundance of benzene observed in hydrothermal gases relative to saturated hydrocarbons (Capaccioni et al., 1993). Cyclic hydrocarbons are enriched in gases originating at T 6 cyclic hydrocarbons as intermediates. We are investigating the mechanisms for formation of benzene from cyclic hydrocarbons under laboratory conditions. The reactions of cyclohexane, cyclohexene and cyclohexadiene have been studied at 300 °C and 85 bar. Benzene production is observed, together with various oxidation, hydration and isomerization products, depending upon the conditions. Dehydrogenation of cyclohexadiene to form benzene is very efficient in water alone, but the corresponding reaction of cyclohexane gave negligible benzene even after reaction for 10 days. However, formation of both benzene and cyclohexene from cyclohexane was enhanced in the presence of minerals, in particular, sphalerite. Experiments with varying ratios of cyclohexane and sphalerite showed that dehydrogenation is a surface catalyzed reaction. Experiments in D₂O showed that sphalerite very efficiently catalyzes breaking C-H bonds, even when conversion to benzene is low. For cyclohexene, benzene formation is negligible compared to oxygenation products in the absence of minerals, but sphalerite catalyzes formation of both benzene and cyclohexane. Finally, solution phase oxidation using Cu(II) forms primarily oxygenation products, suggesting that formation of benzene requires surface catalysis by minerals.

Capaccioni B., Martini M., Mangani F., Giannini L., Nappi G. & Prati F. 1993. Light hydrocarbons in gas-emissions from volcanic areas and geothermal fields. *Geochem. J.*, 27, 7-17.

Seewald J.S. 1994. Evidence for metastable equilibrium between hydrocarbons under hydrothermal conditions. *Nature*, 370, 285-287.

Taran Y. & Giggenbach W.F. 2004. Evidence for metastable equilibrium between hydrocarbons in volcanic gases. In: Warty R.B. & Seal R.R. Eds., *Water-Rock Interaction*. 193-195. A.A. Balkema, Leiden.

B. Conference Proceedings

AGU FALL MEETING

San Francisco | 14 – 18 December 2015

V21D-07
Mineral-catalyzed dehydrogenation of C₆ cyclic hydrocarbons: results from experimental studies under hydrothermal conditions

Tuesday, 15 December 2015: 09:45
308 (Moscone South)

*Stefania Venturi*¹, *Franco Tassi*², *Ian Gould*³, *Everett Shock*³, *Edward D. Lorange*⁴, *Christiana Bockisch*³ and *Kristopher Fecteau*³, (1)University of Florence, Dipartimento di Scienze della Terra, Florence, Italy, (2)University of Florence, Florence, Italy, (3)Arizona State University, Tempe, AZ, United States, (4)Vanguard University, Department of Chemistry, Costa Mesa, CA, United States

Abstract:

Volatile organic compounds (VOCs) are ubiquitously present in volcanic and hydrothermal gases. Their relative abundances have been demonstrated to be sensitive to physical and chemical parameters, suggesting VOCs as potential tools for evaluating deep reservoir conditions. Nevertheless, reaction pathways for VOC production at hydrothermal conditions are still poorly understood. Reversible catalytic reforming may be responsible for the high abundance of benzene observed in hydrothermal gases relative to saturated hydrocarbons. The dehydrogenation of n-hexane to benzene could proceed with C₆ cyclic hydrocarbons as intermediates, as suggested by the relative enrichment in cyclic hydrocarbons observed in gases originating at T < 150 °C. In this study, laboratory experiments were carried out to investigate the production of benzene from cyclic hydrocarbons at 300°C and 85 bar. At these conditions in pure water, negligible benzene is produced from cyclohexane after 10 days. The presence of a mineral phase, especially sphalerite, favored the formation of both benzene and cyclohexene. The efficiency of dehydroaromatization reaction increased at increasing mineral/cyclohexane ratio, pointing to a surface catalyzed reaction. The catalytic action of sphalerite on the C-H bonds was confirmed by the large abundance of deuterated cyclohexane resulted in D₂O experiments. The same experiment carried out using cyclohexene in pure water mainly produced methyl-cyclopentenenes (via isomerization) and cyclohexanol (via oxygenation). In presence of sphalerite, the production of significant amounts of benzene confirmed the critical role of this mineral for the aromatization of cyclic compounds under hydrothermal conditions. Contrarily, products from cyclohexene solution phase oxidation using Cu(II) mainly consisted of oxygenated VOCs.



Soil gas composition from the 2001-2002 fissure in the Lakki Plain (Nisyros Island, Greece): evidences for shallow hydrothermal fluid circulation

Stefania Venturi (1,2), Franco Tassi (1,2), Christos Kanellopoulos (3), Orlando Vaselli (1,2), Chiara Caponi (1), Andrea Ricci (4), Alessio Raspanti (1), Andrea Gallorini (1), Jacopo Cabassi (1,2), and Georges Vougioukalakis (3)

(1) Department of Earth Sciences, University of Florence, Via G. La Pira 4, 50121 Florence (Italy), (2) CNR – Istituto di Geoscienze e Georisorse, Via G. La Pira 4, 50121 Florence (Italy), (3) Institute for Geology and Mineral Exploration, 70 Messoghion Street, GR-11527 Athens (Greece), (4) Department of Biological, Geological and Environmental Sciences, University of Bologna, Porta S. Donato 1, Bologna (Italy)

Nisyros volcano (Aegean Sea, Greece) is currently classified in the "Very High Threat" category (Kinvig et al., 2010). Although the last volcanic activity, consisting of phreatic eruptions, occurred in the 19th century, Nisyros experienced an intense seismic activity during 1996-1998 accompanied by ground deformation and changes in the chemistry of fumarolic gases (Chiadini et al., 2002), pointing to a renewed unrest. Between November 2001 and December 2002, a NNE-oriented 600 m long fissure opened in the vegetated central part of the Lakki Plain. The fissure, 1-5 m wide and up to 15-20 m deep, showed neither vertical displacements nor gas release. No changes in the seismic and volcanic activity were observed during or after this event, which was interpreted as related to collapse of the upper caldera floor fine sediment cover (<50 m thick) induced by hydrothermal fluid circulation (Vougioukalakis and Fytikas, 2005). In June 2015, diffuse CO₂ flux measurements, in combination with sampling and chemical analysis of the interstitial soil gases, were performed in (i) the fissure bottom, (ii) the adjacent vegetated areas in the Lakki Plain, (iii) the near hydrothermal craters (Stefanos, Kaminakia, Lofos domes), and (iv) sites located outside the caldera (blank values). The fissure showed neither temperature (<30 °C) nor CO₂ fluxes (<10 gm-2d-1) anomalies with respect to the blank sites and the Lakki Plain, with values strikingly lower than those measured in the hydrothermal craters (up to 98 °C and 208 gm-2d-1, respectively). Contrarily, the CO₂ concentrations in the interstitial soil gases from the fissure (up to 513 mmol/mol) were markedly higher than the background values and comparable with those measured in the craters (up to 841 mmol/mol). Relatively high H₂S, H₂ and CH₄ contents in soil gases from the fissure confirm the hydrothermal origin of these soil gases. However, their CH₄/CO₂ ratio were lower than those measured in the soil gases from the craters, suggesting the occurrence of oxidation processes during the underground migration of the hydrothermal fluids toward the peripheral areas of the caldera. While the low-permeable sediment cover in the Lakki Plain conceals the underneath hydrothermal gas flow, preventing the typical surface manifestations (high temperature and CO₂ flux), the chemistry of the interstitial gases reveals that deep-sourced fluids circulate within the deep permeable layers beneath the Lakki Plain enhancing alteration processes and formation of shallow collapsing structures.

Chiadini G., Brombach T., Caliro S., Cardellini C., 2002. *Geophys Res Lett*, 29(16), 1759.

Kinvig H.S., Winson A., Gottsmann J., 2010. *Nat Hazards Earth Syst Sci*, 10.

Vougioukalakis G.E., Fytikas M., 2005. In Fytikas M., Vougioukalakis G.E. (Eds.), *The South Aegean Active Volcanic Arc, Present Knowledge and Future Perspectives, Developments in Volcanology*, Elsevier, Amsterdam The Netherlands, 2005, pp. 161–163.

Appendix C

Research Projects

C. Research Projects



UNIVERSITÀ
DEGLI STUDI
FIRENZE
DST
DIPARTIMENTO DI
SCIENZE DELLA TERRA



ALMA MATER STUDIORUM
UNIVERSITÀ DI BOLOGNA



Istituto Nazionale di
Geofisica e Vulcanologia

WEST
Systems



Studio multiparametrico sulle emissioni gassose naturali presso Cava dei Selci e Solfatara di Pomezia (Colli Albani, Roma): sviluppo di un protocollo di misura per la definizione di traccianti geochimici atti alla valutazione dell'impatto ambientale di aree affette da degassamento diffuso dal suolo

Cava dei Selci e Solfatara di Pomezia (Colli Albani, Roma)

5, 6, 7 Aprile 2016

Partecipanti:

Università degli Studi di Firenze

Prof. Franco Tassi
Prof. Orlando Vaselli
Dr. Stefania Venturi
Dr. Chiara Caponi
Dr. Jacopo Cabassi
Dr. Francesco Capecchiacci

Università di Bologna

Prof. Bruno Capaccioni
Dr. Andrea Ricci

INGV-Roma

Dr. Alessandra Sciarra
Dr. Daniele Cinti
Dr. Tullio Ricci
Dr. Giuseppe Etiope

INGV-Palermo

Dr. Giorgio Capasso
Dr. Roberto Di Martino

WEST Systems s.r.l.

Dr. Giorgio Virgili
Dr.ssa Ilaria Minardi

Comitato Organizzatore: Prof. Franco Tassi, Dr. Stefania Venturi, Dr. Chiara Caponi, Dr. Alessandra Sciarra

Census of Deep Life Cover Sheet

PROJECT INFORMATION

A geomicrobiological study on soils and sediments affected by hydrothermal fluids from Solfatara Crater (Campi Flegrei, Italy): life adaptation in extreme environments

Option 1

Latitude/longitude N 40°49'45.98" / E 14°7'49.76"

Principal Investigators

Name: FRANCO TASSI

Address: Department of Earth Sciences, University of Florence, Via G. La Pira 4, 50121 Firenze (Italy)

Phone #: +390552757477

e-mail: franco.tassi@unifi.it

Name: STEFANO FAZI

Address: Water Research Institute, National Research Council (IRSA-CNR), Via Salaria km 29.300, CP10, 00015 Monterotondo, Roma (Italy)

Phone #: +390690672790

e-mail: fazi@irsa.cnr.it

Co-Investigators

Name: STEFANIA VENTURI

Address: Department of Earth Sciences, University of Florence, Via G. La Pira 4, 50121 Firenze (Italy)

Phone #: +390552757507

e-mail: stefania.venturi@unifi.it

Name: ORLANDO VASELLI

Address: Department of Earth Sciences, University of Florence, Via G. La Pira 4, 50121 Firenze (Italy)

Phone #: +390552757508

e-mail: orlando.vaselli@unifi.it

Name: JACOPO CABASSI

Address: Department of Earth Sciences, University of Florence, Via G. La Pira 4, 50121 Firenze (Italy)

Phone #: +390552757507

e-mail: jacopo.cabassi@unifi.it

Name: SIMONA ROSSETTI

Address: Water Research Institute, National Research Council (IRSA-CNR), Via Salaria km 29.300, CP10, 00015 Monterotondo, Roma (Italy)

Phone #: +390690672697

e-mail: rossetti@irsa.cnr.it

Brief project abstract with statement of objective

Volcanic and hydrothermal areas represent extreme environments affected by high temperatures, low soil pH, significant diffuse gas emissions and high soil interstitial gas and metal contents. In such areas, microbial life develops in harsh and spatially rapidly changing environments, affecting and being affected by the local geochemical conditions. Solfatara Crater (Campi Flegrei, Italy) represents a perfect natural laboratory to study the interplay between microbial communities and CO₂-rich fluids uprising from deep hydrothermal reservoirs. Here, microbial activity was suggested to exert a trivial control on hydrothermal emissions from diffuse degassing (Tassi et al., 2015a). We propose 16S rDNA amplicon V4V5 and V6 regions sequencing of Bacteria and Archaea collected from 12 sites within Solfatara Crater, including soil samples from two different depths (10 and 30 cm) along 5 vertical profiles and 2 sediment samples from acidic mud pools. Complete geochemical data, including temperature, pH, EC, WHC, total carbon and nitrogen, gas fluxes and composition, water composition, trace metal contents, soil and sediment mineralogical composition, will be provided. The DNA sequencing of soil and sediment samples from this multi-disciplinary study site will produce a detailed picture of biodiversity in hydrothermal environments and will give insights into the complex relations with the chemical and isotopic features of the fluid constituents involved in the microbially-driven processes.